AN ENGINEERING STUDY OF COMPRESSION AND FOULING OF CHROMATOGRAPHIC MATRICES.

Thesis submitted for the degree of

Doctor of Philosophy

by

Gerardo AGUILERA SORIANO

The Advanced Centre for Biochemical Engineering
Department of Chemical and Biochemical Engineering
University College London
Torrington Place
London WC1E 7JE

March 1995

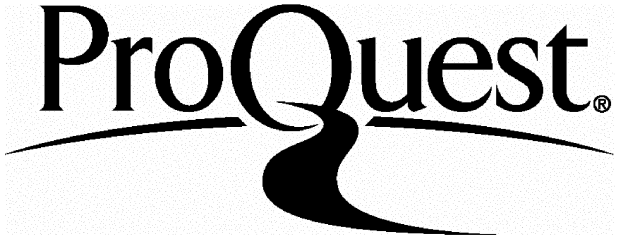

To my Parents, Mariela and all my Family.

ACKNOWLEDGEMENTS.

First of all I would like to thank Dr. N. J. Titchener-Hooker for his continuous support and optimism during these years. His help and advice were invaluable to the writing of this thesis. I would like to express my gratitude to Dr. M. Turner for the great interest he showed in my research project. I would also like to acknowledge Dr. Basset whose experience in the domain of soil mechanics was of great assistance in the conduction of the compression experiments. This thesis would not have been possible had it not been for the work and assistance of D. Webb, J. Graham and B. Bartram who patiently constructed the rigs needed for the estimation of the model parameters. I would also like to thank M. Vale whose support in the field of electronics was of great value. I feel greatly indebted to D. Hearle whose practical experience was essential to the collaborative work which resulted in the last chapter of this thesis. Finally I would like to thank all my colleagues for their valuable contributions and friendship.

ABSTRACT

An engineering study of compression and fouling of chromatographic matrices.

The soft or semi-rigid matrices used in the chromatographic separation of biomolecules have the tendency to compress at high flow rates limiting the throughput and therefore the process productivity.

The first part of this study has focused on the effects of bed compression on column hydrodynamics and chromatographic performance. The predictive capabilities of two hydrodynamic models developed for columns packed with compressible matrices have been assessed. These models were used to predict the pressure drop and the maximum flow rate that can be achieved with a specific matrix for particular sets of column dimensions. In order to evaluate the models the mechanical properties of Sepharose 6B and Sepharose Cl-6B have been measured by means of experimental techniques similar to those employed in soil mechanics.

In order to analyze the effects of bed compression on column performance, key chromatographic parameters were measured with gel filtration columns packed under different compression conditions. Pulse techniques, in particular the HETP method, were used to determine the distribution coefficient, the intraparticle diffusivity coefficient and the axial dispersion coefficient. These parameters have been inputted into a chromatography model to simulate the chromatographic peaks obtained with compressed gel filtration columns in order to corroborate the validity of the estimated parameters.

Chromatographic columns are prone to fouling, however the level of contaminants that can be accepted by a particular column and therefore the required degree of sample pretreatment are not well defined. In the second part of this study the changes that occur in the transport parameters, when a column is fouled with a process stream containing different levels of foulants, have been determined in order to assess the effects of fouling on the matrix and bed structure and therefore on column performance.

The results of this study will enable better prediction of chromatographic separations carried out with columns operating at conditions closely resembling those encountered at the process scale level.

CONTENTS

5. FOULING AND CHROMATOGRAPHIC PERFORMANCE.

6. CONCLUSIONS AND FUTURE WORK.

LIST OF FIGURES

Chapter 3

Chapter 4

Chapter 5

LIST OF TABLES

CHAPTER 1

INTRODUCTION

1.1 General overview.

Large-scale chromatography has come of age as a method for biotechnological separations. Many biological products are already isolated and purified by means of chromatographic techniques on a commercial scale. Their number continues to increase, partially as a result of the possibilities offered by genetic engineering. However, the design and operation of large-scale columns is far from being optimum, and a significant number of problems remain to be solved. Among them are the classical problems of bed compression, typically associated with the use of soft and semirigid matrices, as well as the fouling problems that occur with all types of matrices. The present work has focused on the study of these problems in relation to their effects on column chromatographic performance.

The continuous advances in computer technology and the development of mathematical and numerical algorithms have made possible the use of modelling and simulation as tools to aid the understanding and solution of a great variety of problems. In the chemical industry, process simulation has played an important role in process development and control for many years. On the other hand suitable models for simulating bioprocesses have started to appear only very recently. The aim of this thesis is also to contribute to the development of modelling and simulation tools, and to make use of such tools in order to derive information about the effects that bed compression and fouling have on column chromatographic performance. This information will serve to improve the design, operation and performance of this important unit operation.

In the present chapter the fundamental concepts used in the field of chromatography and in the description of column performance are reviewed. The hydrodynamics of packed columns in relation to compressible matrices is presented together with the most relevant models used in its description. Finally the fouling of chromatographic matrices is dealt with, including a description of the main fouling components found in biological process streams. This will set the context within which the present study will be carried out and it will lead to the definition of its aims.

Initially the place of chromatography within the biotechnology industry is considered in relation to its commercial interest and its importance to bioprocessing.

1.1.1 Commercial perspective.

The rapid development of biotechnology and the requirements placed on the purity of biopharmaceutical products have drastically increased the importance of column-based liquid chromatography in purification and isolation processes. The substances concerned include complex organic molecules, e.g., antibiotics, and proteins, e.g. enzymes and monoclonal antibodies. Particular emphasis has been placed on the isolation and purification of high value products, such as therapeutic products. The high degree of purification required by these products and the fact that chromatography is practically the only unit operation capable of achieving this level of purification has made this operation one of the most important and widely used separation processes in biotechnology.

TABLE 1.1 Chromatographically purified biological products used as human therapeutic agents.

Product	**Use**
Albumin	plasma substitution
Colony stimulating factors (CSFs)	promotion of white cell formation
Epidermal growth factor (EGF)	wound healing
Erythropoeitin (EPO)	anaemia in dialysis patients
Factor VIII	haemophilia
Human growth hormone (HGH)	growth disorders
Human insulin	diabetes
Interferons	treatment of cancer and infectious diseases
Interleukin-2	cancer treatment
Monoclonal antibodies (MAb)	cancer treatment and diagnosis, general diagnosis, affinity chromatography
Platelet derived growth factor (PDGF)	promotion of white cell formation
Superoxide dismutase (SOD)	myocardial infarction therapy
Tissue plasminogen activator (tPA)	dissolution of blood clots
Tumour necrosis factor (TNF)	cancer treatment and diagnosis

Liquid chromatography as a production method for therapeutic agents was first established with the production of insulin and serum proteins. It received a boost with the commercial success of tissue plasminogen activator (tPA), erythropoeitin (EPO), and colony stimulating factor (CSF) (see table 1.1. and 1.2) and more recently, the introduction of a larger number of products among them interferon β1B (Betaseron) and recombinant DNase (Pulmozyme), has further established process liquid chromatography in the biotech market. Table 1.1 gives a list of some of the most important human therapeutic agents with an indication of their use, while table 1.2 shows the ten top biotechnology drugs in the market (all of these drugs are proteins). This latter table provides a clear idea of the size of the biotechnology market. The production of all these agents and proteins requires at least one chromatographic step.

Table 1.2 Top ten biotechnology drugs on the market.

Product	**Developer**	**Marketer**	**Net sales 1993, $m**
Neupogen	Amgen	Amgen	719
Epogen	Amgen	Amgen	587
Intron A	Biogen	Schering-Plough	572
Humulin	Genentech	Eli Lilly	560
Procrit	Amgen	Ortho Biotech	500
Engerix-B	Genentech	SmithKline Beecham	480
RecombinNAK HB	Chiron	Merck	245
Activase	Genentech	Genentech	236
Protropin	Genentech	Genentech	217
Roferon-A	Genentech	Hoffman-La Roche	172
Total sales of top ten			4,288
Total industry sales			7,700

Source: *The Economist*. February 25th 1995.

The number of other substances produced by the human body which are potential drugs with good prospects of becoming commercially successful is rapidly increasing. To date 24 biopharmaceuticals are on the market (Werner, 1994) and over 250 new products are in phase I, II or III of clinical trials (Edgington, 1994). Each of these products is likely to have sales in the order of tens or even hundreds of millions of dollars annually when approved (see table 1.2). As more of these products get into the market the importance of chromatography as a powerful purification process will continue to increase.

Process scale liquid chromatography serves three basic industry segments: food chemistry, drug, and biotech product separations. The latter accounts for the largest share of the pharmaceutical market. The process liquid chromatography market has been estimated in 200 million dollars each year (Richards, 1989).

According to the scale of operation, liquid chromatography can be categorised in three functional markets: analytical, preparative and process. The sales for analytical chromatography columns have settled to a growth rate of 8-10 % annually, while sales of preparative and process scale equipment have experienced an annual increase of 15-20 % (Richards, 1989). An exact definition of process and preparative chromatography has not been settled and estimates of the size of the market vary greatly according to the definition.

Column liquid chromatography has proved so far to be economical even for the production of some common drugs, however in the future it will have to compete with other technologies, such as membrane chromatography and expanded bed chromatography, which are already available in the market, continuous chromatography, which is under research, and process scale electrophoresis.

1.1.2 Process perspective.

The production of highly purified biomolecules requires a complex series of operations. Traditionally, these operations are split into those of upstream processing, in particular fermentation, and a series of separation and purification operations commonly referred as downstream processing.

Downstream processing can be divided into four main stages: (1) extraction; (2) initial purification; (3) final purification; and (4) product polishing. Figure 1.1 presents a typical downstream processing sequence for the production of an intracellular product.

An extraction step is employed in the case of intracellular products, and is most frequently carried out by mechanical methods, normally using homogenisation (Bonnerjea et al, 1986), which is based on liquid shear. The removal of cell debris from the extract has traditionally been

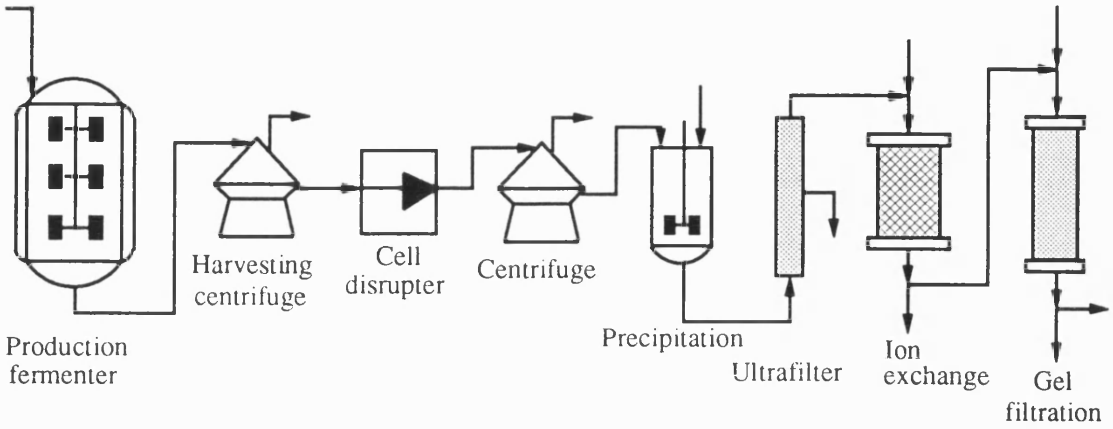

Fig. 1.1 Process flowsheet for the production of an intracellular molecule.

accomplished by centrifugation using large, continuous-flow centrifuges. Cross flow filtration, using either tubular or flat membranes at high shear forces can now be used as an acceptable alternative to centrifugation, and in some cases can give a better clarification of the extract (Scawen et al, 1990).

In the crude, clarified extract the product is very diluted. For this reason the initial steps of purification must be able to concentrate the product. Methods such as two-phase aqueous separation or precipitation can be employed for this step. However, in most cases a more selective step, involving some form of adsorptive chromatography is used, e.g. methods based on ion exchange, hydrophobic or affinity interaction. The final purification step (high resolution stage) will often involve more highly resolving chromatography (Bonnerjea et al, 1986)

The last step, product polishing, is most frequently encountered in the case of therapeutic proteins and often involves the removal of pyrogens or polymeric forms of the product. Pyrogens can be removed by means of anion exchange chromatography, while polymeric forms are removed by gel filtration, which has the added advantage that it can include a buffer-exchange step. Therefore the protocol is very often finished with a gel filtration step (Bonnerjea et al, 1986).

Analysis of the above downstream processing operations, suggests that chromatography is at present the most likely technique to be used for the process purification of high-value products in biotechnology, especially in the high resolution steps. In fact chromatography has become an

integral part of the biotechnology industry. This is due not only to its high separating power, but also to its flexibility, simplicity and efficiency.

A measure of the importance and acceptance of this technology can be seen in new guidelines being developed by the Parenteral Drug Association of Philadelphia, for standards for chromatographically separated drugs, and by the acceptance of liquid chromatography as a drug purification technology by the US Food & Drug Administration (Richards, 1989). In the case of therapeutic agents, these licensing authorities already consider at least one chromatographic step essential for their purification (Jagschies, 1988 and Sofer and Nyström, 1989).

It is therefore expected that the use of chromatography in the biotechnology industry will continue to increase as the new products of the recombinant DNA and hybridoma technologies are accepted and are introduced to the market. New developments will attempt to reach the same levels of purity with fewer more specific chromatographic separations, at higher yield and in a more economical way.

Tied to this trend is the increasing equipment automation and heavier use of instrumentation and monitoring, to simplify the steps involved and to ensure process reproducibility. These key elements, together with the sanitary design are already driving changes in equipment design (McCormick, 1987).

Finally, it should be mentioned that present process-scale chromatography usually involves scaled-up versions of linear elution (volume overloading). This approach suffers from two main disadvantages, poor utilization of the stationary phase and excessive consumption of eluent[1]. Economic analysis of industrial chromatography has shown that solvent costs account for 70% of the total costs (Dwyer, 1984). Nonlinear modes on the other hand require a more careful design but do not suffer these disadvantages, permitting the separation of much higher amounts with far less solvent consumption. It is expected that the development of the theory of nonlinear chromatography and the experience being gained at the preparative level will stimulate the application of nonlinear techniques at the process scale.

1.2 Fundamentals of chromatography.

Chromatography is a very versatile and diverse separation process. Three different modes of operation have been defined, and the number of mechanisms and principles of separation is

[1] The eluent is the solvent, buffer or mobile phase passed through a chromatographic column in order to carry out the separation and elution of the components of a sample.

increasing. Therefore the field of chromatography constitutes not only a single technique but a growing group of techniques. In this section the three modes of operation, and the techniques of interest in the preparative and process scale separation of biomolecules are discussed, as well as the distinctive characteristics between the three different scales of operation: analytical, preparative and process scale chromatography.

Finally, the important properties of biopolymers in relation to their chromatographic separation are discussed.

1.2.1 Definition.

Chromatography is generally defined as a separation process wherein a multicomponent mixture is introduced into a two-phase system, one being stationary, in which the mixture of components have different distribution coefficients and are separated due to their differential migration through the system.

However, in the case of the chromatographic separation of biopolymers, where adsorption is frequently irreversible on chromatographic time scales[2], this definition no longer holds and a new definition, in which the different components are separated due to differences in their residence times within the system, is starting to be introduced (Lee et al, 1988)

1.2.2 Chromatographic modes of operation.

The classical modes of operation as enunciated by Tiselius are elution, displacement and frontal chromatography (Lee et al, 1988). These three modes of chromatography share the same operational features: they are carried out with columns, and require the same sorbents and equipment. Although the three modes can be used at the preparative and process level, most of the processes developed involve elution chromatography, only a few frontal chromatography and none of them, displacement chromatography. According to this, the present work will focus on elution chromatography.

[2] Proteins and other biopolymers adsorbed under strong binding conditions may take hours, days or weeks to desorb spontaneously. Such sorption has been called irreversible on the time scale of chromatographic interest (Lee et al, 1988).

1.2.2.1 Frontal analysis chromatography.

In frontal analysis chromatography , the mixture to be analyzed enters the chromatographic bed continuously at the start. Since the components have different affinities for the stationary phase, they are partially separated as the front of the least adsorbed component breaks through first, followed by a series of mixed fronts. Frontal chromatography is extremely useful for the separation of binary mixtures, when the desired product is lesser retained than the impurities to be removed. In this case, a large amount of feed can be processed and pure product withdrawn until the first impurity breaks through. In multicomponent separations on the other hand, frontal analysis offers an efficient way of loading the column. Here, operation under conditions of strong binding is advantageous, since high loading is achieved and a large fraction of the stationary phase is utilised. This loading method offers the added benefit of recovering a fraction of the least retained component in pure form. The other feed components that are adsorbed during the loading process can be separated subsequently by stepwise or gradient elution or by displacement.
This mode of operation is used in affinity chromatography (see section 1.2.3.5), where the high selectivity of the stationary phase results in a strong and very selective binding of the desired product. The column is first loaded in the frontal analysis mode and only the desired product binds to the stationary phase while the rest of the impurities break through. The loading operation is stopped when the desired product breaks through at a certain predetermined concentration. Then, the column is washed to remove the remaining impurities and the product is obtained by means of an elution step.

1.2.2.2 Elution analysis chromatography.

In elution chromatography a narrow band of the sample is applied to one end of the column and the chromatogram is developed by passing a mobile phase which has lesser affinity for the stationary phase than any component of the feed. The various sample components migrate through the column at different rates and exit at the other end of the column. Two classes may be distinguished on the basis of solvent strength: isocratic elution, where the strength of the eluent entering the column is constant during the chromatographic run, and gradient elution, where the eluent strength is changing continuously. Elution chromatography may be carried out in either the linear or the non-linear ranges of the sample isotherms. Analytical chromatography uses linear elution almost exclusively, but the method is limited to low sample concentrations and therefore the utilisation of the stationary phase is very inefficient. Non-linear elution is better suited to the

demands of preparative separations as higher production rates can be expected.

1.2.2.3 Displacement analysis chromatography.

Displacement chromatography is a preparative technique best suited for the separation of closely related compounds. Its application in large-scale protein separation is yet to be explored. The major problem here is to find suitable macromolecular displacers that are readily available in pure form at a reasonable cost.

In displacement chromatography the sample is injected onto the column either as a narrow band or in the frontal mode, in which case it is partially separated. The migration of zones is achieved by feeding a substance which is called the displacer or desorber after the injection of the sample. The displacer has a higher affinity for the stationary phase than any of the components in the sample. The displacer front drives the sample mixture through the column, eventually forcing all the components to move at its velocity. As a result of the mutual competition for the active sites, the components are separated into adjacent quasirectangular bands, ordered according to their affinity for the stationary phase. At this point the separation is complete and the bands have reached a final pattern, the so called "isotachic" state, after which no further change occurs. Ideally, the process results in a fully developed displacer train so that the feed components are completely separated. In practice, less than complete separation in a single run is realised and subsequent rechromatography of the mixed zones may be required (Lee et al, 1988).

1.2.3 Chromatographic techniques.

Among all the different chromatographic techniques developed and employed at the laboratory level, only some of them have proved so far to be useful in the separation of biomolecules at the preparative and process scale level. Here, the techniques normally used in the biotechnology industry are presented.

1.2.3.1 Size exclusion chromatography.

Size exclusion chromatography also known as gel filtration or gel permeation, can actually be considered as a kind of partition chromatography. The partition of the solute between very similar

mobile and stationary phases is governed by several factors. The predominant one is the so-called molecular sieve effect by which the three-dimensional network in the beads sterically hinders diffusion of the solute into the interior liquid contained within the gel beads. This hindrance is a function of the molecular dimensions of the solute and the density of the network. The degree of hindrance can range from nothing to the total solute exclusion. Totally excluded solute molecules, passing only through the void volume of the gel bed, are eluted first, the other molecules following in increasing order of intraparticle diffusivity. A fractionation on the basis of relative molecular size is thus accomplished.

1.2.3.2 Ion exchange chromatography.

Ion exchange chromatography is the process which involves the reversible exchange of ions between an ion exchange media or material and an ionisable substance or substances in solution. Many biological molecules possess net charge the size and sign being dependent on the solution pH. This property is utilized in ion exchange chromatography for selective adsorption onto a carrier derivatized with charged groups.
Sample constituents bind to the exchanger at low ionic strengths. The strength and selectivity of binding for a given protein are controlled by the initial pH and ionic strength. Bound substances are eluted selectively by increasing the ionic strength or changing the pH.
This technique is well suited for large scale applications because it has a high capacity, is selective, has a concentration effect, and can be used to isolate many proteins in one step (Sofer and Nyström, 1989).

1.2.3.3 Hydrophobic interaction chromatography.

Hydrophobic interaction chromatography is a method by which substances are separated due to the different strengths of the hydrophobic interactions with an uncharged adsorbent media which contains hydrophobic groups. An advantage of hydrophobic interaction chromatography is that it can separate components of similar size and charge on the basis of their differences in hydrophobicity.
Most proteins (not only "hydrophobic" proteins) possess hydrophobic regions on their surface which allow interaction with a hydrophobically derivatized matrix in aqueous surroundings. Phenyl, butyl, and octyl residues are the common ligands used in hydrophobic interaction

chromatography. The hydrophobic properties of phenyl matrices are suitable for purifying most proteins under mild conditions (Jagschies, 1988).
Hydrophobic interaction is affected by the action of specific salts or the polarity of the solvent. Proteins can be adsorbed by a hydrophobic matrix at high salt concentrations, and unbound material washed away. The bound materials are then eluted selectively with an eluent of decreasing polarity in a second step. Decreasing salt gradients are used generally, but further reduction of polarity by addition of non-polar organic solvents may be necessary.

1.2.3.4 Reverse phase chromatography.

Reverse phase chromatography is the most commonly used technique in high performance liquid chromatography (HPLC). Hydrophobic interactions are also utilised in reverse phase chromatography for the separation of components. However, whereas hydrophobic interaction chromatography is a nondenaturing method, proteins are usually denatured by the nonpolar solvents used for elution from the highly hydrophobic reverse phase chromatography matrices. Nevertheless, reverse phase chromatography is the prime method for the analysis of peptides and proteins as well as for peptide purification since it is capable of high resolution and sensitivity. In certain cases, it is also used for the preparative chromatography of proteins (Lee et al, 1988).

1.2.3.5 Affinity chromatography.

One of the most specific methods for isolating and purifying biologically active molecules is affinity chromatography. This process depends on the selective and reversible formation of a complex between the solute to be recovered and a complementary binding substance, most often called the ligand, immobilized on an insoluble support (the adsorbent matrix).Many different types of ligands have found application in affinity chromatography including those exhibiting high specificity toward a particular type of biomolecule (i.e. monoclonal antibodies, protein A, enzyme inhibitors), and group specific ligands exhibiting specificity towards classes of biomolecules (i.e. immobilized metal ions).
Because of the high selectivity of affinity media, very large volumes of dilute product solution can be processed, and the number of processing steps can be significantly reduced. The capacity of the gel is not reduced by the binding of numerous foreign proteins, which occurs with ion-exchange or hydrophobic interaction chromatography. However, affinity chromatography compared

with other techniques is more expensive, has a lower capacity and is more susceptible to fouling (Scawen et al, 1990)

The sample mixture is generally applied to the column at low ionic strength and in the neutral pH range. After nonbound impurities are washed out, the product can be eluted by using a gradient of increasing ionic strength or by reducing the pH.

Purification factors of well over 1000 can be achieved with affinity chromatography, although the mean enrichment obtained in practice is only 100-fold (Jagschies, 1988). Higher values can often be obtained with only relatively impure samples.

1.2.4 Analytical, preparative and process scale chromatography.

This section is intended to establish the characteristics that make analytical, preparative and process chromatography different from each other, as well as the relation between each other within a industrial separation process.

Analytical chromatography is classically carried out in order to obtain information regarding the composition of a mixture. The separated components of the mixture are not collected to a specific degree of purity. Although chromatography separates the components of the analyzed mixture, providing pure components diluted in the mobile phase, once the components are identified and quantified, the eluent and the separated solutes are considered as waste. Thus, the cost of separation is measured in terms of the amount of money spend per analysis or per piece of information, not in terms of the amount of money required for the production of product prepared. Analytical chromatography is used because is fast, powerful, convenient and flexible but not because it prepares pure compounds.

Preparative chromatography on the other hand is carried out for the purpose of isolating purified chemical substances. For this reason preparative separations are best carried out at the highest concentrations at which good separation is achieved in order to increase throughput and enhance the utilization of the stationary phase. The operating conditions differ considerably from the experimental conditions used with analytical chromatography, since the assumptions are different, and the process is operated by the biochemical engineer rather than the chromatographer who works in the laboratory.

Some researchers have considered preparative chromatography and process chromatography as being virtually the same (Guiochon and Katti, 1987), however others (Knox and Pyper, 1986) have made a distinction. Knox and Pyper (1986) have considered the purpose of preparative chromatography to be solely the isolation and purification of chemical compounds while they have

defined process or production chromatography as liquid chromatography carried out for the purpose of commercial production. In this case the purified compounds obtained are prepared for sale and the cost of production becomes important. Maximum production per unit time must be achieved in order to save on investment and running cost. In this way process chromatography is distinguished from preparative chromatography in that the cost element becomes important. They have also differentiated them by their scale. They considered the scale of preparative chromatography to be normally larger than analytical chromatography, but ranging from micrograms to grams per run, while the scale of process chromatography will normally be within the range of milligrams to kilograms per run.

In relation to the operating conditions, the equipment and media used, there are some important differences that must be pointed out. Analytical chromatography is often synonymous with high-pressure or high performance liquid chromatography, while process chromatography is usually thought of as low-pressure chromatography[3]. Chromatographic media used for analytical separations are often not suitable for production because they can suffer from low capacity and high per gram cost[4] . Also analytical methods may be harsh, utilising partially or fully denaturing conditions that may destroy the biological activity. In contrast, manufacturing procedures rely on mild conditions that separate molecules based on surface differences, using soft gels which are more likely to preserve biological activity (Builder and Hancock, 1988). Thus, these characteristics of the chromatographic sub-groups make each less appropriate for the other's function and allow a clear distinction between the operating conditions, equipment and packings used at the analytical scale and those used at the process scale level.

Finally it must be mentioned that analytical chromatography plays an important role within the industrial production processes, where there is a need for rapid, sensitive and convenient analytical techniques to monitor biosynthetic and separation processes and to measure product purity in quality control. In this respect, analytical chromatography is already used for on-line analysis of the column effluent in process scale chromatography, to check the product quality in a given purification scheme and has been used to aid the recovery process by providing data that can result in a more controlled fermentation process (Builder and Hancock, 1988). Future developments in analytical chromatography aim at reducing the time for routine analysis, to fulfil regulatory

[3] This situation is starting to change due to new developments in column and packing technologies (Colin et al, 1990) and although reports on commercial production are scarce, many pharmaceutical companies are already using large-scale HPLC (Kroeff et al, 1989), or are studying this possibility.

[4] This has resulted in the need to develop packing materials with preparative and process scale applications in mind. A recent example of these developments is perfusion chromatography (Afeyan et al, 1990).

requirements and to meet production schedules (Lee et al, 1988). Furthermore with present trends in reducing the time for protein separations, analytical chromatography is expected to find increasing use in "on-line", and "off-line" process monitoring.

1.2.5 Chromatography of biopolymers.

The fact that proteins vary in molecular weight, hydrophobicity, isoelectric point, and thermal and chemical stability and reactivity, makes a generally applicable approach to their chromatographic separation impossible (Verzele, 1990). At the same time, due to these properties, biopolymers present a rather complicated and unusual adsorption behaviour. In the first instance, biopolymers can exhibit slow binding kinetics, and in this case equilibrium is not reached under experimental conditions.

Biopolymers have a complex three-dimensional structure which can deform upon accommodation at the surface of the stationary phase. Its conformation and orientation on the adsorbent surface depend not only on the operating conditions, but also on the concentration of the various adsorbates, including itself, on the stationary phase. Interactions between the biopolymer molecules may occur, either at the surface or in solution, and can drastically affect the sorption behaviour. If a relatively large number of free binding sites is available, the adsorbed biopolymer is likely to bind at several points on the stationary phase. However, if many other molecules are already adsorbed onto the stationary phase, the biopolymer may bind at fewer sites. In this case the tendency to suffer a conformational change as a consequence of multipoint adsorption could be less than when there is a greater number of binding sites available to each feed molecule. This could lead to the conclusion that under certain conditions, biopolymers might suffer less conformational change in preparative (overloaded) than in analytical chromatography (Lee et al, 1988).

The fact that biopolymer molecules can bind to several points on the stationary phase makes this interaction very strong, so strong that on the time scale of chromatographic interest, the sorption of biomolecules can be considered irreversible. For this reason, biopolymers cannot be chromatographed using isocratic conditions (Verzele, 1990) as can small and medium molecular weight compounds. Instead, size exclusion chromatography, in which there is no adsorption, or various forms of gradient liquid chromatography must be used. Such gradients include solvent gradients, in which the solvent composition eventually becomes sufficiently strong as to desorb the protein; buffer gradients; pH gradients; or salt concentration gradients, as in hydrophobic interaction chromatography.

Desorption of proteins from the stationary phase can also be promoted by addition of solvents or acids that modify the protein's conformation, such as trifluoroacetic acid, isopropyl alcohol, or acetonitrile. However, this can sometimes cause denaturation of sensitive proteins. Although the weight recovery of the protein mass injected onto the liquid chromatography system is important, the possible loss of biological activity of enzymes is most critical.

1.3 Description of chromatographic performance.

Since chromatography first appeared as a separation tool several concepts and parameters have been introduced to describe the chromatographic peak, the band spreading associated with it and the power of separation of a chromatographic process. Equations have been derived to relate these parameters with the operating conditions and column characteristics.
Chromatographic models have also been developed to describe and to predict the chromatographic peaks resulting from a particular separation.
In this section a review of some of the main concepts used to describe the chromatographic performance is made.

1.3.1 Concept of theoretical plate and efficiency.

The model of the theoretical plate was introduced into chromatography by Martin and Synge (1941). In this concept, the chromatographic column is considered to be composed of a series of hypothetical layers or plates (perpendicular to the direction of zone migration) in which the solute concentrations in the participating phases are assumed to be in equilibrium. The chromatographic column is thus comparable with a series of mixing vessels the length of each being identical with the thickness of the above layers. This thickness represents in the plate theory, one height equivalent to a theoretical plate, HETP or H.
The HETP can be expressed by the relationship

$$H = \frac{\sigma_L^2}{Rut_R} = \frac{\sigma_L^2}{L} \qquad (1.1)$$

where R is the retardation factor, t_R is the retention time for a particular component, u the fluid interstitial velocity, σ_L is the elution peak standard deviation measured in column length units and L is the bed length (see Giddings, 1965, for full explanation of the meaning of R). From the above

equation it can be seen that, the smaller the value of H, the smaller is the chromatographic band spreading per unit length of column, and the more efficient is the column. As a consequence H is often used as a measure of column efficiency.

In some instances, it may be more appropriate to express the standard deviation in time or volume units, as

$$\sigma_L = \sigma_t Ru = \frac{\sigma_V Ru}{Q} \tag{1.2}$$

where Q is the volumetric flow rate of the mobile phase. The plate height can also be expressed as

$$H = \frac{\sigma_t^2 Ru}{t_R} = \frac{\sigma_V^2 Ru}{V_R Q} \tag{1.3}$$

where V_R is the retention volume.

The number of theoretical plates, N, is given by

$$N = \frac{L}{H} \tag{1.4}$$

The quantity N is proportional to column length L , so that if the operating conditions are kept constant, an increase in column length results in an increase in N.

Since,

$$L = Rut_R = \frac{RuV_R}{Q} \tag{1.5}$$

N can be calculated from the following equations:

$$N = \left(\frac{L}{\sigma_L}\right)^2 = \left(\frac{t_R}{\sigma_t}\right)^2 = \left(\frac{V_R}{\sigma_V}\right)^2 \tag{1.6}$$

If the value of N is high, then the relative band spreading should be small and the column more efficient. The value of N is approximately constant for different bands in a chromatogram, for a given set of operating conditions (a particular column and mobile phase, with mobile-phase velocity and temperature constant). Therefore, N is a useful measure of column efficiency: the relative ability of a given column to provide narrow bands and improved separations.

1.3.2 Dynamics of zone spreading.

When a sample zone travels along a chromatographic column the width of the zone continuously increases owing to a multitude of different mechanisms collectively known as dispersion processes. The separation obtained from the different velocities of sample components is counteracted by dispersion, which tends to decrease the resolution of these compounds.
The dispersion processes occurring in any chromatographic process have been divided according to the originating causes into: i) chromatographic band broadening or dispersion and ii) extracolumn band broadening. The former relates to the dispersion that occurs within the column and the latter to that occurring due to processes outside the column.

1.3.2.1 Chromatographic band broadening.

In a pioneering work of utmost importance Van Deemter and his co-workers (1956) derived the now famous Van Deemter equation for packed columns, relating the efficiency of separation (band spreading) to various physical and operating parameters in chromatography. The development of this equation was based on the rate theory, previously developed by Van Deemter for gas chromatography.
The increasing variance of a band during migration, as first shown by Van Deemter et al (1956) for gas chromatography, arises from three kinetic or dynamic processes, which occur independently within the column. These include axial molecular diffusion along the column, resistance to mass transfer between and within phases, and the influence of various flow inequalities and disturbances. Because these three dispersive processes are both independent and random, the variances produced by them (i.e. the σ_z^2) are added to give the total variance produced by the three together. Accordingly the total plate height, H, is made up as a sum of contributions from the three processes, that is,

$$H = H_{diff} + H_{flow} + H_{masstransfer} \qquad (1.7)$$

Each of these contributions is now discussed along with its dependence upon flow velocity.
In a packed bed the path of the mobile phase through the interstitial space between the solid particles is neither straight nor uniform, but tortuous and random. Thus, some molecules of the mobile phase may have a shorter path than others and move ahead of the average or the maximum concentration profile while those with longer paths fall behind. This phenomenon results in spreading of the molecules. This kind of dispersion was recognized by Van Deemter and was

called "eddy diffusion". Band broadening due to this multipath process is proportional to the support-particle diameter and to the non-uniformity of the packing and gives a plate height contribution independent of fluid velocity,

$$H_{flow} = 2\lambda d_p = A_o \tag{1.8}$$

where 2λ is the geometrical constant and a measure of the packing non-uniformity in the column. Giddings (1965) pointed out that molecules would also diffuse across the streamlines and would, in reality, sample randomly-varying velocities more frequently than if they remain fixed to the streamlines. Due to this, the dispersion in a real system is less than in a hypothetical one in which the molecules are imagined to be fixed to the streamlines. The more times the solute molecules can sample streamlines in their passage down the column the less will be the dispersion arising from flow inequalities. In fact the dispersion arising from flow inequalities and disturbances shows a weak positive dependence upon velocity. Although no theory accurately describes this dispersion mechanism, experiments (Knox, 1982) show it to be given to a good approximation by,

$$H_{flow} = A' u^{1/3} \tag{1.9}$$

or in a reduced form by,

$$h = \frac{H}{d_p} = A\nu^{1/3} \tag{1.10}$$

where A'and A are constants which are thought to increase slightly with the capacity factor k', although this is not well established (Knox, 1982), and ν is the reduced velocity which is defined as follows:

$$\nu = \frac{u d_p}{D_m} \tag{1.11}$$

where D_m is the diffusivity of the solute in the mobile phase. The reduced velocity represents the ratio of the rate of flow over a particle (u/d_p) to the rate of diffusion over a particle(D_m/d_p^2).

In practice, values of A chiefly reflect how well a column is packed. Well packed columns have an A value of between 0.5 and 1, while poorly packed columns have larger values, usually ranging between 2 and 5.

The second process that is responsible for band broadening is that of longitudinal diffusion.

Whether the mobile phase in the column is moving or at rest the solute molecules tend to diffuse randomly in all directions until there is no concentration gradient. In practice, however, complete and uniform distribution of the solute molecules throughout the mobile phase in the column does not occur because the mobile phase is flowing continuously in a certain direction and because the time spent by a solute in the mobile phase is limited. Thus, the broadening due to this effect is directly proportional to the interstitial tortuosity and to the diffusivity of the solute in the mobile and stationary phases and is inversely proportional to the mobile phase linear velocity,

$$H_{diff} = \frac{2\gamma D_m + 2\gamma_s D_s k'}{u} = \frac{B_o}{u} \qquad (1.12)$$

where D_s, is the solute diffusivity in the stationary phase, k' is the capacity factor, γ and γ_s are the obstruction factors, whose value may be between 0.5 and 1.0 depending on the packing (Van Deemter et al, 1956), normally $\approx$ 0.6.

The contribution to band broadening by longitudinal diffusion can also be expressed in a reduced form as follows,

$$h_{diff} = (2\gamma + 2\gamma_s k' \frac{D_s}{D_m})(\frac{1}{\nu}) = \frac{B}{\nu} \qquad (1.13)$$

B is generally taken to be about 2, but it must vary with k', and this variation should be taken into account in precise calculations. A better approximation for B would be (Knox, 1982)

$$B \sim 1+k' \qquad (1.14)$$

The other major factor that contributes to band broadening relates to the resistance to mass transfer. In a two-phase system, the transfer of a solute from one phase to another is not instantaneous because the solute molecules take a finite amount of time to traverse from the bulk of one phase to the interface and then to enter the other phase. As one phase is continuously moving the solute molecules will also move a certain distance in the mobile phase during this time and equilibrium does not occur.

With porous column-packing particles, the mobile phase within the pores is stagnant (not in the case of perfusion chromatography, (Afeyan et al, 1990). Sample molecules move in and out of these pores by diffusion. Those molecules that happen to diffuse a short distance into the pore and then diffuse out, return to the mobile phase quickly, and move a certain distance down the column, while those molecules that diffuse further into the pore spend more time in the stationary phase and less time in the external mobile phase. These molecules move a shorter distance down the column. This results in an increase in molecular spreading.

After molecules diffuse into a pore, they penetrate the stationary phase or become attached to it in some fashion. If a molecule remains attached to the stationary phase longer than other molecules it spends a shorter time in the mobile phase and travels a shorter distance along the column. Again this produces band spreading.

Rigorous theoretical treatment of the dispersion due to mass transfer in the stationary phase, given by Giddings (1965), shows that this contribution to plate height is,

$$H_{mass\ transfer} = \frac{R(1-R)d_p^2}{30\gamma_s D_m}u = C_o u \qquad (1.15)$$

where R is the retardation factor representing the ratio of solute zone velocity to mobile phase velocity. In a reduced form this contribution is represented by

$$h_{masstransfer} = q\frac{k'}{(1+k')^2}\frac{D_m}{D_s}\nu = C\nu \qquad (1.16)$$

where

$$k' = \frac{1-R}{R} \qquad (1.17)$$

and q is a configurational factor reflecting the particle shape and its internal pore structure. For spherical particles q = 1/30 (Knox, 1982).
In practice C is often found to be in the range 0.05-0.2 (Knox, 1982).

The total plate height obtained by adding together the contributions from the three independent dispersion processes, is then

$$H = A_o + \frac{B_o}{u} + C_o u \qquad (1.18)$$

this is the so-called Van Deemter equation. It represents a landmark in the development of the theory of chromatography. Its importance stems from the fact that it inter-relates the physical parameters within the column that contribute to band broadening and thus the efficiency of the column.
The reduced form of the equation was proposed by Knox (1977) and is now called the Knox equation,

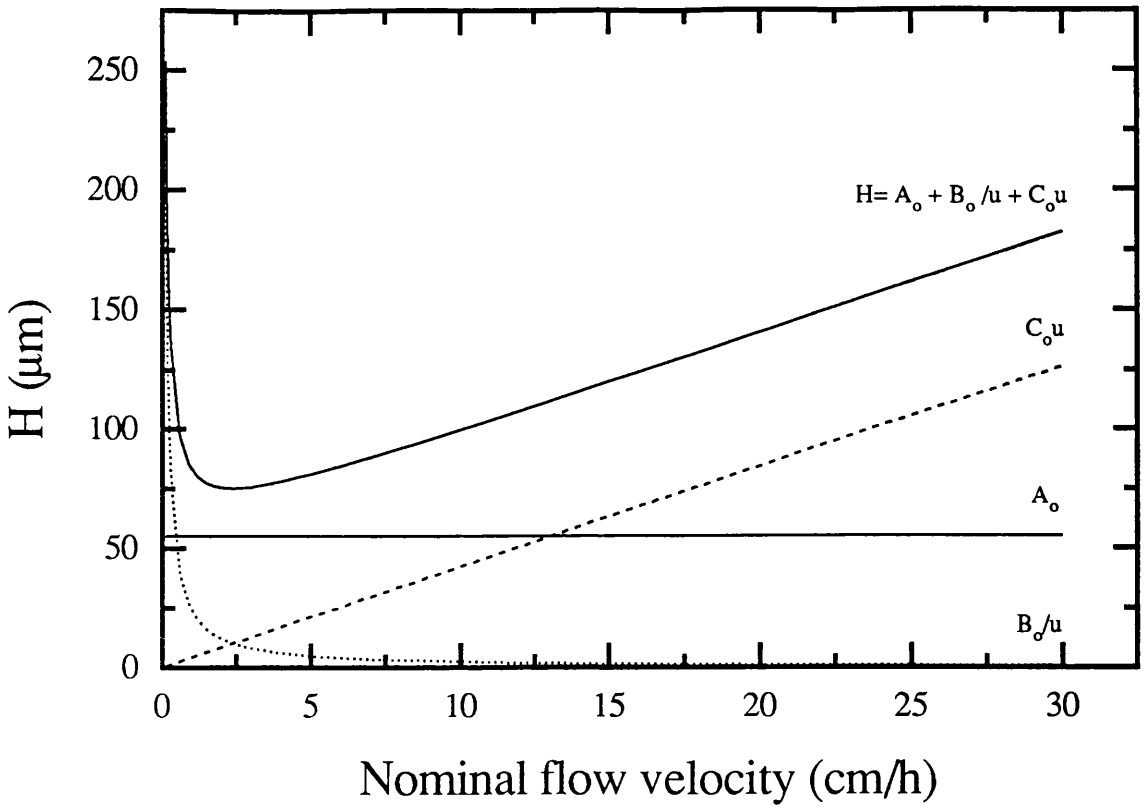

Fig. 1.2 Zone broadening as measured by plate height H, for large solutes in size exclusion chromatography. A_0, B_0 and C_0 are the terms of the Van Deemter (1956) equation. A_0= 55 μm, B_0= 200 $\mu m^2/s$ and C_0= 0.5 s.

$$h = Av^{1/3} + \frac{B}{v} + Cv \qquad \textbf{(1.19)}$$

The main advantage of expressing the plate height in terms of reduced parameters is that data obtained with different particle sizes and different mobile phases can be directly compared.

A typical plot of the Van Deemter equation for large molecules can be seen in Fig. 1.2. It can be observed that for large molecules the contribution of longitudinal diffusion is negligible. This is a consequence of the low diffusion coefficients of large molecules.

As already mentioned, the efficiency of a column is related to its number of theoretical plates. Small values of H or h mean large number of theoretical plates and more efficient columns. A central goal in liquid chromatography practice is the attainment of small H values for a maximum N and highest column efficiency. From the preceding equations it can be seen that H or h can be reduced by reducing the values of the terms A, B and C. And for a given set of A, B and C values the plate height can be minimized by selecting an appropriate value of the mobile phase velocity, u. From the latter equation it can be shown that the reduced plate height shows a minimum value around the range 2-3 at a reduced velocity in the range 3-5.

Apart from the Van Deemter (1956) and the Knox (1977) equations, several other plate height

equations have been derived starting from slightly different assumptions, but a recent review of the various equations shows that the Van Deemter equation (1956) is presently the most accurate one for describing zone broadening in size exclusion chromatography (Katz et al, 1983).
In general small H or h can be obtained by using a small particle size and a narrow size distribution, stationary and mobile phases of high diffusivity, minimum stationary phase thickness and mobile phase velocity near or slightly above the optimal value of u as determined by the Van Deemter plot for a particular system.

1.3.2.2 Extracolumn band broadening.

In addition to the band broadening produced in the column as a result of the phenomena discussed above, the various instrumental parts of the chromatograph also contribute to band broadening. Their relative contribution to band broadening increases with increasing efficiency of the column. The chromatograph contributes to reduce the apparent column efficiency mainly through the dispersion occurring in the injection system, the connection between injection port and column and between the column and the detector, and the detector cell volume. The detector time response should also be considered.
The total variance of a Gaussian peak is given as an additive function of the various contributions:

$$\sigma_T^2 = \sigma_{col}^2 + \sigma_{inj}^2 + \sigma_{conn}^2 + \sigma_{det}^2 \qquad \textbf{(1.20)}$$

where the subscripts of the different terms refer to the column, injection port, connecting tubes and the detector respectively.
The band broadening due to the injection is a function of three variables, namely injector design, sample volume, and injection profile (Ravindranath, 1989), while the contributions due to the connecting tubes, are highly dependent on their length and radius. The connecting tubes should be as short and narrow as possible (Martin et al, 1975). Finally in the case of the detector, its flow properties (resulting from the shape of the flow cell), its volume and the response time can all contribute to band broadening (Martin et al, 1975). If the cell volume is less than 10% of the peak volume, the variance arising from this source is insignificant (Ravindranath, 1989).
The value of the total variance, σ^2_T, is governed by the main contributor to bandspreading and is only marginally affected by the other contributory variances.

1.3.3 Chromatographic resolution.

The resolution R_s is a measure of the separation of the elution peaks, and is defined as the ratio of the distance between the peak maxima, to the mean band width of the two neighbouring peaks. This is expressed for peaks 1 and 2 as,

$$R_s = \frac{2(t_{R_2} - t_{R_1})}{(w_2 + w_1)} \qquad (1.21)$$

where t_R is the retention time, and w is the peak width at baseline. For a Gaussian peak $w=4\sigma_t$, and the above equation can also be expressed as,

$$R_s = \frac{(t_{R_2} - t_{R_1})}{2(\sigma_{t_2} + \sigma_{t_1})} \qquad (1.22)$$

Resolution can be related to selectivity α, retention k', and efficiency N, through the following equation

$$R_s = \frac{1}{4}\frac{(\alpha - 1)}{\alpha}\sqrt{N}\,\frac{k'}{(1+k')} \qquad (1.23)$$

This is a fundamental equation which allows resolution to be controlled by varying α, N and k'. Separation selectivity as measured by α is varied by changing the composition of the mobile phase and/or stationary phases. Separation efficiency as measured by N is varied by changing the column length or solvent velocity (or by switching to a different column packing). Finally retention as measured by k', the capacity factor, is varied by changing solvent strength (the ability of the mobile phase to provide large or small k' values for a given sample).

1.4 Hydrodynamics of chromatographic columns.

One of the basic processes determining the separation performance of column-based chromatography is the convective transport of solute along the column. The hydrodynamic behaviour of the column is therefore of great importance. This behaviour is highly dependent on the properties of the packing materials, the packing procedure and column dimensions. Characteristics such as particle shape, particle size distribution and rigidity significantly determine

the structure of a packed bed. Inhomogeneities related to the presence of the column walls also affect the solute transport and column performance. In this section these phenomena are treated in relation to their impact in preparative and process scale chromatography. Hydrodynamic models for compressible beds used in the determination of important design parameters, such as pressure drop and column dimensions are also reviewed.

1.4.1 Chromatographic matrices.

The matrix is the most important part of any column chromatographic system, since it is the differential interactions with this stationary phase and the mobile phase that cause the separation of the sample components.
In this section the most important characteristics of the matrices used for process scale chromatography will be discussed in relation with the implications for process performance.

According to Clonis (1987) and Cooney (1984) an ideal matrix for large-scale chromatography should have the following properties:

a) Insoluble and chemically stable- to withstand harsh cleansing agents and derivatization chemistry for ligand coupling.
b) Hydrophillic and inert- to minimize non-specific adsorption.
c) Highly porous and permeable- so the biomolecules can freely penetrate the matrix particles interior.
d) Rigid- to resist compression at high flow rates.
e) Derivatizable- possessing an adequate number of functional groups.
f) Available in beaded form- for good flow characteristics.
g) Inexpensive and reusable.
h) Resistant to microbial degradation.

Apart from the above mentioned charateristics particle size and particle size distribution are also of great importance. The use of small particles in chromatography is advantageous. The smaller the bead diameter, the larger the interfacial surface area and the shorter the time required for a molecule to diffuse and reach the interior of the bead. Consequently, the efficiency of the adsorption-desorption step is improved by reducing the particle diameter. At the same time, however, the pressure drop and the compressive forces on the matrix increase, as these are inversely proportional to the matrix particle diameter.

The average particle diameter of packings in preparative and process chromatography ranges from 20 to 200 μm. Packings with average particle diameter between 40 and 60 μm provide a good compromise between column pressure drop, plate number and analysis time (Unger and Janzen, 1986).

A narrow particle size distribution is also required for the generation of stable and efficient columns. A particle size distribution with a d_{p90}/d_{p10}[5] ratio of 1.5-2.0 of the cumulative distribution is adequate (Unger-Janzen 1986).

Beaded packings of uniform shape, rather than fibrous or irregular supports, are preferred in order to achieve a highly dense and stable bed, with improved flow and packing characteristics.

In the case of protein separations the pore size of the packing material affects the recovery of the protein from the column. The main concern is to achieve a surface that is fully accessible to the solute. This consideration has led to the development of the so-called wide-pore supports for the separation of biopolymers. Stationary phases with considerably large pore sizes (30-100 nm) are used to avoid irreversible retention of proteins in the small pores of conventional packing materials, and therefore a loss in recovery. Another advantage of using large pore diameters is the increased diffusivity of the solute molecules. The pore size distribution of most stationary phases is adequate for most needs, however, even large-pore stationary phases have some small pores, so there is always the possibility of some protein being retained within the column. Pores smaller than 4 nm should be absent, to avoid slow kinetics, slow regeneration and fouling (Unger and Janzen, 1986).

Other important matrix characteristics that should be considered in preparative or process scale chromatography are non-specific adsorption and the formation of fines. These two characteristics are responsible for fouling. Fouling of the support surface might take place through preferential adsorption or reaction of active components of the sample mixture. Also colloidal fines or particulates from hydrolisates might be deposited in the pores between the interstices of the packing particles, mainly at the column top, and cause significant changes in column permeability. Fines generation is associated with the brittleness of the matrix and also with fibrous or irregular granular forms. Therefore it is preferable to use matrices that are spherical (to avoid abrasion that causes fines), rigid and strong, perhaps with a small degree of elasticity (Cooney, 1984).

The matrix must also be highly resistant to microbial degradation, the addition of antimicrobial agents (sanitization) and the harsh cleansing (regeneration) conditions to which it is subjected. The main concern is the chemical stability of the matrix, but this must include substituted groups such

[5] The parameters d_{p90} and d_{p10} represent respectively the particle diameter d_p below which 90% and 10% of the particles in the distribution are found according to their size, this is that 90% or 10 % of the particles in the distribution are smaller than d_{p90} or d_{p10}.

as ligands, spacer arms, and ionic or hydrophobic groups, in the range of conditions that the matrix will be subjected to. This is of particular importance in the production of pharmaceutical products, since any products that may be released from the matrix from chemical degradation or autoclaving could find their way into the final product, unless they are removed during the remaining process steps.

Packings for use in large-scale chromatography should be available at an economical price. The price is determined by the particle shape, the particle size and size distribution, the degree of purity, the extent of surface modification, etc. Spherical particles are more expensive than irregular particles, while with decreasing average particle size, size classification processes are increasingly reflected by higher cost. Narrow cuts are more difficult to produce than those with a broad size distribution and this is also reflected in the cost. Chemical bonding of adsorbents and supports raises their price. Specific bonding reagents, such as for the synthesis of chiral and affinity packings, further increase the price. In such an analysis it must be borne in mind that in the case of process chromatography media cost is not simply a measure of the purchase price, but is related to the amount of support consumed per unit product produced. Therefore it is determined by the lifetime, capacity, and efficiency of the packing. The working life of a support depends on the physical and chemical properties already mentioned, and the quality of the sample and the buffer solutions.

Most protein separations are performed on soft gels derived primarily from polysaccharides (Janson and Jönsson, 1989; Verzele, 1990). Although these soft gels do not have the efficiency of silica gel-based small-particle stationary phases, they are hydrophilic, and appear to be more inert than the pore surfaces of rigid macroporous matrices, reducing in this way the degree of non-specific adsorption (Dawkins, 1990). However, their lack of rigidity has posed serious problems in the design, operation and scale up of chromatographic processes and has resulted in the design of composite matrices. These composites are obtained either by encapsulating a soft gel in a macroporous, inert and rigid matrix, i.e. Macrosorb KAX (Sterling Organics), or by introducing microporous gel forming polymers into the pores of macroreticular gels, i.e. Sephacryl (Pharmacia). These matrices combine the hydrodynamic advantages of a more rigid structure, with the biological advantages of the gels, hydrophillicity and low non-specific adsorption.

Improved cross-linked gels have also been developed, i.e. Sepharose CL and Fast Flow Sepharose (Pharmacia), as well as entirely synthetic polymeric matrices, i.e. Trisacryl (IBF), Toyopearl (Toyo Soda), Fractogel TSK (Merck), etc. They all present higher mechanical strength than traditional gels and possess suitable characteristics for protein separation. However, they are not as rigid as inorganic supports, and have retained some degree of compressibility (Goward et al, 1989).

On the other hand, truly inorganic materials, based on silica, although ideal in terms of rigidity,

have found relatively few applications for the large-scale isolation of proteins. This is due to its denaturing effects, high non-specific adsorption (Scawen et al, 1990) and its instability at alkaline pH (Janson and Jönsson, 1989). It appears that silica-base matrices will probably not be useful overall in industrial-scale purification of proteins (Clonis, 1987).

It is apparent that the mechanical strength of a matrix, its particle size and its particle size distribution have the greatest influence over the hydrodynamic properties of a packed bed. The economics of process-scale operations, which require the throughput to be maximised by employing a high flow rate, are therefore strongly affected by these matrix properties.

1.4.2 Studies related to bed compression.

The study of compression in packed beds is relevant not only to the field of chromatography but also to the fields of dead-end filtration and cell/enzyme immobilisation.

As cake filtration is an important and widely used solid-liquid separation process, it has been studied extensively in the past beginning with the classical work of Ruth et al (1933). Wakeman (1978) attempted an analysis of the formation and growth of compressible filter cakes based on the principles of continuity, Darcy's Law and the knowledge of porosity (or solidosity profile of the cake). Other workers, in particular Tiller (1975), have extended the scope of the theory of filtration. However, in dead-end filtration cakes are of increasing length due to the inherent characteristics of the filtration process, therefore theoretical and empirical analysis are not directly transposable to column-based chromatography.

In immobilised cell/enzyme technology, the use of packed bed reactors and soft supports is quite common. The hydrodynamics of this type of reactors therefore resembles that of the compressible chromatographic beds.

Various studies on bed compression have been carried out in the area of immobilised enzyme beds. Klein et al (1979) tested the mechanical stability of polymeric catalyst-beads by means of two measuring apparatus, the "Duromater" and the "Pfizer Hardness Tester". They found that the compression behaviour of single catalyst particles obtained from polymer entrapment of whole cells was a function of the nature of the polymeric carrier, the amount of cell loading and particle size. They also carried out hydrodynamic studies of packed beds with different packing materials and different particle sizes, and concluded that if the particle size was small then the turbulent flow region is never reached in practice and any deviation from linearity of the Δp vs u curve indicates directly deformation and compression of the packed bed.

Norsker et al (1979) developed an apparatus to measure the permeability of glucose isomerase

beds, as a function of applied pressure. This information was used in Darcy's equation to predict the pressure drop of pilot scale beds. In their analysis they considered the effect of time on the permeability and pressure drop of these immobilised enzyme beds.

In order to avoid compaction of soft immobilized cell beds, Furui and Yamashita (1985) developed a column equipped with a horizontal baffle. They found the pressure drop of this column to be smaller than that of a non-modified one.

In the field of chromatography similar approaches to reduce bed compaction have been previously followed. Sachs and Painter (1972) used glass beads as an internal support with Sephadex columns, to enable the gel to withstand much greater operating pressures without being compressed. This approach, however, has been abandoned due to the inherent loss in resolution. The mechanical properties of single chromatographic beads have been studied by Golden and Irving (1972) and Andrei et al (1994). The effect of mechanical forces on ion-exchange resins (250-300 μm) treated and non-treated with acid/alkali solutions was approached by Golden and Irving (1972). They found that non-treated resin beads break under forces of 3-6 N, while treated beads will only withstand forces of 1 N or less. Andrei et al (1994) studied the micro-compression of single Sephadex beads (20-400 mμ) and found the elastic modulus of this material to be in the order of 10^5 Pa.

Various researchers have studied the effects of compression on column efficiency and resolution. Experimenting with cross-linked Sephadex gels, Edwards and Helft (1970) found that resolution doubled when compressing a bed to about 75% of its freely settled volume. The interparticle volume was halved, while the intraparticle volume was reduced only by about 5% as a result of the compression. They believed that reduced channelling produced by compression was the reason for the decrease in the plate height.

In a similar experiment Fishman and Barford (1970) found the resolution of a Sepharose 6B column to improve as it was increasingly compressed.

Hjertén et al (1988) and Liao et al (1988) have shown that columns of compressed, cross-linked, non-porous agarose beads for ion-exchange and hydrophobic interaction chromatography permit high flow rates at relatively low pressures, and that resolution is virtually independent of flow rate (at constant gradient volume), even at extremely high flow-rates and for large bead diameters. They explained the high resolution obtained as being a consequence of the deformation of the compressed beads, resulting in a decrease in the average distance between them which, in combination with the lack of permeability for proteins, has a favourable effect on the partition rate of solutes between the beads. Hjertén et al (1991) has also suggested the occurrence of flow patterns which favour rapid transport between the mobile and the stationary phases, as a

consequence of bed compression.

Horváth (1990) carried out experiments utilising gigaporous supports (20 μm beads, pore size 4000-5000 Å). He packed columns with the same support but at different pressures and found that the higher the packing pressure the smaller the plate height obtained. He also compared the performance of column packed at high pressure (precompressed) and that of columns being compressed by increasing the eluent flow rate (with and without bed height adjustment). Improved performance of the precompressed bed was observed. This was attributed to a reduction in interstitial volume and channel diameter, resulting in a reduction of the interparticular diffusion resistances. The increase in the relative magnitude of the transparticular flow was thought to also contribute to the improved performance. In all cases the existence of a maximum flow rate was observed, at which efficiency rapidly decreased as a result of the destruction of the bed structure.

The processes involved in compressible beds from the bulk solid mechanics point of view have been discussed by Johanson (1979). His qualitative discussion was based on the analysis of equilibrium forces acting on an element of solid containing a moving fluid, and solid and fluid flow rule equations. He pointed out that bed permeability will depend upon the solids contact pressure, fluid flow rate and the compressibility of the particles, and discusses the development of large pressure drops near the bottom of compressible packed beds.

Levison et al (1991) studied the influence of bed height adjustment (packing density) on the flow performance of a process-scale axial flow column packed with the ion-exchanger Whatman DE52. They found that the linear flow rate/pressure drop relationship was significantly influenced by overcompression.

Employing the technology of dynamic axial compression, Colin, et al (1990) studied the effect of compression pressure on column efficiency using rigid particles of different sizes and shapes. They found that there is a minimum pressure above which the compression pressure has no effect on column efficiency, corresponding to the required pressure to overcome the friction forces of the seals on the column walls. They pointed out that there is also a maximum at which column efficiency deteriorates, this is probably as a result of destruction of the particles under high mechanical stress.

A few studies have been carried out in order to compare the properties of soft packings with those of incompressible composite packings. Goward, et al. (1989) compared Macrosorb KAX-CM, an incompressible kieselguhr-agarose composite, with a conventional agarose gel, CM-Sepharose Fast Flow, for the large scale purification of L-asparginase from *Erwinia chrysanthemi*. They found that although Macrosorb KAX-CM had better pressure/flow characteristics and the matrices were identical on criteria of purity, the protein was eluted from CM-Sepharose in a smaller volume.

Wall effects are important in liquid chromatography because they influence the ease of packing,

column efficiency, and column hydrodynamics and life expectancy. Verzele et al (1989) have divided the wall effects into three different types: the direct wall effect, the bridging effect and the thermal wall effect. In the case of compressible packings the direct wall effect is of greater importance. In this effect the walls of the container hold the packing in position as a result of direct interaction with the packing material. It is mainly due to friction forces, however it could also be expected as the result of physico-chemical interactions such as hydrogen bonding, dipolar, or van der Waals forces. Consequently small bore columns are more stable than large preparative columns because the wall holds the packing in position better than in wider preparative columns. The distance along the column diameter to which this wall effect extends has not been thoroughly studied and therefore has not been clearly defined. Some researchers have suggested that this effect extends to 10 particle diameters away from the column wall, and have considered that it can be neglected for column diameters greater than 5 centimetres (Janson and Hedman, 1982). Others consider that columns with a length between 20 and 40 cm are stable only when their internal diameter is less than 2-5 cm (Colin et al, 1990).

1.4.3 Hydrodynamic models for porous materials.

Chromatographic separation depends on both diffusion and flow through porous media. There is a requirement to achieve plug flow, fast solute transport and high flow rates, in order to obtain good resolution and high productivity. The study of the flow of fluids through porous materials is therefore of great importance in chromatography. Some of the most relevant models describing fluid flow through porous media are presented in this section.

1.4.3.1 Darcy's Law.

Stokes and Navier were the first to formulate the general force-acceleration equations for fluids over a century ago (Giddings, 1965). However, in practice the Navier-Stokes equation has been found extremely intractable even for moderately simple geometries. In chromatography the geometry of the flow space is quite complex and is therefore far beyond exact treatment.
The mathematical difficulties associated with the Navier-Stokes equation have led to various empirical approaches. Foremost among these and of great value in the classical studies of porous materials, is Darcy's Law (Darcy, 1856). Darcy developed an empirical equation based on measurements of the flow of water through sands and sandstones, which may be represented as,

$$u_o = \frac{K}{\mu}\frac{\Delta P}{L} \qquad (1.24)$$

where u_o is the linear flow velocity, K is the permeability, $\Delta P/L$ represent the pressure gradient along the net flow or z axis. This is the fundamental equation of permeability, and is only valid at low velocities (Giddings, 1965). The law is closely analogous to Poiseuille's Law for the flow of viscous fluid through a circular capillary, namely,

$$u_o = \frac{d_e^2}{32\mu} \cdot \frac{\Delta P}{L} \qquad (1.25)$$

where d_e is the capillary diameter or the equivalent diameter of a channel and μ the fluid viscosity. Numerous capillaric models have been developed. These models are based on the principle that flow through the interstices in porous media is much like flow through fine capillary tubes. In the simplest case a granular bed is pictured as a bundle of uniform, equal capillaries parallel to the direction of flow. Other models assume capillaries of unequal diameter, capillaries with a nonuniform bore, interconnected capillaries, nonparallel capillaries, etc.

Fluid flow through porous media is accurately described by Darcy's Law only for rigid particles. Very recently a corresponding expression for compressible materials has been derived by Jönsson and Jönsson (1992). This model equation which they called the steady-state flow equation for compressible media, describes how the porosity and fluid flow through a compressible medium are influenced by hydraulic and/or mechanical pressure. However, the lack of adequate compressibility and permeability relationships still restricts the use of this equation.

1.4.3.2 The Kozeny-Carman equation.

The Kozeny-Carman equation (Carman, 1937) has been derived from Darcy's equation by using dimensionless numbers as suggested by Blake (1922). The equation can also be derived from capillaric models. In deriving the equation, Kozeny (Carman, 1937) considered that if, in any section of the bed normal to the direction of flow, the fractional free area for flow is εA, then the average velocity parallel to the direction of flow must be u_o/ε. However, based on the fact that the path of any element of the fluid through the bed is sinuous, u_o/ε, must represent only the component of velocity parallel to the direction of flow. Thus, the time taken for such an element of fluid to pass over a sinuous track of length, L_e, at a velocity $(u_o/\varepsilon)(L_e/L)$, corresponds to that taken to pass over a distance, L, at a velocity, u_o/ε. In short the true value of the flow velocity

through the interstices is, $(u_o/\varepsilon)(L_e/L)$. With these considerations, he arrived at the following equation,

$$u_o = \frac{\epsilon^3}{k\mu S^2}\frac{\Delta P\, g}{L} \tag{1.26}$$

where k is defined by,

$$k = k_o\left(\frac{L_e}{L}\right)^2 \tag{1.27}$$

The value of the constant, k, was determined by Kozeny (Carman, 1937) to be 5.0 for streamline flow through the packed bed. S is the surface area per unit volume of packed bed.
In the case of spherical particles

$$S = \frac{6(1-\epsilon)}{d_p} \tag{1.28}$$

and the Kozeny-Carman equation becomes

$$u_o = \frac{d_p^2}{180\mu}\,\frac{\epsilon^3}{(1-\epsilon)^2}\,\frac{\Delta P}{L} \tag{1.29}$$

The importance of this equation resides in the fact that it relates the permeability to the porosity of the medium,

$$K = \frac{d_p^2}{180}\frac{\epsilon^3}{(1-\epsilon)^2} \tag{1.30}$$

Analysis of a great deal of data has led to a change in the value of the constant from 180 to 150, resulting in the Blake-Kozeny equation (McCabe and Smith, 1976).
These equations were developed for the flow of fluids through rigid porous media, however, extensions have been made in order to make possible the use of these equations with beds of compressible particles.

1.4.3.3 Models for compressible beds

For non-compressible beds the pressure drop at low Reynolds numbers < 10, is a linear function of flow rate; and the flow resistance is constant.

In the case of beds packed with non-rigid particles the bed void fraction and therefore the resistance to flow vary with the degree of particle deformation. The deformation in turn is a function of the pressure drop, the column length and the column diameter. With this type of particle the pressure drop through a bed is a non-linear function of linear flow rate. Models for compressible beds, in which these variables have been related, are presented in this section.

Joustra et al (1967) modified Darcy's equation to fit the properties of Sephadex gels by assuming an exponential relation between the permeability K, and the pressure drop ΔP. This assumption led to the following equation:

$$u_o = \frac{K}{\mu}\frac{\Delta P}{L} = \frac{K_o\, e^{-a\frac{\Delta P}{L}}}{\mu}\frac{\Delta P}{L} \qquad (1.31)$$

where a and K_o are constants. K_o represents the permeability when no pressure is being applied on the bed, this is the permeability at zero pressure drop (no flow). a is a constant for a particular gel, and is a function of the column dimensions and the particle rigidity.

According to this equation there is a flow rate maximum corresponding to the optimal pressure drop (i.e. the largest pressure drop just before clogging occurs), which according to hydrodynamic considerations is determined by the state of compression of the bottom section of the column (this section being subjected to the largest compression force). In their analysis, they considered the force exerted by the weight of the gel to be small when compared to the pressure drop, and since their model did not take into account friction forces against the column walls, they assumed the supporting force of the column wall to be negligible for beds of diameters larger than 15 cm. The optimal pressure drop is, therefore almost independent of bed height, and depending on the column diameter it may also be almost independent of column diameter. The assumptions made in the development of this model should result in poor predictions of experimental data in particular when wall friction is important.

Buchholz and Godelmann (1978) considered that the flow through a compressible bed must take into account varying hydraulic radii R_h in the flow path, caused by particle deformation. The pressure drop then becomes a function of bed height h, u_o, and R_h. Based on this consideration, they developed a model based on elastic deformable spheres with a modulus A defined by

$$\frac{\Delta R}{R_p} = A\ \Delta P \qquad (1.32)$$

where R_p is the particle radius, and ΔR, represents the particle deformation. They calculated $\Delta P=f(h)$ by approximation and compared the results with $\Delta P = f(u_o)$, which was experimentally determined. The approximation was achieved by calculating the pressure drop at each layer of spheres forming the bed (in a dense column packing) by means of the Hagen-Poiseuille equation, and using this information to evaluate the particle deformation and the reduction of void volume at each of these layers. The sum of all these losses in pressure and void fraction gave the total loss along the column. By using this model it was found that the main pressure drop and occlusion occurred at the bottom of the fixed bed.

In a study related to glucose isomerase reactors Verhoff and Furjanic (1983) developed a model which uses the Kozeny-Carman equation to describe the fluid dynamics. They analyzed the forces acting on a bed of deformable particles and derived a model that predicts the solids pressure at each position along a column. The force analysis included the weight of the particles as well as the drag force on the particles due to the flow of a fluid, and unlike all the previous models, it considered the support from the walls of the container resulting from friction forces arising at this location. These researchers were unable to develop a satisfactory theoretical description of the change in void volume as a function of applied pressure, and used the following empirical relationship to complete their model, (full derivation of this model is presented in section 2.2),

$$\epsilon = \frac{\epsilon_o}{(1+\alpha P_s)} \qquad (1.33)$$

The model was used to investigate the influence of the wall friction coefficient, the column dimensions, the particle size, and the matrix compressibility on column hydrodynamics. Verhoff and Furjanic (1983) also suggested experiments for testing various deformable materials for use in packed beds and employed the model to predict the performance of plant-scale equipment.

Davies and Bellhouse (1989) in a study of the permeability of beds of agarose-based particles, developed a model based on the following force balance on a cross-sectional element of a column,

$$\frac{dP}{dz} + \frac{d\sigma}{dz} + \frac{4}{d_c}\tau = 0 \qquad (1.34)$$

where P is the piezometric fluid pressure, σ is the mean effective interparticle stress in the direction of flow z, τ is the shear stress at the column wall and d_c is the column diameter. In the

balance the stress caused by the weight of the particles was neglected (full description of this model is shown in section 2.2). In their analysis, it was assumed that the permeability $K = f(\sigma)$, and they related τ to σ by means of a constant factor B, so that $\tau = B\sigma$. It is through the constant B that the wall support was taken into account. Two limiting cases were considered, that of a short column in which the shear stress at the column wall vanishes and that of a long column in which the gradient of direct stress becomes negligible and the pressure drop is considered to be entirely resisted by the wall shear. The maximum linear flow rate through columns of given dimensions was determined as well as the changes in permeability that occur along columns of different length to diameter ratios when operated at their maximum linear flow rate. This model was tested against experimental data obtained with Sepharose CL-4B columns. The model predictions agreed with the experimental curves.

In a more recent study involving Sephadex gels, Mohammad et al (1992) developed empirical correlations to model pressure drop curves. They used the following modified version of Joustra's (1967) empirical equation to fit their experimental pressure drop curves.

$$\Delta P = \frac{\mu u_o L}{K_o d_p^2} \phi \exp(a u_o L) \qquad \textbf{(1.35)}$$

where

$$\phi = 1 + \frac{1}{C_1(1 - u_o L / u_{o,cri} L)} \qquad \textbf{(1.36)}$$

K_o is the permeability of the unstressed bed, $u_{o,cri}$ is the critical linear velocity (maximum obtainable linear flow rate), and a and C_1 are constants. The change in bed length with compression was taken into account by the term $u_o L$ where L represents the experimentally measured bed length corresponding to the particular value of u_o. Based on these equations Mohammad et al developed a scaling procedure for compressible beds which keeps separation, pressure drop and feed throughput constant. The main drawback of this approach is the requirement to carry out the experimental measurement of pressure drop curves in order to conduct any scaling procedure.

Although the models developed by Verhoff and Furjanic (1983) and by Davies (1989) have been tested against experimental data with success, it is necessary to carry out more experimental work to fully verify their predictive capabilities and generality. Also more theoretical work is needed in order to increase the understanding of the hydrodynamics of compressible packed beds which will lead to the development of improved models.

1.5 Fouling in chromatography.

The problem of fouling in preparative and process-scale chromatography is of considerable importance. Two problems arise from fouling: loss of column performance and matrix deterioration.

When an adsorbent is being fouled, it continuously loses capacity due to the non-specific adsorption of foulants on the matrix support surface and on the ligands (loss of specific sites of adsorption), therefore its performance is continuously deteriorated.

Fouling also results in the mechanical blockage of the matrix pores, impeding the solute access to the inner matrix surface. This again leads to the loss of support capacity, and if the foulants build up in the matrix particles interior, access to solutes becomes restricted with consequent effects on performance. On the other hand if foulants deposit in the interstitial space reducing the void fraction, the bed permeability will be modified resulting in an increase in the pressure drop or in a reduction of the flow rate. Further changes will occur if the matrix is a soft gel, and the flow rate is to be kept constant, due to the increasing pressure drop. The blockage of pores between the support particles may adversely affect the column efficiency by causing uneven flow in the bed.

Fouling is an important cause of adsorbent deterioration, since the continuous fouling of adsorbents will require the continuous use of regenerating and cleaning agents under relatively severe conditions.

Regeneration of support media is required for techniques other than gel filtration, in which sample material is bound to the matrix and then eluted with a change of eluent conditions. Any remaining material must then be removed from the matrix by a regeneration procedure, for example by changing the pH, increasing the ionic strength of the buffer, or adding salt in the case of ion exchange chromatography. Reequilibration follows regeneration to bring the matrix to the starting conditions. These procedures however may not be sufficient to remove all non-specifically adsorbed material, so the matrix must be cleaned periodically.

Cleaning procedures can consist of washes with acid and/or alkali solutions, detergents or solutions of dissociating agents. Sodium hydroxide solutions are preferred (Cooney, 1984). Sorbent deterioration as a result of the use of these more severe conditions is more likely than during routine operation and so cleaning is restricted to occasions when its use is mandatory. For many pharmaceutical materials where interbatch cross-contamination is not permitted, this may involve cleaning after each run but in other instances, the quality of the feedstock will dictate cleaning needs. In the latter case, the regularity of the cleaning procedure is dependent on the degree to which strong, non-specific binding occurs. Therefore in the case of feedstocks containing high

levels of fouling components, cleaning will be more frequent and adsorbent deterioration will occur more rapidly. This will be reflected in the production costs, which will be higher not only because the adsorbent will have to be replaced more frequently but also because the cost of the reequilibration buffer used after each cleaning procedure will increase.

In practice, the frequency of the cleaning procedures can be set according to a difference in peak shape during elution, build-up of back pressure across the column, discolouration of packing or detection of contamination in the eluent (Pettersson, 1989). Normally cleaning is performed every 5-10 cycles (Pettersson, 1989).

The cleaning and washing agents must be controlled rigorously as any operational solution, since detrimental materials such as pyrogens will build up on many resins.

Different factors, involving not only the sample chemical composition, but also the matrix chemical structure, lead to fouling. In the following sections these factors are discussed and some practices to prevent or alleviate this problem are pointed out.

1.5.1 Matrix chemistry and structure.

The fact that all matrix surfaces have their own chemical structure, contain chemical groups and bind solvents make them liable to interact not only specifically with the solute or solutes to be separated, but also non-specifically with other solutes found in solution. The non-specific interactions are often relatively weak, but where polymeric ligates or cells are involved, a large number of weak interactions occur and can lead to strong binding. Many of the compounds of interest, especially those of high value are polymers such as proteins (including enzymes and antigens), nucleic acids or polysaccharides. These compounds are always mixed in a solution containing many other polymers and compounds of similar and different chemical structure which can interact with the matrix surface, making it highly susceptible to non-specific binding. Many of these compounds are often amphoteric, and frequently contain a large number of ionizable groups, some of which are ionized virtually at all usable pHs. Many other bioactive compounds and materials are lipophilic to a varying degree and are capable of non-polar interactions with hydrophobic surfaces. Indeed, many amphoteric polymers, such as proteins, have substantial hydrophobic regions in the molecule (usually but not by any means confined to the interior of their highly folded structures). The opportunities for hydrophobic interactions are therefore also very considerable. This diversity of interactions makes the provision of inert matrices very difficult.

The matrix chemical properties as well as the structure of the chemical groups attached to it are of great importance in relation to non-specific interactions and fouling:

I) Matrix. The matrix chemistry is a very important factor which determines considerably the degree of non-specific adsorption. Some of the highly hydrophillic polysaccharide matrices, notably agarose, have very low non-specific adsorption in aqueous solutions. This applies also for polyacrylamides. However, highly hydroxylated polymers (Spheron), even though designed specifically for biological work, have some non-specific adsorption. Silica and glass show substantial non-specific adsorption (due to silanol groups). Polystyrene on the other hand shows strong hydrophobicity even when it has ion-exchange groups and can cause a substantial degree of denaturation of proteins. Phenol formaldehyde polymers, seem to have a less drastic effect. Fouling can also occur when support particles are mechanically damaged. Freshly fractured surfaces can lead to non-specific binding of proteins to high energy planes around a fracture.

II) Ligand or bonded groups. Depending on its structure the ligand in affinity chromatography or the bonded groups in other types of chromatography (i.e. ion-exchange, hydrophobic interaction, etc) can also encourage non-specific adsorption. Thus for example fatty acid ligands especially those with longer alkane chains will almost certainly interact with non-polar molecules or non-polar regions in macromolecules, in a non-specific manner. Similarly many ligands or bonded groups are charged at certain pH and hence will interact to some degree with other charged groups or molecules.

III) Coupling chemistry. In affinity chromatography, the reaction used to activate the available matrix may itself lead to the introduction of charged groups, resulting in the creation of ion-exchange capacity, with the consequent non-specific adsorption.

IV) Spacer arm. Again, in the case of affinity chromatography, the use of spacer arms, although highly valuable may lead to non-specific adsorption. In general the spacer arm needs careful design to minimise non-specific adsorption, while in many cases there must be sufficient interaction to enhance the actual affinity of the ligand. There is little real guidance on the design of the spacer arm except that hydrophillic non-ionic chains tend to minimise non-specific adsorption, while hydrophobic arms tend to maximise it.

It must be borne in mind that the possible non-specific interactions previously mentioned do not necessarily lead to fouling. In many cases these non-specifically bound compounds are easily removed from the bed, however, in many other cases they bind strongly to the matrix and fouling results.

Apart from the above mentioned factors concerning the matrix, the eluent composition is also

important in order to minimise non-specific adsorption, and to control fouling. Ionic effects in gel filtration for example, can be minimise by the use of high ionic strength solutions (Pharmacia, 1991a). It must be remembered, however, that increased ionic strength tends to enhance hydrophobic interactions, so an effective compromise is required.

1.5.2 Main fouling components in chromatography.

There are quite a few components in a fermentation broth that can foul a chromatographic sorbent. Pirotta (1985) in a study involving antibiotic fermentation broths and ion exchange resins, specified the components commonly found in the fermentation broth that can foul the chromatographic support. This is the list of fouling components he indicated together with the most important factors which influence their adsorption on matrices and adsorbents. Some suggested procedures for their removal are also included (Pirotta, 1985 and Pettersson, 1989).

A) Antifoaming agents, waxes, and oils. Most of these substances are hydrophobic and, consequently, can be adsorbed to hydrophobic matrices through electrostatic attraction. In this type of interactions it is important to consider the nature and molecular size of the antifoam, wax or oil, the resin porosity, the contact time with the support, temperature, and ionic strength of the solution. When this type of non-specific adsorption occurs the matrix can be regenerated by: eluting the fouling compound with a suitable organic solvent; the use of a dilute regenerant solution at the highest possible temperature; hydrolysing the foulants by means of chemical or biological agents; the use of a suitable surfactant.

B) Suspended solids. When a filtered broth is passed over a chromatographic support, and the solute is adsorbed, the composition of the broth changes and often precipitation occurs. The precipitated solids must be removed as frequently as economically possible, in order to prevent more serious problems such as, microbial infection in the column, matrix clumping and bed channelling. The most simple way of removing suspended solids is by backwashing the bed. However, in some cases precipitation is slow and this operation might not be sufficient. The use of a low foaming surfactant in the backwashing procedure, in that case should be considered. In some situations, the solids dissolve by simply changing the pH.

C) Fatty acids, phenolic substances, thiols. These compounds can react with the anionic groups

of ion exchange resins and/or be adsorbed on the support surface by electrostatic forces. Lipids tend to clog columns. If standard regeneration procedures are not capable of eluting these compounds, the use of a less concentrated regenerant should be considered, 2% NaOH or even 0.5% NaOH, can be used instead of the standard 4% NaOH. The use of aqueous solvent solutions or even pure organic solvents should also be considered. Regeneration conditions when this type of fouling occurs are important, since unsuitable regeneration conditions could precipitate substances such as, polyphenols and irreversibly foul the matrix.
An alternative for solubilizing and removing lipids on heavily contaminated supports is to elevate the temperature. Extremely contaminated matrices may require treatment with high temperature and sodium hydroxide (Sofer, 1987). Phenolic substances and, especially thiols can polymerise and film-coat the support. In this case, oxidising agents to break the formed film should be considered.

D) The presence of heavy metals, such as Fe, for example, must be avoided, since these heavy metals can act as catalysts for radical de-crosslinking reactions, deteriorating the matrix.

E) Proteins. Proteins react to all types of matrices but to different extent and with different mechanisms. Proteins also tend to react with almost all types of the previously described impurities present in the fermentation broths. The treatments for the elution of fouling proteins vary depending on the type of proteins involved (Pettersson, 1989). These could be soluble proteins, precipitated proteins or hydrophobic proteins (lipoproteins). Alkali or acid solutions, and low and high ionic solutions have been used, as well as enzymatic treatment in the case of precipitated protein.

Apart from the foulants mentioned by Pirotta (1985), there are others equally important (Pettersson, 1989). The following list continues the one above. The cleaning in place procedures developed to remove these fouling components are included in the list:

F) Nucleic acids. This type of foulant can be removed by means of alkali or acid solutions, followed by salt solutions.

G) Endotoxins. In this case, sodium hydroxide solutions are used to inactivate and remove endotoxins, but detergents and ethanol solutions have also been used.

H) Virus. Heat or pH treatment are used to inactivate and remove viruses, but sodium hydroxide solutions can also decontaminate and inactivate viruses (Sofer, 1987).

Finally, on the list:

I) Microbial contamination itself has been considered as a type of fouling (Unger and Janzen, 1986). This type of fouling is usually prevented by mobile phase additives. Sanitization procedures are carried out to prevent build up of microbial contamination and to reduce the amount of living microorganisms contaminating the column. Numerous antimicrobial agents including solutions of ethanol, formaldehyde, sodium azide, or Merthiolate can be employed. However, it is a good practice to avoid using toxic materials for sanitizing the matrices, because there is danger that they may find their way into the product. Again, sodium hydroxide solutions are the preferred option due to its sterilizing capabilities and the fact that it destroys pyrogens and does not contaminate the product.

Alternative solutions have been proposed to solve fouling problems when the cleaning procedures do not help to restore the chromatographic performance. These are based on the fact that most contamination occurs in the top 5-10 cm of the gel bed (Pettersson, 1989). When a column is fouled, first the flow should be reversed to try to eliminate the foulants on the top portion of the bed. If this action does not work, then the top part of the bed is replaced. If flow and performance are not restored, the column must be repacked or the matrix must be replaced.
Besides the above mentioned cleaning, regeneration and sanitization procedures other actions should be taken in order to avoid and reduce fouling problems:

I) All buffers and cleaning and solutions should be filtered through 0.45 micron, or, preferably 0.22 micron filters.

II) Sample pretreatment should be examined to remove particulates, lipids and endotoxins. Particulates can be removed by centrifugation and microporous- or ultrafiltration (Sofer, 1987). Lipids on the other hand can be removed by Gauze filtration, product precipitation, flotation, temperature drop or adsorption (Pettersson , 1989). Endotoxins removal is usually accomplished during ion exchange chromatography. Removal of lipids and endotoxins prior to chromatography, although desirable, is not always possible.

The type of fouling components encountered in the sample to be injected onto a chromatographic column is highly determined by its source. The main fouling components identified, according to the product source are as follows (Pettersson, 1989):

i) Plants extracts. The high content of charged polyphenols in plant extracts can cause severe loss of capacity, especially at low ionic strength. Plant extracts also contain a big amount of coloured substances that can cause contamination and fouling.

ii) Tissue extracts. With this type of product source the main problem is the high lipid content. These compounds can bind to the matrix surface, and hydrophobic proteins can bind to these complexes. Fouling by lipids can be detected by the increase in pressure drop due to clogging of the matrix, and in some cases by the appearance of a grey or discoloured zone on the matrix.

iii) Microbial fermentation. The secretion systems of some microorganisms require the use of silicon-based antifoams which can foul the matrix. Also cell membranes have a high lipid content. In the particular case of *E. coli*, endotoxins can produce fouling and contamination problems.

iv) Mammalian cell culture. In general, fouling is small with these systems. Major contaminants from culture broth may vary considerably, depending on specific nutrient requirements of cell line. The secretion systems of this type of cells require the use of antifoaming agents which can act as foulants.

1.5.3 Studies on fouling in chromatography.

A few studies have been carried out in order to investigate the effects of fouling on the matrix performance, however most of these studies have been qualitative rather than quantitative. In most of them fouling has been found to be the factor causing detrimental effects on the matrix performance, however, no attempt has been made to quantify the effect of this phenomenon in relation to the inlet stream composition.

The mechanisms of silica fouling in processes for the recovery of metal values employing ion exchange resins or carbon adsorption have been studied (Ritcey, 1986 and Guowei et al, 1988). In the case of recovery of uranium, it was found that fouling of ion exchange resins occurred through silica polymerisation inside the resin beads as well as on the outside, resulting in loss of capacity and kinetics (silica interferes with the rate-controlling diffusion process of ions in and out of the resin matrix) and thus plant capacity (lower flow rates must be used unless the silica is removed). The silica content of resin may increase if not controlled and the beads may ruptured through failure of the resin cross-linking.

The resin fouling also resulted in increased consumption of reagents for elution. More desorption

feed solution is needed to desorb the poisoned resin to the same low uranium concentration, compared with the fresh resin desorption, even though the poisoned resin has a lower saturation capacity than the fresh resin.

These researchers also studied the carbon adsorption used in many CIP gold plants, where fouling due to silica deposition is a major problem. Here again, fouling affects the gold loading on the carbon sites and the kinetics. Since the gold loading value determines the size of the carbon stripping and reactivation plant, and kinetics control the loading, then this factor is a major concern in optimizing the performance and determining the cost of CIP processes for gold recovery. The entire system is thus, very sensitive to fouling.

Kril et al (1987) have reported the reduction of the dynamic capacity of ion-exchange resins or activated charcoal beds due to microbial fouling. The fact that the sorbents co-adsorbed organic and inorganic matter which could serve as nutrients, facilitated microbial growth. The studies were carried out for the case of water-treatment process.

New matrices have been developed which are more chemically stable and less prone to non-specific adsorption. Stewart et al (1990) have developed novel perfluorocarbon supports bearing adsorptive dyes. These polymers are stable to extremes of pH and are resistant to oxidising agents and significant non-specific adsorption of proteins is absent.

1.5.4 Fouling models.

Until now no models have been developed specifically to represent the fouling phenomenon in chromatography. However, the models used for catalyst deactivation and membrane fouling could provide useful information for the development of a fouling model for chromatography. Therefore some of the most important models in catalyst fouling and membrane fouling will be reviewed briefly in this section.

There is a substantial number of fouling models in ultrafiltration, where flux reduction occurs as a result of protein deposition on the membrane. The nature of this deposition has been studied, and solute and membrane properties as well as the solution environment and operating conditions have been considered.

Fane and Fell (1987) have reviewed the fouling models in ultrafiltration. They are divided into semiempirical and fundamental models. Both types of models are constituted by a main equation which gives as a result the flux changes with respect to time. The main concern in these models is the evaluation of the deposit (or fouling) resistance or permeability as time passes and the foulant builds up.

Mechanistic models for long-term flux decline have also been developed in protein ultrafiltration. Fane and Fell (1986) developed one such model assuming that protein in the concentrated layer adjacent to the membrane slowly aggregates to form a deposit of reduced voidage and increasing resistance. Protein aggregation is based on flocculation theory and assumes that the protein molecules behave as hard spheres with double-layer interactions.

In chromatography it is required to develop a model which takes into consideration the changes in void volume and permeability with respect to time due to the time dependent foulant deposition in the interparticle space. Fouling protein could aggregate and build up in the interstices as a result of flocculation processes as it is considered to occur in ultrafiltration.

In the case of catalyst deactivation, models have been developed that take into account not only the loss of activity due to surface coverage by foulant components but also the blockage of the catalyst support pores which result from the building up of the foulant on the active sites where it was first deposited (Beeckamn and Froment, 1979). The access of the reactant to the active sites inside the support particles is restricted by foulant deposition or completely hindered by pore blockage. The catalyst deactivation has been mathematically related to the foulant content of the catalyst. Mathematical relationships have also been developed to determine the rate of coverage and the rate of catalyst deactivation as a result of foulant deposition and pore blockage.

Models developed for catalyst deactivation have involved not only microporous and mesoporous catalysts, in which one of the major causes of deactivation is pore plugging as mentioned above, but also macroporous catalysts (Kissinger and Khang, 1989). In the latter the absence of diffusional resistance will allow for a more uniform deposition of foulant throughout the catalyst and their larger pore radii will allow for the accumulation of much larger amounts of foulant before pore plugging becomes of concern.

In chromatography, loss of capacity due to fouling results from surface coverage and pore blockage. Both of these phenomena must be considered in the development of a model.

1.6 Aims of Project.

In process-scale chromatography the general objective is to reach the specified purity, at the highest possible yield, at the lowest possible cost and in the shortest possible time. The achievement of this objective implies the optimisation of the design, operation and performance of the process.
Within this context, the overall objectives of the project are:

A) To provide useful information in order to assist the optimisation of the design, operation and performance of large-scale chromatography.

B) To investigate experimentally and by means of modelling and simulation tools, the effect of bed compression and fouling on the separation performance of chromatographic columns.

C) To contribute to the development of modelling and simulation tools, by means of which the chromatographic performance of columns operated under realistic conditions could be predicted.

The flow rate in a chromatographic separation should not exceed a critical value determined by matrix compressibility and diffusion kinetics. In process-scale chromatography of biopolymers, where soft gels are widely used, the lack of rigidity of these matrices is the cause of one of the major problems associated with large-scale chromatography, that of bed compression. The tendency of these matrices to compress at high flow rates, with the resulting rise in back pressure has limited the depth of the gel which may be used, as well as the particle size. In relation to this problem and to the possible beneficial effects of bed compression reported by some researchers (see section 1.4.2) the objectives of the compression studies conducted as part of this thesis are as follows:

1) To study the fluid dynamics of beds packed with compressible supports in order to contribute to the development and improvement of modelling tools that will aid in the assessment of the effects that the different operating variables, and the column and matrix dimensions have on the hydrodynamic behaviour of columns packed with compressible particles.

2) To study the effects that changes in the bed and matrix structure resulting from bed compression have on the efficiency and separation performance of chromatographic operations.

The information obtained will provide a basis on which columns packed with soft or semirigid supports could be better designed, operated, and scaled-up.

Matrix fouling in preparative and process-scale chromatography is of great importance since it affects column performance and leads to matrix deterioration, which in turn result in an increase in the costs of separation. However, very little work has been carried out in this area and much remains to be studied in order to understand fully the effects and mechanisms of fouling. Accordingly the aims of the fouling studies carried out as part of this work are as follows:

1) To study experimentally and by means of modelling and simulation tools the effects that foulant deposition have on the efficiency and separation performance of chromatographic beds in order to derive mathematical relationships that would allow the prediction of these effects.

2) To develop and test a methodology for the analysis of the effects of fouling on the bed and matrix structure and therefore on chromatographic performance.

The information obtained will contribute towards the understanding of the effects of fouling on column performance and will aid the operation and optimisation of chromatographic separation steps.

According to the above mentioned objectives the present thesis has been structured as follows. Chapter 2, deals with the effects of matrix compression on column hydrodynamics and analyses the most relevant models used in the prediction of flow rate-pressure drop curves. In doing so it looks in some detail at the parameter estimation methods used in this area.
Chapter 3 introduces the chromatography model later used in the analysis of the effects of matrix compression and fouling on column performance, as well as the numerical methods employed in its solution. It also deals with some important aspects of transport in fixed porous beds in order to set the theoretical background required for the compression and fouling studies covered in the next two chapters.
The analysis of the effects of matrix compression on column performance is presented in Chapter 4. The pulse techniques and in particular the HETP (height-equivalent-to-a-theoretical-plate) method are introduced in this chapter. The HETP technique is used in this study in order to estimate the parameters that characterize chromatographic performance.
In Chapter 5 the fouling of chromatographic matrices and its effects on column performance are analyzed, and the method of moments used in the estimation of transport and equilibrium

parameters, looked at in detail.

Finally in Chapter 6 general conclusions are drawn, while pointing out the main contributions of this thesis. Possible future developments in the study of matrix compression and fouling within the chromatographic field are also suggested.

1.6.4 Concluding Remarks.

Chromatography is a well established isolation and purification process in the biotechnology industry. Its importance will continue to grow, as the biotechnology industry introduces more of its products to the market. This will certainly continue to expand the chromatographic market, despite the increasing competition of other newly developed separation techniques.

Although chromatography is recognized as the technique which allows the highest degree of purification of biomolecules, and is already widely used in industry, its design and operation are far from being optimum. Its design, process scale-up, and optimisation are mostly carried out empirically. A number of problems need to be addressed if this situation is to be improved.

Relatively few modelling and simulation studies of the whole chromatographic process have been made and used in order to carry out process optimisation. It is expected that the development of new and more rigorous models will aid in the solution of a variety of process problems, among them, bed compression and fouling, as addressed in this thesis.

CHAPTER 2

COLUMN HYDRODYNAMICS AND MATRIX COMPRESSION.

2.1 Introduction.

An important and often critical factor in the design, operation and scale-up of chromatographic columns is the ability of the support material to resist bed pressure drop. The vast majority of packing materials used in the separation and purification of biopolymers are compressible to different degrees. Due to this characteristic at certain critical column dimensions and flow rates these packings tend to compact (reversibly) as a result of the hydrodynamic forces they are subjected to. This tendency poses a series of practical disadvantages:

A) Compression reduces the porosity of packed beds and therefore limits the flow rate and throughput. It has been observed (Joustra et al, 1967, Mohammad et al, 1992) that there is a maximum flow rate beyond which a bed will clog due to the high compression of the support at the bottom of the column. Therefore it has been advised to use packing flow rates that correspond to 80% of the maximum flow rate and to run the column at no more than 80% of the packing flow rate (Sofer and Nyström, 1989). This means that operating flows could be very low.

B) The elasticity and compressibility of porous gels that fractionate in the high molecular weight range precludes the use of long columns for large scale fractionation. In fact until the introduction of a special column design providing stability and support for the packing material, it was virtually impossible to fractionate on highly porous gels on a large scale (Janson and Hedman, 1982).

C) It precludes the use of small particle sizes. Although resolution increases with decreasing gel particle size, the flow rate characteristics of compressible matrices militate against the use of all but coarse or medium gels (Delaney, 1989). Therefore, it is normally better to increase the column length and/or diameter, and use standard grade gel rather than to use a short column with a superfine gel.

D) Gel compression makes design and scaling-up of separations difficult (Mohammad et al, 1992).

It is not possible to simply increase the column dimensions and still maintain the correct flow and pressure drop. When the column diameter increases, the chromatographic bed becomes unstable because of the loss of wall support. The matrix therefore compresses more freely and the flow rate characteristics of the bed change.

E) Operational costs of chromatographic columns are determined in part by the pressure drop required to realise a given flow rate (Chisti and Moo-Young, 1990). The pressure drop in the case of compressible packings is largely affected by their tendency to compact. Therefore matrix compressibility has an effect on operational costs.

F) Compression occurs also with time possibly due to reaccommodation of the packing or to a fatigue process. This phenomenon is related to the existence of unstable regions formed in the bed during the packing process. Such regions have bridges of particles (arches) surrounding empty spaces. The bridges eventually collapse (because of shear forces resulting from the flow of solvent, for instance, or because of mechanical vibration). The particles then reorganize and the whole bed settles, usually forming a gap at the column inlet. At this point, the column's efficiency is dramatically reduced (Colin et al, 1990). Fouling could also be a cause of compression with time since it reduces the bed permeability (Petersson, 1989).

On the positive side it has been reported that beds that have been highly compressed can provide improved performance (Edwards and Helft, 1970; Fishman and Barford, 1970). Hjertén et al (1988) and Liao et al (1988) have shown that columns of compressed, cross-linked, non-porous agarose beads for ion-exchange and for HIC permit high flow rates while the resolution is virtually independent of flow rate at constant gradient volume. Horváth (1990) in his studies with gigaporous particles has found the efficiency of packed columns to be higher the greater the packing pressure and has observed drastic deformation of the particles with the concomitant reduction in column permeability.

It seems therefore that bed compression has on one hand a clearly detrimental effect on the flow rate-pressure drop dependence and hence on the throughput and economics of the chromatographic operations while on the other hand it may improve column performance. Both of these effects have not been thoroughly studied and it is not clear as yet what the real effects are and the extent of these on column performance and the economics of the chromatographic operation.

In the present chapter the effect that bed compression has on the flow rate-pressure drop dependence has been approached. The aim would be to be able to predict the pressure drop given the column dimensions, flow rate, viscosity and density of the fluid as well as properties

describing the mechanical behaviour of the column matrix. Such a prediction will enable the determination of the best packing flow rate as well as the maximum flow rate that can be utilised for a particular matrix and column, the size of the pump needed to achieve the required pressure and the operating conditions and costs. At present optimal operating pressures must be established empirically, and this is usually done during packing when flow rate-pressure drop curves are generated (Delaney, 1989). Besides in the case of gel filtration flow rate data is also required to estimate column capacity.

Several studies concerning the modelling and the prediction of the hydrodynamics of compressible beds have been carried out (see section 1.4.2), amongst them the most relevant works have been those conducted by Verhoff and Furjanic (1983) and Davies (1989) and therefore constitute the basis of the present study.

The objective of this chapter is to analyze the most relevant hydrodynamic models available in the literature, to test their predictive capabilities and to develop methods for the estimation of the mechanical properties of soft matrices.

2.2 Hydrodynamic models for compressible packed beds.

When fluid is passed through a compressible bed, the pressure drop of the fluid causes a solids pressure or interparticulate stress to develop in the packing material (Carman, 1933). The particles in the bed then compress and deform under the compressive stress reducing the porosity and therefore limiting the flow rate. This deformation is brought about by unbalanced forces in the bed. As it can be seen in fig. 2.1, the particles in the bed are in contact with the surrounding particles and with the liquid flowing past them. They form a skeleton which transmits the total hydrostatic pressure P to the bottom of the column. On the other hand as the liquid passes through the bed, it progressively loses pressure which is commensurate with the friction that has been overcome. Wherever there is contact between particle and particle, the total pressure, P, is transmitted. But in the voids, where contact is between particle and liquid, only the residual pressure of the liquid is impressed upon the particle. If the fluid lost pressure is ΔP, then it impresses a pressure, $P-\Delta P$, upon the particles. The particles are therefore subjected to an unbalanced or deforming force, $P-(P-\Delta P)$, i.e. ΔP. This compressive force is the effective interparticulate stress or the solids pressure P_s, as it will be referred to in the remaining part of this chapter.

In the present study the hydrodynamic model derived by Verhoff and Furjanic (1983) and that developed by Davies (1989) have been analyzed and experimentally tested with two compressible

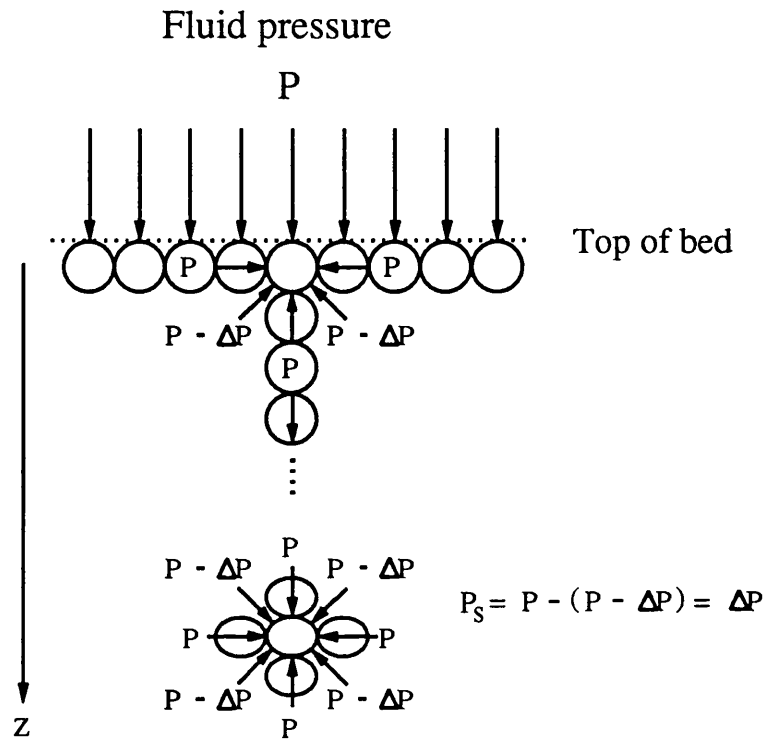

Fig. 2.1 Particle compression resulting from the unbalanced forces acting upon them. Wherever there is contact between particles, the total fluid pressure P, is transmitted. In the voids only the residual liquid pressure is impressed upon the particles. The particles are therefore subjected to a deforming force ΔP, this is the effective interparticle stress σ, or the solids pressure, P_s.

chromatographic matrices, Sepharose 6B and Sepharose CL-6B (Pharmacia LKB Biotechnology). The model developed by Verhoff and Furjanic (1983) was originally used to aid the design and scaling up of glucose isomerase reactors but its generality allows its use in other systems. The phenomena considered in its derivation were the flow through porous media, the compressibility of the matrix particles, the wall friction support, and the interaction between the fluid dynamics and the solid mechanics (see section 1.4.3.3 for details).

Fig. 2.2 shows the analysis of the forces acting on a cross-sectional element of bed packed with a compressible matrix. These forces include the weight of the particles, the support from the column walls, and the drag force exerted by the fluid flow.

Except during settling (packing) there is no acceleration of the particles inside the column, so the sum of forces is zero and the force balance is

$$dF = dF_g + dF_F + dF_W \qquad (2.1)$$

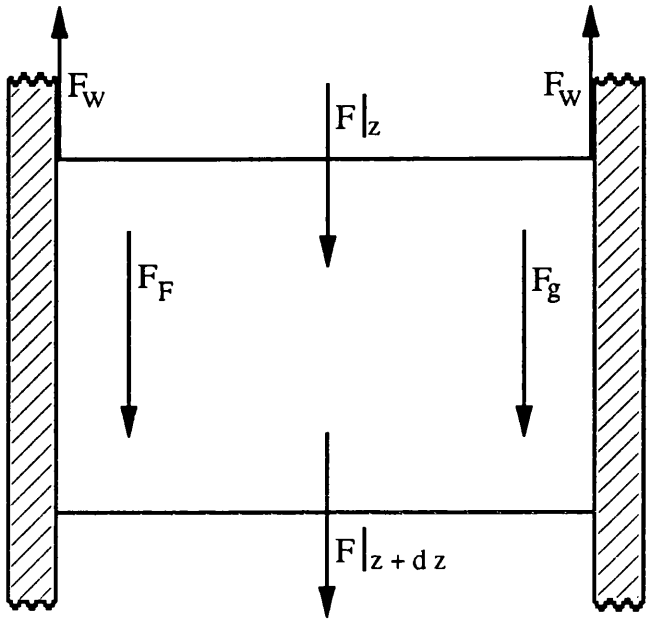

Fig. 2.2 Forces acting on a compressible packed bed. F_W, force due to the support from the column walls, F_F, drag force due to the fluid flow and F_g, force due to the weight of the particles.

Force F_g is due to the weight of the particles, and its contribution is

$$dF_g = AdP_g = \pi R^2(\Delta\rho)(1-\epsilon)dz \tag{2.2}$$

where A is the cross-sectional area of the bed, P_g is the corresponding solids pressure due to F_g, R is the column radius and ε the bed void fraction. The distance along the column axis is defined by z, and

$$\Delta\rho = (\rho_s-\rho_L)g \tag{2.3}$$

ρ_s being the density of the stationary phase, while ρ_L is the density of the liquid phase.
The downdrag force F_F due to the fluid flow follows the Kozeny-Carman form

$$dF_F = AdP_F = \pi R^2 f\frac{(1-\epsilon)^2}{\epsilon^3}dz \tag{2.4}$$

where P_F is the solids pressure due to F_F and

$$f = \frac{150\mu u_o}{\Phi^2 d_p^2} \tag{2.5}$$

here μ is the fluid phase viscosity and u_0 is its linear velocity. The particle diameter is represented by d_p, and Φ corresponds to a shape factor that has been introduced to account for particle deformation.

The pressure drop along the column can be evaluated by

$$\frac{\Delta P}{L} = \frac{1}{L}\int_0^L \frac{150\mu u_o}{\Phi^2 d_p^2}\frac{(1-\epsilon)^2}{\epsilon^3}dz \tag{2.6}$$

Support from the column walls follows the treatment of pressures of granular solids in silos by McCabe and Smith (1976).

$$dF_W = SdP_W = \pi R^2 \omega P_s dz \tag{2.7}$$

where S is the lateral surface area of the bed, P_W is the solids pressure associated with F_W and the wall support coefficient ω is defined as

$$\omega = \frac{2\mu' K'}{R} \tag{2.8}$$

here K´ is the ratio of lateral to vertical pressure and μ' is the coefficient of wall friction.

Combining the above equations and dividing by the volume A dz, of the differential element the basic model for the solids pressure as derived by Verhoff and Furjanic (1983) is obtained

$$\frac{dP_s}{dz} = \Delta\rho(1-\epsilon) + f\frac{(1-\epsilon)^2}{\epsilon^3} - \omega P_s \tag{2.9}$$

This model was completed by taking into account the physical properties of the compressible matrix by means of an empirical relationship between the matrix compressibility, α, the initial void fraction of the unstressed bed, ε_0 and the solids pressure, P_s,

$$\epsilon = \frac{\epsilon_o}{1 + \alpha P_s} \tag{2.10}$$

where ε is the void fraction at a given value of solids pressure.

The model is applicable only in the laminar flow region and is based on the following assumptions:

A) The particles composing the packing material are monodisperse. The model does not take into account the existence of the particle size distribution of the matrix. However an appropriate mean value of particle diameter will be used (see section 2.3.2.4).
B) The interparticle friction force is negligible. The model considers that the friction forces between the particles are small enough to be negligible.
C) The radial variation of the axial stresses or compressive forces is small and can be neglected.
D) The fluid phase is incompressible.

Davies (1989) developed a model which is basically a modified version of the one previously described. He neglected the weight of the gel particles assuming their density is very similar to that of the fluid in which they are immersed since they are highly hydrated, Sepharose CL-4B (Pharmacia LKB Biotechnology) was used to verify the model. The concept of stress normally used in soil mechanics was employed by Davies (1989) to refer to the pressure resulting from compressive forces. He then used interparticulate stress σ instead of solids pressure P_s. These two concepts are equivalent and will be used without distinction in the remaining part of this chapter. Since stress determines the degree of particle deformation and hence the geometry, bed porosity and permeability depend on stress. Therefore Davies (1989) substituted the permeability function already used by Verhoff and Furjanic (1983) in its model derivation, defined according to the Blake-Kozeny equation (Bird et al, 1960) as:

$$K = \frac{d_p^2 \phi^2}{150} \frac{\epsilon^3}{(1-\epsilon)^2} \qquad \textbf{(2.11)}$$

for an empirical function of the form

$$K = f(P_s) = K_o \exp\left(-\frac{\sigma}{\sigma_o}\right) \qquad \textbf{(2.12)}$$

where K_0 is the permeability of the uncompressed bed, $\sigma=P_s$ is the effective interparticulate stress or solids pressure acting directly along the column axis, and σ_0 is a constant representing the matrix rigidity (equal to the inverse of matrix compressibility, α (see eq. 2.10)). This function was determined experimentally and represents the dependence of permeability on stress. The friction against the tube wall or wall shear stress was considered by Davies (1989) to be proportional to

the axial stress, $\sigma = P_s$, with B as the proportionality constant. The resulting model equation was

$$\frac{d\sigma}{dz} = \frac{dP_s}{dz} = \frac{u_o\mu}{K(P_s)} - \frac{4BP_s}{D} \qquad (2.13)$$

Taking into account the weight of the particles and since the constant B corresponds to the product $K'\mu'$ (see eq. 2.8), and $P_s = \sigma$, the model equation can be rewritten as

$$\frac{dP_s}{dz} = \Delta\rho(1-\epsilon) + \frac{u_o\mu}{K(P_s)} - \omega P_s \qquad (2.14)$$

In this case the pressure drop through a column is evaluated by

$$\frac{\Delta P}{L} = \frac{1}{L}\int_0^L \frac{u_o\mu}{K(P_s)}\,dz \qquad (2.15)$$

Equations 2.9 and 2.14 have the same form and they differ only in the way the permeability K is expressed. These are the two model equations which predicting capabilities are to be tested. In the following sections the materials and methods used in the determination of the model parameters as well as in the verification of the two models are presented.

2.3 Materials and methods.

2.3.1 Chromatographic system.

The chromatographic system, i.e. instrumentation, matrices, buffer and chemical components, used in the first part of this work is described in this section. This includes the study of the effects of matrix compressibility on column hydrodynamics (chapter 2) and the study of the effects of bed compression on chromatographic performance (chapter 4).

2.3.1.1 Chromatographic matrices.

Two soft matrices were used as part of the experimental system, Sepharose 6B and Sepharose CL-6B (Pharmacia LKB Biotechnology). These gel supports are prepared from agarose and have a spherical shape. In its natural state agarose occurs as part of the complex mixture of charged and

neutral polysaccharides referred to as agar, a component of seaweed. Agarose is the less sulphated polysaccharide present in agar. It is a linear polysaccharide made up of alternating D-galactose and 3,5-anhydro-l-galactose units. Sepharose is prepared from agarose obtained by a purification process which removes the charged polysaccharides to give a gel with only a very small number of charged groups. Bead-shaped gels suitable for chromatography are formed by cooling 2-15% aqueous solutions of agarose dispersed in a non-polar organic solvent in the presence of suitable emulsifiers. The individual polysaccharide chains form double helices which subsequently aggregate to form bundles during the formation of stable gels (see fig. 2.3). The gel so formed has a highly hydrated hydrophillic structure and is extremely porous. Sepharose has been prepared at three different agarose concentration 2, 4, and 6% to give the three different types of Sepharose 2B, 4B and 6B.

Although the structure of Sepharose is stabilized by hydrogen bonding and not by covalent cross-links, it can still be used under most of the conditions encountered in gel filtration. It is stable in water and salt solutions over the pH range 4-9 and in the absence of dissociating agents. With respect to its physical stability, Sepharose melts on heating above 40 °C and the bead structure may be irreversibly damaged on freezing. Consequently Sepharose cannot be sterilised by autoclaving.

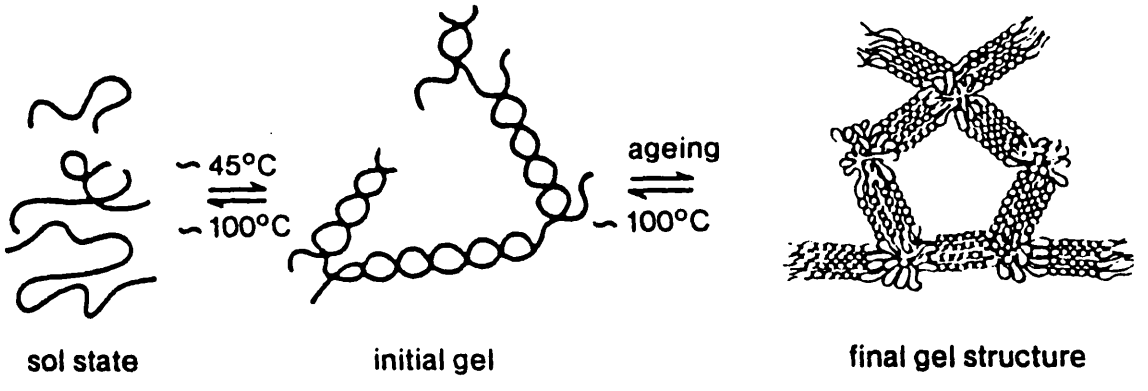

Fig. 2.3 Gel structure of agarose.

Sepharose CL is prepared from Sepharose by reaction with 2,3 dibromopropanol under strongly alkaline conditions. This produces a cross-linked agarose gel with substantially the same porosity as the parent gel but with greatly increased physical and chemical stability. After the cross-linking, the gel is desulphated by alkaline hydrolysis under reducing conditions yielding a gel with an

extremely low content of ionizable groups which shows even lower non-specific adsorption than the parent non cross-linked gel. Sepharose CL can be used in aqueous media in the range pH 3-12 and its higher physical stability allows the use of higher flow rates (maximum flow rates are typically 50% higher than those obtained with the corresponding types of Sepharose B). In contrast to the parent gels, Sepharose CL can be sterilized repeatedly by autoclaving at pH 7, 121°C without significant changes in porosity or rigidity.

The pores of Sepharose 6B particles consist of spaces between fibres, therefore in practice there is a continuous spectrum of pore dimensions. The pore size distribution of Sepharose 6B has not been reported in the literature[1]. However, its porosity has been standardised using molecules of known molecular weight/size. Its useful molecular weight fractionation range for globular proteins is 10×10^3 to 10×10^6 (Pharmacia, 1991a).

In the cross-linking procedure of Sepharose CL-6B it is primarily the agarose chains within the bundles which are cross-linked. The size of the channels formed by the bundles is thus not much affected by the cross-linking and therefore the pore structure, permeability, fractionation range and selectivity curves for globular proteins are virtually the same as those of its parent gel Sepharose 6B (Pharmacia, 1991).

In summary Sepharose gels have many of the desired properties for the fractionation of biopolymers, such as hydrophillicity, a highly porous structure and minimal non-specific adsorption. They are sufficiently rigid for use on a laboratory scale, and for production in specialised equipment to accommodate its undoubted compressibility which is due to its xerogel character. Due to these characteristics these gels were selected for the present study.

2.3.1.2 Model proteins.

The study of chromatographic column performance involves the analysis of the dispersion (bandbroadening) that a pulse undergoes as it travels down the column, and the effect of this dispersion on the resolution between two different components. In order to study this dispersion phenomenon five globular proteins were selected to be used as part of the experimental system, i.e. ribonuclease A, ovalbumin, γ-globulin, β-amylase and apoferritin.

The selection of these proteins was based on their availability, purity, cost, molecular weight and the need for baseline or nearly baseline resolution for a pair of them (ribonuclease A and γ-

[1] By the application of a capillary pore diffusion model, Ackers and Steere (1962) estimated the pores of 4% agar gel to be approximately 40 nm in diameter, while Janson and Jönsson (1989) have reported an average pore diameter of about 30 nm for the same beaded gel concentration with average d_p= 90 μm.

globulin) to facilitate the analysis of the effects of compression on resolution. γ-globulin in particular was selected mainly due to its analogy to monoclonal antibodies (immunoglobulin-G is the main component of the γ-globulin fraction).

All the model proteins were bought from Sigma Chemical Company. Ribonuclease A from bovine pancreas was essentially protease-free, type XII-A (cat. no. R-5500). It has a molecular weight of 13 700. Ovalbumin from chicken egg was of grade VI and approx. 99% pure (cat. no. A-2512). Its molecular weight is 45 000. Bovine γ-globulins from Cohn fractions II and III were approximately 99% pure (cat. no. G-5009). These fractions contain different types of globulin all of them of slightly different molecular weight, however, the difference is negligible and for the purpose of the present study the properties of the γ-globulin fraction can be considered to be those of the immunoglobulin-G which is its main constituent. Its molecular weight is 156 000.

β-amylase was from sweet potato and for use as a molecular weight marker (cat. no. A-8781). Approx. molecular weight 200 000. Finally apoferritin was from horse spleen and also for use as a molecular weight marker (cat. no. A-3660). Its molecular weight is 441 000.

2.3.1.3 Void volume markers.

The interparticle void volume V_o, was required to evaluate the bed void fraction ε and subsequently the equilibrium and transport parameters. It was measured using a totally excluded molecule, blue dextran 2000. The void volume is usually determined from the injection point of the marker to the apex of the eluted peak (Hagel, 1989). Blue dextran 2000 was bought from Pharmacia LKB Biotechnology (cat. no. 17-0712-01).

To determine the total void volume V_T, acetone was use as a marker. A solution of 5 µl of acetone per ml of buffer was prepared and 200 µl samples were injected (Hussain et al, 1991). The acetone peak was also used to assess the quality of the bed packing and the column efficiency (Hagel, 1989).

2.3.1.4 Buffer.

The buffer used in all the following experiments was: 0.05 M potassium dihydrogen orthophosphate Analar grade (BDH Ltd), 0.20 M sodium chloride Analar grade (BDH Ltd.), 0.02 % sodium azide (Sigma Chemical Co. Ltd). The pH was set at 7.0 by adding 4 M sodium hydroxide solution (Analar grade, BDH Ltd).

For Sepharose 2B, 4B and 6B, investigators (Crone, 1974) have suggested that ionic interactions are not eliminated until 0.2 M ionic strength. On the other hand for the classical carbohydrate gels, hydrophobic interactions do not come into play until the ionic strength exceeds 0.36 M (Schmidt et al, 1980). According to these findings the concentration of sodium chloride was set to 0.20 M. Sodium azide was used to prevent microbial growth. Previous to its use the buffer was vacuum degassed and all the particulates were removed using a 0.2 μm filter (Millipore Inc).

2.3.1.5 Experimental apparatus.

The experimental apparatus consisted of a FPLC (Fast Protein Liquid Chromatography) system from Pharmacia LKB which included the following parts:

a) LCC-500 controller. 32 Kb memory.

b) Two high precision pumps P-500. These pumps work at constant flow within the range 1-499 ml/h, up to a maximum pressure of 4 MPa (40 bar). They are equipped with a membrane pressure sensor which consists of a diaphragm that contracts or expands with pressure changes causing the resistance in an electronic bridge to change. This gives a signal that is proportional to the backpressure, i.e. 0.5 MPa/mV. The signal is amplified and relayed to the pressure output which can be connected to a recorder or to an A/D interface.

c) Two high precision pumps P-6000. These pumps work on the same principle as the P-500, but have a flow rate range of 0.1-99.9 ml/min and provide pressures up to 2 MPa (20 bar).

d) Valve MV-7. A 3 position, 7-port motorized valve used as an automatic injection valve.

e) Valve MV-8. Motorized valve used as an automated selection valve for columns.

f) Single path UV monitor UV-1. It measures absorption at 280 nm.

The output signal of the UV monitor and the pressure sensor were connected to a computer which was used to store and process the data. The system consisted of the following parts:

g) PS/2 IBM 386 Model 55 SX, 20 MHz, 40 Mb hard disk.

h) A/D interface PE NELSON 900 series. Model 970 with 256 Kb memory.

i) Chromatography software. Turbochrome 2.1 from PE NELSON.

2.3.2 Parameter estimation.

The hydrodynamic models described in section 2.2 require a number of parameters to be determined or estimated in order to carry out any possible prediction. Figs. 2.4a and 2.4b show the liquid, matrix and column properties required to be measured for input into each of the corresponding models, to give as result the solids pressure and the void fraction at each axial position along the column, as well as the column pressure drop for a particular value of the liquid flow rate.

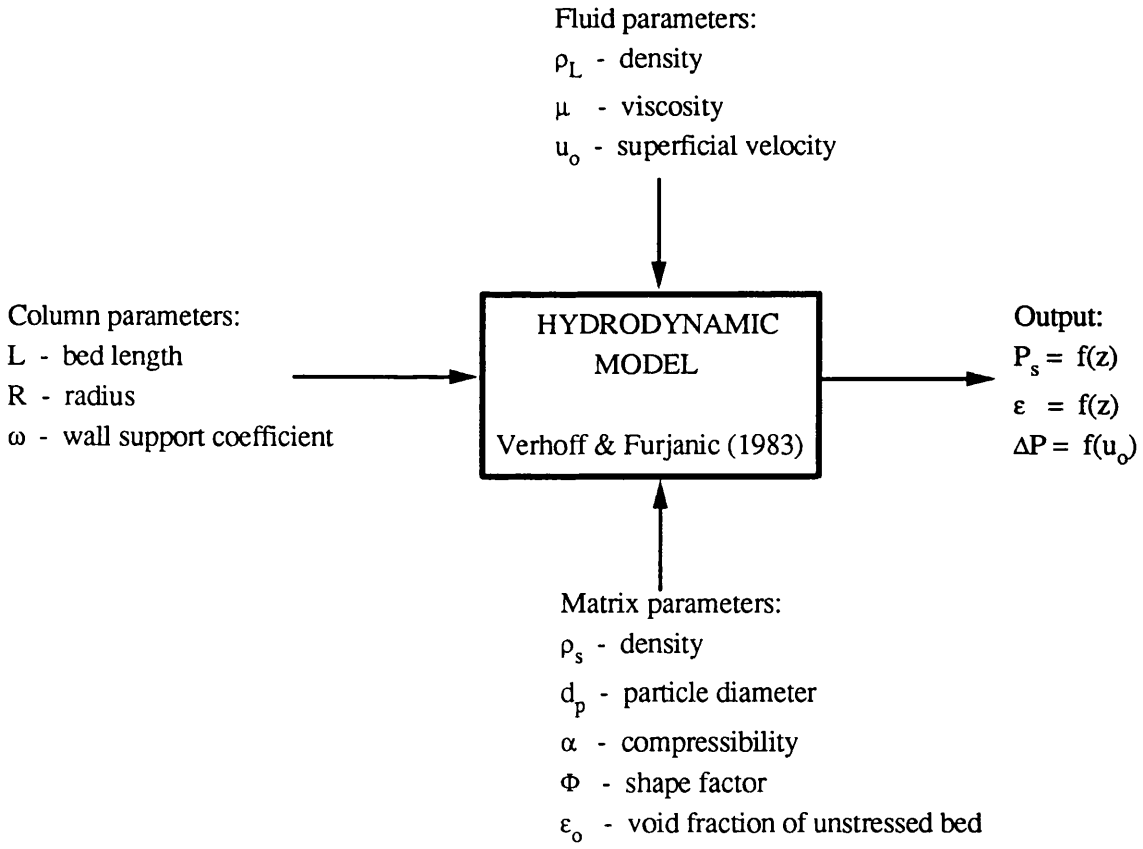

Fig. 2.4a Parameters required by the hydrodynamic model developed by Verhoff and Furjanic (1983), and model output.

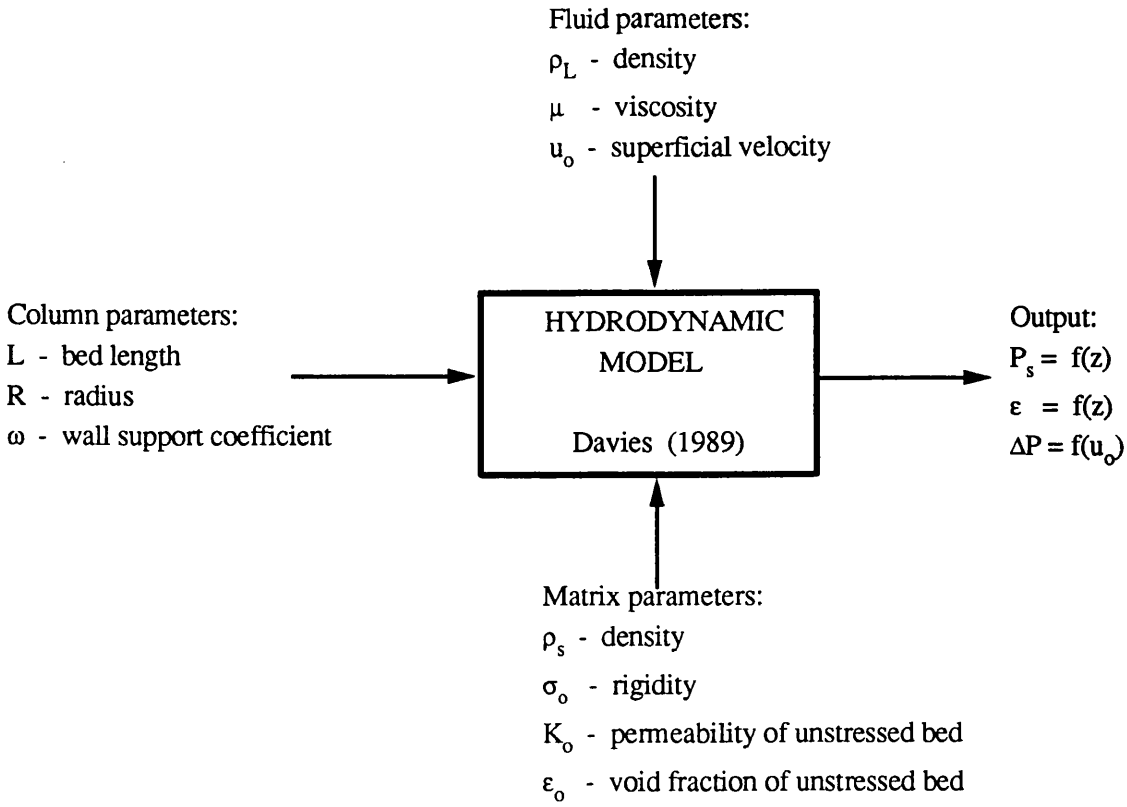

Fig. 2.4b Parameters required by the hydrodynamic model developed by Davies (1989), and model output.

2.3.2.1 Determination of buffer viscosity.

The viscosity of the buffer (0.05 M phosphate, 0.20 M sodium NaCl and 0.02% sodium azide, pH= 7.0) was measured at a range of temperatures with a Contraves Rheomat 115 (Contraves Industrial Products Ltd), using a bob and cup system. The results are shown in table 2.1.

Table 2.1 Viscosity of the phosphate buffer at different temperatures.

Temperature °C	20.0	21.0	22.0	24.0	25.0	28.0	29.0	30.0
Viscosity (mPa-s)	1.118	1.114	1.105	1.097	1.088	1.043	0.910	0.884

2.3.2.2 Determination of buffer density.

To measure the density of the phosphate buffer a specific gravity bottle with a volume of 50 ml at 20 °C was used. The density of the buffer was very close to that of water, ρ_L= 1.0041 g/ml at 20 °C.

2.3.2.3 Measurement of chromatographic particles density.

The density of the Sepharose 6B particles was estimated by means of the following procedure: An exact volume of gel slurry (Sepharose 6B and phosphate buffer) was weighed and left overnight for the beads to settle. The volume of the settled gel was measured as well as the volume of the buffer on the top. Since the density of the buffer is known, the weight of the settled gel was found by difference, and by assuming its void fraction to be 0.4 the gel density was calculated. It was found to be ρ_s= 1.0575 g/ml.
The density of Sepharose CL-6B as measured by means of the same methodology was very much the same as that of Sepharose 6B, i.e. ρ_s= 1.0587 g/ml.

2.3.2.4 Measurement of particle size distribution and mean particle diameter.

To measure the particle size distribution of the Sepharose 6B and Sepharose CL-6B particles an image analyzer was used, the Magiscan 2A system (Joyce-Loebl Ltd). A sample of the gel beads was placed in a haemocytometer (depth 0.2 mm) and the diameter of 300 beads was measured using the point to point function of the image analyzer. Before the measurement was carried out the particles were left in contact with the phosphate buffer overnight so that they would swell and acquire the size they would have during all the experiments. The resultant size distributions of the two types of Sepharose are shown in fig. 2.5. The bead size range obtained compared very well with the manufacturer's reported range i.e. 45-165 μm.
The mean value of the particle diameter d_p to be used in permeability models, including the Kozeny-Carman (Carman, 1937) and the Blake-Kozeny (Bird et al, 1960) equations, is of considerable importance. It has been found (Rumpf and Gupte, 1971 and Dullien, 1979) that the most consistent results are obtained if the surface average value of d_p is used. This is defined as follows:

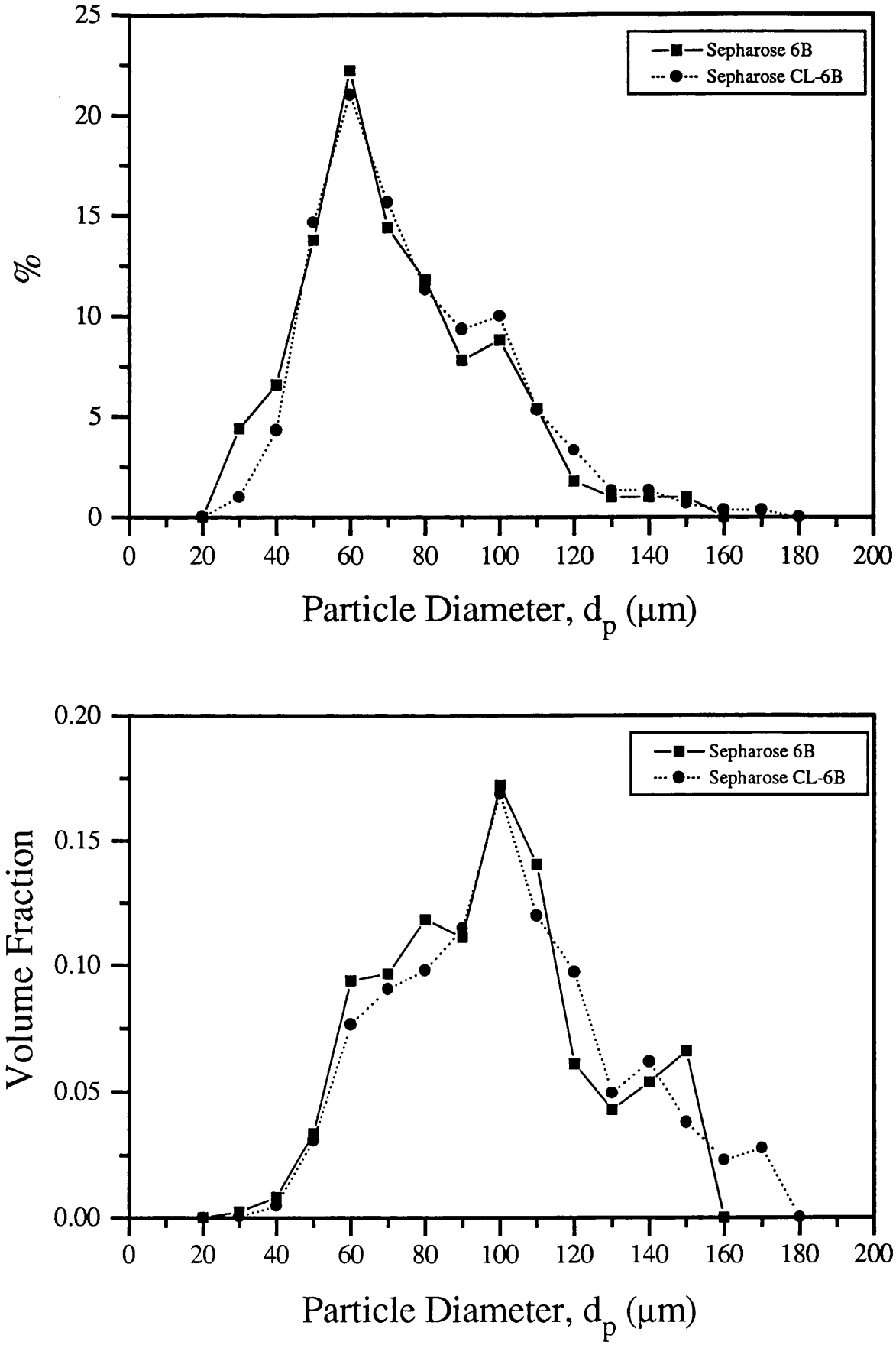

Fig. 2.5 Particle size distribution of Sepharose gels used in this study. Percentage frequency distribution (top) and volume fraction distribution (bottom).

$$d_{p_{mean}} = \frac{\left[\int_0^\infty d_p(d_p^2)n(d_p)\mathrm{d}d_p\right]}{\left[\int_0^\infty d_p^2 n(d_p)\mathrm{d}d_p\right]} \qquad (2.16)$$

where $n(d_p)$ is the particle size distribution. Rasmuson (1985a) also suggested that the appropriate average particle radius R_p to be used in chromatographic models is that giving an equivalent surface area per unit volume of particles (surface average radius). The average radius R_p can be calculated directly from the measured particle size distribution using the following equation which is the discrete form of the previous equation.

$$R_p = \frac{\sum_{i=1}^{N} R_{p_i}^3}{\sum_{i=1}^{N} R_{p_i}^2} \qquad (2.17)$$

By means of eq. 2.17 the mean particle diameter of Sepharose 6B was found to be d_p= 88 µm and that of Sepharose CL-6B, d_p= 92 µm. These values compare very well with those reported in the literature. Andersson (1985) reported the mean particle diameter for Sepharose 6B and Sepharose CL-6B to be around 110 µm. Davies (1989a) determined a mean particle diameter of 86 µm for Sepharose CL-4B while Boyer and Hsu (1992) found a value of d_p= 92 µm for Sepharose CL-6B.

2.3.2.5 Determination of matrix compressibility and wall support coefficient.

The wall support coefficient, ω was measured in two different ways, each involving a different procedure, a compression cell and an oedometer-type cell.

Compression cell. The rig used in the first procedure is shown in fig. 2.6. Its construction was based on the compression cell used by Verhoff and Furjanic (1983). A small glass tube (ID= 16 mm) surrounded by a protecting screen was used to contain the gel sample. Beds of approx. 9 cm were formed by allowing 75% (v/v) gel slurry (25% buffer and 75% settled gel) to gravity settle. The gel slurry was previously degassed under vacuum. At the bottom of the glass tube a porous support (copper sinter) was placed to allow the liquid to flow out and to retain the gel beads. The piston head was made of PTFE in order to produce a good seal against the tube walls while largely reducing the friction force between these two surfaces. A good seal between the piston head and the tube walls was required so that the bed would not drain dry and the gel particles would not escape during bed compression. To measure ω, a constant pressure was exerted on the

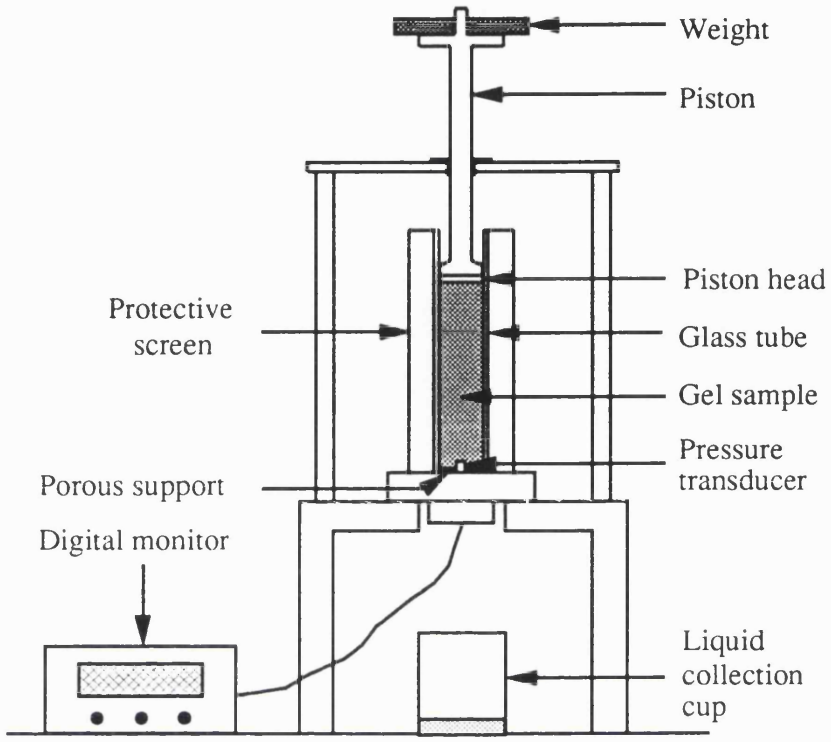

Fig. 2.6 Compression cell used in the determination of the wall support coefficient ω and the matrix compressibility α of Sepharose gels.

top of the bed by means of weight loads. A period of 12 hours was allowed for the bed to consolidate. Then the pressure transmitted to the bottom of the bed was measured by means of a miniature pressure transducer EPX-10W-50A (Entran Ltd).

By neglecting the density term and since no flow is passed through the bed allows eq. 2.9 to be reduced to

$$\frac{dP_s}{dz} = -\omega P_s \qquad \textbf{(2.18)}$$

the solution of which is

$$P_s(z) = P_o e^{-\omega z} \qquad \textbf{(2.19)}$$

where P_0 is the applied pressure at the top of the bed, and since the pressure transducer was placed at the bottom of the column, $P_s(z)$ corresponds to the transmitted pressure at this position. The wall

support coefficient ω, was evaluated by means of this equation. The load required to overcome the friction between the piston head and the column walls was measured by carefully adding weights on top of the piston until it began to slide down when the glass column was empty. This load was subtracted from the total load applied on the bed in order to obtain P_o. The correction was made before using eq. 2.19 to evaluate ω, and before the evaluation of α.

In the experiment previously described the change in bed length when a load was applied was also measured. This information and eq. 2.10 were used for the evaluation of matrix compressibility α, according to the following assumptions: A) any decrease in volume is due to loss in the interparticle void volume only, B) the pressure is constant throughout the whole sample and C) the void fraction of the unstressed bed[2] was ε_o= 0.4.

In order to measure the changes in bed length the rig was placed on a surface plate and the bed height was measured by means of a vernier height gauge. Experiments employing the compression cell were carried out using a series of increasing weight loads for each set. Four sets were conducted with each Sepharose gel.

Oedometer-type cell. The second procedure was based on a method of soil mechanics suggested by Basset (1992) and based on the premise that the friction force between the packing and the column walls becomes negligible as the column diameter tends to infinity. By applying a series of stresses on beds of increasing diameter and measuring their degree of compression, it is possible to extrapolate the degree of settlement that a bed of infinite diameter would experienced under such an applied stress. Subsequently this information can be used to evaluate the wall support coefficient ω.

This procedure involved the construction of a special rig as shown in fig. 2.7, and the use of three different diameter glass tubes (precision bore), i.e. 16 mm, 30 mm and 50 mm. The rig design was a modified version of the oedometer cells used in consolidation tests in soil mechanics (Scott, 1969). In order to avoid contact and therefore friction between the piston head and the tube walls, a gap of 0.050 mm was left between these surfaces. This gap was small enough to avoid the leakage of gel particles.

Initially a series of consolidation experiments were carried out with this oedometer-type cell and the 50 mm diameter glass tube to determine the rate of settlement and therefore the loading period required by these particular gels, i.e. Sepharose 6B and Sepharose CL-6B. A shallow bed of

[2] This assumption seems quite reasonable according to the values reported in the literature for packed beds with rigid spheres. The intermediate void fraction for random-poured packings is in the range 0.4-0.38. These packing consist of a combination of local regions of random-loose (ε= 0.42) and random-close packings (ε=0.36) (Reyes and Iglesia, 1991)

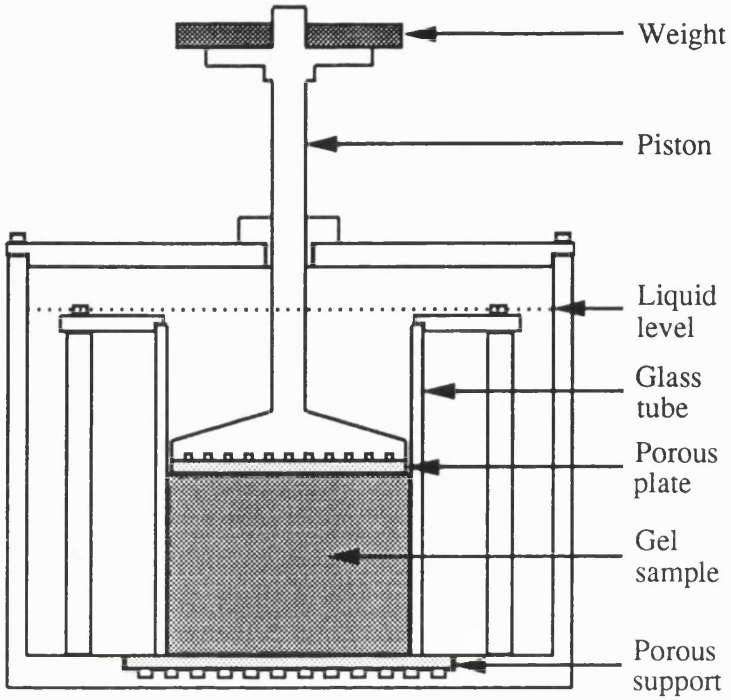

Fig. 2.7 Oedometer-type cell used in the consolidation experiments carried out in order to determine the wall support coefficient ω, and the matrix compressibility α of Sepharose gels.

approximately 4.5 cm was formed by allowing degassed 75% (v/v) gel slurry to gravity settle inside the 50 mm glass tube. The bed was loaded vertically and a record was made of settlement against time. When the settlement was substantially complete, the load was increased. A standard load increment ratio of 2:1 (the load was doubled at the end of each stage) and a loading period of 48 hours were used in these tests. Porous plates were placed at the top and bottom of the sample so that it could freely drain from both surfaces. The liquid level outside the glass tube was always above the top of the gel bed so as to prevent the bed from draining dry. The widest diameter glass tube (ID= 50 mm) was used in this set of experiments so that the wall support was almost negligible[3].

Following the determination of the loading period, a series of experiments was carried out with both gel matrices and the oedometer-type cell, this time all three glass tubes of increasing diameter were used. The experimental procedure was basically the same as that used in the previous consolidation experiments. The loading period was reduced to 24 hours and different initial bed lengths were used according to the tube diameter so that the area of contact between the gel matrix

[3] Although not very well established it is considered that wall support is negligible for column diameters greater than 5.0 cm (Cox, 1990).

and the tube walls was fairly constant in all cases. Accordingly the initial bed lengths were of 4.75 ± 0.05 cm with the 16 mm diameter tube, 2.52 ± 0.03 cm with the 30 mm diameter tube, and 1.52 ± 0.03 cm with the 50 mm diameter tube. The area of contact was 23.8 ± 0.3 cm^2. The changes in bed length of these samples were measured while the load was doubled at the end of each period. As in the previous experiments the rig was placed on a surface plate and the bed height was measured by means of a vernier height gauge.

To determine the matrix compressibility α, the measured bed lengths in the latter set of experiments were used to determine the changes in void ratio e, as a function of applied pressure (see fig. 2.12). This information in turn was used to derive the corresponding values for an infinite diameter column (see fig. 2.13). Eq. 2.10 was used for the evaluation of α according to the same assumptions made in the previous procedure (compression cell). Since α was evaluated for the column of infinite diameter, no correction to account for frictional forces was required. The evaluation of the wall support coefficient by means of this procedure is presented in section 2.4.1.

2.3.2.6 Permeability measurement.

The permeability of both Sepharose gels was measured as a function of applied stress, in order to define the empirical relationship (eq. 2.12) and to determine the matrix compressibility α.

The measurement of permeability as a function of stress was carried out using a permeability cell similar to that used extensively by Grace (1953) for testing filter cake materials and to that used by Davies (1989) for the measurement of permeability of Sepharose CL-4B beds (see fig. 2.8). As with the oedometer-type cell a gap of 0.05 mm between the walls of the glass tube and the piston was allowed so that no friction occurred between these surfaces. This gap was small enough as to impede the leakage of gel particles.

The experimental measurements were carried out according to the following procedure. Sepharose gel slurry was prepared with about 75% (v/v) of settled gel and 25% (v/v) of 50 mM phosphate buffer. A measured volume of degassed slurry was then allowed to settle in the glass tube (diameter 1.6 cm) for a few hours in order to form a bed approx. 1 cm high. The bed was then compressed between two porous surfaces by means of weights placed on a loading platform as shown in fig. 2.8. Buffer was allowed to flow through the gel bed at constant pressure. The flow rate was measured by collecting the flowing buffer for a constant period of time and then weighing it. The load on the bed was increased every 30 min. This period of time was sufficient for the bed to fully consolidate under the increasing load.

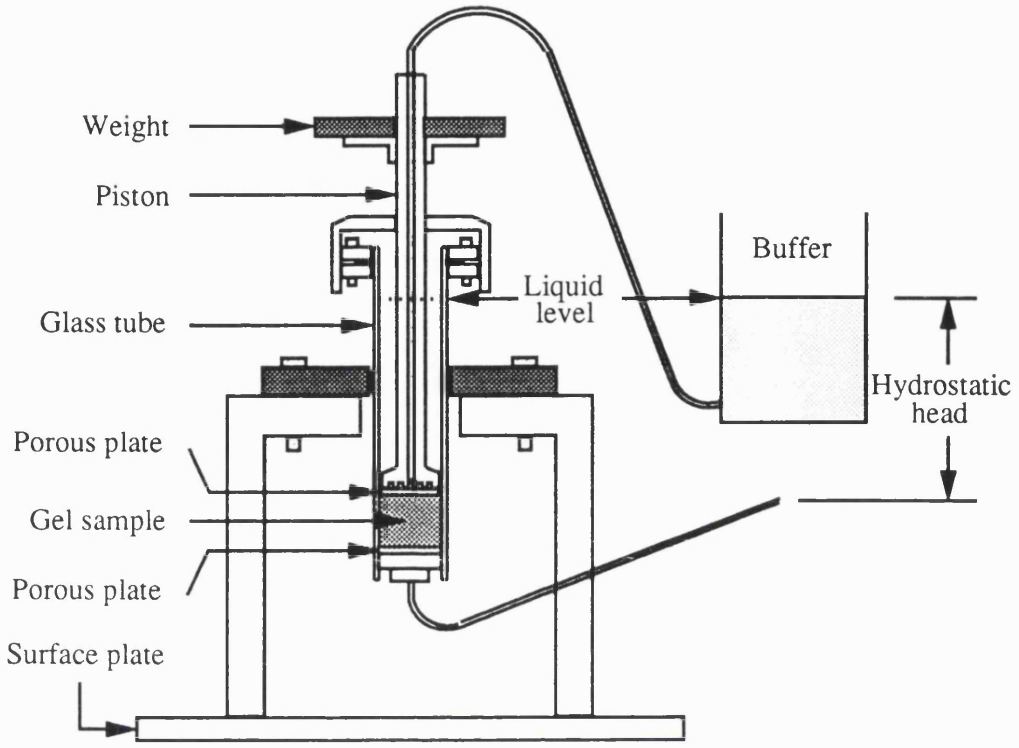

Fig. 2.8 Cell used to determine the permeability of Sepharose gels as a function of applied pressure.

In order to measure the bed height every time it was compressed, the apparatus was placed on a surface plate and the height of the loading platform was measured with a vernier height gauge. Very shallow beds were used so that the weight of the gel and the friction against the column walls were negligible. If the ratio of bed height to diameter does not exceed 0.6, the effect of wall support is negligible (Grace, 1953) and the porosity and the stress distribution within the bed can be considered to be uniform. The pressure head (<5 cm) was small enough as to produce only a small stress relative to the loading pressure. Therefore the bed was not disturbed by the flow and the bed could be considered homogeneous. The compressive stress was assumed constant throughout the whole of the bed. The calculation of permeability was based on the height of the bed in its compressed state and was carried out by means of Darcy's Law (1856). The total pressure head applied on the system (gel bed plus permeability cell) was corrected by subtracting the pressure drop caused by the cell only, before evaluating the bed permeability. Two sets of permeability experiments were conducted with each Sepharose gel.

2.3.3 Experimental determination of flow rate-pressure drop curves.

The evaluation of the predictive capabilities of the hydrodynamic models of Verhoff and Furjanic (1983) and Davies (1989) involve the comparison of experimental flow rate-pressure drop curves with those simulated by these models. The schematic representation of the system configuration used in the experimental measurement of flow rate-pressure drop curves is shown in fig. 2.9.
The following columns were used in the experiments: XK16/10, HR16/30, XK16/70, XK26/40, XK26/100 and XK50/40 (Pharmacia LKB Biotechnology). These columns have three different diameters, i.e. 1.6, 2.6, and 5.0 cm, and different adjustable lengths.
The P-500 pumps were used with all the columns with the exception of the XK50/40 which used the P-6000 pumps.

In order to ensure that there were no particulates that might clog the columns, in addition to filtering the buffer, a 0.45 μm filter (Pharmacia LKB Biotechnology) was placed upstream of the column. Frits were also placed at the top and bottom of the beds.
All the columns were packed by allowing degassed 75% (v/v) gel slurry (75% settled gel and 25% phosphate buffer) to gravity settle until the bed height became constant (approx. 5 hours). The top column adaptor was then inserted down very carefully to avoid bed compression. For this reason a very small gap (approx. 2 mm) was left between the adaptor and the top of the bed. When the flow rate was increased the bed compressed and the gap increased. Since pushing down the adaptor could itself cause additional compression, the adaptor was left fixed at its initial position for the whole experiment.

Flow rate was increased step by step until close to the critical flow rate (maximum flow rate) at which point the pressure drop did not equilibrate. At each flow rate, the bed was allowed to equilibrate so that the pressure drop and the bed length were constant. The period of time needed for equilibration depended very much on the column dimensions. For the shortest column 10 min was sufficient, for the medium length columns 30-40 min were required and for the longest column it took 60-90 min before equilibrium was reached. The bed length and the pressure drop at each flow rate were recorded.
The pressure drop due to the system which includes connecting tubing, column and adaptors, valves, filter, frits and net rings, was also measured as a function of flow rate. This extra-column pressure drop was obtained for each column by measuring the pressure drop across an empty column (no packing). Phosphate buffer was used in all the experiments (see section 2.3.1.4), which were carried out at room temperature, 23-27 °C.

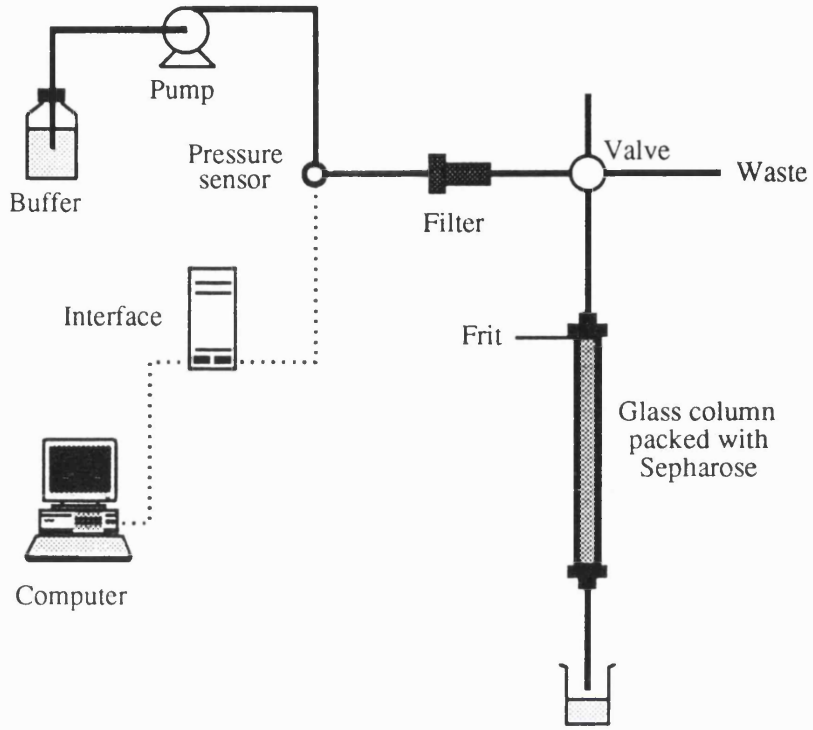

Fig. 2.9 System configuration used for the experimental measurement of the flow rate-pressure drop curves of the Sepharose gel beds.

2.3.4 Experimental determination of bed void fraction under different compression conditions.

In order to test the model capabilities to predict the bed void fraction, this parameter was measured for a column compressed at different flow rates. A XK 16/70 column (Pharmacia LKB Biotechnology) was packed with degassed 75% (v/v) Sepharose 6B slurry in phosphate buffer, at an initial flow rate of 0.3 ml/min. This produced a bed of 52.35 cm. The bed void fraction was measured by passing a 2.5 mg/ml solution of blue dextran 2000 at a flow of 0.1 ml/min through the column. The flow rate was then increased in steps. At each step the column adaptor was carefully pushed down to the top of the compressed bed, and the bed void fraction measured. The system configuration used in this experiment is presented in fig. 4.3 (see section 4.2.2.2).

2.3.5 Numerical methods.

Given the form of the equations describing both models tested in this study an analytical solution was not possible. Numerical integration was therefore needed. In this section the numerical methods used to solve the mathematical equations which describe each of these models, and that employed in the parameter fitting procedure to determine $k=150/\Phi^2$ are presented.

2.3.5.1 Solution of model equations.

Both the hydrodynamic model developed by Verhoff and Furjanic (1983), equations 2.9 and 2.10, and the set of equations 2.12 and 2.14 which constitute the model developed by Davies (1989) were solved using a classical fourth-order Runge-Kutta method (Flannery and Teukolsky, 1989). Equation 2.6 or eq. 2.15 which describe the pressure drop along the column were integrated simultaneously with the model equations. The integrations were carried out using 200 steps of constant size.

The iterative procedure used in the estimation of the wall support coefficient ω and the matrix compressibility α and described in section 2.4.1, was also carried out by means of the Runge-Kutta method. All the simulations and parameter estimations were carried out employing a SUN SPARC station 1 (Sun Microsystems Europe, Inc).

2.3.5.2 Determination of $k=150/\Phi^2$.

In order to carry out simulations with the model of Verhoff and Furjanic it is required to evaluate the constant $k=150/\Phi^2$ (see eqs. 2.4, 2.5, 2.6 and 2.9 in section 2.2). Its value was determined by fitting the model eqs. 2.9 and 2.10 to experimental pressure drop curves. The NAG Fortran Library routine E04FDF was used to carry out the optimisation. This routine uses a quasi-Newton algorithm for finding the minimum of a sum of squares of nonlinear functions. The derivatives of the function are not required by this routine, only the function values at each point. The routine is used for unconstrained problems. The objective function was the following sum of squares,

$$S = \sum_{i=0}^{n} [y_i - f(x_i)]^2 \qquad (2.20)$$

where n is the number of experimental points, y_i are the experimental values and $f(x_i)$ represents

the function values obtained with the hydrodynamic model. Depending on the number of experimental points to be fitted and the goodness of the initial values the optimisation procedure took between 10 and 25 min of computing time.

2.4 Results and discussion.

In this section the results of the compression experiments are presented and discussed. Initially the different methodologies used in the estimation of the model parameters are discussed in relation to the resulting values of these parameters. This is followed by the evaluation of the capabilities of the models tested to predict flow rate-pressure drop curves as well as bed void fraction.

2.4.1 Consolidation experiments and the measurement of matrix compressibility and wall support coefficient.

Compression cell. The values of the matrix compressibility α, obtained with the compression cell shown in fig. 2.6, were within the range α=5.85 - 7.86x10^{-2} kPa^{-1}, with an average value of α=6.75x10^{-2} kPa^{-1} for Sepharose 6B, and α=3.55 - 5.05x10^{-2} kPa^{-1}, with an average value of α=3.85x10^{-2} kPa^{-1} for Sepharose CL-6B. As expected Sepharose CL-6B is more rigid than Sepharose 6B and therefore its corresponding value for compressibility is smaller. Although these parameter values were of comparable magnitude to those reported in the literature, i.e. α=15.27x10^{-2} kPa^{-1} for Sepharose CL-4B (Davies, 1989), they proved to be smaller than those obtained using the permeability cell (section 2.4.2). The use of a narrow column diameter (1.6 cm) and a rather long sample (approx. 9.5 cm) occasioned the friction against the glass walls to give strong support to the gel samples. This may explain why the gels appeared to be more rigid (small values of α) than expected. Another reason for this discrepancy resides in the assumption made for the evaluation of α, i.e. all losses in void volume correspond only to losses in interparticle volume and hence that the intraparticle volume remains constant. This assumption applies for low loads when rearrangement of the gel particles from a loose, random packing to a more dense packing occurs. It is unlikely to apply at high loads when particle deformation is more significant. The value of the wall support coefficient, ω obtained with the compression cell (utilising a 1.6 cm diameter glass column, described in section 2.3.2.5), ranged from 0.014 to 0.102 cm^{-1}, with an average value of ω=0.043 cm^{-1} for Sepharose 6B, and from 0.028 to 0.124 cm^{-1}, with an average value of ω=0.064 cm^{-1} for Sepharose CL-6B. These values are very small when compared to

values in the literature (see table 2.2). Davies (1989) in his study of Sepharose CL-4B found the value of the angle of internal friction, θ, to be 14°, and that of the angle of friction against glass, δ, to be 7°. Since the ratio of lateral to vertical pressure $K' = 1-\sin\theta$, and the coefficient of friction $\mu' = \tan\delta$, the value of the wall support coefficient ω for a 1.6 cm diameter column can be evaluated to be 0.233 cm^{-1}. The disagreement in wall support coefficient values is probably due to inaccuracies in the measurement of the transmitted pressure. This results from the uneven load distribution caused by the presence of the pressure transducer itself (Basset, 1992). Error in the measurement of the friction force between the piston head and the column walls could also have contributed to this discrepancy. The uncertainty in the measured values of ω and α led to the implementation of the second procedure used in this study in order to corroborate their value and/or to improve the accuracy of their determination.

Oedometer-type cell. The results obtained from the initial consolidation tests with the oedometer-type cell and Sepharose 6B are presented in figs.2.10 and 2.11. The graph of settlement vs $\sqrt{}$(time) (fig.2.10) shows the occurrence of instant and delayed compression (Bjerrum, 1967). This type of behaviour is typical of those materials with a very large structural viscosity, which is the case of the Sepharose gels analyzed. For these materials the dissipation of the pore pressure is very rapid and almost all the settlement is secondary (Bjerrum, 1967), as can be seen in the figure. In fig. 2.11 the settlement vs log(time) curve shows again that the consolidation of these gels is dominated by secondary compression resulting from particle deformation.

From this set of experiments it was concluded that a standard loading period of 24 hours was sufficient for the settlement of these gels to be substantially completed.

In fig. 2.12 the results from the consolidation tests using gel samples contained in glass tubes of three different diameters and the oedometer-type cell are presented. These graphs clearly show the effect of increasing the column diameter on wall support. For a particular value of applied stress, as the column diameter increases the resulting void ratio e, becomes smaller as a consequence of the diminishing support from the column walls.

This information has been used in fig. 2.13 to determine the stress that an infinite diameter column needs to experience so that it compresses to a particular value of void ratio. It can be observed that the stress diminishes linearly as the column diameter increases at constant void ratio. At the infinite diameter value the bed would compress with no support from the column walls. Finally in fig. 2.14 the stress vs void ratio curves have been replotted, this time including the curve corresponding to the infinite diameter column. This curve has been used to evaluate the compressibility α of these gels by means of eq. 2.10 , with $\varepsilon_o = 0.4$. Since in this case friction is negligible, no correction is needed for the evaluation of this parameter. The values obtained were $\alpha = 13.76\times10^{-2}$ kPa^{-1} for Sepharose 6B and $\alpha = 10.78\times10^{-2}$ kPa^{-1} for Sepharose CL-6B.

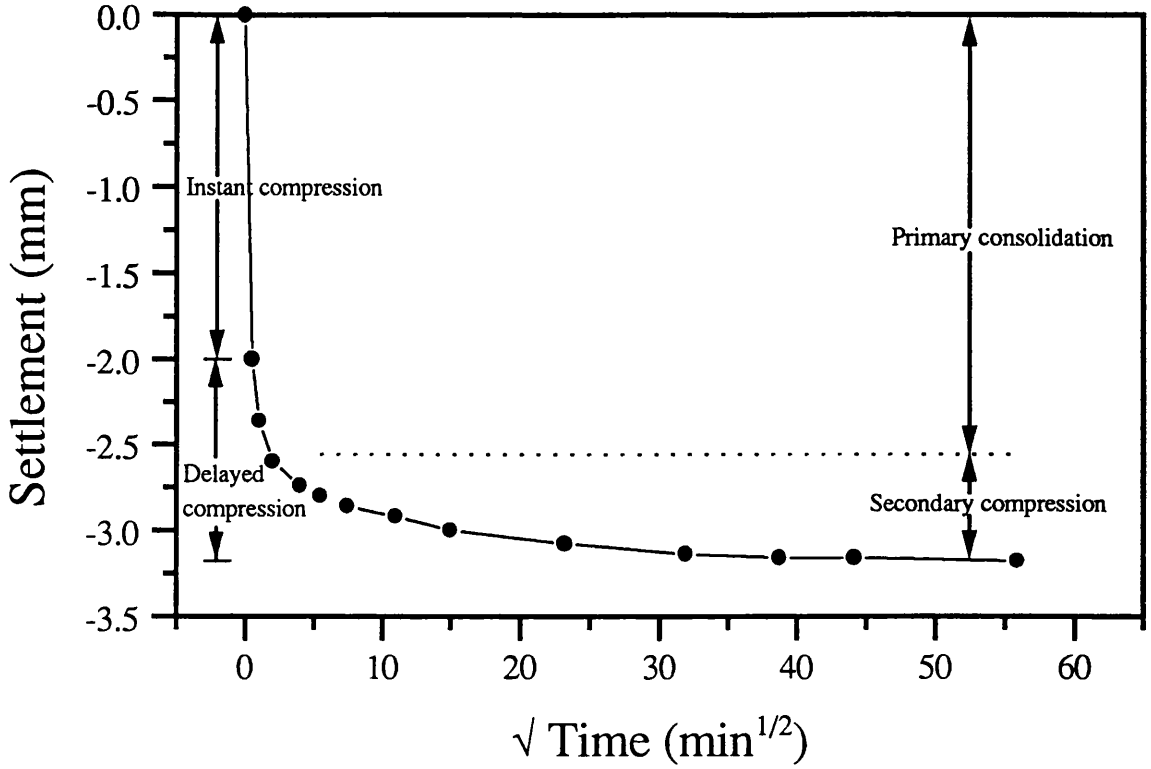

Fig. 2.10 Consolidation of Sepharose 6B. The plot shows the presence of instant and delayed compression. Gel sample, 5 cm diameter and initial length of 3.91 cm , loaded with 10 kPa.

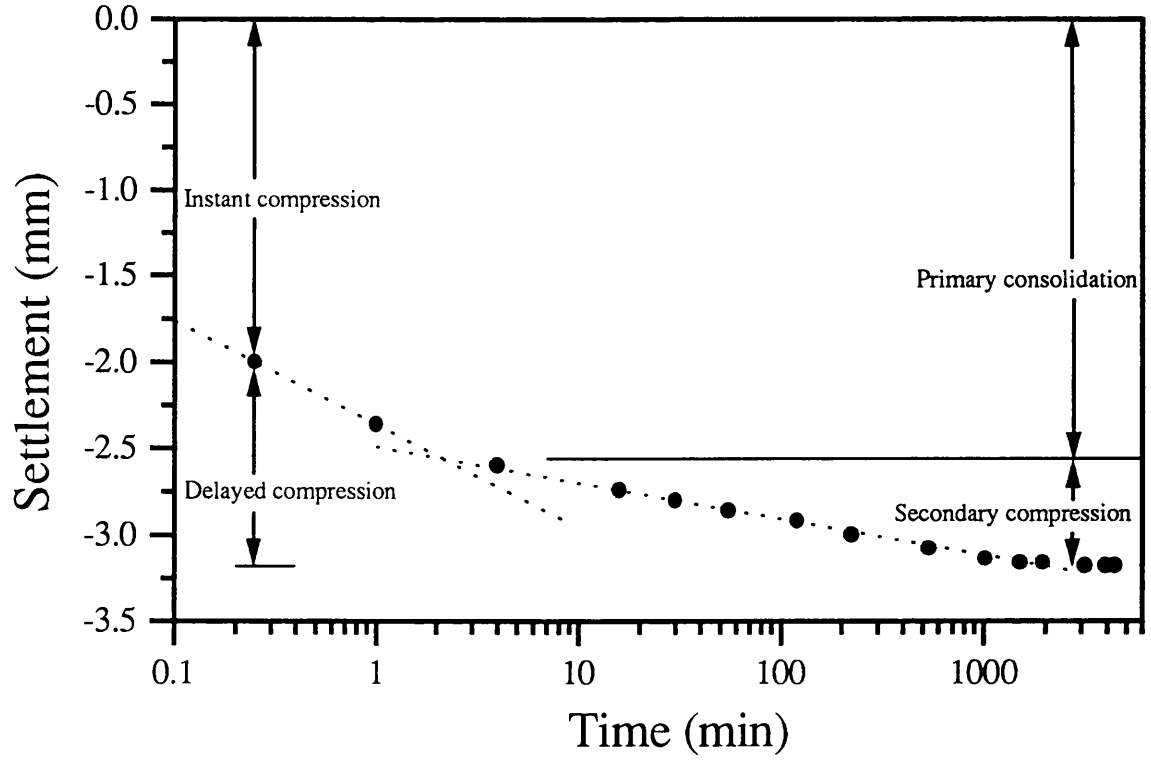

Fig. 2.11 Consolidation of Sepharose 6B. The consolidation process is dominated by secondary compression. Gel bed, 5 cm diameter and initial length of 3.91 cm loaded with 10 kPa.

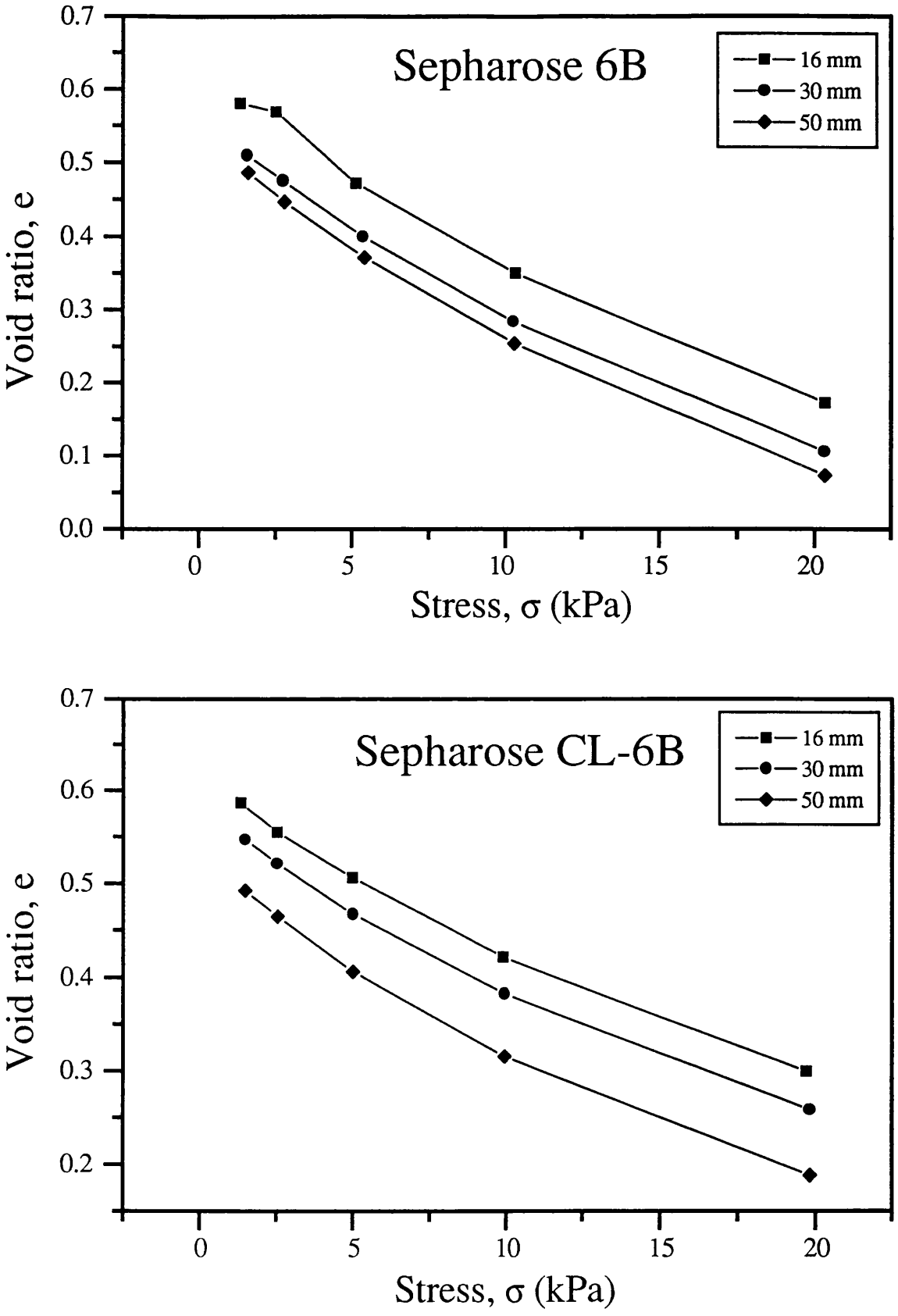

Fig 2.12 Consolidation of Sepharose gels. Void ratio e, of gel samples of three different diameters, as a function of applied stress σ. The bed lenght of each of the samples was set so that the lateral area was initially equal for the three gel samples (see section 2.3.2.5). A standard loading period of 24 h was used.

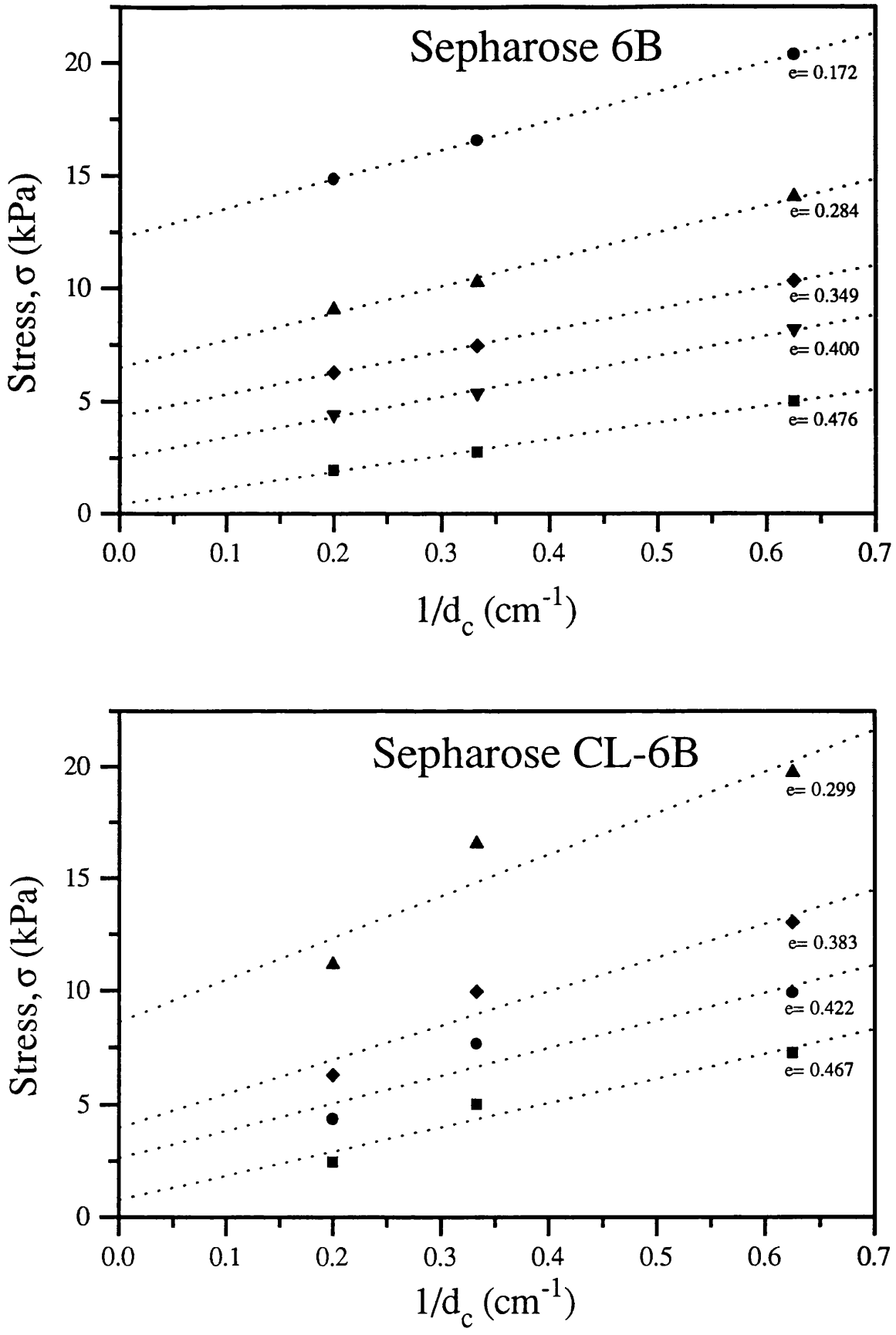

Fig 2.13 Stress required to compress a gel sample contained in a glass column of diameter d_c, to a particular value of void ratio, e. The corresponding stress for a column of infinite diameter where frictional forces against column walls are negligible, is obtained from the y-intercept of the lines of constant void ratio, e.

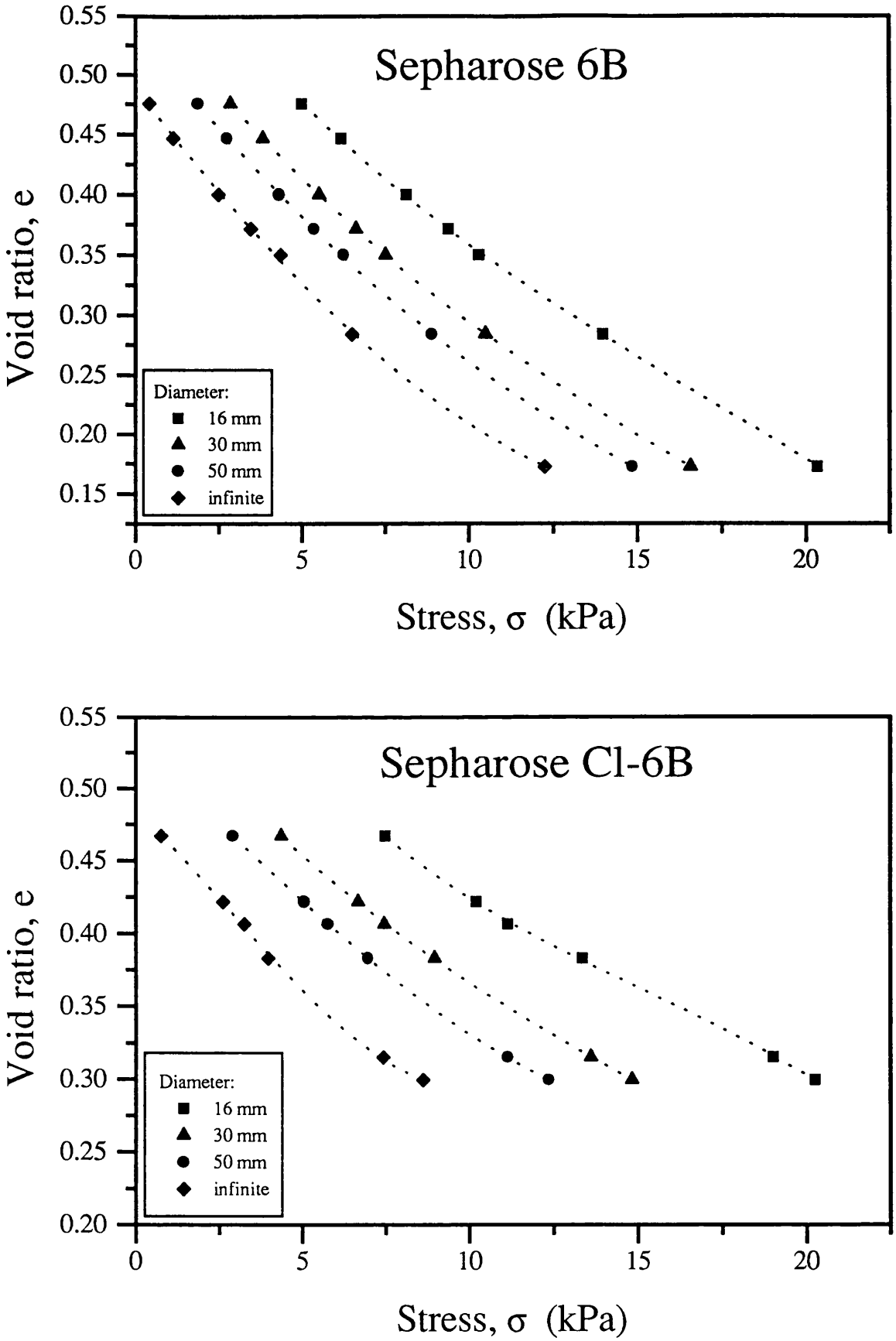

Fig. 2.14 Void ratio e, as a function of stress σ, of Sepharose samples of different diameter. The curve corresponding to a sample of infinite diameter, obtained from fig. 2.13., is also shown. A standard loading period of 24 h was used.

In a different evaluation an iterative procedure which involved the use of the hydrodynamic model and the information contained in fig. 2.14 was used to estimate the value of the wall support coefficient ω, as well as that of the matrix compressibility α. Since there was no fluid flow through the bed in these experiments, eq. 2.9 simplifies to

$$\frac{dP_s}{dz} = \Delta\rho(1-\epsilon) - \omega P_s \qquad (2.21)$$

where again the void fraction, ϵ is a function of the bed compressibility α, and the solids pressure P_s, according to

$$\epsilon = \frac{\epsilon_o}{1 + \alpha P_s} \qquad (2.22)$$

and it is related to the void ratio e, by

$$\epsilon = \frac{e}{1 + e} \qquad (2.23)$$

The solution of these equations 2.21 and 2.22 was carried out numerically (see section 2.3.5.1) using the following initial conditions:

$$\begin{aligned} P_s &= \sigma_T , \quad z = 0 \\ \epsilon &= \epsilon_T , \quad z = 0 \end{aligned} \qquad (2.24)$$

where the value of interparticulate stress at the top of a gel sample σ_T, was equal to the applied pressure on the bed, and the value of void fraction at the top of the bed ϵ_T, was that corresponding to the void ratio of a column of infinite diameter subjected to a stress equal to σ_T. The iterative estimation of the wall support coefficient and the matrix compressibility was carried out by varying their values until the void fraction of the bed as determined by numerical integration matched the experimentally measured value of ϵ_{av}, the average void fraction of the sample to a tolerance of 10^{-2}. This is the matching condition:

$$\epsilon_{(theoretical)} \approx \epsilon_{av,(experimental)} \qquad (2.25)$$

The numerical integration of ϵ along the bed to determine its average void fraction was performed simultaneously with the solution of the model equations (eqs. 2.21 and 2.22).

The previously obtained value of matrix compressibility α, was used as an initial guess, while the values of ϵ_T and ϵ_{av} were obtained by linear interpolation from the curves in fig. 2.14. ϵ_T was

interpolated from the infinite diameter curve, and ε_{av} from the experimental curve corresponding to the column diameter being used in the present numerical calculations. The values of the remaining parameters were: ε_o= 0.4, and the value of L, was the experimentally measured value of bed length when compressed under the stress σ_T.

The values of the wall support coefficient obtained by means of the previous iterative procedure were for the case of a 16 mm diameter column: ω=0.318 cm^{-1} for Sepharose 6B and ω=0.343 cm^{-1} for Sepharose CL-6B. As expected the value of ω was almost the same for both these gels since their composition and properties are very similar (see section 2.3.1.1) and therefore their interaction with the glass walls must be of a comparable degree.

On the other hand the average matrix compressibility values obtained were: α= 12.5x$10^{-2}$$kPa^{-1}$ for Sepharose 6B and α= 9.95x10^{-2} kPa^{-1} for Sepharose CL-6B. These values are of the same order of magnitude of those reported by Davies (1989) (see table 2.2).

The parameter values obtained with this procedure were consistent with experimental observations, as confirmed by the simulations of the pressure drop curves (see section 2.4.3). However, some discrepancies existed mainly in respect to the wall support coefficient ω, which appeared to be approx. 70% higher than reported values from the literature for similar gels (Davies, 1989). The values of matrix compressibility α, were very much the same as those determined along with permeability in section 2.4.2 (see table 2.2).

These discrepancies result from a number of sources of error within the parameter determination procedure. Sample disturbance was occasioned when the bed was initially loaded with a weight (piston placed at the gel surface). It is highly probable that when the piston was introduced into the glass tube containing the gravity settled gel, some degree of preconsolidation occurred. However, as noted earlier (see section 2.4.1) the most important source of error was the assumption that volume reduction occurred solely as a result of the loss of interparticle void volume. Since gel particles deform under compression (Horváth, 1990; Andrei et al, 1993), it is clear that intraparticle void volume is also lost especially at high weight loadings of the sample. Another possible source of error was the probable trapping of the largest gel particles between the tube glass walls and the head of the piston. This could have produced extra friction. Difficulties in alignment of the piston could also have resulted in the addition of extra-friction forces, since contact between the piston head and the tube glass walls might have occurred.

2.4.2. Permeability of Sepharose gels.

Figure 2.15. shows the results of the compression-permeability test, on semilogarithmic axes. It

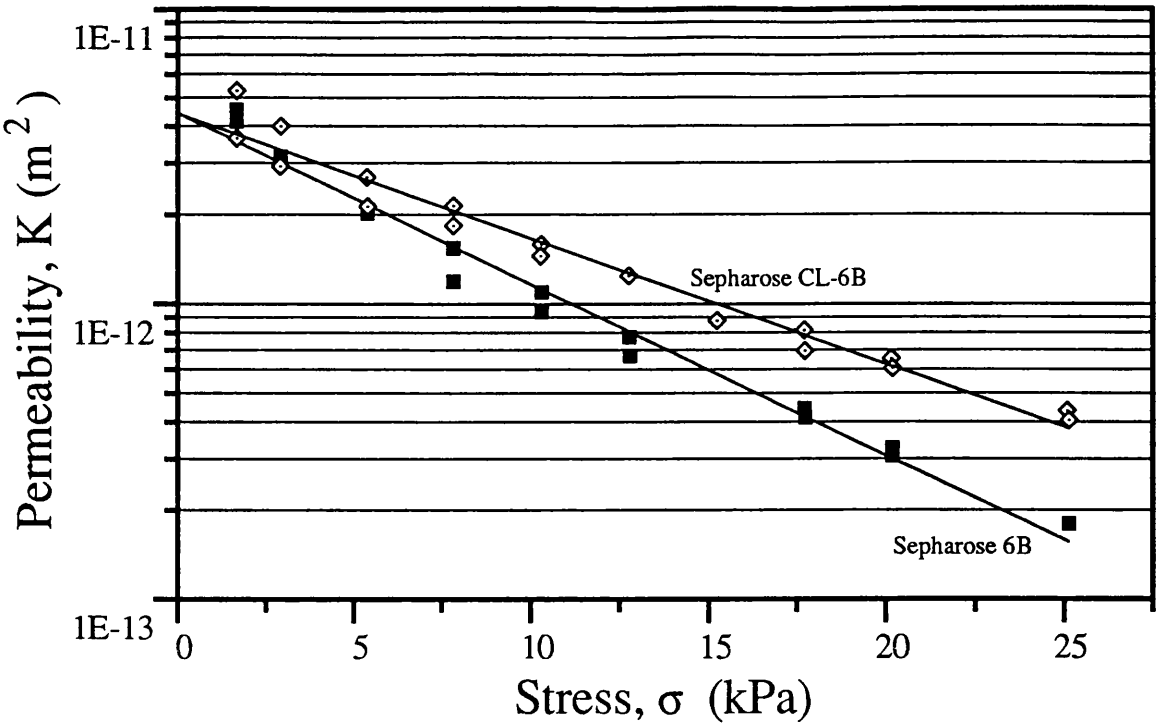

Fig. 2.15 Permeability of Sepharose gels as a function of applied stress, as measured with rig shown in fig. 2.8. Equation 2.12 has been used to fit the experimental points.

can be seen that straight lines are obtained for both Sepharose 6B and Sepharose CL-6B. The model equation for the dependence of permeability on stress is accordingly to Davies(1989) of the form:

$$K = K_o \exp(-\sigma/\sigma_o) \qquad (2.26)$$

where K_0 corresponds to the y intercept and represents the permeability of the unstressed bed. On the other hand σ_0 is the reciprocal of the line gradient and is proportional to the matrix rigidity. The values of these parameters were obtained as $K_0 = 4.44 \times 10^{-12}$ m^2 and $\sigma_0 = 17.27$ kPa for Sepharose 6B, and as $K_0 = 4.43 \times 10^{-12}$ m^2 and $\sigma_0 = 23.59$ kPa for Sepharose CL-6B. This experiment was fairly reproducible as can be seen from the superposition of the experimental points in fig. 2.15. The parameter values are accurate within about ± 8 %.

The value of K_0 was practically the same for both gels. This seems reasonable since their particle size distributions are very similar and therefore the porosity of the unstressed settled gel (randomly packed bed) was expected to be very much the same for both gels.

From fig. 2.15 it can be observed that the slope of the line corresponding to Sepharose 6B is steeper than that one of Sepharose CL-6B. This is in agreement with its larger compressibility α, or its smaller rigidity as expressed by the value of the parameter σ_0. A line corresponding to a non-compressible matrix would have a slope of zero ($\alpha = 0$, $\sigma_0 = \infty$).

Table 2.2 Matrix model parameter values as determined by different procedures.

Experimental Procedure	Matrix compressibility $\alpha=1/\sigma_o$ (kPa^{-1})	Wall support coefficient $\omega=2K'\mu'/R$ R= 0.8 cm (cm^{-1})	$K'\mu'$	Friction[A] coefficient μ'	Angle of friction[F] δ
SEPHAROSE 6B					
Compression cell (fig. 2.6)	6.75×10^{-2}	0.043	0.0172	0.023	1.3°
Oedometer-type cell (fig. 2.7)	12.5×10^{-2} 13.76×10^{-2} [B]	0.318	0.127	0.168	9.7°
Permeability cell (fig. 2.8)	13.3×10^{-2}	-	-	-	-
SEPHAROSE CL-6B					
Compression cell (fig. 2.6)	3.85×10^{-2}	0.064	0.0256	0.034	1.93°
Oedometer-type cell (fig. 2.7)	9.95×10^{-2} 10.78×10^{-2} [B]	0.343	0.1372	0.181	10.26°
Permeability cell (fig. 2.8)	9.76×10^{-2}	-	-	-	-
Reported values (Davies, 1989)[C]	15.27×10^{-2}	0.199	0.0795[D]	0.123[E]	7°

Notes: **A.** These values have been estimated assuming $K'= 1-\sin\theta$ (Jaky, 1944), where the angle of internal friction $\theta= 14°$ (Davies, 1989). Therefore $K'= 0.758$.
B. These values were calculated using the consolidation curve of an infinite diameter column. All other values in this row were evaluated by the iterative procedure described in section 2.4.1.
C. These parameter values correspond to Sepharose CL-4B.
D. This value corresponds to $B= K'\mu'$ as calculated with Konrad's equation for the active mode of failure (Davies, 1989).
E. This value was obtained directly from $\mu'= \tan\delta$, using the reported value of $\delta= 7°$.
F. These values were calculated by means of the equation $\mu'= \tan\delta$.

The values of these constants compared very well with those obtained by Davies and Bellhouse (1989) for Sepharose CL-4B, i.e. $K_o= 4.3 \times 10^{-12}$ m^2 and $\sigma_o= 6.55$ kPa (see table 2.2). This value of K_o is very similar to those obtained in this study. The particle size distribution of Sepharose CL-4B is the same as those of the gels 6B and CL-6B (Pharmacia, 1991), therefore the packing characteristics of the unstressed gels must be very similar for all of them. According to the values of the parameter σ_o, both of the gels tested appeared to be more rigid than Sepharose CL-4B,

Sepharose CL-6B being the most rigid of the three gels as expected.
A comparison of the matrix parameter values measured by means of the different procedures used in this study and those reported in the literature is presented in table 2.2.

2.4.3 Prediction of flow rate-pressure drop curves.

The values of the matrix compressibility α, obtained with the permeability cell were more reliable than those obtained with the other procedures used in this study since there was less experimental error involved in the use of this rig. Therefore in the following predictions the values of α are those measured with the permeability cell (see table 2.2).
The use of the hydrodynamic model of Davies (1989) for the simulation of experimental flow rate-pressure drop curves showed that the values of the wall support coefficient ω, obtained with the oedometer-type cell were overestimated, while those obtained with the compression cell were underestimated. According to these findings, the value of ω was recalculated using the values of the angle of friction against glass $\delta=7°$, and of the angle of internal friction $\theta=14°$, as determined by Davies (1989). Jaky's equation (1944) was used to evaluate $K'= 1-\sin\theta$, the ratio of lateral to vertical pressure, and the coefficient of friction was evaluated by means of $\mu'= \tan\delta$. The resulting value of $K'\mu'$, i.e. 0.0931, was very reasonable lying between the experimental values determined with the oedometer-type cell and the values reported in the literature (see table 2.2).
Since the experimental values of $K'\mu'$ for both Sepharose gels were very similar, the value of $K'\mu'$ previously obtained was used with both gels in all subsequent simulations. Table 2.3 shows the parameter values used in the simulations with the hydrodynamic model of Davies (1989).
Fig. 2.16 shows the effect of increasing the fluid flow on the transmitted solids pressure, P_s (or interparticle stress σ), down a column packed with Sepharose 6B, while in fig. 2.17 the effect of this increase on the bed permeability is presented. It can be observed that as the flow rate increases the solids pressure correspondingly increases at each position down the bed. As the flow rate continues to increase the solids pressure begins to increase more rapidly at the lower part of the bed. Finally a maximum flow rate or critical linear velocity is reached at which point the solids pressure at the bottom of the bed increases infinitely, occasioning the clogging of the column. Concomitant with these changes the permeability down the bed falls and finally at the critical velocity drops to zero at the bottom of the bed.
In the flow rate-pressure drop measurements carried out in this study, the flow rate was treated as the independent variable in the same fashion as Mohammad et al (1992). It is worth noting that Joustra et al (1967) and Davies (1989) on the other hand treated pressure drop as the independent

variable and measured flow rate at specific values of pressure drop. In this respect Mohammad et al (1992) argued that Joustra et al (1967) and Davies (1989) did not consider the extracolumn pressure drop. In this study the actual pressure drop through the gel matrix was calculated by subtracting the extracolumn pressure drop from the total pressure drop (see section 2.3.3).

Table 2.3 Model parameter values used for the prediction of flow rate-pressure drop curves of Sepharose gels.

Parameter	Davies' Model (1989)		Verhoff & Furjanic's Model (1983)	
Buffer density, ρ_L (g/ml)	1.0041		1.0041	
Buffer viscosity, μ (mPa·s)	1.088		1.088	
Matrix density, ρ_s (g/ml)	6B	1.0575	1.0575	
	CL-6B	1.0587	1.0587	
Matrix compressibility, α (kPa^{-1})	6B	13.3×10^{-2}	13.3×10^{-2}	
	CL-6B	9.76×10^{-2}	9.76×10^{-2}	
Permeability of unstressed bed, K_0 (m)	4.43×10^{-12}		-	
Void fraction of unstressed bed, ε_0	0.4		0.4	
$K'\mu'$	0.0931		0.0931	
$k = 150/\Phi^2$ [a]	-		6B	99.50
			CL-6B	107.88

[a] This parameter was evaluated according to the procedure outlined in section 2.3.5.2.

The simulations of pressure drop curves carried out with the model of Davies (1989), and the corresponding experimental curves determined in this work are presented in figs. 2.18 and 2.19. In these figures the pressure drop per unit length $\Delta P/L_{avg}$ has been plotted against the linear flow rate u_o. Average values of bed length L_{avg}, have been used in the model calculations and to scale the values of ΔP in order to account for bed compression. The plots show a nonlinear relationship between pressure drop and linear velocity, and the presence of a maximum flow rate or critical velocity at which the pressure drop increases very rapidly. This behaviour is characteristic of beds packed with compressible matrices and is in agreement with the findings of Joustra et al (1967),

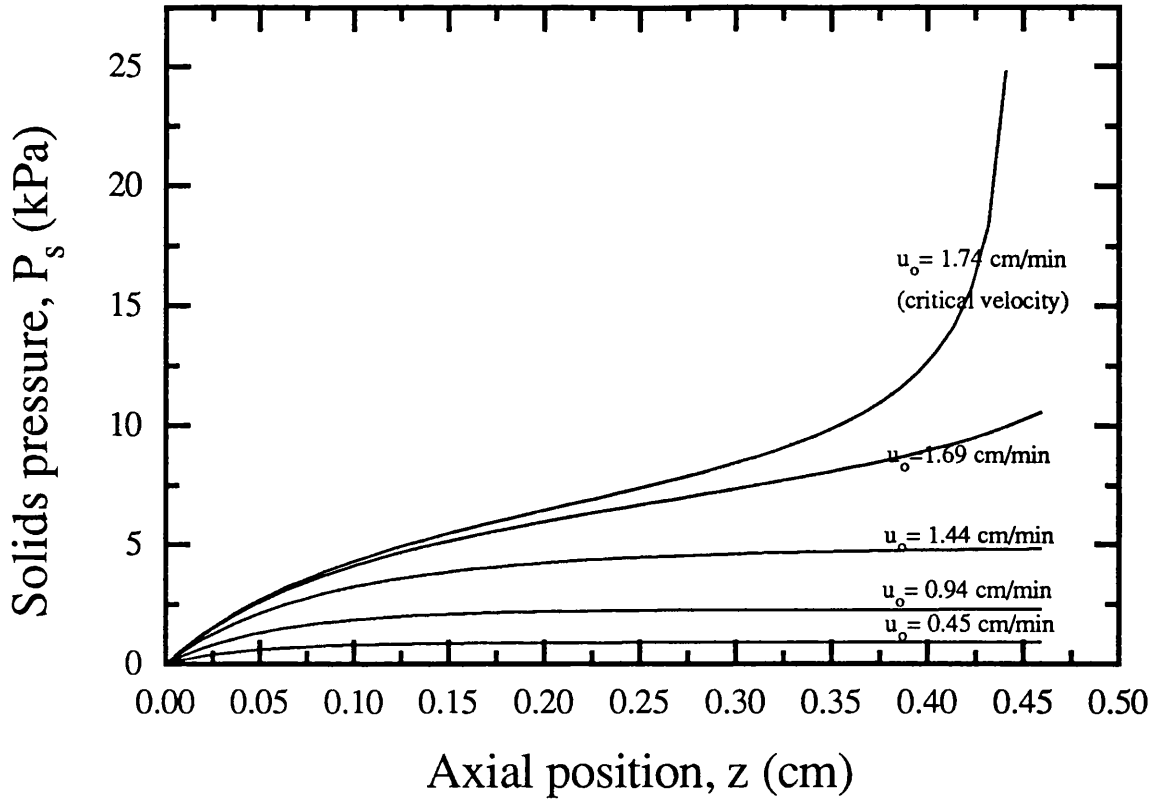

Fig. 2.16 Solids pressure as a function of bed position and flow rate. The simulation was carried out for a column 45.9 cm long, with a diameter of 1.6 cm. The column was packed with Sepharose 6B . The model of Davies (1989) was used.

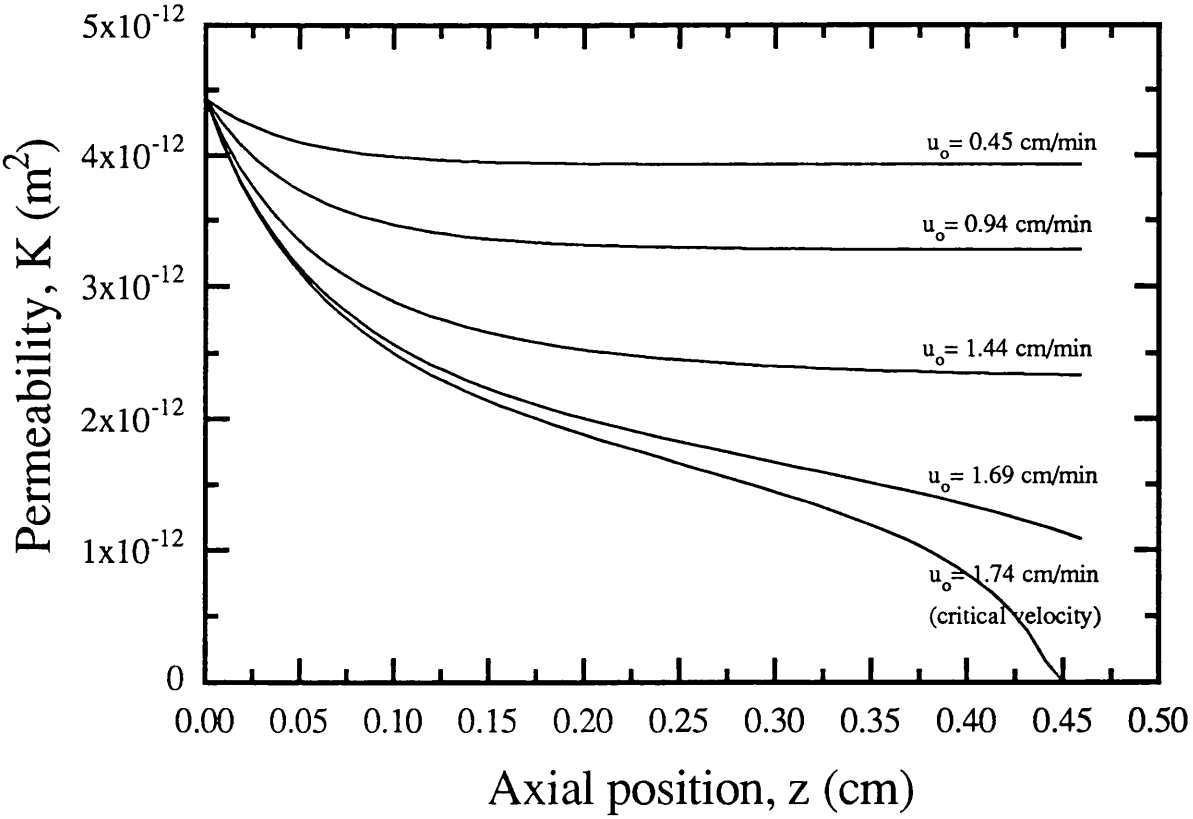

Fig. 2.17 Permeability as a function of bed position and flow rate. Same conditions as in previous figure.

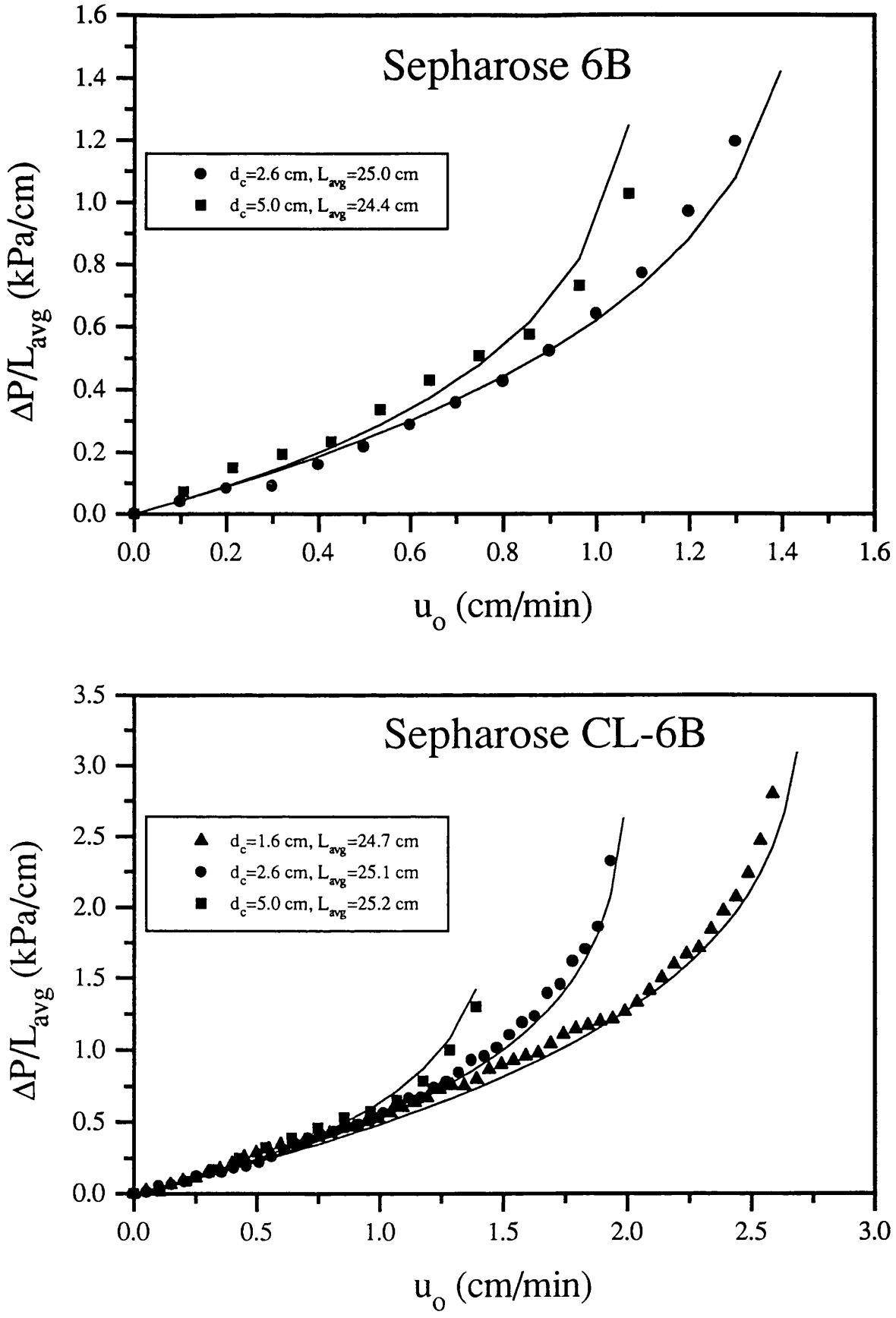

Fig. 2.18 Experimental and theoretical pressure drop curves of columns of different diameter, based on average bed length L_{avg} to account for bed compression. The model developed by Davies (1989) was used to carry out the predictions: ———.

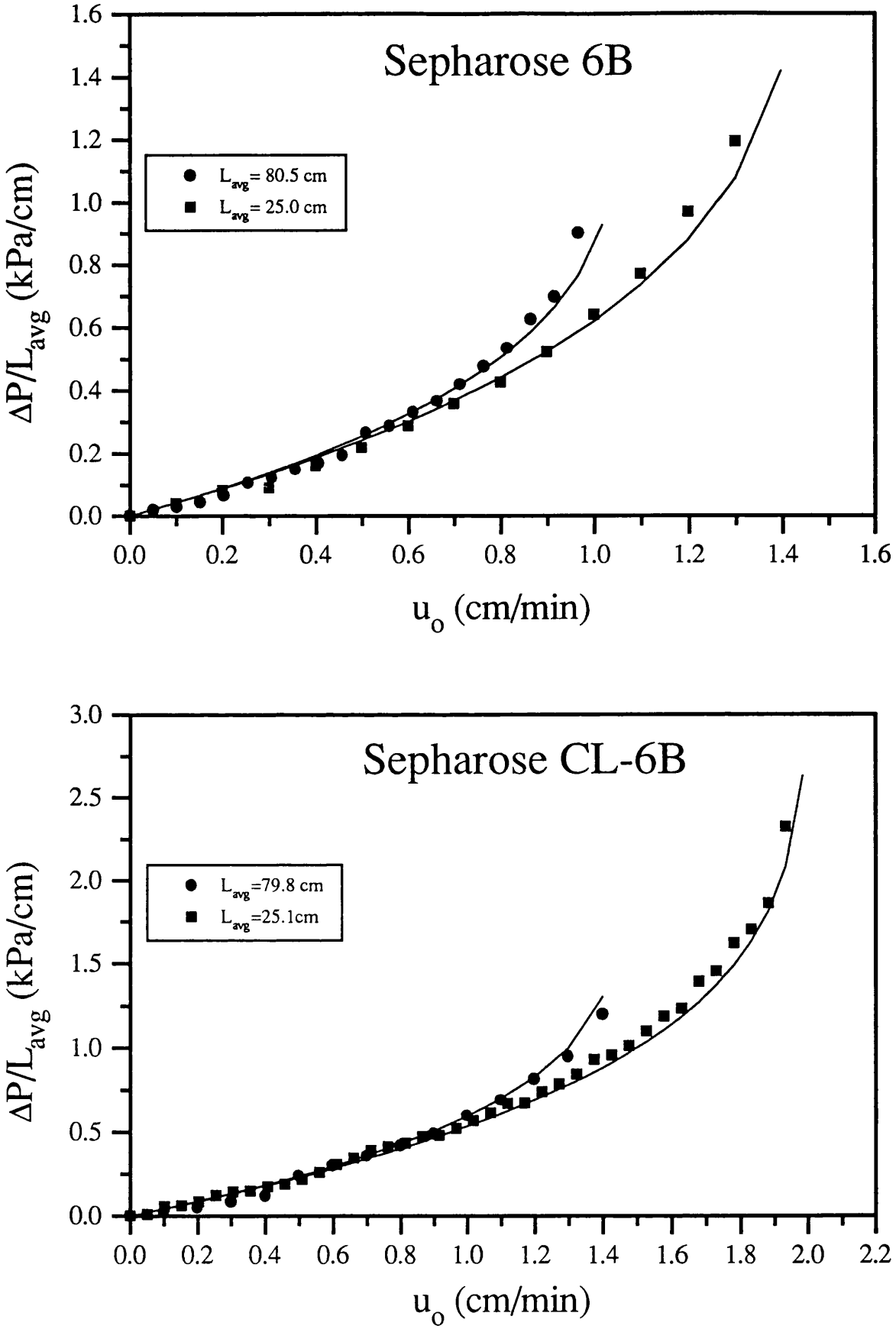

Fig. 2.19 Experimental and theoretical pressure drop curves of beds of constant diameter, d_c= 2.6 cm, and varying length. The curves are based on average bed length L_{avg}, to account for bed compression. The model developed by Davies (1989) was used to carry out the simulations: ———.

Verhoff and Furjanic (1983), Davies and Bellhouse (1989) and Mohammad et al (1992). As mentioned above, the occurrence of this maximum flow rate is due to the presence of a region at the bottom of the bed where the particles are highly compressed as a result of the increasing compressive forces down the column (see fig. 2.16). The existence of this region has been experimentally demonstrated by Parker et al (1987) who showed that the degree of strain of porous compressible media subjected to fluid flow is higher at the bottom.

How particle deformation and therefore the reduction of permeability down a compressible bed affects the pressure drop of columns of different diameters is presented in fig. 2.18. The critical velocity, which occurs when the bed clogs, becomes smaller as the column diameter increases. This dependence of pressure drop on column diameter is explained by the wall support. As the column diameter increases the extent to which the column walls support the bed becomes relatively smaller. This is clearly expressed by the wall support coefficient $\omega = 2K'\mu'/R$, included in the models. Therefore a column of infinite diameter will have no support. (The hydrodynamic models in fact could be used to define with more precision the column diameter at which the wall support could be considered effectively negligible). A comparison between the pressure drop curves of Sepharose 6B and Sepharose CL-6B demonstrates the effect of matrix compressibility. The more compressible a matrix, the smaller the critical velocity for the same column dimensions. The pressure drop curves for columns of equal diameter but different lengths are shown in fig. 2.19. It is observed that the longer the column the smaller the critical velocity. For rigid particles if the length is doubled, the pressure drop will also double. This is not the case in compressible beds where the pressure drop increases non-linearly. Since the solids pressure at a particular position of a bed are equal to the pressure drop up to that same position (see section 2.2), it is clear that for a particular linear flow velocity the pressure drop will be much larger for a longer column and therefore the compression forces acting at the bottom will also be larger. There is also a component of these compression forces due to the weight of the particles, which may or may not be significant depending on their density difference with the fluid, when increasing the bed length.

The experimental pressure drop curves and the predictions carried out with the hydrodynamic model of Verhoff and Furjanic (1983) are shown in fig. 2.20 and fig. 2.21. As in figures 2.18 and 2.19 average values of bed length L_{avg} have been used in the model calculations and to scale the values of ΔP in order to account for bed compression. Since it was not possible to measure or estimate the value of the shape factor Φ as a function of bed position and linear flow rate, the same procedure followed by Verhoff and Furjanic (1983) was applied, where this parameter was bulked into the constant $k = 150/\Phi^2$, which forms part of the flow term coefficient defined by eq. 2.5. Its value was obtained by fitting the hydrodynamic model to an experimental flow rate-

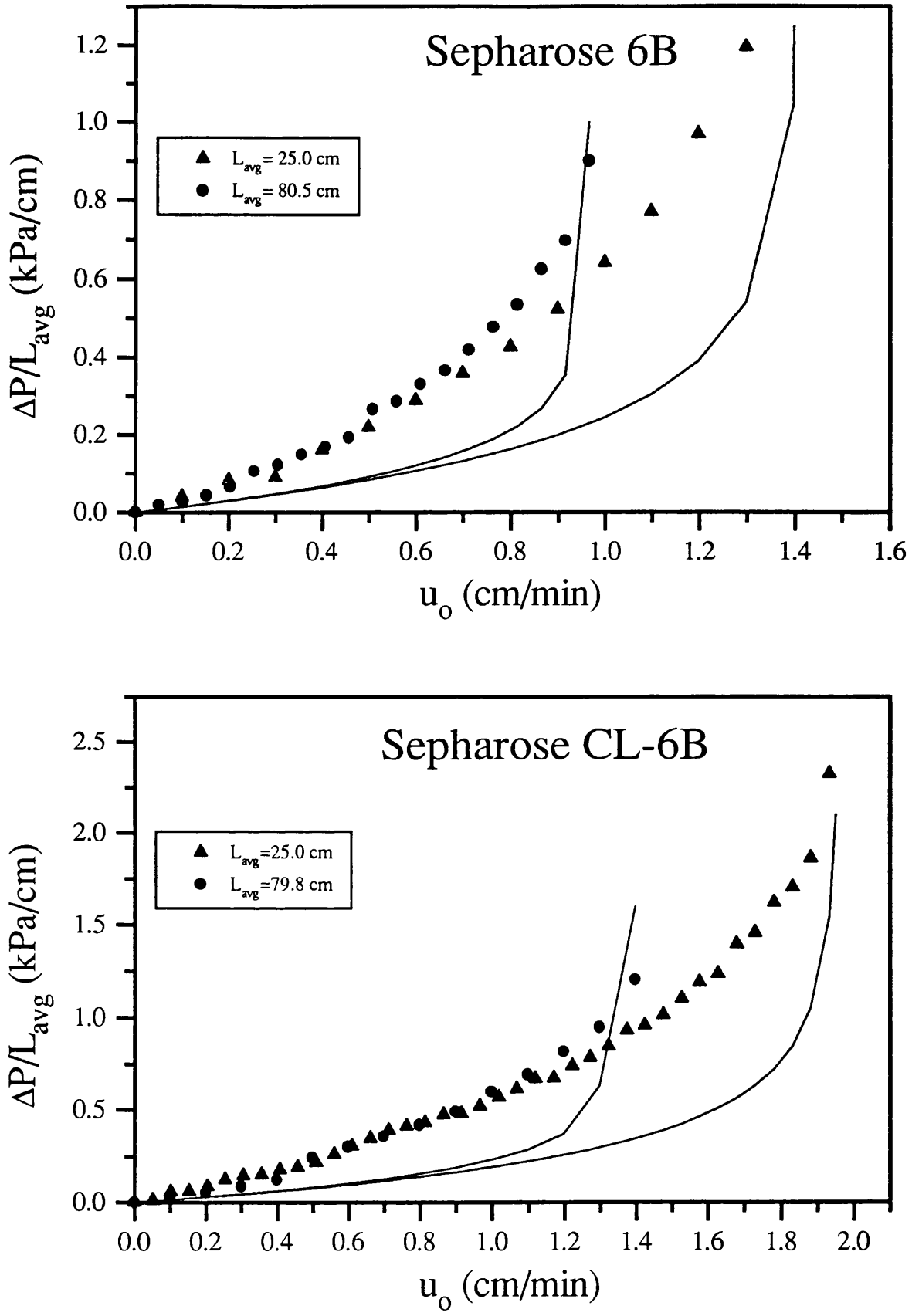

Fig. 2.20 Experimental and theoretical pressure drop curves of columns of constant diameter, d_c= 2.6 cm, and different lengths. The curves are based on the average bed length L_{avg}, to account for bed compression. The model developed by Verhoff and Furjanic (1983) was used to carry out the predictions: ———.

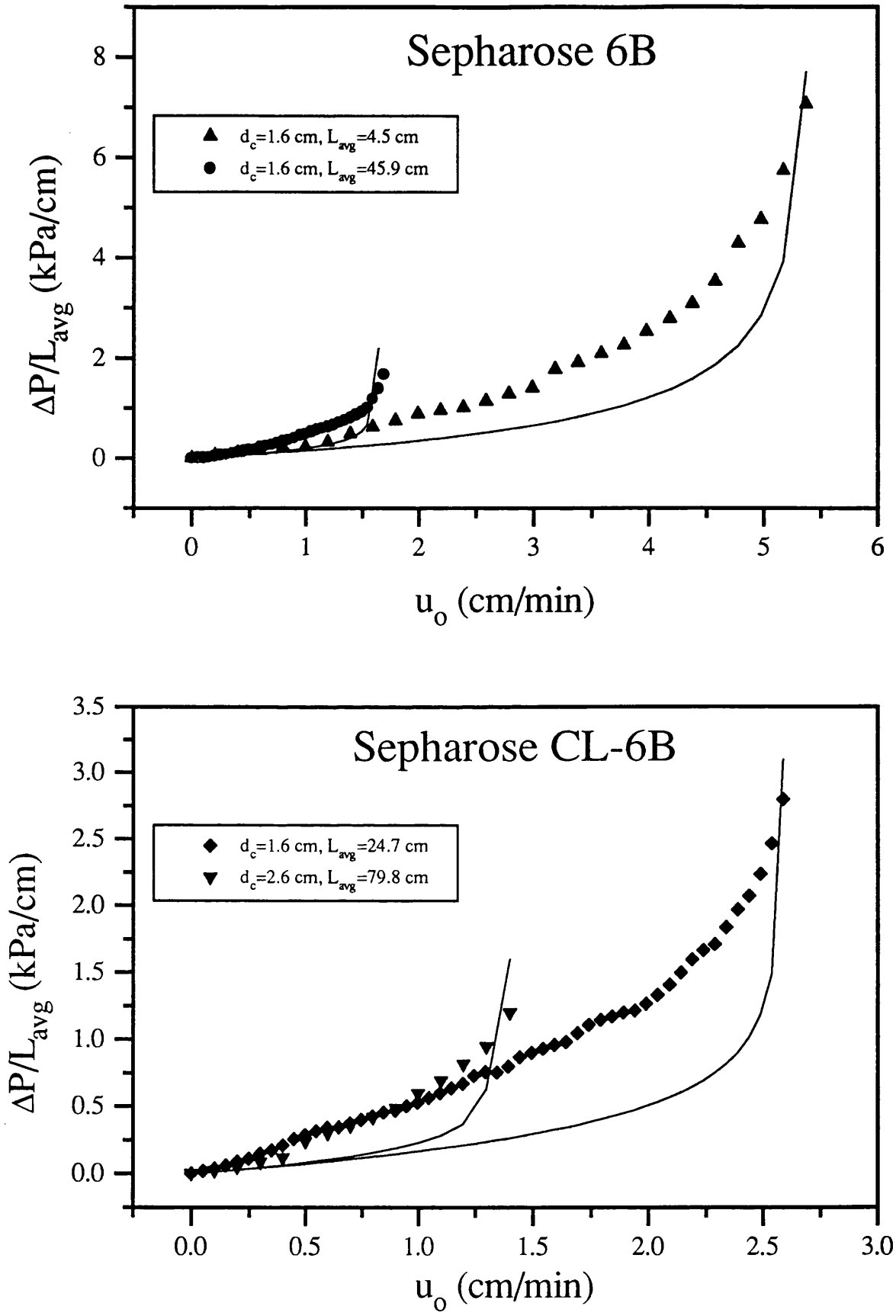

Fig 2.21 Experimental and theoretical pressure drop curves of columns of different dimensions, based on average bed length L_{avg} to account for bed compression. The model of Verhoff and Furjanic (1983) was used to carry out the simulations: ———.

pressure drop curve (see section 2.3.5.2). This means that all the predictions carried out with this model were based on information obtained from experimental pressure drop curves. The value of k so obtained, was used together with the remaining parameter values presented in table 2.3, to simulate the flow rate-pressure drop curves of columns of different dimensions.

One of the major uses of a hydrodynamic model is in the scale-up of compressible beds, either varying bed diameter, bed height or both. Figs. 2.18, 2.19, 2.20 and 2.21 show the predictive capabilities of the two models tested in this study, for different column geometries. From these figures it can be seen that the predictions carried out using the model of Davies (1989) (figs. 2.18 and 2.19) follow closely the experimental curves. On the other hand, the simulations carried out using the model of Verhoff and Furjanic (1983) (figs. 2.20 and 2.21) follow the trend of the experimental curves but underestimate the pressure drop for most of the linear velocity range and all column dimensions. However, both models are capable of predicting the maximum flow rate that can be achieved for a particular set of column dimensions.

The difference in the performance of these two models is due to the accuracy with which the permeability down the column has been described. Therefore it is not surprising that the model of Davies (1989) renders a better prediction. The discrepancies between the experimental curves and the predictions obtained with the model of Verhoff and Furjanic can be explained as a result of the use of the bulked parameter $k= 150/\Phi^2$. This parameter is a measurement of the degree of deformation of the gel particles down the column, the shape factor Φ, being a function of the increasing compressive forces. By carrying out the fitting procedure of an experimental curve only a single value of k is obtained. This constant therefore averages the gradual deformation suffered by the matrix beads down the column at the different compression conditions (flow rates) at which the bed was subjected to. It is clear that this is a very rough estimation of the level of particle deformation. However, it is remarkable that despite this gross approximation the model of Verhoff and Furjanic (1983) is capable of predicting the critical velocity rather well. This means that despite its lack of accuracy along most of the linear flow range, this model can also be used to determine the operating conditions of a chromatographic bed and for scale-up purposes.

In order to improve the predicting capabilities of the hydrodynamic model of Verhoff and Furjanic (1983), it is necessary to describe better the way the shape factor changes as a function of the solids pressure and therefore along the column. This function will also provide information as to how the intraparticle void volume is affected under different levels of compression. NMR imaging techniques (Ilg et al and Höpfel, 1992 and Bayer et al, 1989) could be used to carry out such studies.

The model developed by Davies is very sensitive to the value of K_o, the permeability of the unstressed bed which is directly related to ε_o, the void fraction of the unstressed bed. In this thesis

the values of K_0 compared very well with those found by Davies (1989) as above mentioned, however, the corresponding values of ε_0 (assuming permeability of the Kozeny-Carman type) would be 0.328 for Sepharose CL-6B and 0.336 for Sepharose 6B. These values appear to be very low when compared to the reported values of ε_0 for beds packed with rigid beads, which should correspond closely to the unstressed condition of those packed with compressible beads. Reyes and Iglesia (1991) have reported ε_0= 0.36 for random-close packings, ε_0= 0.42 for random-loose packings and ε_0= 0.40-0.38 for random-poured packings. In this work a value of ε_0= 0.4 has been used. There is therefore a need to determine ε_0 and consequently K_0 with more precision so as to improve the quality of the predictions carried out with these models. Here again NMR imaging (Ilg et al and Höpfel, 1992, and Bayer et al, 1989) could be a very useful tool for determining the porosity of unstressed beds.

Both of the models tested in this study lack of a solid theoretical description of the fluid flow, the two of them have used modified versions of hydrodynamic equations developed for rigid particles. A more fundamental model could be derived by integrating the steady state equation developed by Jönsson and Jönsson (1992) to describe fluid flow in compressible porous media. Its use would improve the description of the column hydrodynamics and therefore the prediction of the flow rate-pressure drop curves.

Table 2.4 shows the maximum flow rate and the changes in length experienced by the different columns used in this study. It can be observed that the % reduction in bed length was very similar for both gels, although the average value shows a slight difference reflecting the small difference in compressibility between the two Sepharose gels studied.

One of the main drawbacks of most of the hydrodynamic models developed to date is that they do not allow for the prediction in the changes of bed length that occur when the bed compresses. Parker et al (1987) studied the steady, one-dimensional flow of an incompressible fluid through a deformable porous material and have used a model which is essentially based on the consolidation equations of Biot (1955). Assuming that the stiffness and permeability of the matrix are functions of the local strain, they predicted the fluid velocity, the matrix height and the distribution of strain as a function of the applied pressure drop. However, their analysis did not consider the friction forces between the matrix and the column walls. An analysis similar to this one could be applied to compressible chromatographic beds so that bed height could be also predicted and thereby improving the prediction of the flow rate-pressure drop curves.

The two models studied do not consider the effects of polydispersity on pressure drop. However, it seems that the use of a mean particle diameter is adequate for modest size distributions (see fig. 2.5). Dewaele and Verzele (1983) worked with two narrowly distributed fractions of silica-based reversed-phase sorbent materials (Alltech) and showed that the pressure drop in columns packed

with mixtures of very different size fractions was well above that predicted by using the arithmetic mean diameter in the Blake-Kozeny equation. In contrast, Yamamoto et al (1986) found that the Kozeny-Carman equation was satisfactory for their columns packed with Toyopearl HW55 media (Tosohaas) which have a reasonably narrow size distribution. It appears therefore that packings with a modest size distribution do not produce major increases in pressure drop over what is expected of their monodisperse counterparts for a given interstitial void fraction.

Table 2.4 Column dimensions and critical velocities.

Packing and column diameter	Maximum flow rate (ml/min)	Critical velocity (cm/min)	Initial length (cm)	Average length (cm)	Final[A] length (cm)	Reduction in length %
Sepharose 6B						
d_c= 1.6 cm	11.0	5.50	4.9	4.5	4.1	16.3
d_c= 1.6 cm	3.50	1.75	50.5	45.9	41.0	18.8
d_c= 2.6 cm	7.40	1.40	27.6	25.0	22.5	18.7
d_c= 2.6 cm	5.05	0.95	88.9	80.5	71.9	19.2
d_c= 5.0 cm	21.6	1.10	27.1	24.3	22.2	18.1
					avge=	18.2
Sepharose CL-6B						
d_c= 1.6 cm	5.30	2.65	27.5	24.7	22.3	19.1
d_c= 2.6 cm	10.3	1.95	27.7	25.0	22.8	17.7
d_c= 2.6 cm	7.40	1.40	88.5	79.8	74.5	15.8
d_c= 5.0 cm	28.5	1.45	27.3	25.2	23.2	15.2
					avge=	16.9

Notes: A. This is the bed length at the critical velocity.

Finally it must be pointed out that although experimental experience has shown the existence of time dependent compression, with the exception of Norsker et al (1979), none of the models developed to date have accounted for this effect. Norsker et al (1979) introduced an empirical relationship between permeability and time into their model to allow for this effect. This type of compression is possibly due to a fatigue time-dependent process and therefore is material specific.

Norsker et al (1979) found that permeability of immobilized glucose isomerase (Sweetzyme) beds was largely reduced in the first two days of operation, with a further 25-30 % reduction after a virtually infinite period of time. In the case of the Sepharose gels time-dependent effects do not seem to be significant as only small changes in length and therefore in permeability have been observed.

2.4.4 Prediction of bed void fraction.

In order to determine the effects of bed compression on the performance of column-based chromatography it is necessary to be able to predict structural properties of packed beds such as the bed void fraction, ε. This property is of great importance since it is not only directly related to porosity but greatly influences the mass transfer properties of the bed. As already mentioned in beds packed with compressible supports the bed void fraction is very much dependent on the weight and rigidity of the matrix, the support from the column walls and the pressure drop across

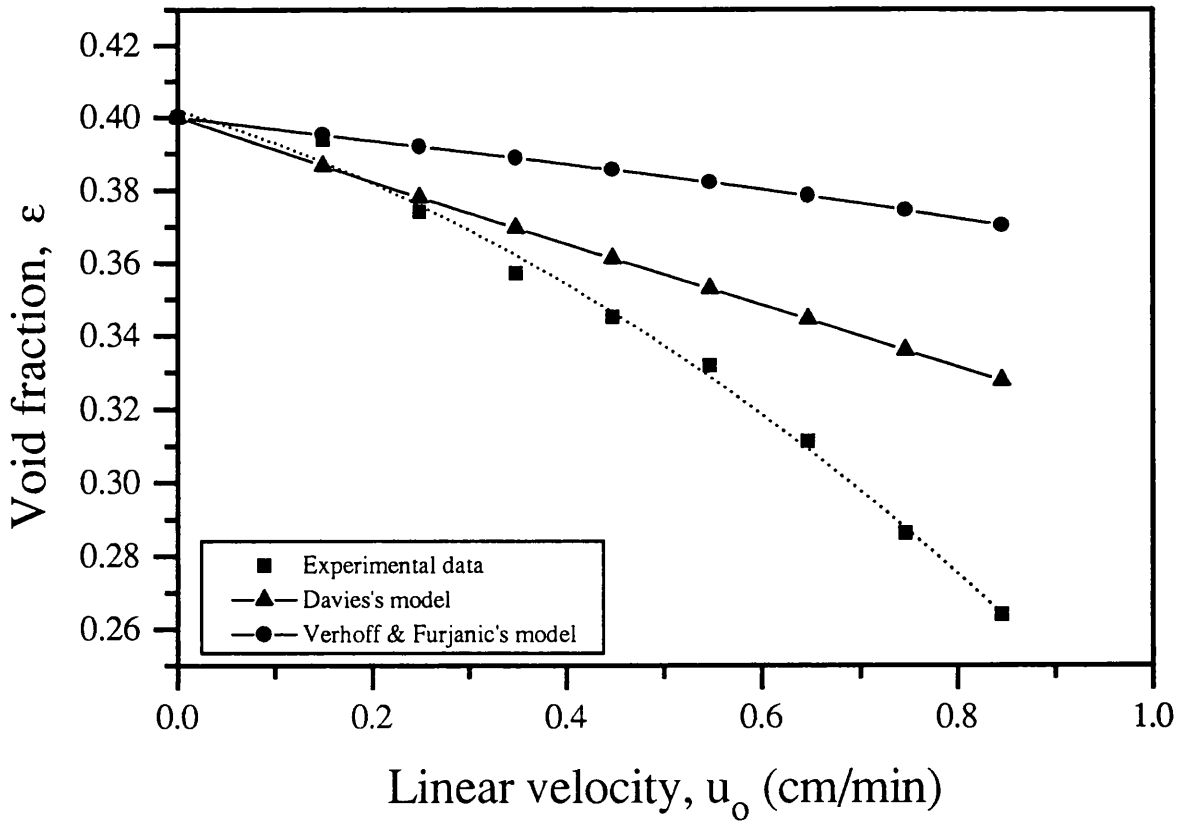

Fig. 2.22 Void fraction of a column packed with Sepharose 6B at different linear flow velocities. The experimental data has been fitted with a second order polynomial to show its trend. The predictions have been carried out with the two models tested in this study.

the column. One of the main reasons the model developed by Verhoff and Furjanic (1983) was tested was the fact that it allows the estimation of the bed void fraction. The relationship between the interparticulate stress and the void fraction (eq. 2.10) was also integrated in the model of Davies (1989), so that this prediction could be carried out.

In fig. 2.22 the experimental measurements of bed void fraction at different compression conditions (flow rates) are compared with the model predictions. It can be observed that both of the hydrodynamic models studied overestimate the experimental curve, although they follow the decreasing trend. The prediction carried out using Davies's model is closer to the experimental curve. This is again the result of the better description of permeability as a function of interparticulate stress down the column, provided by the empirical function $K= K_0 \exp(-\sigma/\sigma_o)$, included in Davies's model (see section 2.2).

These results question the applicability of the mathematical relationship between the solids pressure, matrix compressibility and bed void fraction (eq. 2.10). The following relationship also used with compressible beds was tested. However, its performance was very similar with only a slight improvement.

$$\epsilon = \epsilon_o e^{-\alpha P_s} \qquad (2.27)$$

All the relationships are empirical and at present there is not a satisfactory theoretical description of this phenomena. There is clearly a need to improve the accuracy of these empirical relationships and to develop theoretical correlations. As mentioned above NMR imaging (Ilg et al and Höpfel, 1992, and Bayer et al, 1989) could be of great help in developing a more accurate relationship that will take into account both the intraparticle and the interparticle volume losses.

2.5 Conclusions.

The two models studied are capable of predicting the maximum flow rate that can be achieved with a column packed with a compressible matrix. Therefore both are useful to determine operating conditions and in the upscaling of chromatographic columns. The model of Davies (1989) agreed much more closely with the experimental flow rate-pressure drop curves.

To improve the predictive capabilities of the two models tested, a greater accuracy in the determination of the matrix compressibility α, and the wall support coefficient ω is needed.

The use of rigs involving pressure transducers in their construction, for the measurement of wall support coefficient ω (or friction coefficient μ') may lead to considerable error. This is due to the

uneven distribution of the load produced by the presence of the transducer itself.

The oedometer-type cell (sections 2.3.2.5 and 2.4.1) provides a more accurate way of determining the wall support coefficient ω (or the friction coefficient μ') of a material packed in a column and subjected to compressive forces. The information gained by this methodology is also useful in the determination of the rigidity σ_0, of compressible matrices. However, a number of sources of error are involved in this procedure (see section 2.4.1). There is much to be gained in the accuracy of this procedure if a more precise design and construction of the rig is carried out in order to reduce these sources of error.

Development of models capable of predicting the changes in length undergone by compressible beds subjected to compression will also help to improve the accuracy in the prediction of the flow rate-pressure drop curves.

Studies are needed to determine the variation in intraparticle and interparticle void volume that occurs under different levels of compression. This will provide information not only for a more accurate evaluation of the matrix compressibility α, but also for the development of a description of the degree of particle deformation (Φ=shape factor) down a compressed column. These studies could result in a far more accurate mathematical relationship between compressibility, applied pressure and the corresponding reduction in void volume. This will enable a better prediction of the void fraction (porosity) at each position down a compressed bed, and an improved prediction of the bed void fraction. Such a compressibility relationship would make it possible to use the model developed by Östergren and Trägårdh (1991) to predict the velocity field and dispersion in compressible beds.

Further studies are also needed in order to understand better the effects of polydispersity on pressure drop. Finally, the time dependent compression of these matrices should also be researched to complete the modelling of compressible chromatographic beds.

Development of a complete and successful model and our increasing understanding of the factors that influence the hydrodynamics of compressible chromatographic beds will assure successful design and upscaling of new chromatographic processes.

CHAPTER 3

PROCESS MODELLING AND TRANSPORT PARAMETERS

3.1 Introduction.

This chapter reviews the modelling of chromatographic operations as well as some important aspects of transport in fixed porous beds. The modelling analysis is centred on the description of the model selected for study in this thesis, i.e. the general rate model of size exclusion chromatography, and on the description of the numerical methods used in its solution. These modelling and numerical tools will be used in the study of the effects of matrix compression and fouling on column performance in the next two chapters.

Initially the modelling of column chromatography focusing on gel filtration or size exclusion chromatography (SEC) is outlined (section 3.2). This particular type of chromatography has been selected to be used throughout the present study because of its simplicity as compared with the other types of chromatography. The only rate parameters needed for simulation of SEC chromatographic peaks are intraparticle diffusivities, convective dispersion coefficients, and to a lesser degree fluid-phase mass-transfer coefficients. Furthermore, partition equilibrium is linear up to relatively high concentrations (Jönsson, 1987). Solute-matrix interactions in this type of chromatography are negligible and therefore adsorption constants are not to be considered.

The linearity of the partition equilibrium relationship is of importance since linear chromatography models are more easily solved than the non-linear types. Besides in SEC the solute concentration in the applied sample is generally low, being limited by the viscosity of the sample which must not be so large as to cause hydrodynamic instability (Hagel, 1989). This means that not only the equilibrium distribution coefficient is constant, but all the transport parameters and fluid properties are considered to be independent of concentration and constant.

Subsequently, since axial dispersion, fluid-phase mass-transfer resistance and the solute intraparticle diffusivity are the transport parameters needed to describe the chromatographic process and to characterize its performance, they are looked at with some detail in respect to fixed porous beds. The correlations and methods used in their determination and estimation are briefly

reviewed. Particular emphasis is given to those methods and correlations which are applicable within the range of reduced velocity of interest to modern liquid chromatographic practice. To conclude the numerical method employed in the solution of the size exclusion chromatography model used in this thesis is presented.

It is intended that the theory presented here will provide a basis for the interpretation of the compression and fouling experiments described in the next two chapters.

3.2 Size exclusion chromatography models.

The development of theoretical models for the prediction of the performance of size exclusion chromatography has followed different approaches.

The majority of chromatographers now agree that size separation of molecules can be fully explained on the purely steric basis that large molecules can only partially permeate the pore volume of the support. According to this view, a series of theoretical models have been derived in order to predict SEC calibration curves, also termed exclusion or selectivity curves. In these models it is assumed that the equilibrium distribution coefficient K_d, depends only upon the size and shape of the solute molecules and upon the size and shape of the pores in the column packing material. Using statistical theory for the equilibrium distribution of rigid molecules in inert porous networks, Giddings et al (1968) obtained theoretical relationships to estimate K_d, for solutes of spherical to thin-rod shape and for pores whose shape ranged from circular cross section to an infinite slab. However, these models are of regular geometry and consists of a single uniform pore size, therefore they cannot accurately represent real SEC packings.

More complex models of non-regular geometry and random-sized pores have been derived, among them the random-sized touching sphere model and the uniform-sized random-sphere model give excellent quantitative fits to experimental data (Knox and Scott, 1984). These researchers have also shown that SEC calibration curves can be predicted with remarkable accuracy from mercury porosimetry data, by using a model consisting of an assembly of cylindrical pores having the pore size distribution given experimentally.

Although all these models are capable of predicting K_d and therefore the retention volume V_R of a solute given its molecular weight M, they do not provide any information regarding peak shape and band spreading.

Since the equilibrium relationship in SEC is linear, all the models derived to describe and to predict the elution profile in linear chromatography are applicable. These models can be classed into three broad types: plate or tank-in-series models, statistical models and transport models

(Golshan-Shirazi and Guiochon, 1992b).

Plate models. In the plate models, it is assumed that the column consists of a number of identical equilibrium stages or theoretical plates, placed in series, and that the stationary and mobile phases are in equilibrium at each stage.

There are two categories of plate models. In *the discrete stage distribution or Craig model* (Craig, 1944; Eble et al 1987), a finite volume of eluent is equilibrated step by step, within one theoretical plate in the column after another. In the second category of plate models, there is continuous flow of the mobile phase through a series of stages (Martin and Synge, 1941), this is why it is called *the continuous plate model.* All plate models are by nature approximate since the equilibrium assumption requires a mixing mechanism which is clearly absent from the physical system.

Statistical models. In the second class of linear chromatography models, a microscopic statistical method is used to derive the probability density function of a single solute molecule at a particular column position and time. Giddings (1965) used *the random walk approach* to calculate the profile of the chromatographic band in a simple way. Another probabilistic approach, *the stochastic model,* was introduced by Giddings and Eyring (1955), for the description of the migration of a single solute molecule in chromatography. Their molecular dynamic approach based on statistical ideas treats chromatography as a Poisson distribution process. They derived an expression for the elution profile, or distribution of the residence time of a molecule in the column, assuming random adsorption/desorption processes, with a single type of site on the stationary phase and for a pulse injection. This latter approach did not consider the column axial dispersion and the mass transfer kinetics, and therefore its predictive capabilities are limited.

Transport models. The third approach followed in the modelling of chromatography is the transport approach. This has been widely used to calculate the chromatographic response to a given input function. In this method the transport processes that take place between the stationary phase and the mobile phase as well as the additional dispersion of the solute in the interstices of the packing matrix due to eddy diffusion and molecular diffusion are built into the model, and the chromatographic process is described by a set of partial differential equations which result from the differential mass balance of the solute in a slice of column and its kinetics of mass transfer. Rate models of different levels of complexity have been developed. The most important of them are the equilibrium-dispersive model, the lumped kinetic model and the general rate model of chromatography (Golshan-Shirazi and Guiochon, 1992b). Most of these models have been developed for adsorptive chromatography but size-exclusion chromatography could be treated as a special case, with the adsorption/desorption rate constants and the equilibrium isotherm constant all equal to zero.

In *the equilibrium-dispersive model,* the mobile and stationary phases are assumed to be in

constant equilibrium. The contributions of non-equilibrium effects, e.g. axial dispersion and mass transfer resistances are lumped together in an apparent dispersion coefficient D_a (adsorption/desorption kinetics could also be considered but they are not relevant to the present study dealing with SEC). With these assumptions the model is reduced to a single equation, the differential mass balance of the solute in a slice of column given by:

$$D_a \frac{\partial^2 C}{\partial z^2} - u\frac{\partial C}{\partial z} - \frac{1}{m}\frac{\partial q}{\partial t} = \frac{\partial C}{\partial t} \qquad (3.1)$$

where:

C= solute concentration in mobile phase, mg/cm^3.

q= solute concentration in stationary phase in equilibrium with mobile phase conc. C, mg/cm^3.

t= time, s.

z= axial distance from column inlet, cm.

u= interstitial fluid velocity, cm/s.

D_a= apparent axial dispersion coefficient, cm^2/s.

m= phase ratio, $\varepsilon/(1-\varepsilon)$

ε= bed void fraction.

This model has been discussed by Yamamoto et al (1988), Jönsson (1984) and Golshan-Shirazi and Guiochon (1992a) among others. Its analytical solution has been derived by Lapidus and Amundson (1952) and has a simple Gaussian form when the sample volume is small and the plate number is large.

Yamamoto and Sano (1992) discussed the criteria under which this simplified model is applicable to SEC of proteins and found that for a small sample volume V_F, when

$$N > 22\,[(m + K_d)/K_d] \qquad (3.2)$$

where N is the plate number and K_d the distribution coefficient, the calculated elution curves by the three rate models discussed in this section and the plate theory were hardly distinguishable. They stated that this condition is usually fulfilled in current protein SEC.

In *the lumped kinetic model* of chromatography, the contributions to band broadening due to all the mass transfer resistances are lumped in a single coefficient and a linear driving force model is assumed. The contribution of axial dispersion to peak spreading is treated independently and accounted for by the axial dispersion coefficient D_L. Therefore the behaviour of the chromatographic system is described by the following mass balance equation:

$$D_L \frac{\partial^2 C}{\partial z^2} - u\frac{\partial C}{\partial z} - \frac{1}{m}\frac{\partial C_s}{\partial t} = \frac{\partial C}{\partial t} \qquad (3.3)$$

where C_s is the concentration of the solute in the stationary phase.

The mass transfer kinetics of the solute to the surface of the adsorbent is given by either the liquid film linear driving force:

$$\frac{\partial C_s}{\partial t} = k'_m(C - C^*) \qquad (3.4)$$

where C^* is the solute concentration in the mobile phase which is in equilibrium with the stationary phase concentration C_s, and k'_m is the apparent mass transfer coefficient, or by the solid film linear driving force:

$$\frac{\partial C_s}{\partial t} = k_m(q - C_s) \qquad (3.5)$$

where q is the solute concentration in the stationary phase in equilibrium with the mobile phase concentration C, and k_m is the apparent mass transfer coefficient.

According to Glueckauf (1955), the lumped mass transfer coefficient k_m is related to the film mass transfer coefficient k_f, and to the pore diffusivity D_e, by the equation

$$\frac{1}{k_o k_m} = \frac{m d_p}{6 k_f} + \frac{m d_p^2}{60 D_e} \qquad (3.6)$$

where d_p is the particle diameter and k_o is the retention factor. This equation demonstrates that the contributions of the mass transfer resistances are additive. Lapidus and Amundson (1952) derived an analytical solution for this model, which is also reduced to a Gaussian curve when the sample volume V_F is small and the plate number N is large (Van Deemter et al, 1956).

The general rate model considers simultaneously all the contributions to mass transfer kinetics. This model usually takes into account the axial dispersion, the external film mass transfer resistance, the intraparticle diffusion and the rate of adsorption/desorption. In fact this model is the most sophisticated and comprehensive so far developed (Golshan-Shirazi and Guiochon, 1992b). Ideally in SEC adsorption does not participate in the separation process, therefore this mechanism will not be considered.

The general rate model considers, in a separate and independent manner, all the transport parameters that characterize the chromatographic process. It is these same parameters on which the study of the effects of compression and fouling on column performance (presented in chapters 4 and 5) is based. This model has therefore been selected in this thesis to be used as a tool to aid

the analysis of these effects. In the following sections a description of this model as well as the numerical methods employed in its solution will be outlined.

3.2.1 The general rate model of size exclusion chromatography.

The general rate model of chromatography has been postulated and solved by various researchers (Lenhoff, 1987; Yamamoto et al, 1979; Gibbs, 1989; Davies, 1989; McGreavy et al, 1990) making different considerations and using different boundary conditions and numerical methods. Recently Boyer and Hsu (1992) made used of the Fast Fourier Transform algorithm (FFT) for the numerical solution of the general rate model applied specifically to SEC. Due to the speed and easiness of programming of this algorithm their model description and numerical method have been followed in the present study. The model definition and boundary conditions used by these researchers are presented in this section.

The general rate model makes no simplifications in relation to the transport processes followed by the solute molecules along the chromatography column. However, the migration of the solute molecules inside and outside the matrix particles is considered separately and therefore two mass balance equations are required, one for the mobile phase flowing between particles and one for the stagnant mobile phase inside the particle.

The system considered is a fixed bed of length L, consisting of spherical particles with an average radius R_p. It is assumed that the liquid flow in the column is axially dispersed, and the mass transfer processes occurring include the external fluid mass transfer and the intraparticle diffusion. As already mentioned adsorption is negligible in SEC and is therefore not considered. The mass balance equation in the mobile phase describing this system can be written as (Golshan-Shirazi and Guiochon, 1992b):

$$D_L \frac{\partial^2 C}{\partial z^2} - u\frac{\partial C}{\partial z} - \frac{1}{m}\frac{\partial \hat{C}_s}{\partial t} = \frac{\partial C}{\partial t} \qquad (3.7)$$

where D_L is the axial dispersion coefficient, u is the interstitial linear velocity, m is the phase ratio ($V_m/V_s=\varepsilon/(1-\varepsilon)$) and $\hat{C}_s$ is the solute concentration in the stationary phase averaged over the entire particle. For spherical particles $\hat{C}_s$ is defined as:

$$\hat{C}_s = \frac{3}{R_p^3}\int_0^{R_p} r^2 C_s\, dr \qquad (3.8)$$

The term $\partial\hat{C}_s/\partial t$ is therefore the rate of migration of solute molecules into the particle pores

(averaged over the entire particle), and for a spherical particle it is given by,

$$\frac{\partial \hat{C}_s}{\partial t} = \frac{3M_F}{R_p} \tag{3.9}$$

where M_F is the mass flux of solute from the bulk solution to the external surface of the particle. Assuming a linear driving force at the particle surface and taking into account the particle-to-fluid mass transfer coefficient k_f, M_F is defined as follows:

$$M_F = k_f(C - C_p|_{r=R_p}) \tag{3.10}$$

where C_p is the solute concentration within the pores inside the particle based on the accessible pore volume. It is a function of r, the radial distance from the centre of a particle. Hence the mass balance equation in the mobile phase can be rewritten as:

$$D_L\frac{\partial^2 C}{\partial z^2} - u\frac{\partial C}{\partial z} - \frac{3k_f}{m R_p}(C - C_p|_{r=R_p}) = \frac{\partial C}{\partial t} \tag{3.11}$$

On the other hand the differential mass balance of the solute inside the pores of the matrix particle is given by the following partial differential equation:

$$\epsilon_p\frac{\partial C_p}{\partial t} = D_e\left(\frac{\partial^2 C_p}{\partial r^2} + \frac{2}{r}\frac{\partial C_p}{\partial r}\right) \tag{3.12}$$

where D_e is the effective intraparticle diffusivity and ε_p is the intraparticle inclusion porosity of the solute. A distinction is made in this model between the absolute intraparticle porosity of the stationary phase, which does not appear explicitly in the model, and the solute dependent inclusion porosity ε_p which represents the effective volume fraction of the stationary phase that is accessible to the solute. Indeed, the parameter ε_p is equivalent to the equilibrium distribution coefficient K_d, according to its definition presented in section 3.4. The advantage of using such an inclusion porosity is that there is no need to consider the intraparticle porosity and the rejection factor as separate geometrical parameters (Lenhoff, 1987) which in any case, are difficult to measure separately (Athalye et al, 1992).

Initially the fixed bed is free of solute and at time zero, a pulse injection is introduced at the column inlet. Accordingly the initial and boundary conditions are as follows:

$$C(z,0) = 0 \tag{3.13}$$

$$C_p(r,z,0) = 0 \tag{3.14}$$

$$C(0,t) = \begin{cases} C_o & 0 \le t \le t_o \\ 0 & t_o < t \end{cases} \tag{3.15}$$

$$C(\infty,t) = 0 \tag{3.16}$$

$$C_p(0,z,t) \neq \infty \tag{3.17}$$

In eq. 3.15 C_0 represents the pulse or sample concentration.
The link between the mobile phase and the stationary phase descriptions is provided by the matching condition of flux continuity at the particle surface:

$$k_f(C - C_p)|_{r=R_p} = D_e \left.\frac{\partial C_p}{\partial r}\right|_{r=R_p} \tag{3.18}$$

This equation completes the required set of boundary conditions necessary for the solution of the model equations.

At the column outlet, Boyer and Hsu (1992) used the long-column form of the boundary conditions (semi-infinite column), which assumes that the concentration field decays rapidly at long distances. This is adequate since columns of interest for practical separations are typically long. Indeed the use of these boundary conditions (eqs. 3.15 and 3.16) is justified since the solute flux at the column boundaries is only significant for a relatively short period of time compared to the residence time of the solute in the column. Furthermore the required condition (Lin et al, 1991) for the use of these boundary conditions:

$$4D_L/Lu \ll 1 \tag{3.19}$$

applies to the experimental conditions used in this study (see chapter 4). In any case, as pointed out by Lenhoff (1987), under typical chromatographic conditions axial transport is overwhelmingly convective, and the use of alternative boundary conditions has little effect on the peak shape.
The whole set of equations 3.11 to 3.18 can be solved by Laplace transformation. The Laplace domain solution for the mobile-phase concentration C, at a point z in the bed is given as follows:

$$\bar{C}(z,s) = C_o \exp\left[\left(\frac{u}{2D_L} - \sqrt{\left(\frac{u}{2D_L}\right)^2 + \frac{s}{D_L} + \frac{3k_f}{mD_L R_P}\alpha(s)}\right)z\right] \tag{3.20}$$

where s is the Laplace transform variable and the function $\alpha(s)$ is defined as:

$$\alpha(s) = \frac{\sqrt{\frac{\epsilon_p s}{D_e}}\cosh\sqrt{\frac{\epsilon_p s}{D_e}}R_p - \frac{1}{R_p}\sinh\sqrt{\frac{\epsilon_p s}{D_e}}R_p}{\sqrt{\frac{\epsilon_p s}{D_e}}\cosh\sqrt{\frac{\epsilon_p s}{D_e}}R_p + \left(\frac{k_f}{D_e} - \frac{1}{R_p}\right)\sinh\sqrt{\frac{\epsilon_p s}{D_e}}R_p} \qquad (3.21)$$

Inversion of this expression to obtain an analytical time domain solution is difficult, as it involves the evaluation of an oscillatory integrand which converges very slowly (Rasmuson, 1985b). However, numerical inversion of the Laplace domain solution is possible. In section 3.5 the numerical method used to carry out the inversion in the present study is discussed.
In the remaining part of this section the conditions under which the SEC model is valid are examined. The model is based on the following assumptions:

1) Dispersed plug flow in the bed. This assumption seems to be adequate since non-uniformities in the bulk velocity profile appear to be important as a dispersive mechanism only at flow rates higher than those experienced in liquid chromatography (Johnson and Kapner, 1990).
On the other hand the use of a second order derivative (pseudo-Fickian) term to account for the effect of convective axial dispersion is justified for long, linear systems because the resulting Gaussian solution to a pulse input agrees well with observations on such systems (Athalye et al, 1992).

2) Axial and radial structural homogeneity of the bed. Non-uniformities are neglected.

3) Lateral concentration gradients and radial velocity variations are also neglected.

4) Transport parameters and fluid properties are assumed constant throughout the bed. At the low concentrations used in linear chromatography it is reasonable to assume that the equilibrium distribution coefficient, the transport parameters and the fluid properties are independent of concentration and constant. This a reasonable assumption for low loadings or dilute samples.

5) The particle size distribution (PSD) of the packing media is neglected. The matrix particles are assumed to be monodisperse. Only a few researchers have investigated the effect of polydispersity of packing media on chromatographic performance. Dawkins et al (1977) carried out one of the first studies of PSD effects in gel permeation chromatography using cross-linked polystyrene gels, but they mainly compared distributions with different mean sizes. Their data for a completely excluded solute revealed that plate heights of narrowly distributed and monodisperse media (with

same mean size) are similar.

Nakanishi et al (1978) investigated the performance of sieved size fractions of Sephadex (Pharmacia) gels. They found that the dimensionless Van Deemter plots for different sieve fractions fell onto a single line, when the volume-averaged root-mean-square diameter was used for scaling.

In a very recent work Athalye et al (1992) have shown that existing models of differential chromatography are capable of predicting the behaviour of polydisperse packings in commercially available columns. They carried out experiments using proteins on size-exclusion media with a narrow particle size distribution. Their studies confirmed that such packings perform as well as their more expensive monodisperse counterparts and that a modest degree of polydispersity has no significant effect on separation efficiency. They also mentioned that there is in fact a reason to believe that a moderate degree of polydispersity may be helpful since polydispersed packings give higher packing densities. It appears that monodisperse packings can give rise to long-range wall effects (Knox and Parcher, 1969).

The effect of matrix particle size on the effective intraparticle diffusivity D_e has been investigated by Boyer and Hsu (1992). From the analysis of experiments carried out with fractionated Sepharose CL-6B, they found that protein intraparticle diffusivity in agarose matrices was independent of particle size.

Theoretical analyses on this subject have been carried out by a few workers (Rasmuson, 1985b; Carta and Bauer, 1990) who, by means of numerical solutions of special cases of the chromatography model equations, investigated the effect of PSD on column performance. Rasmuson (1985b) suggested that the appropriate mean particle diameter to be used in the chromatographic models and calculations should correspond to the equivalent surface area per unit particle volume (see section 2.3.2.4).

The general consensus from all these investigations is that polydispersity may have an adverse impact on the broadening of a peak only for very broad or asymmetric PSD in a short bed. For columns with the large number of plates typically necessary for protein separations, it appears adequate to use chromatographic media with a symmetric size distribution of modest breadth.

This conclusion also implies that existing chromatography models that assume a monodisperse particle size should adequately simulate column performance provided the packing media has a narrow PSD and the proper mean particle diameter is used in the calculations (see section 2.3.2.4).

Modern liquid chromatography is almost always conducted in the creeping flow regime, defined for packed beds by the Reynolds number being of the order of unity or smaller. It can be shown from the continuum form of the model equations and on purely dimensional grounds (Bird et al, 1960) that for forced convective transport in the creeping flow regime, the dimensionless transport

coefficients should depend on the Reynolds and Schmidt numbers only through their product, the reduced velocity ReSc (also called the diffusion Péclet number) and on system geometry. The Reynolds and Schmidt numbers are given respectively by:

$$Re = \frac{d_p u \epsilon \rho}{\mu} \tag{3.22}$$

and

$$Sc = \frac{\mu}{\rho D_m} \tag{3.23}$$

The dimensionless transport coefficients, the dispersion Péclet number Pe_L and the Sherwood number Sh (or the Nusselt number Nu), are simply scaled versions of the convective axial dispersion coefficient D_L and the fluid-phase mass transfer coefficient k_f, as defined below

$$Pe_L = \frac{d_p u}{D_L} \tag{3.24}$$

$$Sh = \frac{d_p k_f}{D_m} \tag{3.25}$$

Experience suggest that the most important determinant of the flow geometry in a well-packed, random bed of spheres is the interstitial void fraction ε. It is hence usual to express the dimensionless transport parameters as functions of ReSc and ε in creeping flow. The typical reduced velocity range of interest in liquid chromatographic practice is $1 < ReSc < 200$, with size exclusion chromatography usually conducted below ReSc=50 (Athalye et al, 1992).

3.3 Transport parameters.

The following sections present the correlations and methods used to estimate or to measure the transport parameters that characterize column performance, i.e. axial dispersion, fluid phase mass transfer and intraparticle diffusion. These are also the parameters required by the size exclusion chromatography model in order to carry out peak simulations. Particular emphasis is given to those correlations which are applicable within the reduced velocity (ReSc) range of interest to chromatography.

3.3.1 Axial dispersion.

Axial dispersion in packed beds is generally considered a one dimensional Fickian process which must account for local non-uniformities in the interstitial solvent velocity (eddy diffusion) resulting from the intricate flow paths followed by the fluid around matrix particles, and for local non-uniformities in solute concentration due to axial molecular diffusion. Assuming the effects of eddy diffusion are random and symmetrical they can be expressed as an increase in the diffusion coefficient of the solute in the mobile phase to yield the following equation:

$$D_L = \lambda d_p u + \gamma D_m \tag{3.26}$$

This expression includes an obstruction factor, γ, to correct for the longer flow path due to the presence of the packing particles. The form of the first term of eq. 3.26 was suggested by van Deemter et al (1956) and was later rationalized by Chilcote and Scott (1973).

Lenhoff (1985) has thoroughly reviewed modelling strategies for describing dispersion in randomly packed beds and thus an exhaustive review shall not be attempted here. However, some of the most relevant correlations developed to estimate the axial dispersion coefficient in randomly packed beds will be examined.

The mechanisms of axial dispersion D_L, vary with ReSc (Bear, 1972). Molecular diffusion predominates when ReSc is low. Several investigations (Edwards and Richardson, 1968; Gunn and Pryce, 1969) confirmed that for ReSc<<1, the dispersion coefficient is simply D_m/τ, indicating purely diffusive axial spreading; here τ is the interstitial tortuosity factor, about 1.4 for a packed bed of spheres (Gunn, 1987). Under these conditions D_L/D_m is constant. For very high ReSc values, the dispersion Péclet number approaches an asymptotic value which depends only on the Reynolds number (Miller and King, 1966; Ebach and White, 1958), corresponding to the limit of purely hydrodynamic dispersion (Hiby, 1962). Gunn (1969) correlated this high ReSc limit in the form

$$Pe_L \approx \frac{2p}{(1-p)} \qquad for\ Re > 1000 \tag{3.27}$$

where the adjustable parameter p for a column packed with spheres is found experimentally to be

$$p = 0.17 + 0.33\exp(-24/Re) \tag{3.28}$$

The behaviour for intermediate values of reduced velocity ReSc, the region of importance to chromatography and to the present study, has been analyzed by several workers (Giddings, 1965; Gunn, 1969; De Ligny, 1970; Hejtmánek and Schneider, 1993). Among them Gunn (1969 and

1987) has perhaps performed the most extensive experimental work and has carried out a semi-theoretical treatment which involves the adjustable parameter p given above, leading to the development of a correlation capable of predicting convective axial dispersion coefficients reasonably well over a wide range of conditions for both gases and liquids:

$$\frac{1}{Pe_L} = \frac{(1-p)}{p}[Y + Y^2(\exp(-1/Y)-1)] + \frac{\epsilon}{\tau ReSc} \qquad (3.29)$$

where

$$Y = \frac{p(1-p)ReSc}{4\alpha_1^2(1-\epsilon)} \qquad (3.30)$$

Here α_1 is the smallest positive zero of the Bessel function $J_0(.)$, approximately 2.405 and the bed tortuosity τ= 1.4 for beds of spheres (Gunn, 1987). This expression for Pe_L depends only on the product ReSc when attention is restricted to the creeping flow region (with p=0.17) where it reduces to the widely accepted asymptotic value $D_L = D_m/\tau$. Gunn (1987) also provided an extension of the above correlation to account for macroscopically non-uniform flow and wall effects.

Wakao and Funazkri (1978) proposed a correlation in which the low ReSc asymptote of the effective dispersion coefficient should be dependent on whether solute transfer to the packing occurs or not,

$$\frac{\epsilon D_L}{D_m} = b + 0.5\ ReSc \qquad (3.31)$$

where the value of b is equal to 20 when mass transfer takes place (the inside of the particle is not involved in the mass transfer) and equal to (0.6-0.8)ε when no mass transfer occurs between the particles and the fluid in packed beds. However this correlation has not been widely tested.

Athalye et al (1992) have carried out an empirical fit to data of Miller and King (1966) in order to obtain a conservative upper estimate for the convective dispersion coefficient for intermediate ReSc values (7<ReSc<320) in creeping flow (Re<1). The following result summarizes the data

$$Pe_L = \left(\frac{ReSc}{1-\epsilon}\right)^{-1/6} \qquad (3.32)$$

After comparing the fit to the Miller and King data with other correlations Athalye et al (1992) suggested that the typical behaviour for convective dispersion in packed beds over the intermediate range of reduced velocities, probably lies between the limits given by the expression of Gunn (1969, 1987) and the data of Miller and King (1966). Therefore they used eq. 3.29 and eq. 3.32

as two representative limits of convective dispersion for predictive purposes in chromatography. Hejtmánek and Schneider (1993) obtained axial dispersion coefficients by time-domain fitting of the response peak to square-wave signals. Besides axial dispersion in the column, the fitted model accounts also for regions with ideal mixing and transport delay. The study employed three tracer-liquid-carrier-liquid systems and columns packed with nonporous spherical glass ballotini supports. Their results were expressed in terms of the Bodenstein number, Bo, which is another denomination of the dispersion Péclet number ($Bo= ud_p/D_L$). These workers carried out their experiments in the creeping flow region ($1x10^{-4} < Re < 1$) and derived the following empirical correlation, valid for $0.385<ReSc<580$,

$$Pe_L = Bo = 0.863(ReSc/\epsilon)^{(-0.078)} \tag{3.33}$$

In another recent study utilising fine nonporous spherical glass beads (48-170 μm), Kawai et al (1992), investigated the effect of Reynolds number, particle diameter and particle size distribution on the Péclet number. They proposed the following correlation

$$Pe_L = 1.26\left(\frac{d_p}{d_e}\right)^3\left(\frac{Re}{\epsilon}\right)^{-0.202} \tag{3.34}$$

valid for 5.0×10^{-5} m $< d_p < 2.0 \times 10^{-4}$ m; $0.59 < d_p/d_e < 0.99$ and $1.0 \times 10^{-2} < Re/\varepsilon < 2.0$. Here d_p is the mean particle diameter and d_e is the absolute size constant, this parameter has been introduced in order to take into account the polydispersity of the packing particles. It is defined by means of the expression

$$U = \left(\frac{d_p}{d_e}\right)^m \tag{3.35}$$

where U represents the fraction of surface area of cumulative under size particles, and m is a constant depending on the spread of the size distribution (U=1 for monodispersed particles). These researchers employed samples of 1 N KCl for the determination of the axial dispersion coefficients and therefore their studies apply to the region $3 < ReSc < 625$, and are valid for $1x10^{-2}<Re/\varepsilon<2.0$. The effect of particle size and particle size distribution on the axial dispersion coefficient has also been investigated by Östergren and Trägårdh (1990), in the intermediate range of ReSc ($1<ReSc<158$) in creeping flow ($0.004<Re<0.6$). They used non-porous glass beads as packing material with average diameters of 125-150 μm, and with different particle size distributions ($PSD/d_p(mean)= 0.06-0.21$). Their results showed that a statistical model developed by Saffman (1960) predicted very well the axial dispersion coefficient at the lower range of their measured

ReSc while the model of Harleman (cited in Dullien, 1979) was a good model for the upper end of their measured ReSc. They concluded that particle size distribution has very little influence on the axial dispersion coefficient under chromatographic flow conditions.

In a study of dispersion of a non-retained solute ($NaCl-CaCl_2$) in a column packed with impervious spherical particles, Magnico and Martin (1990) found that the Giddings (1965) coupling equation correctly fitted their experimental data obtained in the range $0.19 < ReSc < 114$ for $Re < 0.4$. Their results validated the physical model of the coupling of the convective and diffusive transport processes on which the Giddings equation is based.

On the theoretical side Koch and Brady (1985) have carried out an asymptotic analysis of dispersion, valid for low volume fractions of randomly configured spheres held fixed in a creeping ambient flow. Their prediction of the convective axial dispersion coefficient, derived for $ReSc >> 1$, does follow the general trend of the experimental measurements taken from the literature, but severely underestimates the data over ReSc values between 1 and 200.

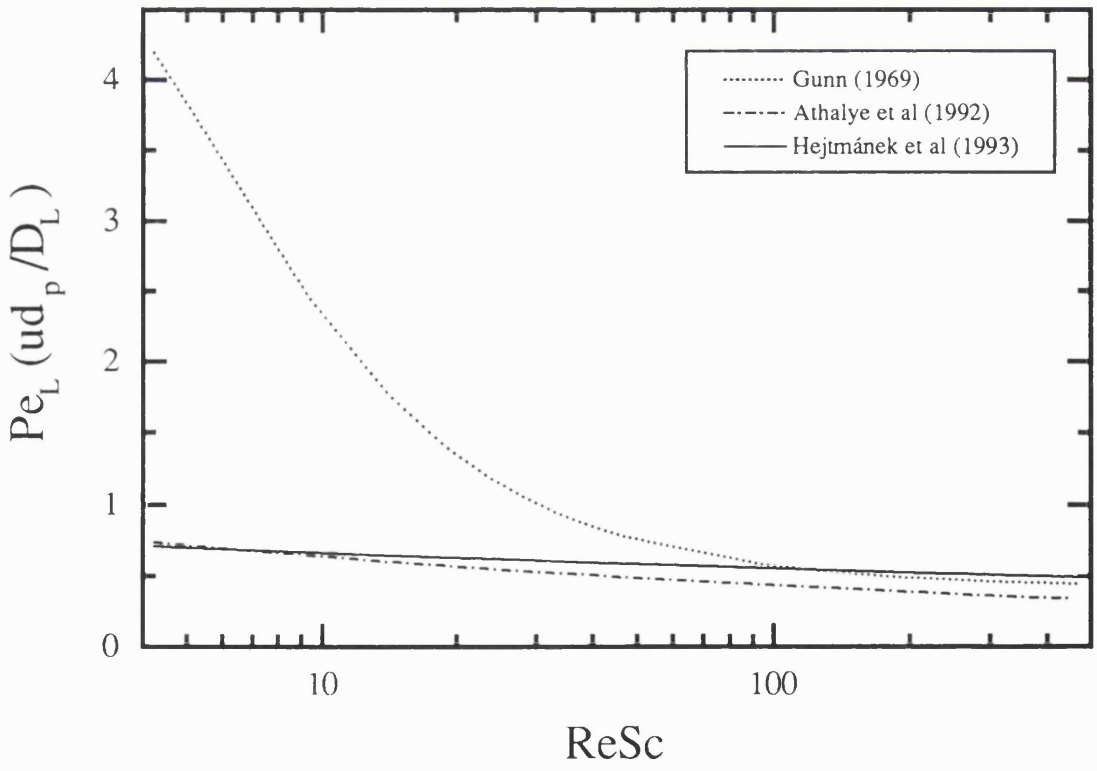

Fig. 3.1 Comparison of the most relevant correlations developed for the prediction of the axial dispersion coefficient within the chromatographic range of operation. Péclet number Pe_L as a function of reduced velocity ReSc. The following parameters were used: ε=0.3343, μ= 0.01118 g/cm-s, d_p= 0.0092 cm, π= 1.0041 g/cm^3, D_m= 6.55x10^{-7} cm^2/s and τ= 1.4. Correlations: ·····, eq. 3.29; -·-·-·, eq. 3.32 and ———, eq. 3.33.

Fig 3.1 shows the three most adequate correlations for the estimation of the axial dispersion coefficient within the conditions of importance to liquid chromatography. Athalye et al (1992) considered their own correlation (based on the data of Miller and King, 1966), and the correlation developed by Gunn (1969) as the limits within which the axial dispersion coefficient should lie for the intermediate range of ReSc. It can be observed from fig. 3.1 that the correlation of Hejtmánek and Schneider (1993) corroborates this suggestion at least within the range 10<ReSc<100. This correlation follows very closely that of Athalye et al (1992) for all the range of interest to liquid chromatography (1<ReSc<200). Within the region 100<ReSc<200 the three correlations follow each other very closely, the correlations of Gunn (1969) and Hejtmánek and Schneider (1993) being even closer to each other. It appears from this analysis that the correlation derived by Hejtmánek and Schneider (1993) follows the expected trend and is probably the most appropriate to be used in liquid chromatography.

From the foregoing discussion and despite the recent efforts it is evident that literature data on the convective axial dispersion under the conditions prevailing in liquid chromatography is scarce and more work is needed to characterize better this parameter, in particular for reduced velocities between 1 and 100 where convective dispersion is poorly understood and there is a need for more information. Also considerable ambiguities remain concerning the effects of particle size distribution, the ratio of column to particle diameter, and interphase mass transfer on the axial dispersion coefficient.

3.3.2 Particle-to-fluid mass-transfer resistance.

As mentioned above, the fluid-phase mass transfer coefficient k_f which characterizes the flux at the particle surface can be expressed in terms of a Sherwood number Sh, or a Nusselt number Nu. For creeping flow and in the absence of natural convection, Nu is a function of ReSc only, on purely dimensional grounds (Karabelas et al, 1971). For large Re, where flow begins to become locally unsteady, Nu may be a function of both Re and Sc, this situation, however, is probably never encountered in liquid chromatography.

Boundary-layer theory predicts the asymptotic functional dependence of Nu for large values of ReSc in creeping flow to be of the form (Sørensen and Stewart, 1974; Stewart, 1987),

$$Nu = \alpha(ReSc)^{1/3} \quad for\ ReSc \gg 1 \tag{3.36}$$

This relationship has been experimentally verified by Wilson and Geankoplis (1966) for random packed beds, and by Karabelas et al (1971) for a dense cubic array with one active sphere. They

obtained $\alpha = 1.09/\varepsilon$. As far as the behaviour at low values of ReSc is concerned, there appears to have been some uncertainty in the literature (Martin, 1978; Wakao and Kaguei, 1982) as to whether the Nu decreases to zero or to a limiting value when ReSc tends to zero. However, both theoretical analysis (Sørensen and Stewart, 1974; Fedkiw and Newman, 1978) and experimental results (Gunn and DeSouza, 1974; Miyauchi et al, 1976) suggest that the Nusselt number approaches a constant value β as ReSc $\rightarrow$ 0, which in turn implies that boundary-layer resistance should be unimportant under most circumstances. Indeed, at the low Reynolds numbers used in chromatographic separations (Re<1), it is unlikely that the particle-to-fluid resistance is the rate controlling step.

Following a procedure for patching up asymptotic results, Athalye et al (1992) used this limiting information to develop the following expression:

$$Nu \approx \left[\beta^3 + \left(\frac{1.09}{\epsilon}\right)^3 (ReSc)\right]^{1/3} \qquad (3.37)$$

where β was given a conservative value of 4.0, according to the findings of Sørensen and Stewart (1974). The behaviour of this cubed averaged form has only been compared with the numerical results of Sørensen and Stewart (1974), giving a uniformly good agreement within 10% over five decades of ReSc (Athalye et al, 1992). Since the contribution of fluid-phase mass transfer resistance to plate height is negligibly small at low ReSc, the large ReSc limit, (i.e. 4.0) seems to be adequate for most practical purposes. This correlation seems to be the only one derived specifically for the range of ReSc used in chromatographic practice, however, it has not been experimentally verified nor has it been fully compared with reported experimental data. All the other correlations to date have been developed by correlating data over a wide range of both ReSc and Re and hence they probably deviate from pure ReSc dependence expected for creeping flow.

The effect of fluid dispersion coefficient on particle-to-fluid mass transfer coefficients in packed beds has been considered by Wakao and Funazkri (1978). These researchers have corrected gas-phase and liquid-phase mass transfer data published in the literature by taking into account the influence of axial dispersion. The corrected Sherwood numbers in the range $3 < Re < 10000$ were correlated by

$$Sh = 2 + 1.1\, Sc^{1/3} Re^{0.6} \qquad (3.38)$$

In this correlation the Sherwood number does not keep decreasing when the Reynolds number tends to zero, and indeed reaches a limiting value, which they found to be approximately 2.

Applying the analogy between heat and mass transfer to particle transfer processes and based on a stochastic model, Gunn (1978) has shown that for particle-to-fluid mass transfer, the dependence

of the Sherwood number (or Nusselt group) upon the Reynolds and Schmidt groups may be expressed as:

$$Sh = (7-10\epsilon+5\epsilon^2)(1+0.7Re^{0.2}Sc^{1/3}) + (1.33-2.4\epsilon+1.2\epsilon^2)Re^{0.7}Sc^{1/3} \quad (3.39)$$

This correlation predicts that the limiting value of Sh, when ReSc→ 0, depends only upon the void fraction of the bed.

Ohashi et al (1981) correlated the particle-to-fluid mass-transfer coefficients for fixed beds making use of the specific power group, $E^{1/3}d_p^{4/3}\rho/\mu$, which includes the energy dissipation rate E. The term E is related to the kinetic energy that is dissipated into heat when the fluid flows against the drag force. These workers defined E, for a bed section equal in height to a single layer of particles as, $E=25(1-\varepsilon)\varepsilon^2 C_{D0}u^3/R_p$, where C_{D0} is the drag coefficient for a single particle based on the superficial velocity u_o. Based on the analysis of a large amount of selected data, in which the effect of natural convection on mass transfer was minimal[1], they obtained the following correlation

$$Sh = 2 + 0.51\left(\frac{E^{1/3}d_p^{4/3}\rho}{\mu}\right)^{0.6} Sc^{1/3} \quad (3.40)$$

which applies within the following range

$$0.2 < \left(\frac{E^{1/3}d_p^{4/3}\rho}{\mu}\right) < 4600 \quad (3.41)$$

$$505 < Sc < 70600 \quad (3.42)$$

In this correlation the specific power group replaces the normally used Reynolds number to express the hydrodynamic effect on mass transfer between flowing fluid and fixed particles. This substitution has allowed the development of a correlation which is applicable over a wide range, from low to high Re

$$10^{-3} < Re < 10^3 \quad (3.43)$$

and which fully covers the range of interest in chromatographic separations 1<ReSc<200.

As already mentioned controversy has existed as to whether the Sherwood number approaches a lower limiting value as the Reynolds number goes to zero or continuous to decrease. However,

[1] In the measurement of fluid-phase mass-transfer coefficients at low flow rates, there is interference by natural convection. The convection effect becomes increasingly important as the Reynolds number decreases beyond certain critical value. This critical Reynolds number above which natural convection may be ignored is generally not clear (Wakao and Kaguei, 1982).

it seems that this matter has been clarified by Wakao and Funazkri (1978) and by the theoretical work of Sørensen and Stewart (1974) and Gunn (1978). They have demonstrated the existence of a limiting value of the Sherwood number. In some of the previous correlations this asymptotic value has been taken as 2. Kehinde et al (1983b) provided experimental evidence to demonstrate that this value is indeed approximately 2. Their experiments covered the creeping flow range $0.025<Re<0.25$.

In fig. 3.2 a comparison of the most important correlations for the prediction of the particle-to-fluid mass-transfer coefficient is presented. It can be observed that the correlation developed by Ohashi et al (1981) follows very closely the correlation of Athalye et al (1992) at the upper range of reduced velocity, ReSc. This latter correlation was specially derived to be applicable within the chromatographic range of operation. The correlation of Gunn (1978) overestimates this trend, while the correlation developed by Wakao and Funazkri (1978) underestimates it. At the lower range of ReSc, Ohashi et al (1981) have taken the limiting value of the Sherwood number to be approximately 2, according to the findings of Kehinde et al (1983b) above mentioned. It is therefore apparent that the correlation of Ohashi et al (1981) is the most suitable to be used in the creeping flow conditions encountered in the chromatographic area.

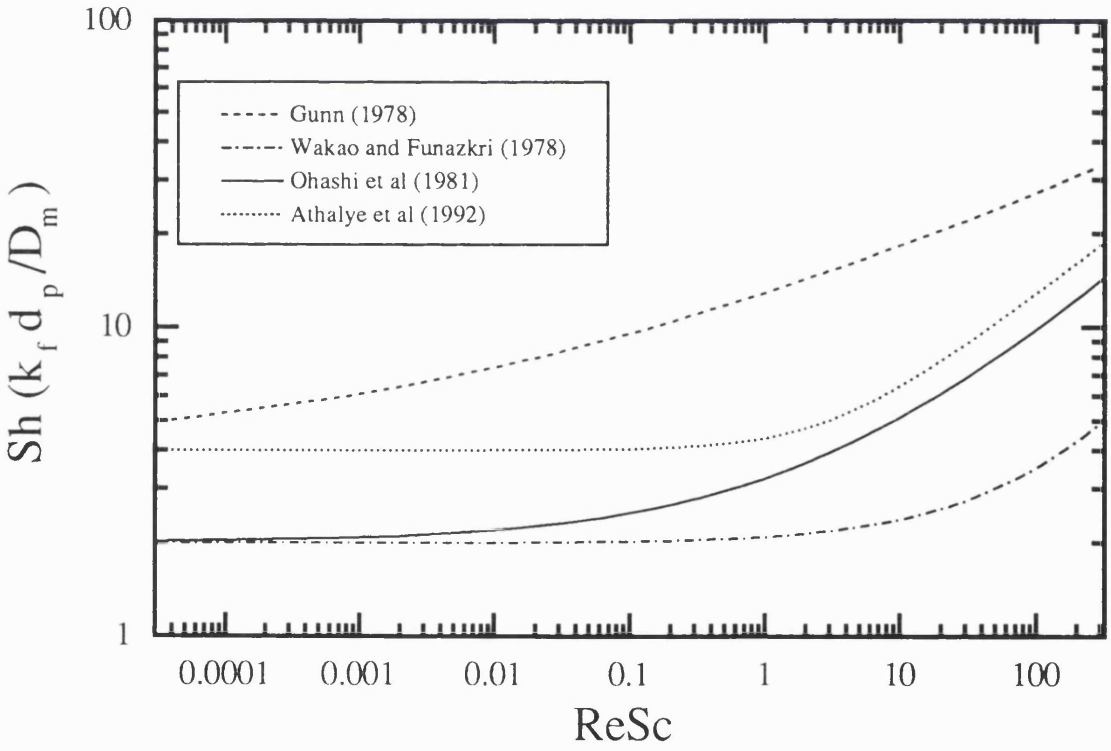

Fig. 3.2 Comparison of the most important correlations developed for the prediction of the fluid-to-particle mass-transfer coefficient, within the chromatographic range of operation. Sherwood number Sh, as a function of reduced velocity, ReSc. The following parameters were used: ε= 0.4, μ=0.01118 g/cm-s, d_p=0.009 cm, ρ=1.0041 g/cm^3, C_{DO}=24/Re and Sc= 10000. Correlations: ------, eq. 3.39;-·-·-·, eq. 3.38;———, eq. 3.40 and ·····, eq. 3.37.

3.3.3 Intraparticle diffusion.

Among the mass-transfer resistances at work in the chromatographic separation of proteins, it seems, at least in the great majority of cases, that intraparticle diffusion is the rate limiting step (Horstmann and Chase, 1989; Skidmore et al, 1990). This situation arises due to the restricted motion experienced by the large protein molecules through the porous network and tortuous paths encountered within the chromatographic matrices. The slow diffusion of proteins is detrimental to process performance, and therefore, determination of the intraparticle diffusivity D_e is very important in the characterization of any chromatographic process.

Several approaches have been followed in order to estimate the effective diffusivity of proteins inside porous supports. Some workers have fitted chromatography models to experimental data (Arve and Liapis, 1987; Johnston and Hearn, 1991; McCoy and Liapis, 1991; Davies, 1989a; Ernest and Hsu, 1991), others have used pulse analysis and HETP theory (Arnold et al, 1985; Ching et al, 1989; Boyer and Hsu, 1992; Ming and Howell, 1993), while some others have developed specific mathematical models to predict this parameter (Laurent and Killander, 1964; Ogston et al, 1973; Cukier, 1984; Boyer and Hsu, 1992). In all of these studies the diffusivity has been assumed to be independent of concentration, this is a reasonable assumption at the low concentrations encountered in linear chromatography. An exhaustive revision is not intended here, and only some of the most relevant works within this field will be outlined.

Early theoretical approaches (Schneider and Smith, 1968) utilised the moments method to determine intraparticle diffusivities and other rate parameters. This method is based on the statistical moments theory of Kubin (1965) and Kucera (1965), the HETP or plate height method being a special case. In these pulse analysis techniques the rate parameters are obtained indirectly by extracting the necessary parameters from the analysis of successive moments or plate heights as obtained from the experimental data. The main drawback of the moments approach is that too much weight is placed on the tail part of the output response corresponding to larger values of time where signal noise and eluting impurities may contribute to inaccurate measurements. Integration and tail truncation errors could be considerable. On the other hand the use of the HETP method is strictly applicable only when the exiting peaks are Gaussian.

Despite their susceptibility to error, pulse techniques have proven useful for quantifying the characteristic rate parameters governing the chromatographic process and have been used by several researchers to determine intraparticle diffusivities of proteins (Arnold et al, 1985; Ching et al, 1989; Boyer and Hsu, 1992; Ming and Howell, 1993). These techniques will be dealt with in more detail in sections 4.2.1 and 5.2.4.

Arve and Liapis (1987; 1988) carried out extensive work on the estimation of kinetic parameters

by matching the predictions of appropriate models with experimental data. They developed a very sophisticated batch adsorption model (Arve and Liapis, 1987) which has been used to estimate intraparticle diffusion coefficients of proteins. Based on the premise that the parameters that characterize the intraparticle mass transfer and adsorption mechanisms are independent of the operational mode (e.g. batch, fixed, fluidized bed), they fitted the predictions of their model to information obtained from finite bath experiments. They indicated that parameters so estimated could be directly used to predict the performance of chromatographic columns.

Following this same consideration, Johnston and Hearn (1991) matched several mathematical models with finite bath experimental data in order to determine the effective diffusivity, D_e of proteins with low isolelectric points, in three different anion-exchangers. They found the correlation between theory and experiment was best when using the most sophisticated model developed by Arve and Liapis (1987), but of the three proteins tested only the largest one, i.e. ferritin, was found to be pore restricted.

In the evaluation of two kinetic models for biospecific adsorption, McCoy and Liapis (1991) found that the estimated value of the intraparticle diffusion coefficient varied according to which of the models was used to carry out the matching procedure with the dynamic batch experimental data. They indicated that while it is a necessary condition for a kinetic model to describe properly the experimental overall mass-transfer resistance, this is not a sufficient condition for the accurate determination of the adsorption mechanism and for the accurate estimation of the values of the rate constants and the pore diffusivity. In the affinity adsorption system used in this study, the variation of the estimated value of the film mass-transfer coefficient k_f, by ±20%, had no significant effect on the dynamic behaviour of batch and column systems. On the other hand the effect of the variation of the estimated pore diffusivity D_e by ±20% on the same both systems was appreciable.

It must be pointed out that the use of this approach, involving the monitoring of the solute uptake by spherical particles in a finite bath, is also prone to experimental errors due to the small particle size used in chromatography which results in a very fast approach to equilibrium. These errors have been studied by Westrin and Zacchi (1991).

Davies (1989a) devised a method for measuring diffusion coefficients of proteins inside gel-filtration media, in which experimental and theoretical breakthrough curves are compared on the basis of the area beneath the curve up to the point where a dimensionless defined time equals unity. Although the accuracy of this method is limited, it was considered that diffusion coefficient values could be obtained within about ±25% of accuracy. Since the use of this method is restricted to solute residence times in the mobile phase that are smaller when compared with the diffusion times in the stationary phases, it is not applicable to rapidly diffusing molecules.

Other researchers, like Ernst and Hsu (1991) have obtained estimates of the intraparticle diffusivity D_e, by fitting the predictions of suitable chromatography models to the experimental peaks obtained from column experiments. To carry out the estimations Ernst and Hsu (1991) have taken advantage of the flexibility and computational efficiency of the Fast Fourier Transform algorithm. These characteristics are most needed when implementing an iterative algorithm such as is generally the case with parameter estimation routines.

Lenhoff (1987) considered that the matching of model predictions with the full chromatographic peak in the time domain would allow a much safer parameter estimation and a more rigorous use of experimental data than other methods which involve moments and plate height calculations. The reason being that the estimation of a parameter value in this way would be based on the information contained in each point of the chromatographic profile.

It has been suggested (Lightfoot et al, 1990) that since intraparticle diffusion appears in combination with other resistances in the integral descriptions needed for parameter estimation, and due to ambiguities regarding the boundary-layer mass transfer resistance and ambiguities caused by non-uniformities and viscous effects, estimates of this parameter from column experiments are unreliable. This suggestion is supported by available estimates which vary over orders of magnitude for similar systems (Arve and Liapis, 1987; Arnold et al, 1985; Graham and Fook, 1982, and Tsou and Graham, 1985). For this reason it has been recommended to seek and develop experimental methods to determine, in an independent manner, not only the coefficient of intraparticle diffusion but all other parameters required (Lightfoot et al, 1990).

Measurements of intraparticle diffusion of macromolecules in chromatographic gels are still scarce. Recently a few techniques have been implemented to carry out these measurements in a direct and independent way. The diffusion of dextran fractions with Stokes radius between 33 and 100 nm have been studied by Key and Sellen (1982), in gels containing 0.3-4% of agarose using the quasi-elastic laser light-scattering method (QELS). However, light scattering, as an alternative means of measuring diffusion coefficients in Sepharose beads is difficult to apply owing to scattering of light by the Sepharose particles themselves (Davies, 1989a). Besides it suffers from the presence of artifacts at high protein concentrations and low ionic strength (Gibbs, 1991).

The reduced coefficient of diffusion, D_e/D_m of several globular proteins have been measured in the AcA-34 gel (Moussaoui et al, 1991) and in Sepharose CL-B gels (Moussaoui et al, 1992) using the technique of fluorescence recovery after photobleaching (FRAP). In this method, a small region of a volume containing a mobile fluorescent molecule is exposed to a brief intense pulse of light, thereby causing an irreversible photochemical bleaching of the fluorophores. The diffusion coefficient is determined by measuring the rate of recovery of fluorescence which results from transport into the bleached region from the unirradiated surroundings. They found that the model

of Ogston et al (1973), i.e. eq. 3.47, seemed more appropriate to describe the sieving properties of microporous gels such as the polyacrylamide AcA-34 gel, than those of reticulated matrices like the Sepharose gels. Their analyses suggested that the obstruction effect is mainly responsible for the diffusion retardation of proteins in these gels.

Gibbs and co-workers (1989, 1991, 1992) measured ovalbumin diffusivities in solution and inside Toyopearl HW65 media at 20°C by means of pulse field gradient NMR. They found that the ratio D_g/D_m is 2.2±0.4 over the concentration range 1-200 mg/ml. In this method the protein was confined to the particle interiors by use of a nonaqueous excluding solvent in the interparticle voids, and NMR signals from the protein were differentiated from those of the polymer particles and the solvents present by selectively labelling the protein with fluorine-containing species. Hence, these measurements although more reliable, also present uncertainties in relation to the efficacy of the labelling technique and the interparticle solution exclusion procedure.

The diffusion coefficient of a solute in gels may depend on the probe distance associated with the method of measurement (Moussaoui et al, 1992). In quasi-elastic laser light scattering method (QELS), the probe distance is a few tenths of a micrometer whereas in FRAP (fluorescence recovery after photobleaching) measurements is of the order of 20 μm. The pulse field gradient NMR technique should give the most accurate results since its spatial resolution is of the order of 10 μm. However, due to the fact that these methods require advanced skills and equipment, and are in some cases not easy to employ, traditional methods are still widely used.

In the field of modelling molecular and matrix network interactions it has been adequate to follow the commonly used practice of considering the intraparticle diffusivity to be proportional to that in free solution, with the proportionality constant depending on the size of the pores relative to that of the solute and on the shape and tortuosity of the pores (Satterfield et al, 1973). Expressions for this proportionality constant, derived from a simplified hydrodynamic model of pore-wall effects and written in terms of solute-to-pore size ratio, have been used successfully in the literature (Satterfield et al, 1973; Walters, 1982 and Ghrist et al,1987).

Early experimental studies showed that the diffusion of proteins in a random network of straight fibres (like the Sepharose structure, see section 2.3.1.1) empirically obeyed the equation (Laurent and Killander, 1964)

$$\frac{D_e}{D_m} = \exp\left(-B r_o c_f^{1/2}\right) \qquad (3.44)$$

where r_o is the interaction radius between the protein and the polymer fibres, c_f is the polymer fibre concentration and B is a proportionality constant.

Ogston et al (1973) were the first to develop a theoretical framework to explain this empirical

equation. Based on a stochastic model, in which the size of the random walk steps are reduced by the presence of the polymer fibres, and considering the interaction radius to be the sum of the fibre radius r_f and the Stokes radius r_s of the protein, they obtained the following equations

$$\frac{D_e}{D_m} = \exp\left[-(r_s + r_f)v_f^{1/2}/r_f\right] \tag{3.45}$$

$$K_d = \exp\left[-(r_s + r_f)^2 v_f / r_f^2\right] \tag{3.46}$$

where v_f is the volume of fibres per total volume and K_d is the equilibrium partition coefficient. From these equations it follows that

$$\frac{D_e}{D_m} = \exp\left[-\sqrt{(-\ln K_d)}\right] \tag{3.47}$$

As the theory of Ogston et al (1973) was derived for spherical molecules, in principle it should be more applicable to globular proteins.

More recently, Cukier (1984) derived a model that described the diffusion of Brownian spheres in a semidilute polymer solution based on the concept of hydrodynamic screening. Considering the polymer molecules to behave like rods, he defined the screening coefficient k_s, which indicated the resistance to flow resulting from the fixed rod network and arrived at the following equation

$$\frac{D_e}{D_m} = \exp[-k_s r_o] \tag{3.48}$$

Based on the models of Ogston et al (1973) and Cukier (1984), and the correlation of Young et al (1980) for the prediction of free diffusivities of proteins, Boyer and Hsu (1992) developed an empirical correlation to estimate protein intraparticle diffusivities in Sepharose gels. After fitting their model to their experimentally estimated values of intraparticle diffusivity of a series of globular proteins in Sepharose CL-6B, they obtained the following correlation,

$$D_e = 8.34 \times 10^{-10}\left(\frac{T}{\mu M^{1/3}}\right)\exp\left[-0.1307(M^{1/3} + 12.45)c_f^{1/2}\right] \tag{3.49}$$

where T is the absolute temperature and μ is the solvent viscosity. The correlation is valid for globular proteins having a molecular weight M in the range $10\,000 < M < 300\,000$, which are diffusing in matrices containing from 2 to 8% agarose. Predictions are expected to be accurate within 25%.

Although it is desirable to estimate the value of protein intraparticle diffusivities independently of the chromatographic model descriptions, as already mentioned the use of the experimental methods

developed to this aim requires advanced skills and sophisticated pieces of equipment. This is why traditional methods, like the pulse techniques are still widely used despite the possible errors involved.

More work is required both in the experimental side to provide more information about measured or estimated protein intraparticle diffusivities in different chromatographic media, and on the theoretical side to improve the quality of the predictions of this parameter by developing a more accurate mathematical model.

3.4 Equilibrium distribution coefficient.

The classical equation describing the phenomenon of size exclusion chromatography is based on the fact that a partition or equilibrium distribution coefficient K_d completely governs this process. Thus, the elution or retention volume V_R of a given chromatographic species is given by the following equation:

$$V_R = V_o + K_d V_i \tag{3.50}$$

where V_o is the column interparticle void volume and V_i is the intraparticle void volume.

For a macromolecule which does not bind to the gel matrix, it is clear from the previous equation that the partition coefficient between the gel and the surrounding solution is equal to the volume fraction effectively accessible to the macromolecule in the gel (Laurent and Killander, 1964)

$$K_d = \frac{V_R - V_o}{V_i} = \frac{V_R - V_o}{V_T - V_o - V_{gel}} \tag{3.51}$$

According to this definition, this parameter is usually denominated as inclusion porosity and denoted by ε_p in the SEC rate models, so that it is directly associated to the gel matrix characteristics.

Partition equilibrium is linear up to relatively high concentrations (Jönsson, 1987), this parameter is therefore a constant within the whole range of concentrations normally used in SEC. K_d is readily measured by chromatographic methods and finite bath experiments, and it can be estimated by pulse analysis techniques. The latter techniques are dealt with in the previous section and with more detail in sections 4.2.1. and 5.2.4.

The analysis of the parameters involved in the description of size exclusion chromatography is now complete and in the following section the numerical method used in the solution of the SEC model is presented.

3.5. Numerical method: Fast Fourier Transform (FFT) technique.

There is at present no analytical solution in the case of a pulse injection, to the general rate model of chromatography (Golshan-Shirazi and Guiochon, 1992), of which the size exclusion chromatography model used in the present study is a special case (eqs. 3.11 to 3.18). Although Carta (1988) has derived an analytical solution for this model, he did not consider axial dispersion (D_L=0) and his approach requires the assumption of a periodical injection. It is therefore necessary to conduct the solution of the general rate model of chromatography numerically.

Lenhoff (1987) implemented a solution of the general rate model for a pulse injection in the Laplace domain, and accomplished the inversion by contour integration in the complex plane. The integral to carry out the inversion into the time domain was conducted numerically.

In the particular case of size exclusion chromatography numerical inversion of the Laplace domain solution of different versions of the general rate model has been accomplished by several workers. Yamamoto et al (1979) neglected the fluid phase mass transfer resistance and carried out the inversion into the time domain either by integration of the complex function or by Fourier series approximation (Crump, 1976). Davies (1989a) used a numerical technique for the inversion of the Laplace transform solution of a gel filtration model used in his method for the determination of protein diffusion coefficients.

Numerical approaches to carry out the inversion of Laplace transforms have been developed by several authors, among them Dubner and Abate (1968) presented a method which relates the inverse Laplace transform to the finite Fourier cosine transform. Their resulting inversion formula is easy to program for digital computation (involving only cosines and exponential functions) but the convergence of the series is generally slow and the valid region in the time domain is restricted to the interval $0 \leq t \leq T/2$ (where the period is 2T). In their analysis Dubner and Abate (1968) first suggested the use and the implementation of the FFT algorithm to significantly reduce the computation time for their numerical method.

Based on the approach of Dubner and Abate, Crump (1976) developed a numerical method which inverts the Laplace transform by means of a Fourier series approximation. By involving the information contained in the sine function of the Fourier series, Crump (1976) reduced the error in the approximation, compared to that of Dubner and Abate (1968), and doubled the interval under which the inverse function is approximated, i.e. $0 \leq t \leq T$.

Hsu and Dranoff (1987) have theoretically justified why the sine function terms should be retained in the final inversion formula. Based on the complete Fourier series approach developed by Crump (1976) these researchers have directly adapted the FFT algorithm to invert Laplace transforms numerically. This technique was found to be very simple, accurate, efficient and generally superior

when compared to other conventional methods (Hsu and Dranoff, 1987).

The FFT algorithm was first used in the field of liquid chromatography by Jönsson (1984) to invert the Laplace transform solution of the linear non-ideal model developed by Grushka (1972). In gas chromatography Villermaux (1974) made used of this algorithm to study the influence of mass transfer processes and kinetic retention mechanisms on peak asymmetry. These researchers, however, did not take advantage of the simplicity and easiness of programming of the Fourier series approach.

Soon after the introduction of the FFT algorithm by Hsu and Dranoff (1987) the numerical method proposed by these workers was applied to the field of chromatography. Hsu and Chen (1987) solved the general rate model by adopting the FFT technique in order to study the influence of intraparticle diffusion and sorption kinetics on the peak shape in linear chromatography. They have also shown how this method can be applied to the prediction of breakthrough curves of a fixed-bed adsorber (Chen and Hsu, 1987), and compared its accuracy and speed with an exact analytical solution and the orthogonal collocation method. Wu et al (1991) developed a method that combines the FFT technique and the orthogonal collocation method to calculate breakthrough curves of nonlinear adsorption systems. Because the FFT technique has advantages of accuracy and computing speed, besides being used to analyze and to simulate chromatographic systems, it has also been used to perform parameter estimation by fitting the time domain solution to experimental chromatographic peaks (Ernst and Hsu, 1991).

Very recently Boyer and Hsu (1992) employed the Fast Fourier Transform (FFT) technique to perform the numerical inversion of the Laplace domain solution of the general rate model for the special case of SEC.

As already mentioned in section 3.2.1 the general rate SEC model as presented by Boyer and Hsu (1992) has been selected to be used in this investigation (The model is described in section 3.2.1). The FFT numerical method which was also followed by these researchers has been chosen to carry out the solution of the SEC model due to its accuracy, easiness of programming and its high efficiency. The Fourier series inversion formula (Crump, 1976) is given by Hsu and Dranoff (1987) in an adapted form to be implemented with the FFT numerical method, while the FFT algorithm has been clearly presented by Hsu (1979).

In the following chapter the effects of matrix compression on chromatographic performance will be looked at, while the effects of matrix fouling on column performance will be dealt with in chapter 5. In both of these investigations the SEC model and the FFT numerical method presented here will be used to aid the analysis.

3.6 Conclusions.

Throughout the present study, size exclusion chromatography (SEC) has been used because of its simplicity. It does not involve adsorption and its performance is characterized only by axial dispersion, particle-to-fluid mass transfer and intraparticle diffusion. Besides the partition equilibrium relationship is linear.

Due to its comprehensiveness and sophistication the general rate model for linear chromatography, as defined by Boyer and Hsu (1992) for size exclusion chromatography, has been employed in the present study to simulate outlet chromatographic peaks. The numerical Fast Fourier Transform (FFT) technique developed by Hsu and Dranoff (1987) has been selected to solve the SEC model. This technique is easy to program, accurate and very efficient.

Existing models of differential chromatography are capable of predicting the behaviour of polydisperse packings if they have a narrow size distribution (Athalye et al, 1992) and the surface average particle diameter is used in the calculations (Rasmuson, 1985b).

More research is needed to improve the understanding and the prediction of the convective axial dispersion coefficient under the conditions prevailing in liquid chromatography, in particular for reduced velocities ReSc between 1 and 100. To date the correlation derived by Hejtmánek and Schneider (1993) seems to be the most appropriate for the estimation of this parameter in the chromatographic range of operation.

On the other hand for the prediction of the particle-to-fluid mass-transfer coefficient it appears that the correlation developed by Ohashi et al (1981) follows the asymptotic behaviour expected at the low ReSc range and it seems to be the most suitable to be used in the creeping flow conditions encountered in the chromatography field. Nevertheless it is unlikely that the fluid phase mass transfer resistance is the rate controlling step within these conditions.

Although sophisticated methods have been developed for the measurement of protein intraparticle diffusivities, these require advanced skills and equipment. As a result traditional methods, which are easy to use, such as the pulse techniques are still widely used to estimate not only this parameter but also the axial dispersion coefficient and the equilibrium distribution coefficient.

CHAPTER 4

MATRIX COMPRESSION AND CHROMATOGRAPHIC PERFORMANCE

4.1 Introduction.

The effects that matrix compression has on the performance of chromatographic columns have not been thoroughly studied. Several researchers have reported improved performance of beds that have been highly compressed (Edwards and Helft, 1970; Fishman and Barford, 1970; Hjertén and Liao, 1988; Hórvath, 1990), see section 1.4.2. However, a satisfactory explanation concerning this improved performance has not been given. In the present chapter an attempt has been made in order to elucidate the effects of bed compression on the transport and equilibrium parameters that characterize the performance of size exclusion chromatography (SEC). The aim here is to distinguish which of these parameters are more affected when a chromatographic bed is progressively compressed and the extent of these effects.

The task therefore consists in conducting an analysis of the process behaviour under different levels of bed compression by estimating the characterizing parameters at each of these conditions. The major effects considered are those on the intraparticle diffusivity, the axial dispersion and the equilibrium distribution. The film mass transfer resistance is in general relatively small under the range of operation of chromatographic separations and will not be experimentally estimated.

Axial dispersion is highly determined by the bed structure and therefore it is expected to be much affected by bed compression. Besides, compression may lead not only to bed structural modifications but also to sorbent deformation, which indeed should have an effect on the partition and intraparticle diffusion coefficients. The aim of this study is therefore to clarify the origin and the extent of the changes effected by bed compression on the performance of SEC.

Pulse techniques, and in particular the HETP (height equivalent to a theoretical plate) method, have been used throughout this study in order to estimate the transport and equilibrium parameters at each compression condition. These techniques are prone to experimental and data analysis errors (Lenhoff, 1987), but they are easy to implement and above all do not require sophisticated pieces of equipment, this is why they are widely used in the field of chromatography (Arnold et al, 1985; Ching et al, 1989; Boyer and Hsu, 1992; Ming and Howell, 1993). A number of test proteins were employed in the pulse experiments so that matrix particle deformation occurring under bed

compression could be followed. (The intraparticle transport of larger molecules will be more affected and it will therefore be more feasible to detect these larger changes).
In the following sections the fundamentals of the HETP method are reviewed (section 4.2.1) followed by a description of the pulse experiments carried out in order to determine the parameters of interest to this study (section 4.2.2.2).

4.2 Materials and methods.

All the materials used in the study of the effects of compression on column performance have been described in Chapter 2, section 2.3.1. This includes the instrumentation, matrices, buffer and chemical components. Virtually the same experimental apparatus has been used as described in section 2.3.1.5. The configuration, however, has been modified and it is described in section 4.2.2.2. The methods used in the measurement of some of the matrix properties, i.e. particle size distribution and mean particle diameter have been covered in section 2.3.2.4, while the methods employed in the measurement of the buffer viscosity and density are presented in sections 2.3.2.1 and 2.3.2.2 respectively. The column packing technique and the bed compression method used in this study are presented here, together with the experimental procedure and conditions under which the pulse analysis was carried out.
Initially the pulse techniques and in particular the height-equivalent-to-a-theoretical-plate (HETP) method are reviewed. This latter method has been used to estimate the equilibrium distribution coefficient, the axial dispersion and the intraparticle diffusivity under different compression conditions. These are the parameters needed in the present analysis.

4.2.1 Pulse techniques and HETP method.

A general form of the pulse analysis, the moments method, has been developed by Smith and coworkers (Schneider and Smith, 1968, and Suzuki and Smith, 1971), based on the statistical moments theory of Kubin (1965) and Kucera (1965). Pulse analysis, in the form of height-equivalent-to-a-theoretical-plate (HETP) equations is a special case of the moments theory which applies only when the chromatographic peaks are Gaussian. Both of these techniques, have been used to obtain rate and equilibrium parameters in a variety of chromatographic systems employing proteins (Arnold et al, 1985; Ching et al, 1989; Boyer and Hsu, 1992; Ming and Howell, 1993). The calculation of peak moments by numerical integration of the experimental data is prone to

error, since small amounts of impurities, tailing, and channelling or shifts in the detector baseline can lead to large variations in the second and higher moments (Chesler and Cram, 1971). Due to this error, when the exiting peaks are Gaussian the simpler approach of the HETP method is preferred.

The pulse analysis method rests upon the relation of the statistical moments of the effluent concentration peak from a bed of porous adsorbent particles, to the rate constants associated with the various steps in the overall adsorption process. In order to establish this relationship a general chromatographic model including axial dispersion, mass transfer through a film surrounding the particle, diffusion into the particle and reversible first-order adsorption on the pore surfaces was solved in the Laplace domain (Schneider and Smith, 1968; Kubin, 1965 and Kucera, 1965). The transformed solution was subsequently used to derive expressions for the peak moments. In the absence of adsorption (the ideal case in SEC), the resulting expression for the first absolute moment of a peak μ_1, or average retention time is given by

$$\mu_1 = \frac{\int_0^\infty C(L,t)t\,dt}{\int_0^\infty C(L,t)\,dt} \tag{4.1}$$

$$\mu_1 = \frac{L}{u}\left[1 + \frac{(1-\epsilon)}{\epsilon}\epsilon_p\right] + \frac{t_o}{2} \tag{4.2}$$

where L is the bed length, u the interstitial fluid velocity, ϵ the column void fraction, ϵ_p the inclusion porosity[1] and t_o is the input pulse time. And the second central moment μ_2', a measure of peak spreading (the variance) is expressed by

$$\mu_2' = \frac{\int_0^\infty C(L,t)(t-\mu_1)^2 dt}{\int_0^\infty C(L,t)\,dt} \tag{4.3}$$

$$\mu_2' = \frac{2L}{u}\left\{\frac{D_L}{u^2}\left[1 + \frac{(1-\epsilon)}{\epsilon}\epsilon_p\right]^2 + \frac{\epsilon_p^2 R_p^2}{15}\frac{(1-\epsilon)}{\epsilon}\left(\frac{1}{D_e} + \frac{5}{k_f R_p}\right)\right\} + \frac{t_o^2}{12} \tag{4.4}$$

where D_L is the axial dispersion coefficient, R_p the particle radius, D_e the effective intraparticle diffusivity and k_f is the particle-to-fluid mass transfer coefficient.

[1] This parameter represents the fraction of intraparticle space that is available to a particular molecule. It is also called intraparticle void fraction and it is equivalent to the equilibrium distribution coefficient K_d.

For a sufficiently long column the exiting peak is Gaussian and the HETP is given by

$$HETP = \frac{\sigma^2 L}{t_R^2} \qquad (4.5)$$

In this case the peak is symmetric and the retention time t_R is identical with μ_1, while the variance σ^2 is also accurately obtained from the peak width without interference from tailing or small baseline shifts.

Substituting the first and second moments in the HETP equation the following expression is obtained

$$HETP = H = \frac{2D_L}{u} + \frac{2\epsilon_p^2 R_p^2 \epsilon(1-\epsilon)}{15(\epsilon+(1-\epsilon)\epsilon_p)}\left(\frac{1}{D_e} + \frac{5}{k_f R_p}\right)u \qquad (4.6)$$

Equations 4.2 and 4.6 constitute the basis of the HETP pulse response analysis. By means of these expressions and two peak properties, the retention time t_R and the variance σ^2, the equilibrium and rate constants can be estimated.

The HETP analysis is strictly valid only for columns with a large number of plates (L/HETP > 30) and when the spreading caused by end effects is small compared with the spreading caused by the transport phenomena, thus pulse techniques (HETP method) should be performed on a long column, even if the actual separation is to be performed on a short one (Arnold et al, 1985). When the bed contains a sufficient number of theoretical plates, Gaussian peaks can be expected if the particle mass transfer can be described by a linear concentration driving force (Arnold et al, 1985). The pulse analysis theory assumes linear equilibrium. This is practically always the case in SEC. Evaluation of the equilibrium distribution coefficient makes use of equation 4.2 which defines the first absolute moment μ_1 or retention time t_R. In this equation the equilibrium coefficient is represented by the inclusion porosity or particle accessible void fraction ε_p. The evaluation requires knowledge of the bed void fraction ε.

From the shape of eq. 4.2 it can be observed that a plot of μ_1-$t_o/2$ or t_R-$t_o/2$ *vs* L/u gives a straight line with a slope equal to $1+\varepsilon_p(1-\varepsilon)/\varepsilon$ which indicates the liquid volume fraction that is available to a tracer molecule. If the pores are not much larger than the tracer, entry of the tracer into the particle may be hindered. If the pores are so small that no tracer can enter, the slope is the interparticle void fraction ε. Knowledge of ε allows the evaluation of ε_p from the slope of the line. The estimation of the axial dispersion and the intraparticle diffusion coefficients involves the use of the HETP expression (eq. 4.6) and the analysis of the peak spreading σ^2 as a function of the interstitial fluid velocity, u.

In the experimental conditions usually encountered in size exclusion chromatography both the quantity D_L/u and the film mass transfer coefficient are affected only slightly by the interstitial velocity in the column (see figs. 3.1 and 3.2). Therefore it is clear from eq. 4.6 that a plot of HETP vs u should give a straight line with D_L/u as the y intercept and the slope depending on the intraparticle diffusion D_e, and the particle-to-fluid mass transfer coefficient k_f. Eq. 4.6 includes all the plate contributions inherent to the processes occurring inside the column, but the extracolumn contributions to peak spreading resulting from the initial sample bandwidth and the mixing in tubing, valves, detector and especially in the distributors are not considered.

Arnold et al (1985) described a method by which the extracolumn effects as well as the fluid film mass transfer resistance contribution can be accounted for so that the intraparticle diffusivity could be evaluated. The method is based on the assumption that the variance of the peak exiting the column is a sum of the variance of each of the contributions:

$$\sigma^2_{Tot} = \sigma^2_{col} + \sigma^2_{extr} \tag{4.7}$$

where σ^2_{extr} is the contribution due to extracolumn effects, and σ^2_{col} the contribution due to the column non-equilibrium effects can in turn be separated into

$$\sigma^2_{col} = \sigma^2_{flow} + \sigma^2_{masstransfer} = \sigma^2_{flow} + \sigma^2_{film} + \sigma^2_{diff} \tag{4.8}$$

where σ^2_{flow} represents the contribution of axial dispersion, σ^2_{film} is the contribution of the fluid film mass transfer resistance and σ^2_{diff} is the contribution resulting from intraparticle diffusion. This equation can also be expressed as plate contributions,

$$H_{col} = H_{flow} + H_{film} + H_{diff} \tag{4.9}$$

Initially the HETP contributions from external sources are evaluated for a given bed and solute by means of the following equation:

$$H_{extr} = \frac{\sigma^2_{extr} L}{t_R^2} \tag{4.10}$$

where the extracolumn contribution σ^2_{extr} is determined according to the experimental procedure outlined in section 4.2.2.3.

The extracolumn plate contribution is essentially constant over the range of fluid velocities used in SEC as can be seen in fig. 4.1. Subsequently this HETP contribution is subtracted from the experimental HETP, so that only the contributions due to the column non-equilibrium interactions are considered in the remaining part of the analysis.

The contribution to HETP due to fluid film mass transfer H_{film}, is calculated by means of the expression:

$$H_{film} = \frac{2\epsilon_p^2 R_p \epsilon(1-\epsilon)}{3k_f[\epsilon+(1-\epsilon)\epsilon_p]^2} \cdot u \qquad (4.11)$$

using correlated values of k_f (see section 3.3.2). This expression has been obtained from eq. 4.6 by assuming the fluid film mass transfer resistance to be the rate limiting step ($D_e=\infty$).
Finally by subtracting this mass transfer contribution from the overall HETP column contributions (eq. 4.6) the following equation is obtained:

$$H-H_{film} = \frac{2D_L}{u} + \frac{2\epsilon_p^2 R_p^2 \epsilon(1-\epsilon)}{15D_e(\epsilon+(1-\epsilon)\epsilon_p)^2} \cdot u \qquad (4.12)$$

As shown in this equation and in fig. 4.1, the difference of the overall column HETP (experimental H minus H_{extr}) and the fluid film HETP have a slope which is inversely proportional to the intraparticle diffusivity.
The axial dispersion coefficient D_L is usually divided into two terms: one for molecular diffusion in the axial direction and the second an eddy mixing term that is proportional to the fluid velocity (see section 3.3.1):

$$D_L = \lambda d_p u + \gamma D_m \qquad (4.13)$$

The molecular diffusion component is negligible for liquid chromatography of large molecules. Therefore the axial dispersion coefficient obtained from the y intercept of eq. 4.12 considers only the effects of the bulk mixing in the interstitial spaces. The whole method is graphically shown in fig. 4.1 for a typical data set.

The present study involves the estimation of the changes in the parameter values that may be associated with the changes in the bed structure and with particle deformation when the bed is subjected to different levels of compression. These parameters are the equilibrium constant, the axial dispersion and pore diffusion coefficients.
The particle-to-fluid mass transfer coefficient has not been estimated by means of the pulse analysis. In a survey of the application of pulse chromatography to the measurement of kinetic and transport properties in packed beds, Gangwal et al (1978) demonstrated that for low Reynolds numbers particle-to-fluid mass-transfer coefficients could not be measured when porous particles

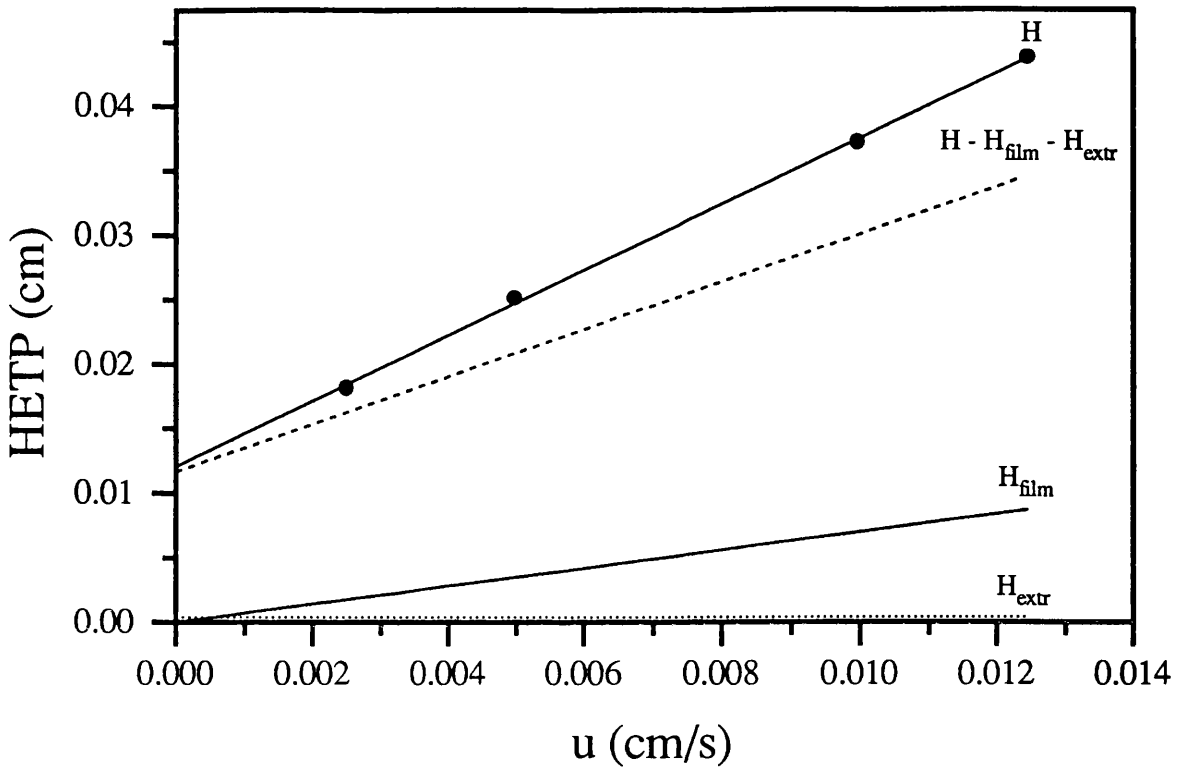

Fig. 4.1 HETP analysis. Procedure for the evaluation of the intrapaticle diffusion contribution to HETP (Arnold et al, 1985). Experimental points correspond to the pulse injection of ribonuclease A to the Sepharose CL-6B column.

are used because the external transport resistance is overpowered by resistances arising from internal diffusion. Indeed, at the low Reynolds numbers common in chromatographic practice (Re<1), and considering the low diffusion coefficients of proteins, it is evident that the boundary-layer resistance could never be the rate controlling step in this type of separation. For these reasons the particle-to-fluid mass-transfer coefficient was instead evaluated by means of the correlation developed by Ohashi et al (1981). This correlation was found to be the most appropriate to be used within the experimental range of reduced velocity, ReSc used in this study (see section 3.3.2).

It has been shown that with a careful choice of experiments and by means of the HETP method the parameters that characterize process performance can be obtained from an analysis of two peak properties, namely the retention time and the peak variance. In the following sections the experimental methods needed to carry out the estimation of these parameters are presented.

4.2.2 Experimental procedures.

4.2.2.1 Packing technique and bed compression method.

Experiments were carried out using a jacketed glass column XK 16/70 (Pharmacia LKB Biotechnology). This column has an I.D.= 1.6 cm and comes with adaptors that allow bed length adjustment. Water from a thermostatic bath LT/LB 8/72 (Grant Instruments Ltd) was circulated through the jacket and the running buffer was kept in the bath in order to maintain the temperature of the whole system constant at 20°C.

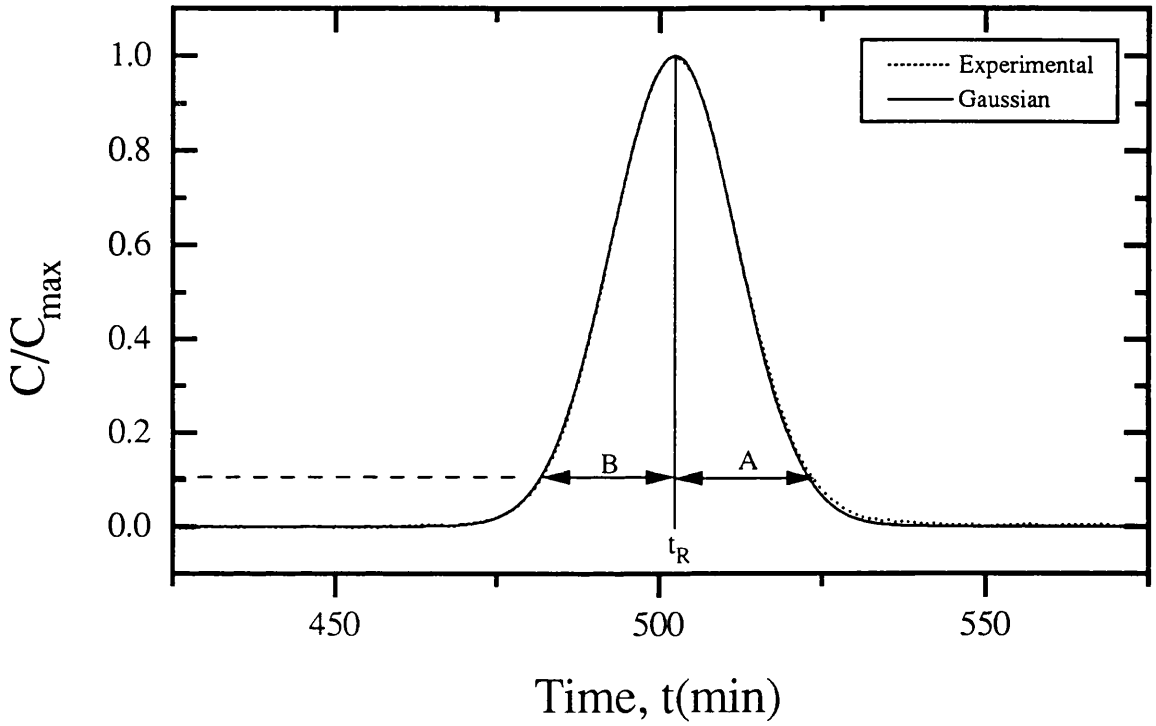

Fig. 4.2 Comparison of experimental acetone outlet peak with Gaussian curve. Definition of symmetry factor, B/A.

The column was slurried packed with either Sepharose 6B or Sepharose CL-6B at constant flow rate according to the packing procedure suggested by Pharmacia (1991a). Approximately 165 ml of degassed 75% (v/v) gel slurry (75% settled gel and 25% phosphate buffer[2]) were used and the flow rate was set to 0.3 ml/min for Sepharose 6B and to 0.6 ml/min for Sepharose CL-6B. After approximately 2-4 hours the gel had settled and the column adaptor was then carefully inserted down to the top of the bed. Then the flow rate was restarted and the top adaptor was continuously moved down in order to eliminate the gap caused by bed compression. This was carefully done

[2] The preparation and exact buffer composition is given in section 2.3.1.4.

Table 4.1 Bed dimensions and packing efficiency characteristics for each of the compression conditions imposed on the Sepharose gels.

Packing or compression Flow rate (ml/min)	Final Bed Length[a] L (cm)	Acetone Flow rate[b] (ml/min)	Number of Plates[c] N	Plate Height H (cm)	Reduced Plate Height[d] h	Symmetry factor[e] B/A	Bed void fraction[f] ε	Interstitial linear velocity u (cm/s)	Reduced velocity[g] ν
SEPHAROSE 6B									
0.3	51.2	0.2	5273	9.71×10^{-3}	1.103	0.975	0.3538	4.71×10^{-3}	3.77
0.5	49.3	0.2	5121	9.63×10^{-3}	1.094	0.974	0.3316	5.03×10^{-3}	4.02
0.75	46.55	0.2	5309	8.77×10^{-3}	0.996	0.982	0.2968	5.61×10^{-3}	4.49
SEPHAROSE Cl-6B									
0.6	51.05	0.2	5737	8.90×10^{-3}	0.967	0.943	0.3343	4.98×10^{-3}	4.17
0.8	50.2	0.2	5507	9.12×10^{-3}	0.991	0.919	0.3241	5.14×10^{-3}	4.30
1.4	49.5	0.2	5014	9.87×10^{-3}	1.073	0.867	0.3133	5.32×10^{-3}	4.45

a. This is the bed length obtained at the end of the packing or compression procedure carried out at each of the specified flow rates.
b. This is the flow rate at which the acetone sample was passed through the column.
c. The number of plates was calculated by means of the acetone peak width at half height.
d. The mean particle diameter d_p determined according to the procedure shown in section 2.3.2.4, was used for this calculation: $d_p = 0.0088$ cm for Sepharose 6B and $d_p = 0.0092$ cm for Sepharose CL-6B.
e. See fig. 4.2 for definitions of A and B.
f. This value was obtained according to the method described in section 4.2.2.2.
g. In this calculation the diffusion coefficient of acetone in water reported by Knox and Parcher (1969) has been use: D_m (25°C)= 1.10×10^{-5} cm^2/s.

until the bed compressed no further. The total packing procedure lasted approx. 8 hours for Sepharose CL-6B and 10 hours for Sepharose 6B. The efficiency of the packing procedure was evaluated by injecting 200 µl of acetone solution (5 µl/ml buffer). The eluting acetone peak was used to measure the number of plates N, the reduced plate height h, and the peak symmetry factor B/A (see fig. 4.2 for definition of A and B). For an efficiently packed bed, h should be smaller than 3 at a reduced velocity of $\nu \approx 5$ (Bristow and Knox, 1977), and B/A should be close to unity, i.e. 0.9-1.1 (Hagel, 1989). The acetone peak was also compared with a Gaussian peak as shown in fig. 4.2. The columns were repacked until a very efficient column was obtained ($h<3$).
Once a bed was efficiently packed the pulse injection experiments described in the next section were carried out. After the pulse runs at this bed height the flow rate was increased to compress further the gel bed. The top adaptor was repositioned following the procedure described above. Additional pulse response experiments were then conducted with the more compressed bed and the procedure was then repeated using a still higher flow rate to achieve further bed compression. A sequence of three of these compression-pulse injection experiments was conducted with each of the two Sepharose columns (6B and CL-6B). Table 4.1 shows the bed dimensions and packing characteristics obtained at each of these compression conditions.

4.2.2.2 Pulse response experiments.

Pulse response experiments were conducted in order to determine the equilibrium distribution coefficient, the axial dispersion coefficient and the intraparticle diffusivities of five model proteins of increasing molecular weight at the different compression conditions at which the Sepharose columns were subjected. The model proteins used in the experiments were the following: ribonuclease A, ovalbumin, γ-globulin, β-amylase and ferritin. The characteristics and source of these proteins are given in section 2.3.1.2.
The physical properties of the proteins studied are listed in table 4.2. These proteins were selected according to their size, purity, availability and cost. The Stokes-Einstein equation was used to calculate the diffusivity of the model proteins in the phosphate buffer used in the experiments:

$$D_m = \frac{k_b T}{6\pi \mu r_s} \qquad (4.14)$$

where D_m is the diffusivity at temperature T (in °K), k_B is the Boltzman constant, r_s is the Stokes radius and μ is the viscosity of the solvent. First the Stokes radius, r_s of the model proteins was evaluated using reported experimental or estimated values of diffusivity in water at 20 °C. The

calculated r_s in turn was used to recalculate the diffusivity according to the viscosity of the phosphate buffer employed in the pulse experiments.

Table 4.2 Physical properties of the tested proteins.

Protein (source)	MW (Da)	D_m in water 20°C (cm^2/s)	r_s (nm)	D_m in buffer 20°C (cm^2/s)	Schmidt number[d] Sc
Ribonuclease A (bovine pancreas)	13 700	11.7×10^{-7} [a]	1.83	10.5×10^{-7}	10 604
Ovalbumin (chicken egg)	45 000	7.3×10^{-7} [a]	2.93	6.55×10^{-7}	17000
γ-Globulin (bovine)	156 000	4.0×10^{-7} [a]	5.35	3.59×10^{-7}	31015
β-Amylase (sweet potato)	200 000	4.18×10^{-7} [b]	5.13	3.74×10^{-7} [b]	29771
Apoferritin (horse spleen)	441 000	3.61×10^{-7} [c]	5.93	3.24×10^{-7}	34365

[a] Reported in Tyn and Gusek (1990).
[b] Calculated with Young's correlation (1980).
[c] Reported in Haën (1987).
[d] $Sc=\mu/\rho D_m$, $\mu= 1.0041$ g/cm^3 and $\rho= 1.118 \times 10^{-2}$ g/cm·s.

All the pulse response experiments were carried out at a constant temperature of 20°C. Calibrated sample loops were used in all of these experiments in order to assure that the injected sample volume was accurate and constant. The experimental apparatus was the same as that described in section 2.3.1.5, but configured in a different manner. A schematic representation of the chromatographic system used in these experiments is shown in fig. 4.3.

Once an efficient column was packed or compressed the following sequence of injections was applied:

A) Total void volume V_T. Acetone samples (5 µl acetone/ml of buffer) of 200 µl were injected to the chromatographic bed at different flow rates in order to determine the total void volume, i.e. interparticle and intraparticle volume (Hussain et al, 1991) and to test the column efficiency by looking at the peak symmetry factor and the reduced plate height (Hagel, 1989), as already mentioned.

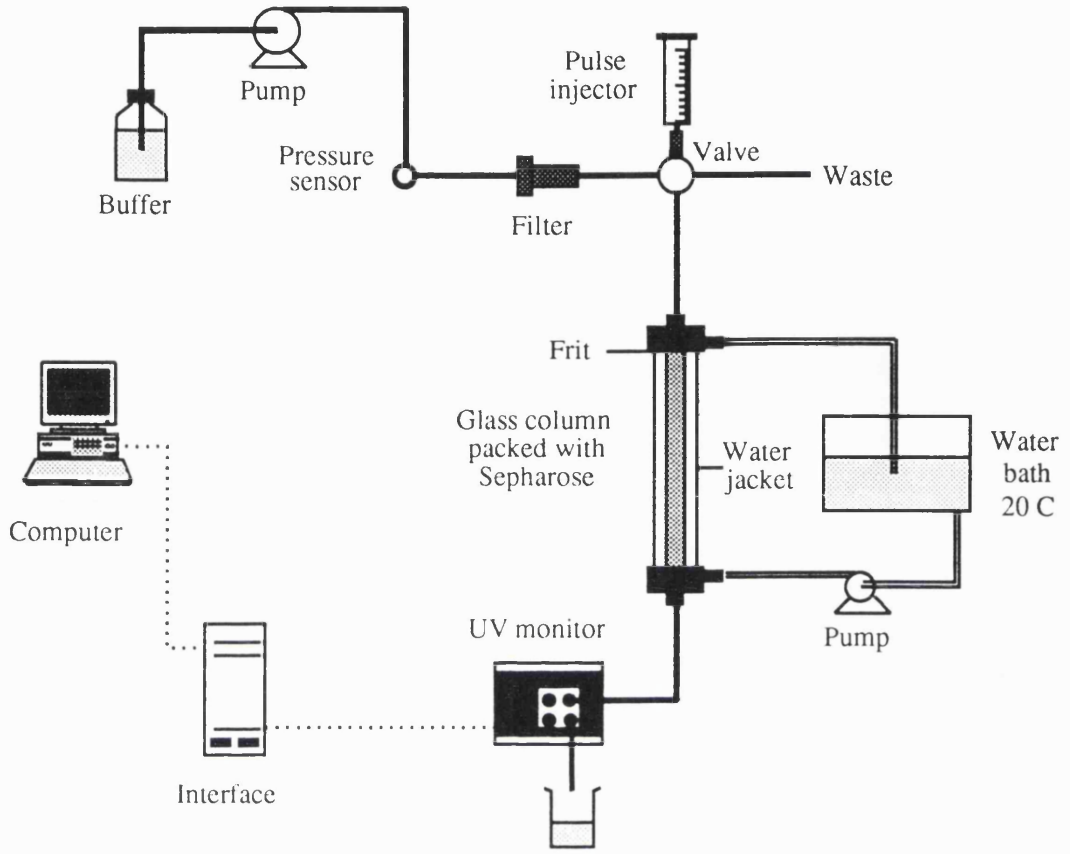

Fig. 4.3 System configuration used in the experimental measurement of the protein chromatographic peaks required by the HETP analysis.

B) Interparticle void volume V_o. 100 µl samples of blue dextran 2000 at a concentration of 2.5 mg/ml were injected to the column to determine the void volume and to check the homogeneity of the bed by watching the progress of the coloured zone of this substance through the bed (Pharmacia, 1991a).

C) Protein HETP measurements. 200 µl samples of each of the five model proteins were injected to the column at a range of flow rates. The sample concentration was 1.5 mg protein/ml of buffer. The sample volume and concentration used in these experiments were such as to make negligible its contribution to peak spreading (a maximum sample volume of 1-2% of the column volume and a maximum protein concentration of 70 mg/ml can be used, Hagel (1989)). The maximum flow rate used in the runs was approx. 80% of the packing or compression flow rate (Sofer and Nyström, 1989), so that the bed did not compress during the experiments.

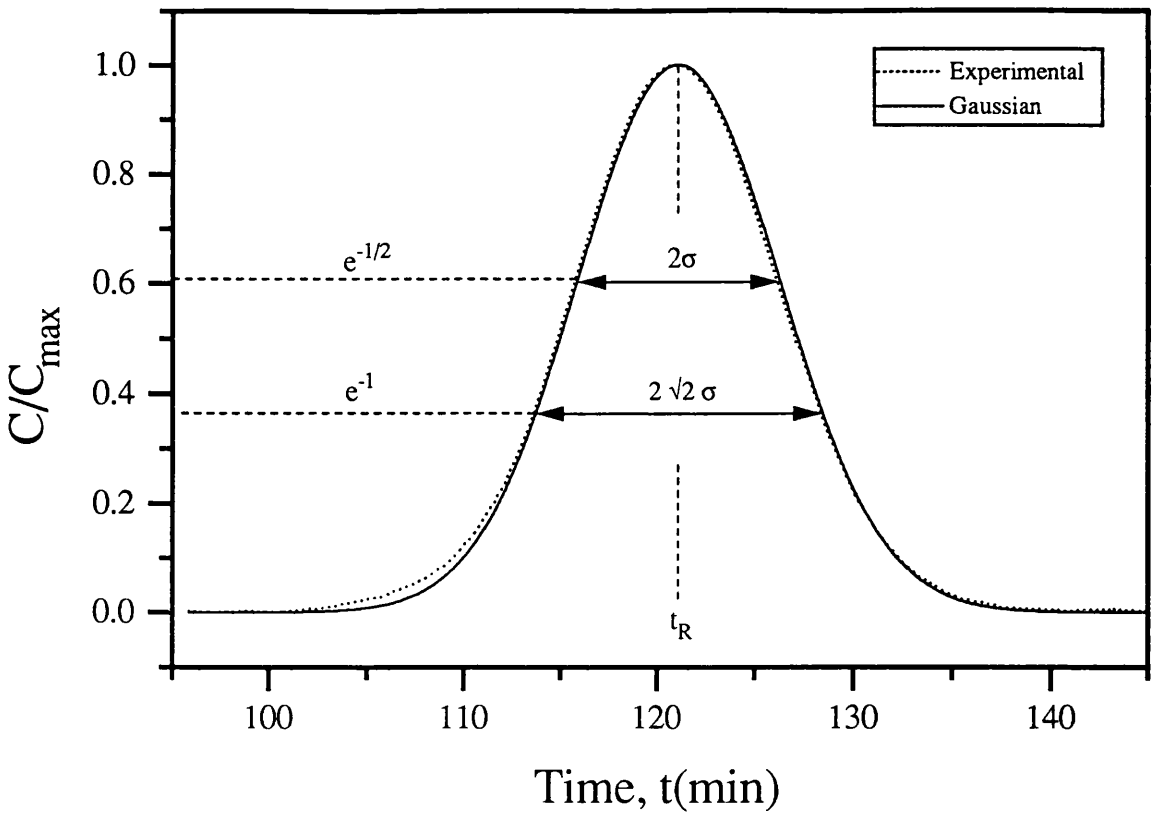

Fig. 4.4 Comparison of the ovalbumin experimental peak with a Gaussian curve. The variance σ^2 is obtained from the peak widths at e^{-1} and $e^{-1/2}$ multiplied by the maximum peak height.

The exiting protein peaks were compared against a Gaussian curve in order to ascertain the applicability of the HETP method. Peaks were very nearly Gaussian over the range of flow rates used in these experiments, as can be seen for an ovalbumin peak in fig. 4.4. The analysis of the experimental data and the determination of the parameters then followed the HETP method (Arnold et al, 1985) outlined in section 4.2.1

The variance σ^2 needed to evaluate the HETP values was obtained from the measured peak widths at $e^{-1/2}$ and e^{-1} multiplied by the maximum peak height (see fig. 4.4). The average value of the two standard deviations (σ) obtained was considered. The peak residence time t_R, was taken to be the time that corresponded to the peak maximum (maximum outlet concentration, C_{max}). A correction was made in order to allow for the system's dead volume, i.e. volume in valves and connecting tubing, according to the following equation:

$$t_R = t_{R,exp} - \frac{V_d}{Q} \qquad (4.15)$$

where $t_{R,exp}$ is the measured experimental retention time, V_d is the volume of dead spaces in the chromatograph, Q is the flow rate and t_R is the actual or corrected retention time.

4.2.2.3 Extracolumn band broadening.

In order to determine the band spreading contribution of the chromatography system and the sample bandwidth, 200 µl pulses of each of the five model proteins were injected onto the XK column containing no gel and in which the two distributors were pushed together (Arnold et al, 1985). The samples were injected at a range of flow rates (0.05-1.5 ml/min). The resulting peaks from these runs were highly non-Gaussian and showed considerable tailing. For this reason in order to estimate the HETP contribution from end effects and sample bandwidth, σ values were obtained only from the outlet peak widths at a corresponding height of $e^{-1/2}C_{max}$. The extracolumn contribution to HETP for a given protein and column was then evaluated by means of eq. 4.10, considering the retention time t_R of that particular protein when passed through the actual bed of length L (see section 4.2.1).

4.3 Results and discussion.

The columns used in the pulse response experiments were very efficiently packed as can be seen from table 4.1. The reduced plate height h obtained with the Sepharose columns was very nearly 1 at reduced velocities of approx. 4 for both columns proving that the bed structure was very homogeneous at the beginning of the pulse experiments.

The resulting h values in table 4.1 also show that in the case of the Sepharose 6B the column became more efficient as compression progressed. The opposite result was obtained with the Sepharose CL-6B, the column lost efficiency with compression.

All the parameters estimated by means of the HETP method at each of the compression conditions at which the Sepharose gels were subjected are presented in table 4.3. This table gives a global picture of the conditions under which the pulse experiments were carried out as well as a global view of the results.

Table 4.3 Estimated parameters at each of the compression conditions at which the Sepharose gels were subjected.

SEPHAROSE 6B						
Compression flow rate: 0.3 ml/min Bed properties: Length[a] L=51.2 cm Void fraction ε=0.3538			Range of operation: Re =0.00033-0.00197 ReSc =3.5-67.9			
Protein	MW (Da)	D_m (cm^2/s)	ε_p	D_e (cm^2/s)	D_L/u (cm)	k_f [b] (cm/s)
Ribonuclease A	13 700	$10.5x10^{-7}$	0.8317	21.9×10^{-8}	0.0071	0.00049-0.00076
Ovalbumin	45 000	$6.55x10^{-7}$	0.6816	11.4×10^{-8}	0.0076	0.00033-0.00053
γ-globulin	156 000	$3.59x10^{-7}$	0.5681	4.0×10^{-8}	0.0119	0.00021-0.00033
β-amylase	200 000	$3.74x10^{-7}$	0.5412	3.7×10^{-8}	0.0085	0.00021-0.00033
Apoferritin	441 000	$3.24x10^{-7}$	0.5119	1.8×10^{-8}	0.0360	0.00019-0.00029
Compression flow rate: 0.5 ml/min Bed properties: Length[a] L=49.3 cm Void fraction ε=0.3316			Range of operation: Re =0.00066-0.00263 ReSc =7.0-90.5			
Protein	MW (Da)	D_m (cm^2/s)	ε_p	D_e (cm^2/s)	D_L/u (cm)	k_f [b] (cm/s)
Ribonuclease A	13 700	$10.5x10^{-7}$	0.8276	25.9×10^{-8}	0.0078	0.00058-0.00083
Ovalbumin	45 000	$6.55x10^{-7}$	0.6800	13.4×10^{-8}	0.0094	0.00040-0.00058
γ-globulin	156 000	$3.59x10^{-7}$	0.5668	4.5×10^{-8}	0.0158	0.00025-0.00037
β-amylase	200 000	$3.74x10^{-7}$	0.5393	4.0×10^{-8}	0.0104	0.00025-0.00037
Apoferritin	441 000	$3.24x10^{-7}$	0.5147	2.1×10^{-8}	0.0394	0.00023-0.00034
Compression flow rate: 0.75 ml/min Bed properties: Length[a] L=46.55 cm Void fraction ε=0.2968			Range of operation: Re =0.00066-0.00395 ReSc =7.0-135.8			
Protein	MW (Da)	D_m (cm^2/s)	ε_p	D_e (cm^2/s)	D_L/u (cm)	k_f [b] (cm/s)
Ribonuclease A	13 700	$10.5x10^{-7}$	0.8253	27.2×10^{-8}	0.0086	0.00059-0.00096
Ovalbumin	45 000	$6.55x10^{-7}$	0.6788	13.8×10^{-8}	0.0105	0.00041-0.00067
γ-globulin	156 000	$3.59x10^{-7}$	0.5639	4.2×10^{-8}	0.0156	0.00025-0.00043
β-amylase	200 000	$3.74x10^{-7}$	0.5384	3.7×10^{-8}	0.0136	0.00025-0.00043
Apoferritin	441 000	$3.24x10^{-7}$	0.5133	2.1×10^{-8}	0.0466	0.00023-0.00040

Table 4.3. Continuation.

SEPHAROSE CL-6B						
Compression flow rate: 0.6 ml/min Bed properties: Length[a] L=51.05 cm Void fraction ε=0.3343			Range of operation: Re =0.00069-0.00344 ReSc =7.3-118.3			
Protein	MW (Da)	D_m (cm^2/s)	ε_p	D_e (cm^2/s)	D_L/u (cm)	k_f [b] (cm/s)
Ribonuclease A	13 700	$10.5x10^{-7}$	0.7722	28.3×10^{-8}	0.0058	0.00056-0.00086
Ovalbumin	45 000	$6.55x10^{-7}$	0.6081	11.6×10^{-8}	0.0063	0.00038-0.00060
γ-globulin	156 000	$3.59x10^{-7}$	0.4779	3.2×10^{-8}	0.0099	0.00024-0.00038
β-amylase	200 000	$3.74x10^{-7}$	0.4473	2.6×10^{-8}	0.0053	0.00025-0.00040
Apoferritin	441 000	$3.24x10^{-7}$	0.3790	1.5×10^{-8}	0.0078	0.00022-0.00036
Compression flow rate: 0.8 ml/min Bed properties: Length[a] L=50.2 cm Void fraction ε=0.3241			Range of operation: Re =0.00069-0.00413 ReSc =7.3-142.0			
Protein	MW (Da)	D_m (cm^2/s)	ε_p	D_e (cm^2/s)	D_L/u (cm)	k_f [b] (cm/s)
Ribonuclease A	13 700	$10.5x10^{-7}$	0.7727	25.8×10^{-8}	0.0056	0.00056-0.00091
Ovalbumin	45 000	$6.55x10^{-7}$	0.6073	11.1×10^{-8}	0.0063	0.00038-0.00064
γ-globulin	156 000	$3.59x10^{-7}$	0.4791	3.2×10^{-8}	0.0111	0.00024-0.00041
β-amylase	200 000	$3.74x10^{-7}$	0.4490	2.5×10^{-8}	0.0102	0.00025-0.00042
Apoferritin	441 000	$3.24x10^{-7}$	0.3761	1.5×10^{-8}	0.0106	0.00022-0.00038
Compression flow rate: 1.4 ml/min Bed properties: Length[a] L=49.5 cm Void fraction ε=0.3133			Range of operation: Re =0.00069-0.00688 ReSc =7.3-236.6			
Protein	MW (Da)	D_m (cm^2/s)	ε_p	D_e (cm^2/s)	D_L/u (cm)	k_f [b] (cm/s)
Ribonuclease A	13 700	$10.5x10^{-7}$	0.7685	26.9×10^{-8}	0.0067	0.00056-0.00107
Ovalbumin	45 000	$6.55x10^{-7}$	0.6069	11.5×10^{-8}	0.0080	0.00039-0.00076
γ-globulin	156 000	$3.59x10^{-7}$	0.4777	3.2×10^{-8}	0.0126	0.00024-0.00049
β-amylase	200 000	$3.74x10^{-7}$	0.4491	2.5×10^{-8}	0.0076	0.00025-0.00043
Apoferritin	441 000	$3.24x10^{-7}$	0.3778	1.5×10^{-8}	0.0144	0.00022-0.00046

[a] The internal diameter of the column was in all cases 1.6 cm.

[b] This coefficient was estimated by means of the correlation developed by Ohashi et al (1981).

The pulse experiments were all carried out in the creeping flow regime (Re<1) and therefore the drag coefficient C_{Do} required in the evaluation of k_f (see section 3.3.2) was calculated by means of Stoke's law, $C_{DO}=24/Re$ (Bird et al, 1960). From table 4.2 it can be observed that the Schmidt numbers fell within the range of applicability of this correlation (505<Sc<70600). On the other hand the values of the modified Reynolds number Re^f in the pulse experiments ranged from 0.06 to 0.50, a little outside of the range of validity of this correlation, $0.2<Re^f<4600$. However, this should not be of significance since as it can be seen in table 4.3 the film mass transfer coefficient varied only very slightly under the conditions employed in these experiments.

The extracolumn contribution to band spreading was virtually negligible in all cases. The extracolumn band broadening was evaluated by means of the following equation:

$$HETP = H_{extr} = \frac{\sigma^2_{extr} L}{t_R^2} \tag{4.16}$$

which can also be expressed as

$$HETP = H_{extr} = \frac{\sigma^2_{extr} u^2}{L\left(1+\frac{(1-\epsilon)\epsilon_p}{\epsilon}\right)^2} \tag{4.17}$$

when t_R is substituted by eq. 4.2 and the term $t_o/2$ is neglected. The plate height from external sources is therefore proportional to 1/L, which means that the end effects becomes less important in longer columns. In the present experiments the Sepharose columns employed were relatively long and this is why the extracolumn contribution to dispersion was virtually negligible.
In the following section the chromatographic peak simulations carried out in order to corroborate the validity of the parameters shown in table 4.3 are presented.

4.3.1 Chromatographic peak simulations.

The validity of the parameters determined by the HETP analysis (shown in table 4.3) was tested by comparing the simulated peaks obtained by means of the SEC rate model (see section 3.2.1), with the experimentally measured outlet peaks.
As previously mentioned the general rate SEC model (see section 3.2.1) as described by Boyer and Hsu (1992) as well as the FFT numerical method (see section 3.5) have been selected to carry

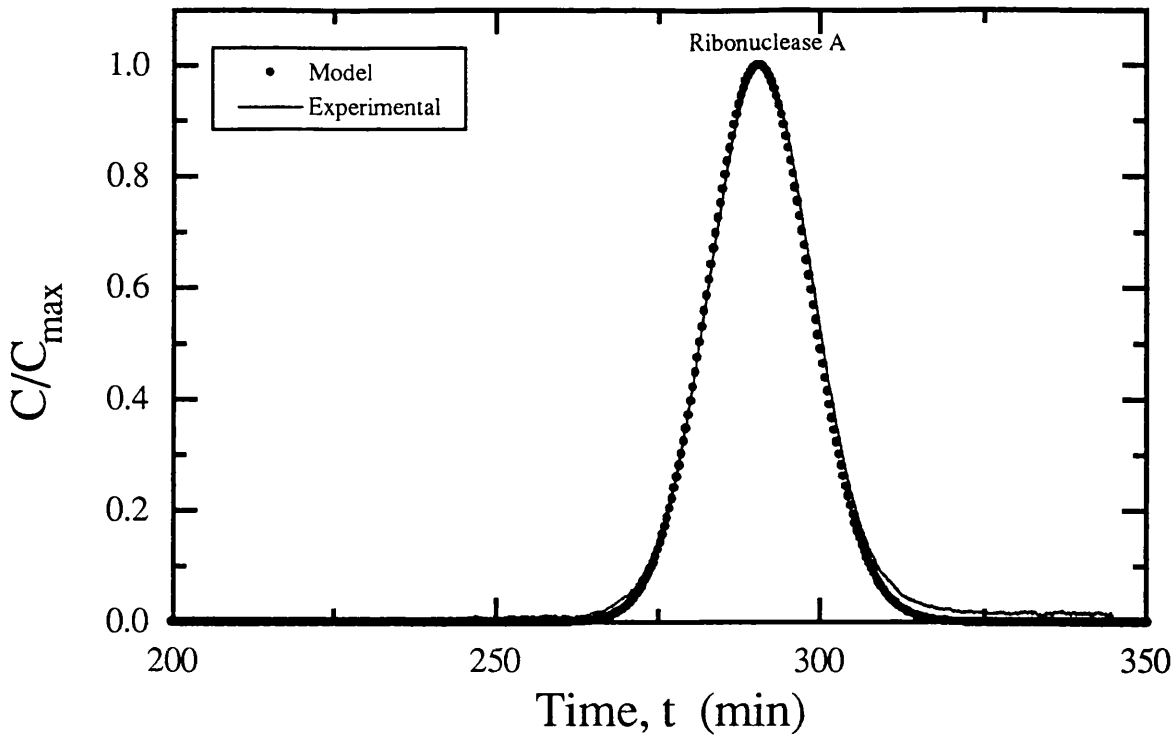

Fig. 4.5 Comparison of experimental outlet peak of ribonuclease A on a column of Sepharose 6B and that predicted with the following parameters: L=49.3 cm, u=7.54 x 10^{-3} cm/s, R= 4.4 x 10^{-3} cm, ε=0.3316 ,ε_p=0.828 , D_e=2.59 x 10^{-7} cm^2/s, D_L=5.88 x 10^{-5} cm^2/s and k_f=7.6 x 10^{-4} cm/s.

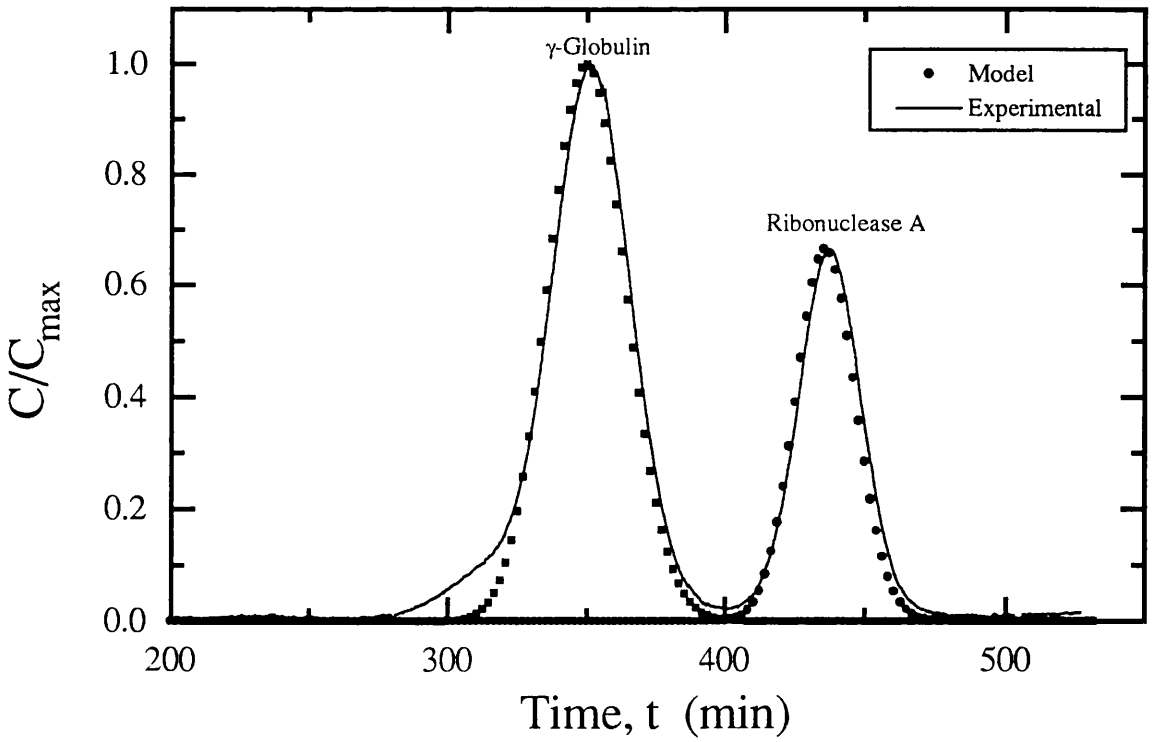

Fig. 4.5a Comparison of experimental outlet peaks of two proteins on a column of Sepharose 6B and those predicted with the following parameters: L=49.3 cm, u=5.03 cm/s, R=4.4 x 10^{-3} cm, ε= 0.3316, D_L=5.93 x 10^{-5} ; γ-globulin: ε_p=0.567 , D_e=4.51 x 10^{-8} cm^2/s, k_f=3.0 x 10^{-4} cm/s; Ribonuclease A: ε_p=0.828 , D_e=2.59 x 10^{-7} cm^2/s, k_f=6.9 x 10^{-4} cm/s.

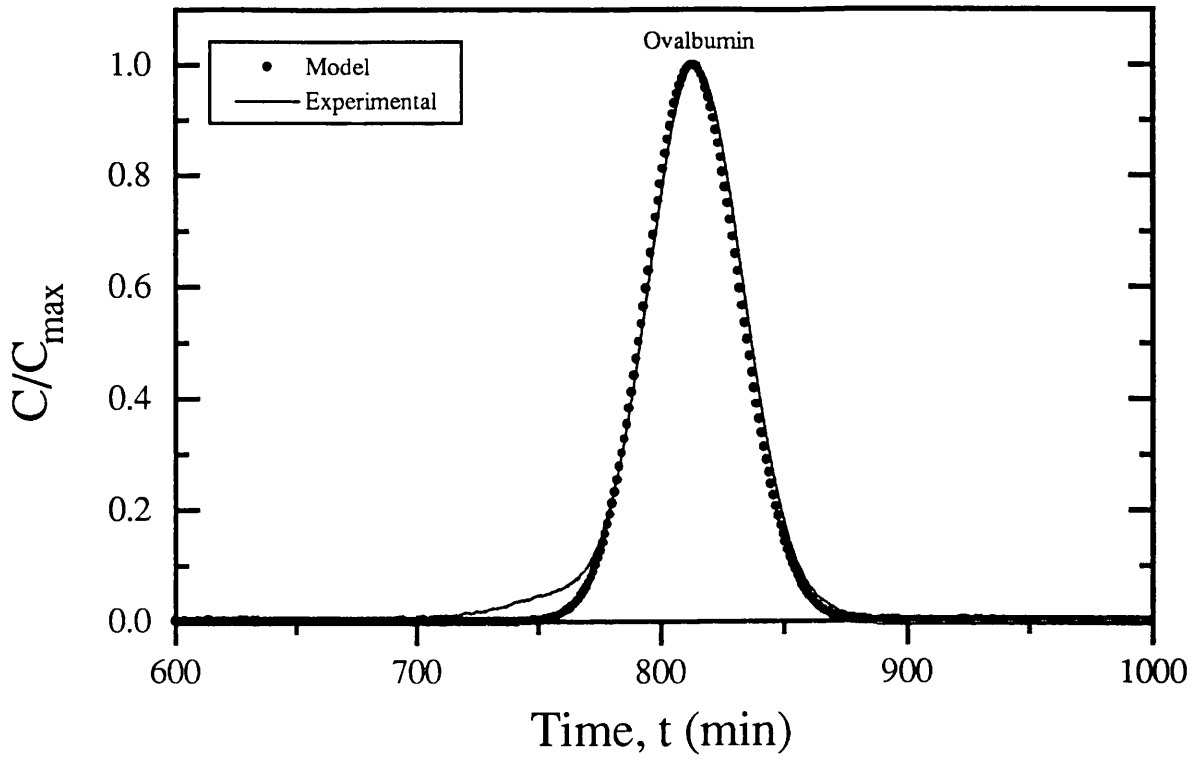

Fig. 4.6 Comparison of experimental outlet peak for ovalbumin on a column of Sepharose 6B and that predicted with the following parameters: L= 51.2 cm, u= 2.36 x 10^{-3} cm/s, R= 4.4 x 10^{-3} cm, ε= 0.3538, ε_p= 0.682, D_e= 1.14 x 10^{-7} cm^2/s, D_L= 6.33 x 10^{-6} cm^2/s, and k_f= 3.9 x 10^{-4} cm/s.

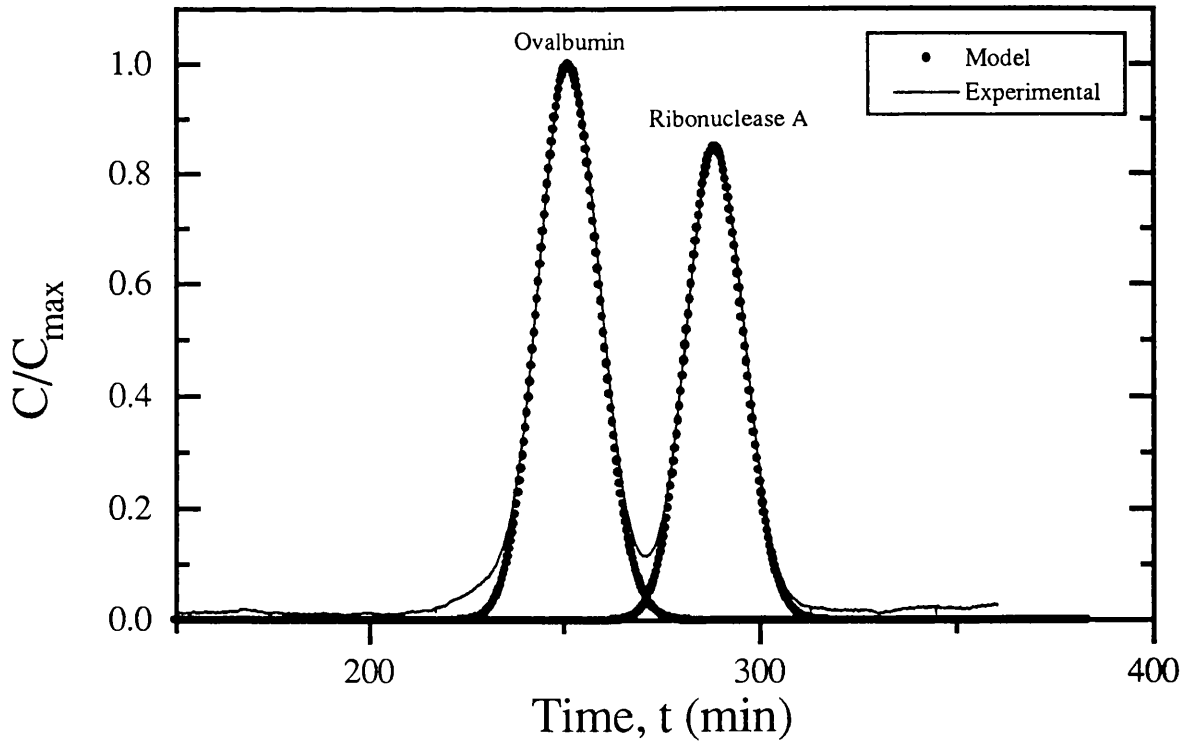

Fig. 4.6a Comparison of experimental outlet peaks of two proteins on a column of Sepharose CL-6B and those predicted with the following parameters: L= 51.05 cm, u= 7.48 x 10^{-3} cm/s, R= 4.6 x 10^{-3} cm, ε= 0.3343, D_L= 1.51 x 10^{-5} cm^2/s; Ovalbumin: ε_p= 0.608, D_e= 1.16 x 10^{-7} cm^2/s, k_f=5.16 x 10^{-4} cm/s; Ribonuclease A: ε_p= 0.772, D_e= 2.83 x 10^{-7} cm^2/s, k_f= 7.4 x 10^{-4} cm/s.

out the chromatographic peak simulations in this investigation.

The FFT method used to conduct the numerical inversion of the Laplace domain solution of the SEC model was implemented in a SUN SPARC station 1 (Sun Microsystems Europe, Inc) using the mathematical software Matlab (The Mathworks, Inc). The Fourier series inversion formula (Crump, 1976) is given by Hsu and Dranoff (1987) in an adapted form to be implemented with the FFT numerical method, while the FFT algorithm has been looked at in detail by Hsu (1979). The built-in functions and language of Matlab (Pro-Matlab version 3.5i) were used to program the algorithm, the program listing is given in appendix A. Examples of the simulated peaks obtained by the use of this program are presented in figs. 4.5, 4.5a, 4.6 and 4.6a. The experimentally obtained peaks are also shown in the figures in order to judge the quality of the predictions and to assess the accuracy of the parameters estimated by the HETP analysis as mentioned above. Both the experimental and the predicted peaks have been normalized with respect to C_{max}, the maximum solute concentration observed for each chromatographic peak. It is apparent that the SEC model predicts very well the experimental outlet peaks. The agreement between the model predictions and the experimental peaks gives confidence in the validity and accuracy of the parameter values determined by the HETP method.

In the following sections the changes suffered by the transport and equilibrium parameters, as determined by the HETP method when the bed was compressed, will be looked at in detail.

4.3.2 Analysis of the equilibrium distribution coefficient.

Examples of the retention time analysis for the test proteins are shown in figs. 4.7 and 4.8, where plots of t_R-$t_o/2$ vs L/u are depicted. The inclusion porosity (intraparticle void fraction) ε_p was determined from the slope of these lines making use of the bed void fraction ε (see eq. 4.2). A greater fraction of the intraparticle volume of the Sepharose particles is available to the smallest molecule, i.e. ribonuclease A, as shown by the largest slope of the corresponding line, while the ferritin being the largest protein tested has the smallest slope. Table 4.4. presents the resulting inclusion porosities of the five proteins for each of the bed compression conditions tested. It can be observed that the inclusion porosity decreases as the molecular weight of the proteins increases. Fig. 4.9 shows the resulting calibration curves for the Sepharose gels tested. It can be seen that the calibration curves of these gels are very close to each other but do not overlay. According to information provided by Pharmacia (1991a) the porosity of Sepharose CL-6B is very similar to that of the parent 6B gel, and it is expected their calibration curves should almost overlay. It is apparent from fig. 4.9 and table 4.4 that the protein molecules had a greater access to the

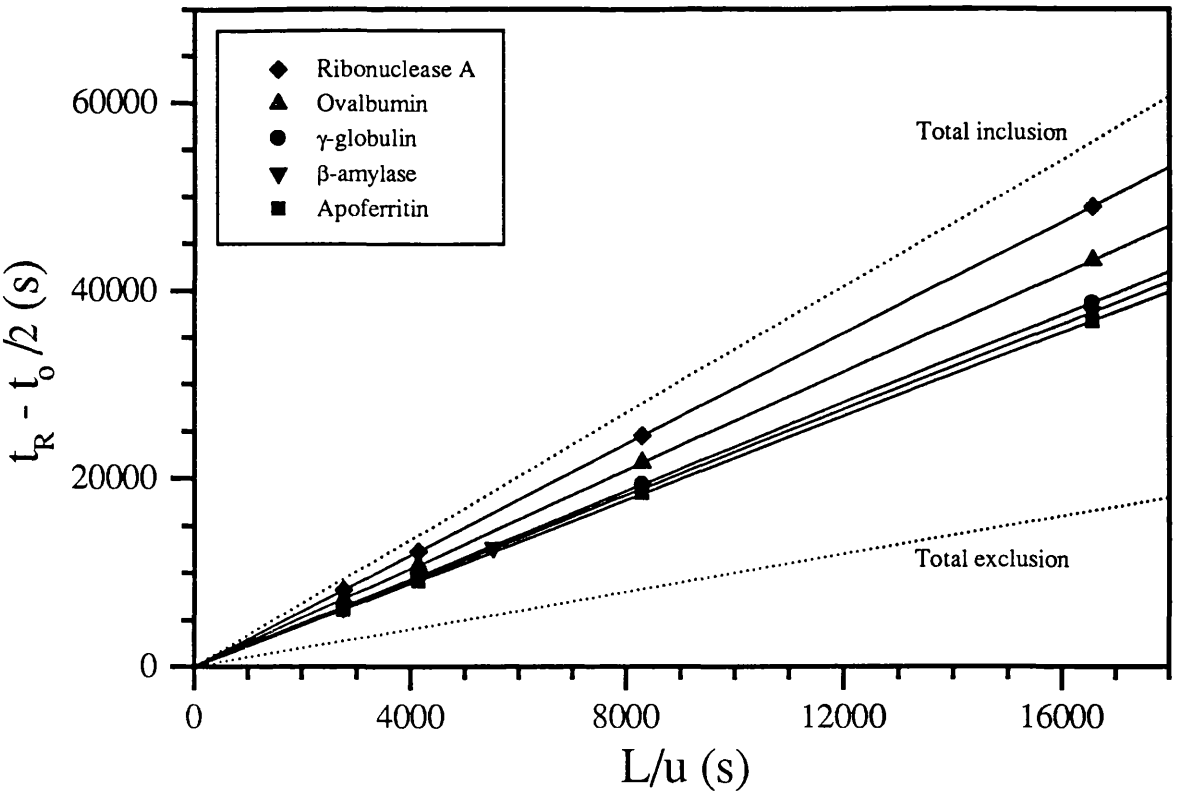

Fig. 4.7 Retention time analysis of outlet peaks of protein pulses on a Sepharose 6B column compressed at a flow rate of 0.75 ml/min to a length, L= 46.55 cm and to a void fraction, ε= 0.2968.

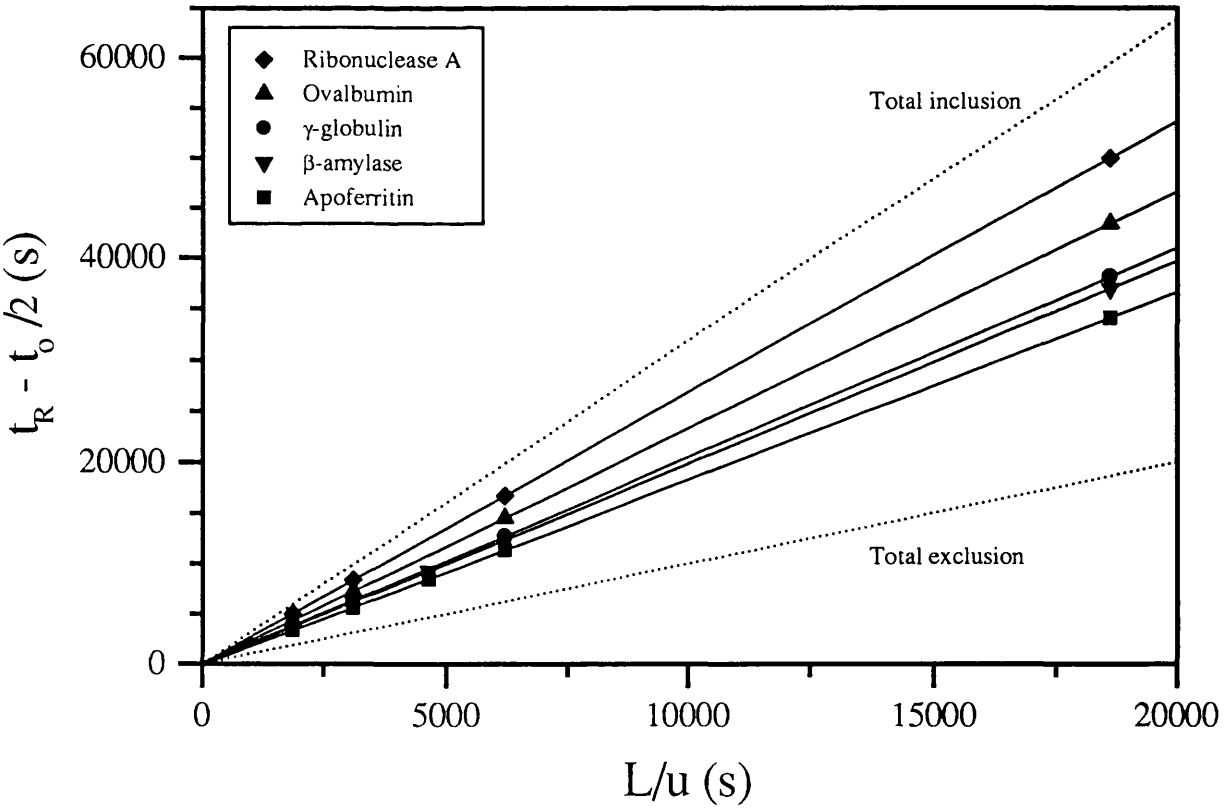

Fig. 4.8 Retention time analysis of outlet peaks of protein pulses on a Sepharose CL-6B column compressed at a flow rate of 1.4 ml/min to a bed length, L=49.5 cm and to a void fraction, ε= 0.3133.

Table 4.4 Inclusion porosities determined by means of HETP analysis for each of the compression conditions at which the Sepharose gel beds were subjected.

SEPHAROSE 6B				
Compression flow rate:		0.3 ml/min	0.5 ml/min	0.75 ml/min
Column properties:		L= 51.2 cm ε= 0.3538	L= 49.3 ε= 0.3316	L= 46.55 cm ε= 0.2968
Protein	MW (Da)	Inclusion porosity[a] ε_p		
Ribonuclease A	13 700	0.832	0.828	0.825
Ovalbumin	45 000	0.682	0.680	0.679
γ-globulin	156 000	0.568	0.567	0.564
β-amylase	200 000	0.541	0.540	0.538
Apoferritin	441 000	0.516	0.515	0.513

SEPHAROSE CL-6B				
Compression flow rate:		0.6 ml/min	0.8 ml/min	1.4 ml/min
Column properties:		L= 51.05 cm ε= 0.3343	L= 50.2 ε= 0.3241	L= 49.5 cm ε= 0.3133
Protein	MW (Da)	Inclusion porosity[a] ε_p		
Ribonuclease A	13 700	0.772	0.772	0.768
Ovalbumin	45 000	0.608	0.607	0.607
γ-globulin	156 000	0.478	0.479	0.478
β-amylase	200 000	0.447	0.449	0.449
Apoferritin	441 000	0.379	0.376	0.378

[a] This parameter represents the fraction of intraparticle void space available to the molecule. It is in fact a representation of the equilibrium distribution coefficient K_d and it is also called intraparticle void fraction.

intraparticle void volume of the 6B-type gel. It is reasonable to expect the 6B gel beads to present a greater intraparticle space since they do not have the CL- groups that may cause extra steric effects in the CL-6B gel. However, the difference between the two calibration curves appears to be greater than expected. The data corresponding to the Sepharose CL-6B follows very closely the correlation provided by Pharmacia (1991a). It is possible that some source of error may be

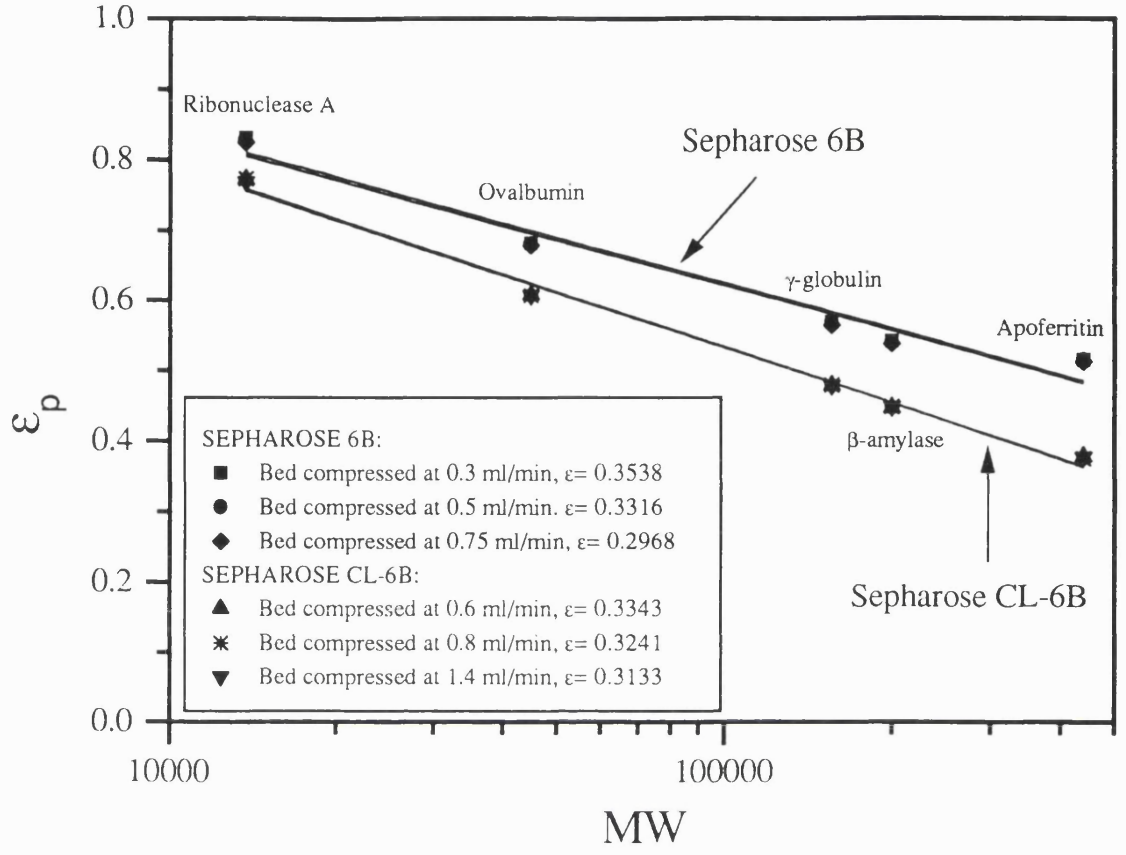

Fig. 4.9 Calibration curves for Sepharose 6B and Sepharose CL-6B columns under different compression conditions.

involved in the HETP analysis of the Sepharose 6B data or that indeed a marked difference exists in the porosity of the gel beads. In any case it is evident from the matching of the calibration curves for this particular gel (6B type) in fig. 4.9, that the error involved, if any, is constant. The inclusion porosities of each of the five proteins were estimated three times (one at each compression condition) and their values were in all cases very similar to each other as can be seen in table 4.4.

A close look at fig. 4.9 also shows that the slope and y intercept of the calibration curves of the Sepharose 6B gels very slightly decreased under compression, while those of the CL-type gel were virtually constant. The slope of the curves depends on the width of the pore size distribution while the y intercept is a function of the mean pore size (Hagel, 1989). This means that the mean pore size of the softer 6B gel slightly decreased while its pore size distribution slightly widened. These changes are, however, so small as to be insignificant. The Sepharose CL-6B bed although compressed at a higher flow rate was strong enough to resist the stresses so their calibration curves show virtually no change.

The very small changes in the calibration curves, caused by bed compression, are in agreement

with the reduction in intraparticle void volume as measured by the acetone pulses and shown in table 4.5. As the Sepharose 6B bed was compressed the intraparticle void volume experienced a reduction of approx. 1.5% (≈1 ml). On the other hand there was virtually no change in intraparticle void volume when the CL-6B bed was progressively compressed. It is apparent that the bed volume was almost entirely reduced at the expense of the interparticle void volume.

Table 4.5 Void volume analysis of Sepharose gel beds during compression.

Bed [a] length L (cm)	Bed void fraction ε	Pulse flow rate (ml/min)	Acetone retention time t_R (min)	Total void volume V_T (ml)	Interparticle void volume V_o (ml)	Intraparticle void volume V_i (ml)	V_i/V_c [b]
SEPHAROSE 6B							
51.2	0.3538	0.1	1004.8	99.93	36.23	63.70	0.62
49.3	0.3316	0.1	965.4	95.98	32.70	63.29	0.64
46.55	0.2968	0.1	907.8	90.23	27.63	62.60	0.67
SEPHAROSE CL-6B							
51.05	0.3343	0.2	497.8	99.01	34.13	64.87	0.63
50.2	0.3241	0.2	489.0	97.25	32.54	64.71	0.64
49.5	0.3133	0.2	481.1	95.67	31.02	64.65	0.65

[a] The column internal diameter was in all cases 1.6 cm.
[b] V_c represents the total column volume.

The evolution of the inclusion porosity of each of the tested proteins when the beds were compressed is plotted in fig. 4.10. As can be seen from this figure and table 4.4, the effect of compression on the intraparticle space available to the molecules was negligible. The inclusion porosity of the tested molecules remained virtually constant as the Sepharose beds were progressively compressed. Only very slight reductions in the protein inclusion porosities in the 6B column were observed (see table 4.4), but they were so small as to be considered significant and not the result of experimental and/or data analysis errors. This result is not surprising since as mentioned above, at the degree of compression experienced by the Sepharose beds in these experiments the reduction in bed volume resulted mainly from particle rearrangement and not from particle deformation. This is why the reduction in the intraparticle void volume was very small and therefore it did not have a significant effect on the inclusion porosities of the proteins.

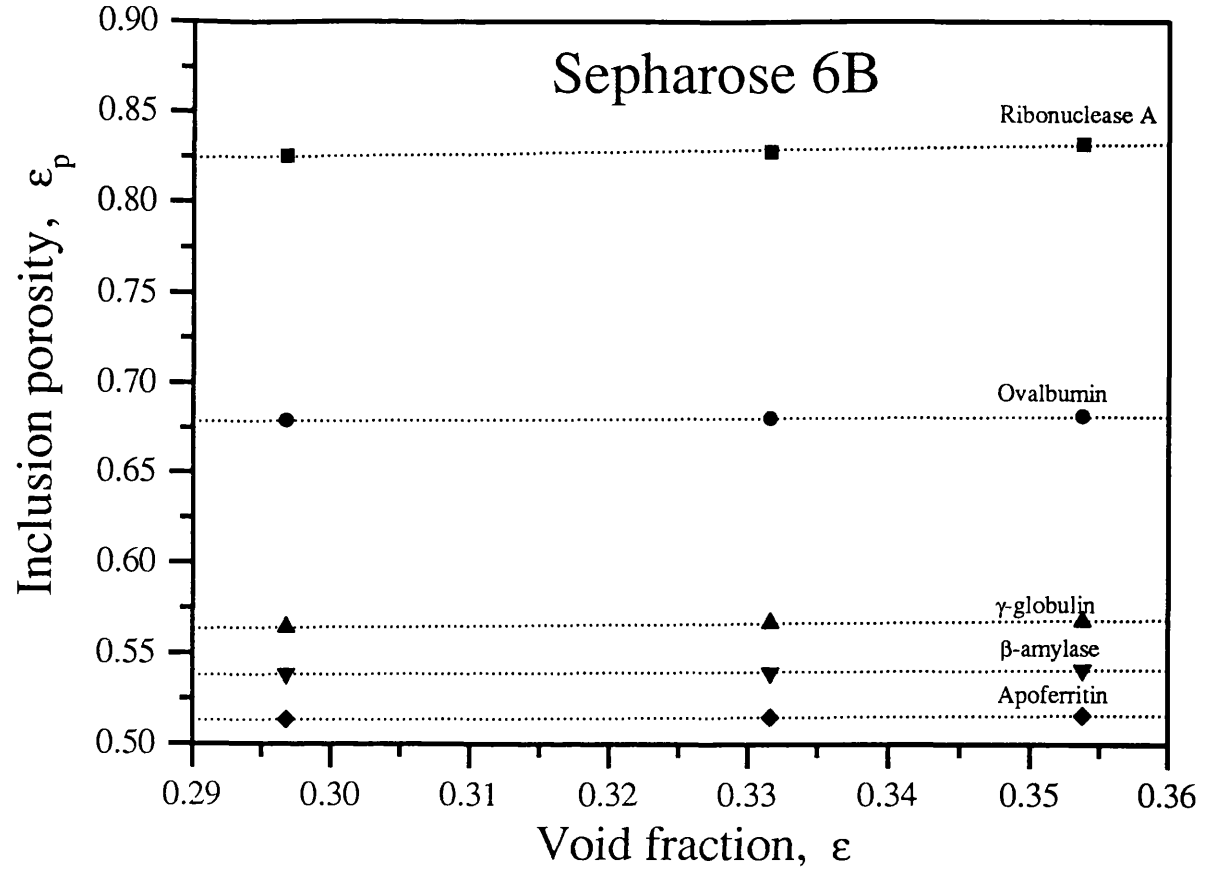

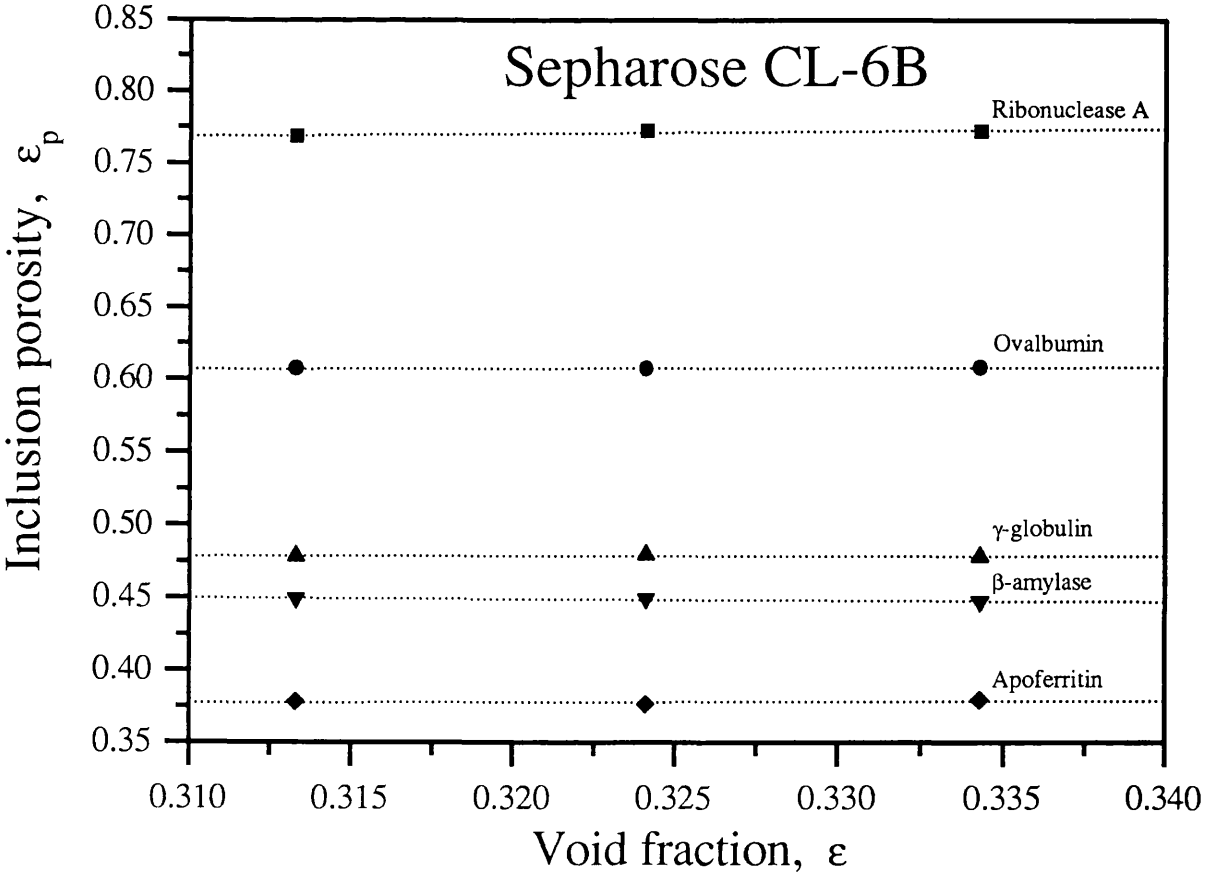

Fig. 4.10 Changes in the intraparticle space available to the protein molecules ε_p, when the bed is progressively compressed as expressed by the bed void fraction ε.

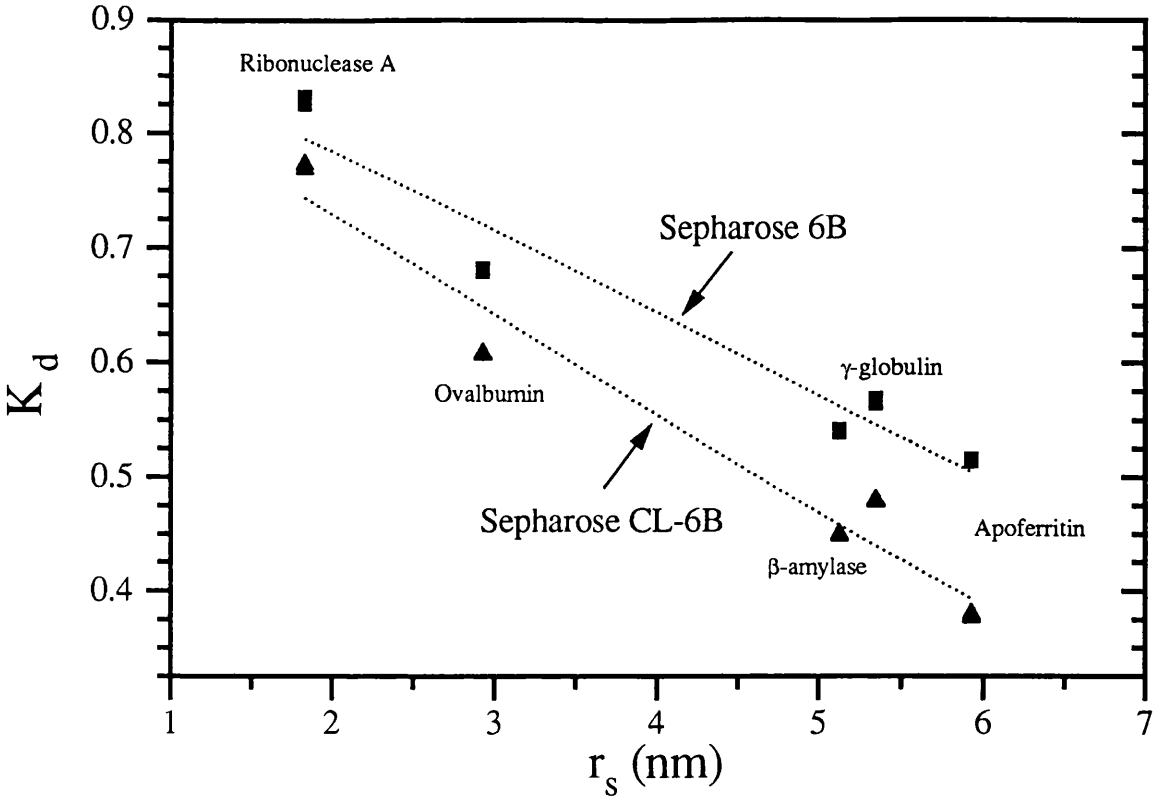

Fig. 4.11 Partition coefficients K_d (or inclusion porosities ε_p) of the five test proteins in Sepharose 6B: ■ , and Sepharose CL-6B ▲ , as a function of the Stokes radius r_s. The dotted lines represent equation 3.46 (Ogston et al, 1973) after curve fitting.

According to the theory developed by Ogston et al (1973) the agarose gel is made up of a random network of straight fibres and the partition coefficient K_d of a spherical molecule is a function of the molecule Stokes radius r_s and the gel fibre radius r_f as shown in eq. 3.46. In fig 4.11 the protein partition coefficients K_d (or inclusion porosities ε_p) have been plotted against the protein Stokes radius, and eq. 3.46 has been fitted to this experimental data in order to estimate the Sepharose fibre radius. The fitting procedure was carried out considering all the K_d values corresponding to each protein for all the compression conditions. In the case of the Sepharose 6B the fibre radius obtained was r_f= 3.8 nm, while for the CL-type gel the value was r_f= 3.5 nm. These results are very close to the value of 2.5 nm estimated for the fibre radius of agarose gels by Laurent (1967) employing gel filtration, and by Öbrink (1968) with light scattering techniques. This agreement gives evidence of the reliability of the inclusion porosities determined with the HETP method.[3]

It can be concluded that the changes in the intraparticle void space and therefore in the protein inclusion porosities when Sepharose gels are progressively compressed are very small even when bed length reductions of approx. 10% of their initial value are experienced.

[3] Boyer and Hsu (1992) found the value of the inclusion porosity of ovalbumin in Sepharose CL-6B to be of 0.610. This value compares very well with those determined here for the same gel.

4.3.3 Evaluation of the axial dispersion coefficient.

HETP *versus* u or Van Deemter (1956) curves of the five test proteins are presented in figs. 4.12 and 4.13. Linear relationships were observed for each of the proteins studied. The Van Deemter curves of large biomolecules do not present the characteristic shape and HETP minimum, because the low diffusivities of protein molecules makes the contribution from longitudinal molecular diffusion negligible. According to eq. 4.12 the axial dispersion coefficient is directly related to the y intercepts in figs. 4.12 and 4.13.

It is apparent in figs. 4.12 and 4.13 that the larger the molecule the larger the resulting plate height for any particular interstitial velocity u. This is certainly a consequence of the lower intraparticle diffusivities of the larger molecules as will be seen in the following section. The exception was the γ-globulin (156 000 Da) in the Sepharose 6B column which had HETP values larger than the β-amylase (200 000 Da). This is due to the larger free diffusivity of β-amylase and the lower values of the axial dispersion coefficient D_L obtained with this molecule.

As can be seen from fig. 3.1 the changes in the dispersion Péclet number Pe_L, according to Athalye et al (1992) and Hejtmánek et al (1993), are negligible within the range of interest to chromatographic separations ($0<ReSc<200$). Therefore it is usual to consider the ratio D_L/u as constant. In table 4.6 the estimated values of the axial dispersion coefficient (D_L/u) are presented and compared with the corresponding values obtained by means of the most relevant correlations applicable to the range of chromatographic operation (see section 3.3.1). It is observed that the experimentally determined values of D_L/u are all of the same order of magnitude as the correlated values. In several cases they lie in between the values predicted with the correlation of Gunn (1969) and those estimated with the correlations of either Athalye et al (1992) or Hejtmánek et al (1993). However, in general the experimental values are smaller than the correlated ones. Although the difference between the experimental and the correlated values of D_L/u is small and could be attributed to experimental and data analysis errors, the differences may be due to the high efficiency of the columns used in the pulse experiments (see table 4.1) with the highly homogeneous structure of the Sepharose beds giving origin to very little longitudinal dispersion. Reported values of D_L/u for similar systems range from 0.027-0.049 (Boyer and Hsu, 1992); from 0.028 to 0.080 cm (Suzuki, 1974) and 0.016 cm (Arnold et al, 1985). These higher values of D_L/u have in some cases been attributed to external sources of dispersion which were not considered in the data analysis (Boyer and Hsu, 1992). In the present study extracolumn effects were negligible.

Han et al (1985) indicated that in the case when dispersion is not constant but depends strongly on bed location, significantly lower values of the axial dispersion coefficient are observed. They

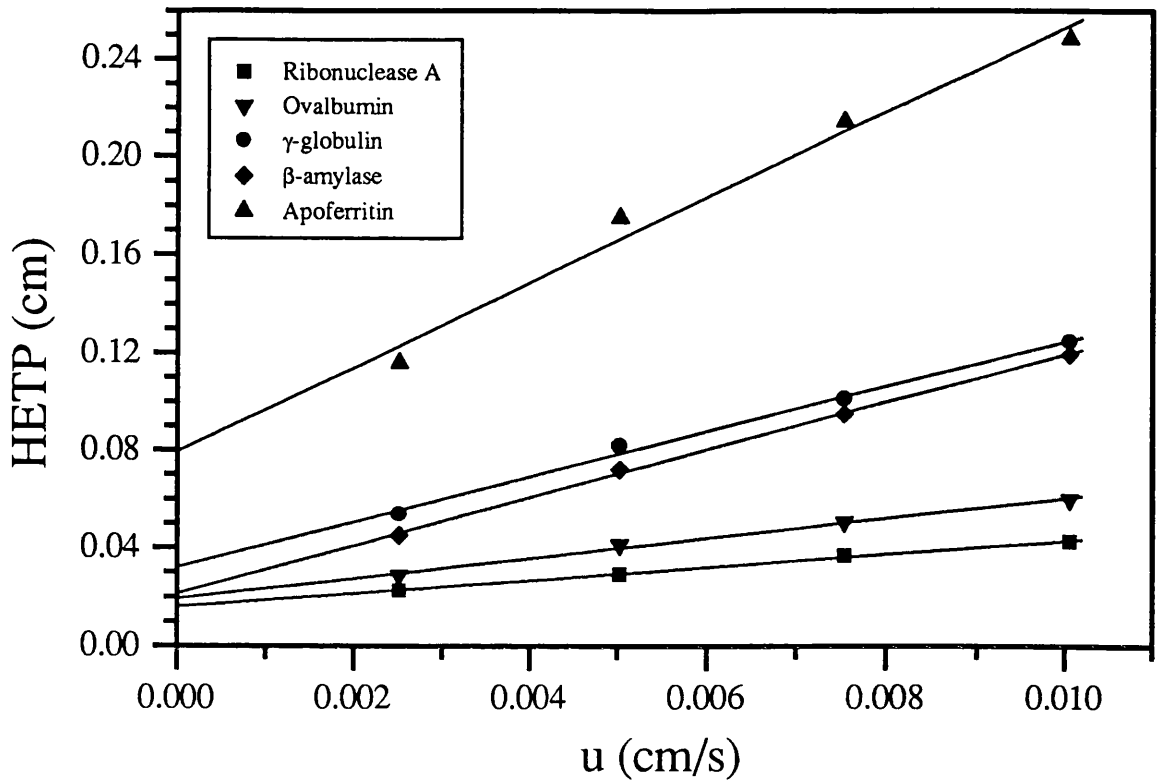

Fig. 4.12 HETP analysis of outlet peaks from protein pulses on a Sepharose 6B column, compressed at a flow rate of 0.5 ml/min to a lenght L=49.3 cm, and to a void fraction of ε=0.3316

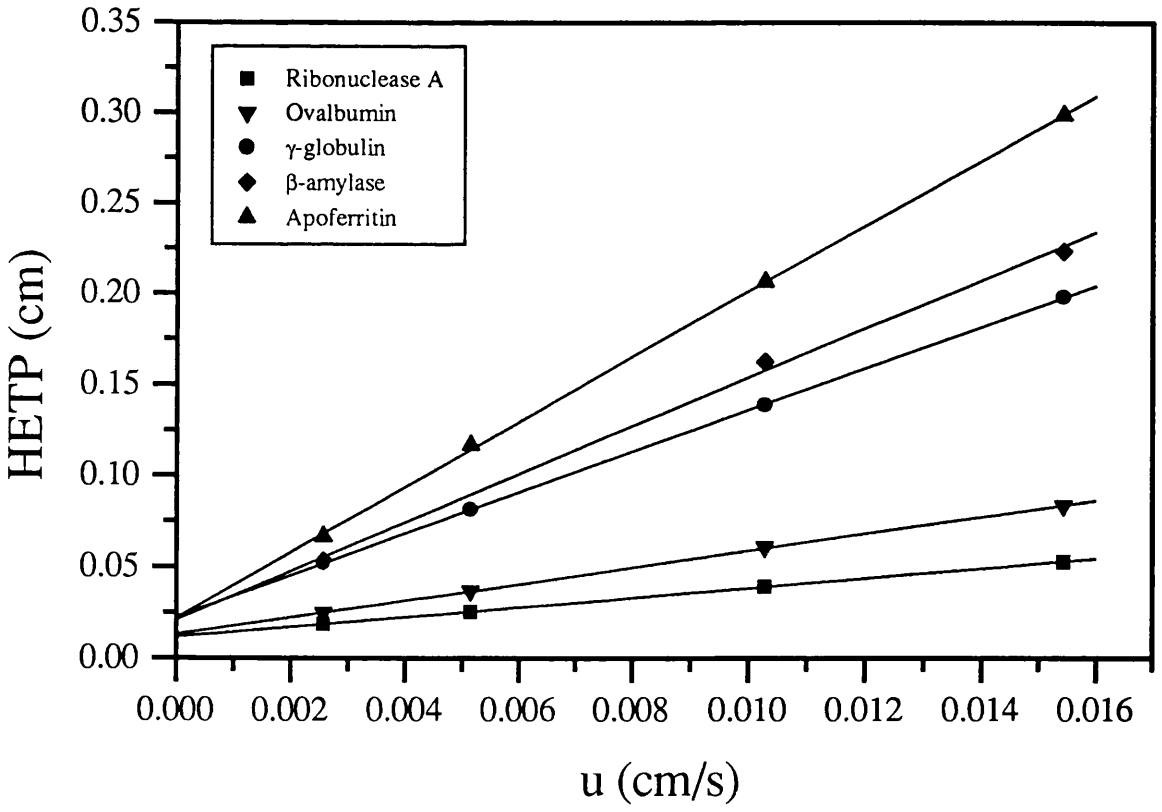

Fig. 4.13 HETP analysis of outlet peaks from protein pulses on a Sepharose CL-6B bed, compressed at a flow rate of 0.8 ml/min to a lenght L=50.2 cm, and to a void fraction of ε=0.3241

found that longitudinal dispersivities for uniform size packings are a function of position in the bed unless the following approximate criterion was satisfied

$$\theta = \left(\frac{L}{d_p}\right)\frac{1}{Pe_P}\left(\frac{1-\epsilon}{\epsilon}\right) \geq 0.3 \qquad (4.18)$$

where Pe_p is a modified diffusion Péclet number defined as $Pe_p = d_p u\varepsilon/D_m(1-\varepsilon)$. Under the conditions of the present pulse experiments this criterion was fully satisfied, θ ranged from 34 to 1960. Although Han et al (1985) suggested that the characteristic length for longitudinal dispersion for the case of nonuniform particle size distributions is much longer than the hydraulic radius of the packing, the very large ratio of L/d_p used in these experiments assures the constancy of the axial dispersion all along the column. Therefore it is correct to assume D_L to be constant and independent of bed location in the present study and it seems reasonable to consider that the experimental values of D_L/u were lower than the correlated ones as a consequence of the high efficiency of the gel beds.

Analysis of the results in table 4.6 also shows the existence of a relationship between the value of the axial dispersion coefficient D_L and the protein molecular diffusivity D_m (see table 4.2). The larger the molecular diffusivity the smaller the value of D_L/u. This is in agreement with the trend shown by the correlated values of D_L/u. This trend occurs due to the variation of the mechanisms of longitudinal dispersion with the diffusion Péclet number, $Pe_p = ud_p/D_m = ReSc/\varepsilon$ (Bear, 1972). At very low values of Pe_p molecular diffusion predominates and D_L/D_m is constant. In the range $0.4<Pe_p<5$ the molecular diffusion is of the same order of magnitude as the eddy or convective diffusion, and the mechanisms are additive. Between Pe_p numbers ranging 5-50 the axial dispersion is caused by convective diffusion combined with transverse molecular diffusion. In this case the two mechanisms interfere with each other and are not additive. The influence of molecular diffusion can be disregarded when Pe_p are higher than 50, and at very high Pe_p (c. 10000) the effects of turbulence and inertia interfere. In chromatographic practice the region of interest is approx. $0<Pe_p<600$ ($\approx 0<ReSc<200$).

In the present studies at a particular compression condition the mechanisms of dispersion vary from one protein molecule to the other according to its corresponding Schmidt number Sc ($Pe_p=ReSc/\varepsilon$), the Pe_p number being larger for the larger molecules. The values of Pe_p ranged from 9.9 to 383.8 for the pulse experiments with the 6B-gel bed and from 20.6 to 668.8 for the experiments with the CL-gel bed. This means that while the dispersion of the ribonuclease A molecules was caused by convective diffusion and transverse diffusion, the dispersion of the apoferritin molecules was caused solely by convective or eddy diffusion. Indeed the larger diffusivities of the smaller protein molecules attenuated the dispersion of these molecules by means

Table 4.6 Comparison of estimated axial dispersion coefficients by means of the HETP method with those predicted by engineering correlations.

SEPHAROSE 6B					
Compression flow rate: 0.3 ml/min Bed properties[a]: L=51.2 cm, ε=0.3538			Range of operation: Re =0.00033-0.00197 ReSc =3.5-67.9		
Protein	Péclet Number Pe_L	Experimental D_L/u (cm)	Correlated values of D_L/u (cm) [b]		
			Gunn [c]	Athalye et al[d]	Hejtmánek et al[e]
Ribonuclease A	1.239	0.0071	0.0046	0.0141	0.0133
Ovalbumin	1.158	0.0076	0.0064	0.0153	0.0138
γ-globulin	0.739	0.0119	0.0094	0.0169	0.0145
β-amylase	1.035	0.0085	0.0092	0.0168	0.0144
Apoferritin	0.173	0.0360	0.0100	0.0172	0.0146
avg. value	0.8688	0.0142	0.0079	0.0161	0.0141
Compression flow rate: 0.5 ml/min Bed properties[a]: L=49.3 cm, ε=0.3316			Range of operation: Re =0.00066-0.00263 ReSc =7.0-90.5		
Protein	Péclet Number Pe_L	Experimental D_L/u (cm)	Correlated values of D_L/u (cm) [b]		
			Gunn[c]	Athalye et al[d]	Hejtmánek et al[e]
Ribonuclease A	1.128	0.0078	0.0056	0.0149	0.0138
Ovalbumin	0.936	0.0094	0.0079	0.0161	0.0143
γ-globulin	0.557	0.0158	0.0112	0.0178	0.0150
β-amylase	0.846	0.0104	0.0109	0.0177	0.0149
Apoferritin	0.223	0.0394	0.0117	0.0181	0.0151
avg. value	0.738	0.0166	0.0095	0.0169	0.0146
Compression flow rate: 0.75 ml/min Bed properties[a]: L=46.55 cm, ε=0.2968			Range of operation: Re =0.00066-0.00395 ReSc =7.0-135.8		
Protein	Péclet Number Pe_L	Experimental D_L/u (cm)	Correlated values of D_L/u (cm) [b]		
			Gunn[c]	Athalye et al[d]	Hejtmánek et al[e]
Ribonuclease A	1.023	0.0086	0.0070	0.0156	0.0143
Ovalbumin	0.838	0.0105	0.0094	0.0169	0.0148
γ-globulin	0.564	0.0156	0.0126	0.0187	0.0155
β-amylase	0.647	0.0136	0.0124	0.0186	0.0154
Apoferritin	0.189	0.0466	0.0131	0.0190	0.0156
avg. value	0.652	0.0190	0.0109	0.0178	0.0151

Table 4.6 Continuation.

SEPHAROSE CL-6B					
Compression flow rate: 0.6 ml/min Bed properties[a]: L=51.05 cm, ε=0.3343			Range of operation: Re =0.00069-0.00344 ReSc =7.3-118.3		
Protein	Péclet Number Pe_L	Experimental D_L/u (cm)	Correlated values of D_L/u (cm) [b]		
			Gunn[c]	Athalye et al[d]	Hejtmánek et al[e]
Ribonuclease A	1.586	0.0058	0.0071	0.0162	0.0147
Ovalbumin	1.460	0.0063	0.0096	0.0176	0.0152
γ-globulin	0.929	0.0099	0.0130	0.0194	0.0159
β-amylase	1.736	0.0053	0.0128	0.0193	0.0159
Apoferritin	1.179	0.0078	0.0136	0.0198	0.0161
avg. value	1.378	0.0070	0.0112	0.0230	0.0156
Compression flow rate: 0.8 ml/min Bed properties[a]: L=50.2 cm, ε=0.3241			Range of operation: Re =0.00069-0.00413 ReSc =7.3-142.0		
Protein	Péclet Number Pe_L	Experimental D_L/u (cm)	Correlated values of D_L/u (cm) [b]		
			Gunn[c]	Athalye et al[d]	Hejtmánek et al[e]
Ribonuclease A	1.643	0.0056	0.0077	0.0166	0.0148
Ovalbumin	1.460	0.0063	0.0103	0.0179	0.0154
γ-globulin	0.829	0.0111	0.0136	0.0198	0.0161
β-amylase	0.902	0.0102	0.0134	0.0197	0.0161
Apoferritin	0.868	0.0106	0.0141	0.0201	0.0163
avg. value	1.140	0.0088	0.0118	0.0188	0.0157
Compression flow rate: 1.4 ml/min Bed properties[a]: L=49.5 cm, ε=0.3133			Range of operation: Re =0.00069-0.00688 ReSc =7.3-236.6		
Protein	Péclet Number Pe_L	Experimental D_L/u (cm)	Correlated values of D_L/u (cm) [b]		
			Gunn[c]	Athalye et al[d]	Hejtmánek et al[e]
Ribonuclease A	1.373	0.0067	0.0101	0.0178	0.0154
Ovalbumin	1.150	0.0080	0.0126	0.0192	0.0160
γ-globulin	0.730	0.0126	0.0156	0.0212	0.0167
β-amylase	1.210	0.0076	0.0154	0.0211	0.0167
Apoferritin	0.639	0.0144	0.0160	0.0216	0.0169
avg. value	1.020	0.0099	0.0139	0.0202	0.0163

a The internal diameter of the column was in all cases 1.6 cm.

b The correlated values shown in this table are the average values of D_L/u over the flow rate range at which the pulse experiments were carried out in each case.

c Values correlated with equation 3.29 (Gunn, 1969).

d Values correlated with equation 3.32 (Athalye et al, 1992).

e Values correlated with equation 3.33 (Hejtmánek et al, 1993).of the transverse diffusion which tended to even the solute front counteracting the effects of convective diffusion.

of the transverse diffusion which tended to even the solute front counteracting the effects of convective diffusion. A similar effect occurred when the bed was compressed. In this case the transition from one mechanism of dispersion to another for a particular protein molecule was promoted by the reduction of interparticle void space which resulted in a larger interstitial velocity u and therefore in a larger Pe_p (Pe_p= ReSc/ε). Hence as the bed compressed the axial dispersion increased due to a change in the mechanisms of dispersion. However, these variations in the values of D_L/u are relatively small and as already mentioned, within the range of reduced velocity of interest to chromatography, i.e. 0<ReSc<200, the value of D_L/u can be assumed constant. In any case it is surprising that the tendency of D_L/u to decrease as the diffusion coefficient D_m increases, although not very pronounced (relatively negligible), was indeed observed with the values of D_L/u estimated by means of the HETP method.

The changes effected by bed compression on the axial dispersion coefficient are shown in fig. 4.14. It is evident that as the interparticle space is reduced by compression the axial dispersion increases. This trend is followed by all the protein molecules studied. In the graph corresponding to the Sepharose 6B the data points of the apoferritin were not included because they were far larger than the values of D_L/u obtained with the remaining molecules, although they followed the same trend (see table 4.6). On the other hand in the graph corresponding to the Sepharose CL-6B in the same fig. 4.14, it is observed that the value points of β-amylase are very scattered, this could be the result of carbohydrate-carbohydrate interactions that may have affected the hydrodynamic behaviour of this molecule in the interparticle space of the Sepharose CL-6B bed.

Analysis of the data in table 4.6 and fig. 4.14 also shows that the relative increase of the experimental values of D_L/u when the bed was compressed is larger than the change in the values predicted with the correlation of Athalye et al (1992) or that of Hejtmánek et al (1993). These correlations are more reliable in the range of operation of chromatography than the correlation of Gunn (1969). From fig. 3.1 it can be seen that the latter correlation does not predict as expected a fairly constant value of D_L/u all along the range of interest to chromatographic practice. According to the theoretical analysis carried out by Östergren and Trägårdh (1991) the zone spreading produced by a homogeneous bed packed with non-porous beads and the spreading produced by an axially compressed bed also packed with non-porous beads are virtually the same. This means that deformation of the particles and therefore the change in the characteristic length of dispersion does not have a significant effect on dispersion. Therefore it appears that the relative higher increase in the experimentally estimated values of D_L/u originated not in the particle deformation caused by compression, but from modifications occasioned on the bed structure by the applied stresses. Pores could have been reduced or blocked as a result of compression

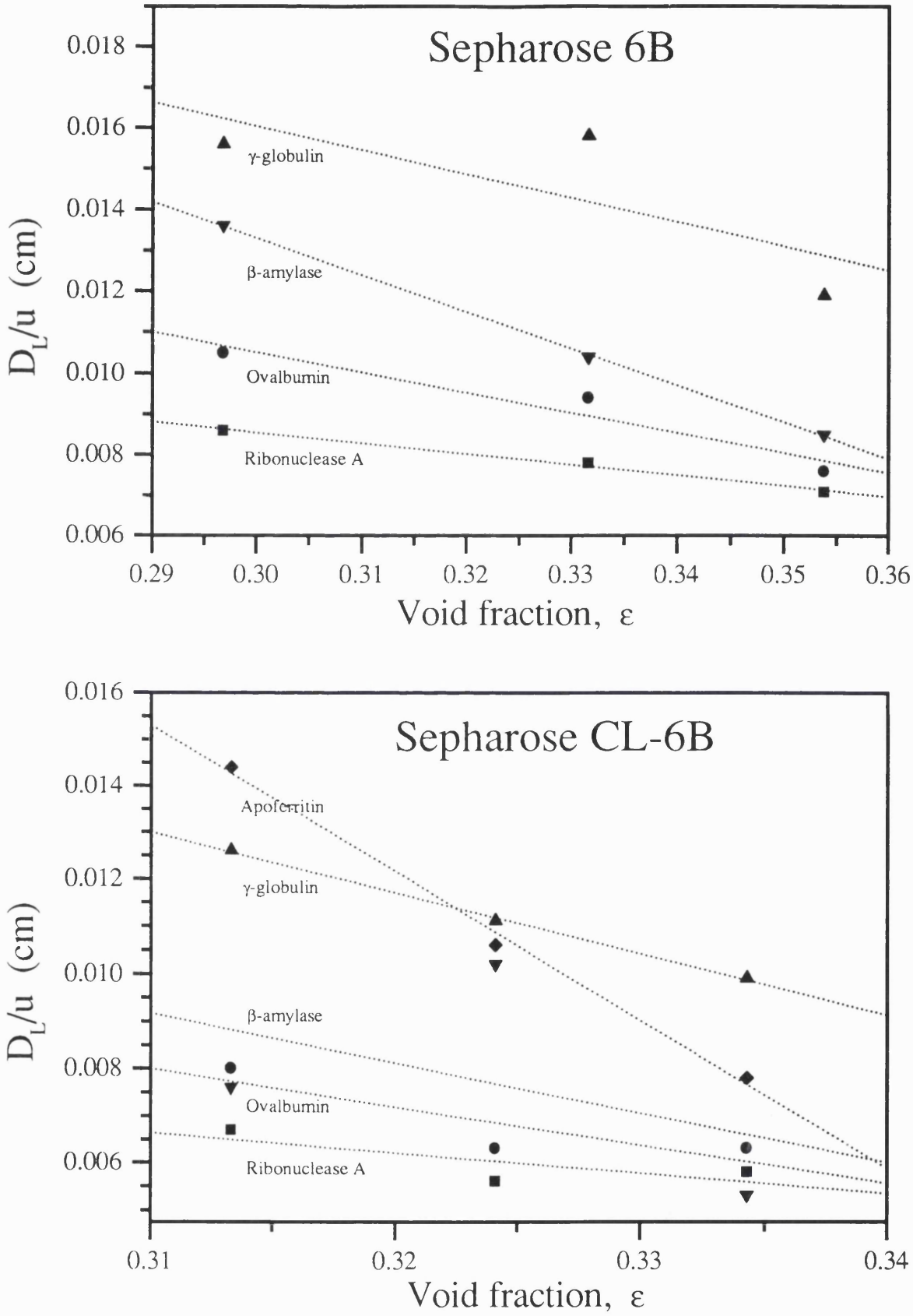

Fig. 4.14 Changes in the axial dispersion coefficient as expressed by D_L/u, when Sepharose columns were progressively compressed, indicated by the reduction in the bed void fraction, ε. ■ ribonuclease A, ● ovalbumin, ▲ γ-globulin, ▼ β-amylase, ◆ apoferritin.

producing disturbances in the flow pattern, hence enhancing the dispersive effects of eddy diffusion. It seems therefore that bed compression can deteriorate column performance by producing bed structural modifications that may lead to flow non-uniformities and thereby to greater dispersion.

4.3.4 Analysis of the intraparticle diffusion coefficient.

From the slope of the HETP *versus* u plots (see figs. 4.12 and 4.13), corrected for the film mass transfer contribution and the extracolumn effects, the effective intraparticle diffusivities D_e of the five proteins studied were estimated, according to eq. 4.12. The film mass transfer coefficient was estimated by means of the correlation developed by Ohashi et al (1981). Under the conditions employed in these experiments the contributions of the film mass transfer were generally small, accounting for less than 15% of the measured plate height. The extracolumn dispersion contributions were virtually negligible in all cases.

The results of this analysis are shown in table 4.7. The evolution of the intraparticle diffusion coefficients D_e of the five model proteins when the Sepharose gels were compressed are plotted in fig. 4.15. Very slight variations in the D_e values of most of the protein molecules are observed. In the case of the Sepharose 6B experiments the intraparticle diffusivities of all the proteins studied increased very slightly with bed compression (see table 4.7 and fig. 4.15). The slight variations of D_e are not significant and are most likely the result of data analysis and experimental errors as will be discussed later in this section. With respect to the Sepharose CL-6B bed, the values of D_e remained virtually constant as compression proceeded. This result agrees very well with the constant values of the inclusion porosities ε_p observed with this gel (see table 4.4). The Sepharose CL-6B column compressed to a lower extent than the 6B column, even though it was subjected to higher stress. This proves its higher rigidity. It can be concluded that at the degrees of compression achieved in this study, bed compression did not have a significant effect on the intraparticle diffusivity D_e of proteins.

Estimated values of the protein intraparticle diffusivities in the Sepharose gels are also shown in table 4.7. The model of Ogston et al (1973), i.e. eq. 3.47, largely overestimates the experimental values of D_e. On the other hand the correlation proposed by Boyer and Hsu (1992), i.e. eq. 3.49, predicts very well all the protein intraparticle diffusivities in the Sepharose 6B gel beads, and very closely the values of D_e in the CL-6B gel beads. This latter correlation only takes into account the

Table 4.7 Comparison between the values of the intraparticle diffusion coefficient D_e estimated by means of the HETP method and those evaluated employing models available in the literature.

SEPHAROSE 6B								
		Column properties[a]:		L= 51.2 cm ε= 0.3538	L= 49.3 cm ε= 0.3316	L= 46.55 cm ε= 0.2968		
Protein	MW (Da)	r_s [b] (nm)	D_m [b] (cm^2/s)	Experimental values: D_e (cm^2/s) (D_e/D_m)			Predicted values: D_e (cm^2/s) (D_e/D_m)	
							Boyer and Hsu[c]	Ogston et al[d]
Ribonuclease A	13 700	1.83	10.5×10^{-7}	21.9×10^{-8} (0.209)	25.9×10^{-8} (0.247)	27.2×10^{-8} (0.259)	32.8×10^{-8} (0.312)	68.1×10^{-8} (0.648)
Ovalbumin	45 000	2.93	6.55×10^{-7}	11.4×10^{-8} (0.174)	13.4×10^{-8} (0.204)	13.8×10^{-8} (0.211)	14.1×10^{-8} (0.215)	35.2×10^{-8} (0.537)
γ-globulin	156 000	5.35	3.59×10^{-7}	4.0×10^{-8} (0.112)	4.5×10^{-8} (0.126)	4.2×10^{-8} (0.116)	4.3×10^{-8} (0.120)	16.9×10^{-8} (0.470)
β–amylase	200 000	5.13	3.74×10^{-7}	3.7×10^{-8} (0.099)	4.0×10^{-8} (0.107)	3.7×10^{-8} (0.100)	3.9×10^{-8} (0.103)	17.1×10^{-8} (0.456)
Apoferritin	441 000	5.93	3.24×10^{-7}	1.8×10^{-8} (0.056)	2.0×10^{-8} (0.063)	2.1×10^{-8} (0.065)	1.9×10^{-8} (0.058)	14.3×10^{-8} (0..442)

[a] The internal column diameter was in all cases 1.6 cm.

[b] See table 4.2 for details of the evaluation of these parameters.

[c] Coefficients evaluated by means of equation 3.49 (Boyer and Hsu, 1992). The value of D_m was taken as shown on this table.

[d] Coefficients evaluated employing equation 3.47 (Ogston et al, 1973), utilising the experimental values of the inclusion porosity ($\varepsilon_p=K_d$).

Table 4.7 Continuation.

SEPHAROSE CL-6B								
		Column properties[a]:		L= 51.05 cm ε= 0.3343	L= 50.2 cm ε= 0.3241	L= 49.5 cm ε= 0.3133		
Protein	MW (Da)	r_s [b] (nm)	D_m [b] (cm^2/s)	Experimental values: D_e (cm^2/s) (D_e/D_m)			Predicted values: D_e (cm^2/s) (D_e/D_m)	
							Boyer and Hsu[c]	Ogston et al[d]
Ribonuclease A	13 700	1.83	10.5×10^{-7}	28.3×10^{-8} (0.269)	25.8×10^{-8} (0.246)	26.9×10^{-8} (0.256)	32.8×10^{-8} (0.312)	63.1×10^{-8} (0.600)
Ovalbumin	45 000	2.93	6.55×10^{-7}	11.6×10^{-8} (0.177)	11.1×10^{-8} (0.169)	11.5×10^{-8} (0.176)	14.1×10^{-8} (0.215)	32.4×10^{-8} (0.494)
γ-globulin	156 000	5.35	3.59×10^{-7}	3.2×10^{-8} (0.089)	3.3×10^{-8} (0.091)	3.2×10^{-8} (0.090)	4.3×10^{-8} (0.120)	15.2×10^{-8} (0.423)
β–amylase	200 000	5.13	3.74×10^{-7}	2.6×10^{-8} (0.069)	2.5×10^{-8} (0.068)	2.5×10^{-8} (0.067)	3.9×10^{-8} (0.103)	15.3×10^{-8} (0.408)
Apoferritin	441 000	5.93	3.24×10^{-7}	1.5×10^{-8} (0.046)	1.5×10^{-8} (0.047)	1.5×10^{-8} (0.047)	1.9×10^{-8} (0.058)	12.1×10^{-8} (0.372)

[a] The internal column diameter was in all cases 1.6 cm.
[b] See table 4.2 for details of the evaluation of these parameters.
[c] Coefficients evaluated by means of equation 3.49 (Boyer and Hsu, 1992).The value of D_m was taken as shown on this table.
[d] Coefficients evaluated employing equation 3.47 (Ogston et al, 1973), utilising the experimental values of the inclusion porosity ($\varepsilon_p=K_d$)

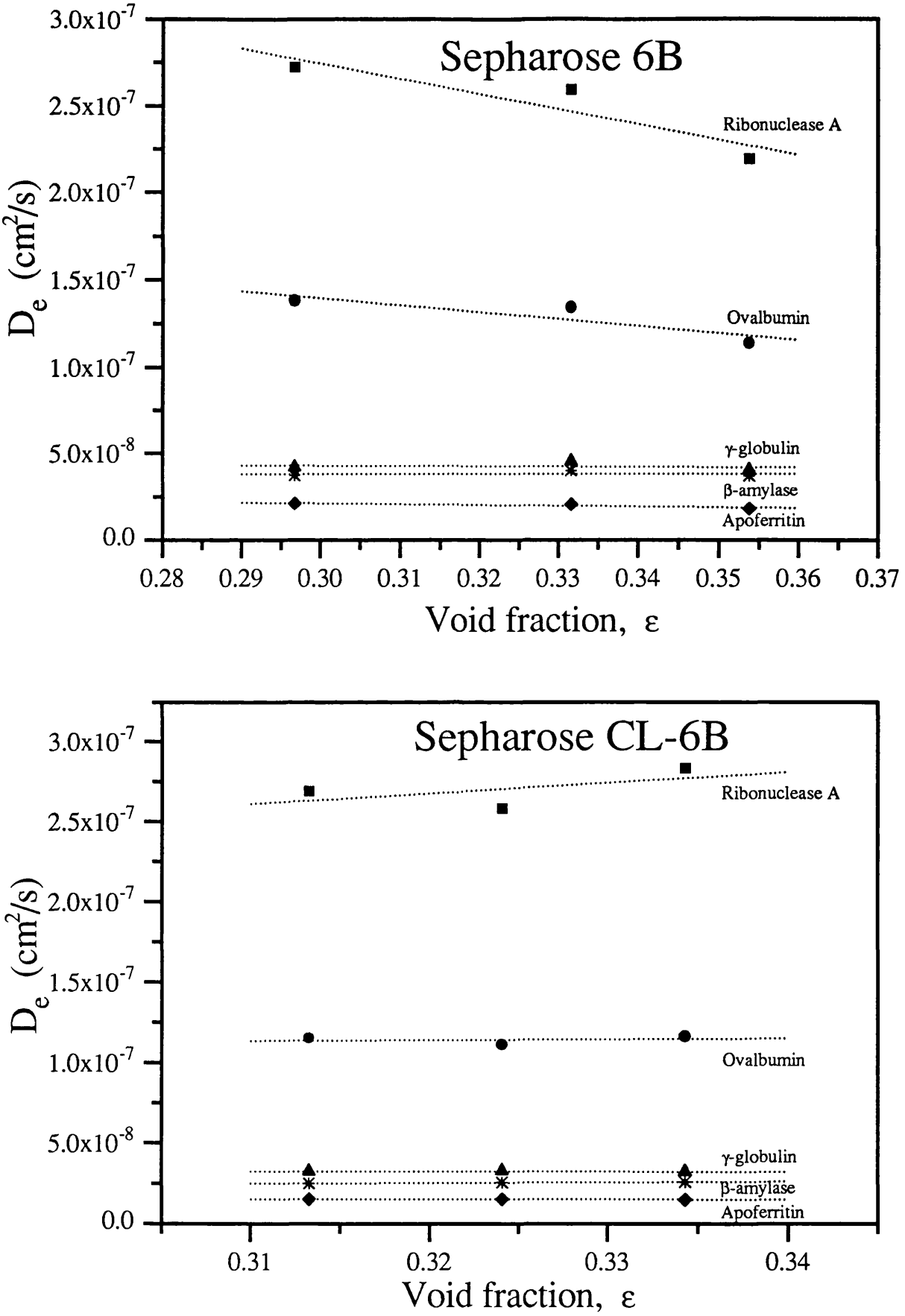

Fig. 4.15 Changes in the intraparticle diffusion coefficient D_e of the five model proteins when columns of Sepharose gels were progressively compressed as indicated by the reduction in the bed void fraction ε.

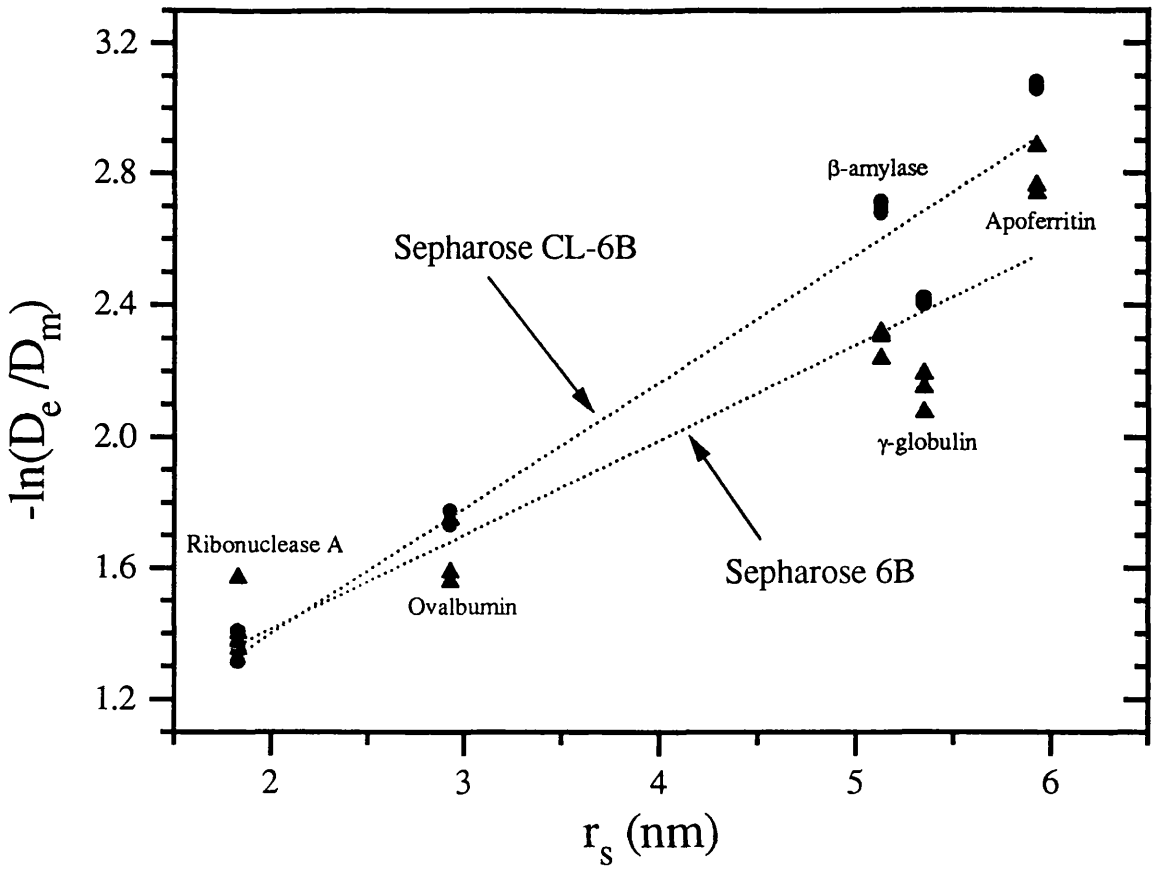

Fig. 4.16 Analysis of hindered diffusion of proteins in Sepharose 6B: ▲ , and Sepharose CL-6B: ● , according to Ogston et al (1973). The dotted lines represent equation 3.45 after curve fitting.

agarose fibre concentration c_f, and does not allow for any distinction between the 6B and the CL-6B gel structures. Hence the equal values of D_e predicted for any of the agarose gels studied. Analysis of the hindered intraparticle diffusion of proteins in the Sepharose gels is presented in fig. 4.16, according to the theory developed by Ogston et al (1973). The dotted lines represent the curve fitting of eq. 3.45. All the values of D_e for each of the Sepharose gels have been considered in the fitting procedure in order to estimate the value of the agarose fibre radius r_f. In the case of the 6B gel data set the estimated value was r_f= 2.89 nm, while for the CL-6B data set r_f= 1.64[4]. These values are surprisingly close to the reported radius of agarose fibres, i.e. r_f= 2.5 nm, determined by gel filtration (Laurent, 1967) and by light scattering (Öbrink, 1968). These results provide further evidence in regards to the reliability of the parameters determined in this study and are close to those calculated from consideration of the inclusion porosity (see section 4.3.2).
In fig. 4.17 the experimental values of D_e have been correlated according to the model equation proposed by Boyer and Hsu (1992):

[4] The value of r_f estimated by Boyer and Hsu (1992) for Sepharose CL-6B was of -2.3 nm.

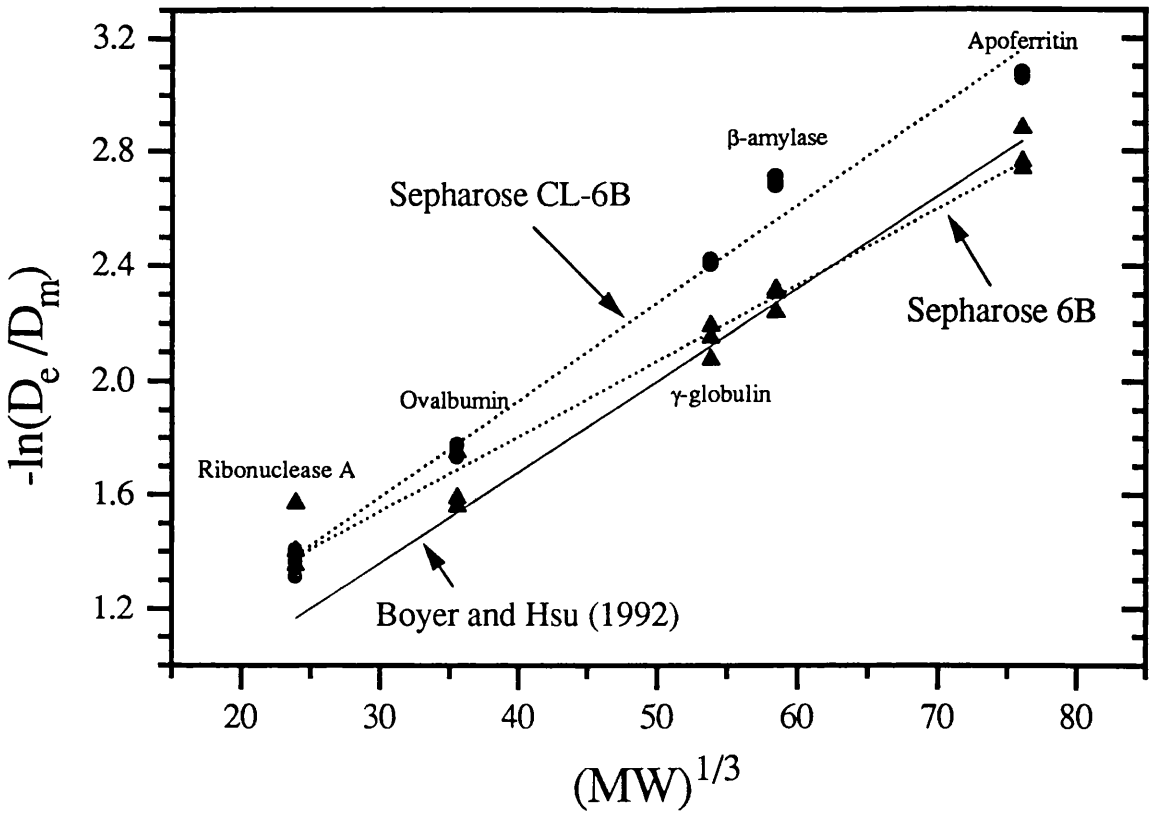

Fig. 4.17 Analysis of the correlation proposed by Boyer and Hsu (1992) for the estimation of restricted protein diffusion in Sepharose gels:———. Dotted lines represent the best fit of eq. 4.19 to the data obtained with Sepharose 6B: ▲ and Sepharose CL-6B: ● .

$$\ln\left(\frac{D_e}{D_m}\right) = -A\,(MW^{1/3} + B)\,c_f^{1/2} \qquad (4.19)$$

The solid line in the figure corresponds to the correlation as determined by these authors, with coefficients A=0.1307 and B=12.45. The corresponding coefficients obtained with the Sepharose 6B data set generated in this thesis were: A=0.1078 and B=28.259; and with the Sepharose CL-6B: A=0.1385 and B=16.852. As already discussed this correlation closely matched the experimental values of D_e, therefore it seems that the form of eq. 4.19 is correct, however, more experimental data is required to refine the values of the coefficients involved.

Finally fig. 4.18 shows the changes in the experimental values of plate height HETP for a particular protein, i.e. ribonuclease A, when the Sepharose 6B column was compressed. It is observed that as compression proceeded (ε decreased) the axial dispersion in the bed increased, as denoted by the increase in the value of the y-intercept. At the same time for the major part of the linear velocity range u, the values of the plate height HETP decreased as indicated by the decrease in the slope of the lines. Since the slope and the bed void fraction decreased with compression the value of the intraparticle diffusivity D_e slightly increased (see table 4.7) according

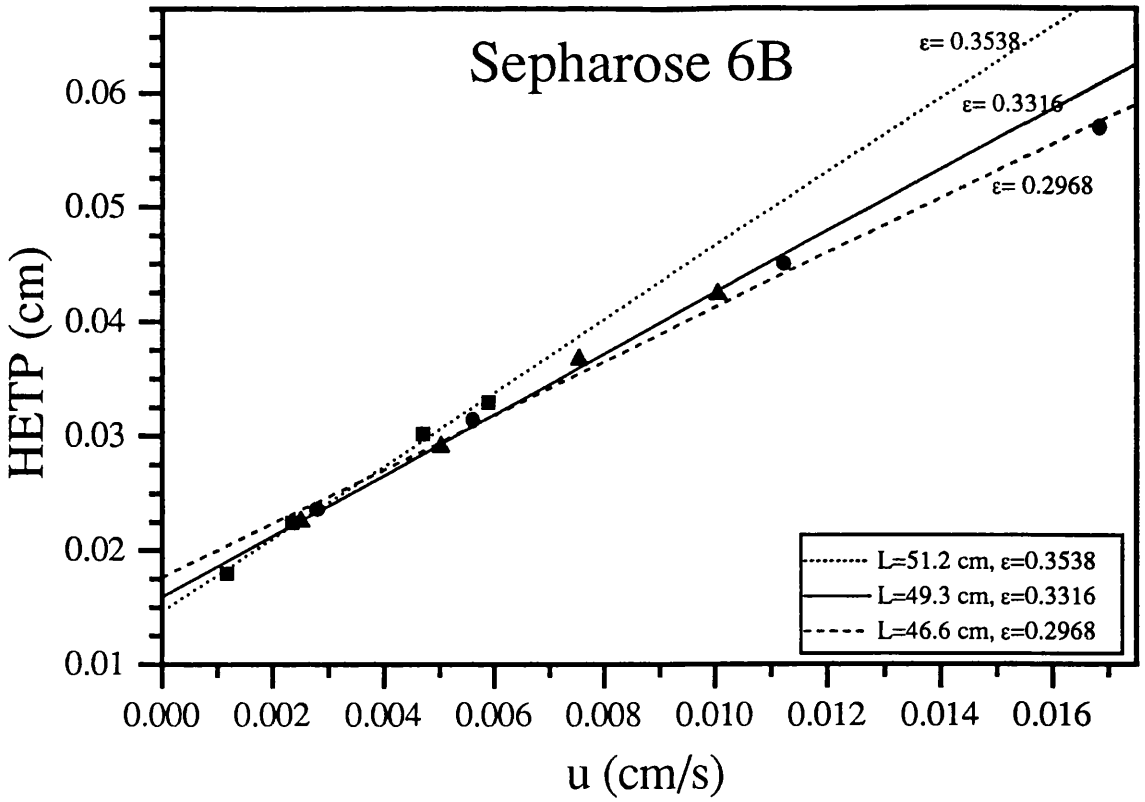

Fig. 4.18 Changes in the plate height HETP of ribonuclease A when the Sepharose 6B column was compressed as indicated by the reduction in bed void fraction, ε.

to eq. 4.12 which was used in the evaluation of D_e (see section 4.2.1). The slight improvement in the column performance as the bed was compressed is in agreement with the increase in efficiency determined with the acetone pulse as shown in table 4.1. This improvement was shown virtually by all the proteins tested with the Sepharose 6B column and it was possibly due to the faster solute partition caused by the reduction in the interparticle transport distances as suggested by Liao and Hjertén (1988). Horváth has considered that a possible reduction in the interparticular diffusion resistances may be responsible for the increase in efficiency under bed compression. Hjertén et al (1991) have also suggested that flow patterns that favour rapid transport of solutes between the mobile and the stationary phases may occur in compressed beds. However, the increase in performance experienced by the Sepharose 6B column, was reflected in an increase in the value of the intraparticle diffusivity D_e (see table 4.7). It appears that the model used in this analysis does not account for the possible increase in the velocity of molecular interparticle transport and therefore bulks this effect in the intraparticle diffusivity. Possible changes in the fluid film mass transfer coefficient, greater than those predicted by the correlation of Ohashi et al (1981), may have occurred as a result of bed compression and these could also be reflected in an increase in the intraparticle diffusivity.

In the case of the Sepharose CL-6B column the experimental values of the plate height HETP

slightly increased as the bed was progressively compressed as shown in fig. 4.19 for ribonuclease A. This reduction in the column efficiency agrees with the behaviour observed when the acetone pulses were injected onto the bed (see table 4.1). The intraparticle diffusivity of the five proteins studied did not change with bed compression as already discussed and the loss in column efficiency was due to an increase in the axial dispersion as indicated by the increase in the y-intercept of the lines. The Sepharose CL-6B column did not compress to the same degree as the 6B gel bed, despite the higher flow rate applied to this column. This is probably why the beneficial effects of compression were not experienced to the same extent by the CL-type column and therefore its performance diminished as a result of the higher dispersion, instead of increasing as it was the case with the Sepharose 6B column.

It appears therefore that bed compression could improve column performance by reducing the interparticle distances that solute molecules need to travel, but it can on the contrary deteriorate performance by provoking changes in the bed structure that lead to variations in the flow pattern and hence to greater dispersion. Depending on the balance of these two opposite effects bed compression will be beneficial or detrimental to column performance.

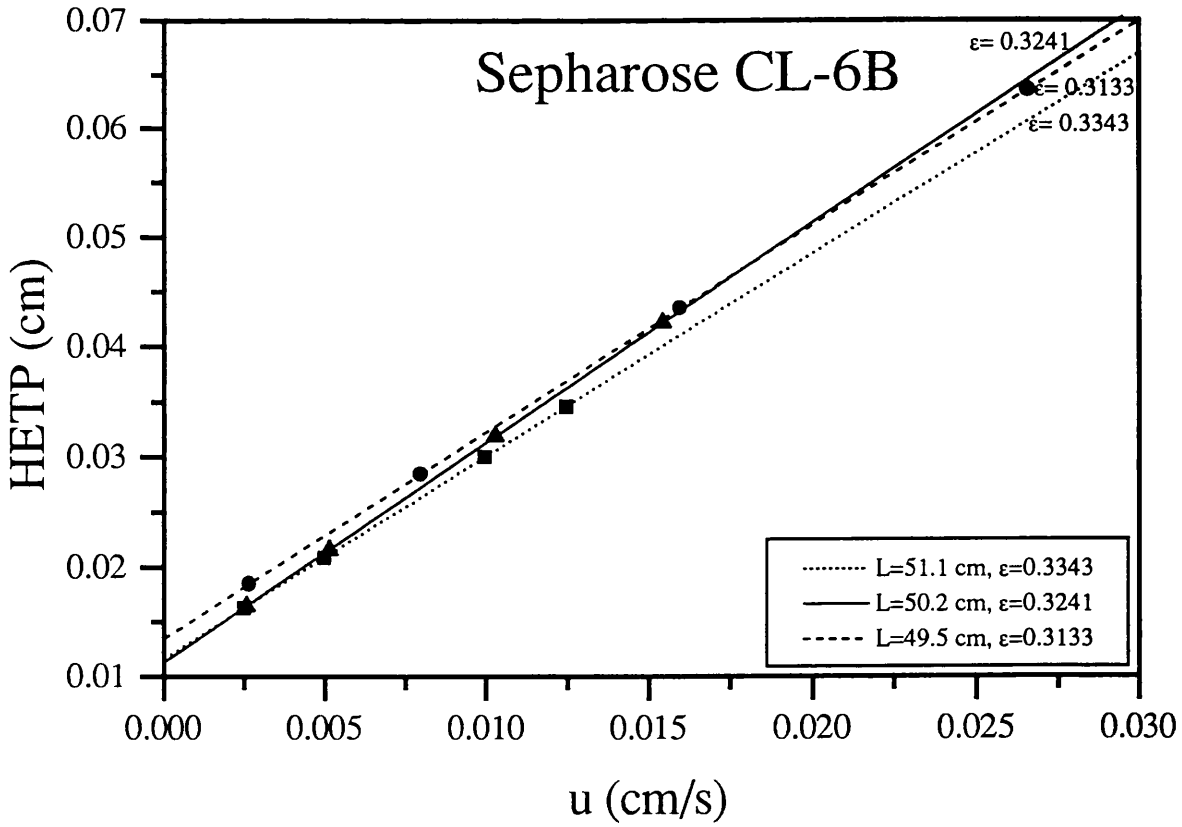

Fig. 4.19 Changes in the plate height HETP of ribonuclease A when the Sepharose Cl-6B column was progressively compressed as indicated by the change in void fraction, ε.

4.4 Conclusions.

The HETP method is less prone to data analysis errors, however, it is only applicable when the exiting peaks are gaussian. In the present study the columns used were long enough to generate Gaussian peaks. This was confirmed by comparison of results against a Gaussian curve. The considerable length of the two Sepharose columns also meant that the extracolumn contributions to peak dispersion were virtually negligible in all cases. The validity of the parameters determined by the HETP method was confirmed by the matching of experimental outlet peaks with the simulations generated by means of the general rate model of SEC (see section 3.2.1).

Although both Sepharose columns were significantly compressed it appeared that the reduction of the bed volume was mainly caused by a reduction in the interparticle void volume. Only a very small fraction of the intraparticle void volume was lost in the case of the Sepharose 6B column which was much more compressed than the CL column. Very slight reductions in the protein inclusion porosities were observed and it appears therefore that bed compression although deforming the matrix particles does not significantly affect the porosity of Sepharose gels and hence the intraparticle space available to the diffusing molecules. The validity of the protein inclusion porosities estimated by the HETP method was tested by means of the theory developed by Ogston et al (1973). A model equation defined by these authors was used in order to estimate the fibre radius r_f of the agarose gels. Resulting values of r_f were very close to those reported in the literature.

The experimentally estimated values of the axial dispersion coefficient expressed as D_L/u compared well with the correlated values, although they were in general slightly lower. It is considered that this is a consequence of the surprisingly high efficiency of the Sepharose columns used in these experiments. Bed compression increased the values of D_L/u for all the proteins studied mainly as a result of bed structural modifications that led to flow non-uniformities. Bed compression did not affect significantly the intraparticle diffusivity D_e of the five proteins tested. This result agrees very well with the very low changes experienced by the inclusion porosities ε_p of these molecules.

The reliability and validity of the D_e values obtained by means of the HETP method was corroborated by estimating the value of the agarose fibre according to the theory of restricted diffusion developed by Ogston et al (1973). The experimental values of D_e in the Sepharose 6B and CL-6B gel beads were very well predicted by the correlation proposed by Boyer and Hsu (1992).

It is probable that bed compression could have a beneficial effect on performance by reducing the interparticle distances travelled by the diffusing molecules and therefore speeding up solute partition. This must be balanced against deleterious effects generated by modifying the bed

structure causing flow non-uniformities which will enhance dispersion. More experimental work is needed in order to understand fully the effects of bed compression on column performance. However, in the light of the present results it appears that bed compression has a much greater effect on the column hydrodynamics than on its chromatographic performance.

CHAPTER 5

FOULING AND CHROMATOGRAPHIC PERFORMANCE

5.1 Introduction.

Chromatographic matrices are prone to fouling, in particular when they are used in a packed-bed configuration. Fouling is an important problem in chromatographic separation and purification since its occurrence has a detrimental effect on column performance. However, very little work has been carried out in this area (see section 1.5.3) and much remains to be studied in order to fully understand the effects and the mechanisms of fouling.

In this chapter the fouling study carried out as part of this project is presented. The study is centred on the effect that different levels of foulants present in a real process stream have on column performance. In order to discriminate in a more precise manner the effects of fouling on the bed and matrix structure the variations in column performance were monitored by measuring the change in the transport parameters, i.e. equilibrium distribution coefficient, intraparticle diffusivity and axial dispersion coefficient, that occurred when freshly packed columns were subjected to different degrees of fouling.

Size exclusion chromatography (SEC) was used to conduct this study. The simplicity of this type of chromatography make it suitable for this work which constitutes a potential starting point for a more profound fouling study. The method of moments was used to carry out parameter estimation. Although this pulse response method is prone to error it continues to be used in the field of chromatography (Ching et al, 1989; Boyer and Hsu, 1992; Ming and Howell, 1993) due to its ease of implementation and because it does not require costly pieces of equipment. The changes in the parameters that characterize the performance of SEC when a column is fouled will provide insight into the fouling process and the distribution of the foulants inside the chromatographic bed.

The aim of the present study was to attempt to establish a relationship between the degree of fouling to which a column is subjected and the subsequent change in the transport and equilibrium parameters, and hence its performance. This relationship will constitute the basis on which the performance of chromatographic columns operated under fouling conditions could be predicted.

This study was also aimed at determining which of the different chemical compounds among the whole range of foulants present in a biological stream, was mostly responsible for fouling.
In the first part of this chapter the materials and methods used to obtain and process the experimental data are presented together with a description of the assays conducted in order to analyze the chemical composition of the fouling and effluent streams. In the remaining sections the results are outlined and discussed.

5.2 Materials and methods.

5.2.1 Chromatographic system.

The chromatographic system used to obtain the experimental data required for the evaluation of column performance under both non-fouling and fouling conditions is described in this section.

5.2.1.1 Chromatographic matrix.

All the experiments were carried out using Sepharose 4 Fast Flow (Pharmacia LKB Biotechnology). This gel filtration matrix is not available in the market and was kindly provided to us by Pharmacia LKB Biotechnology (Uppsala, Sweden). The importance of this gel resides in the fact that it is used as the base matrix for the manufacture of Protein A Sepharose 4 Fast Flow and Protein G Sepharose 4 Fast Flow (Pharmacia LKB Biotechnology) which are widely used for the recovery and purification of monoclonal antibodies from cell culture at both laboratory and process scale.
Sepharose 4 FF is a beaded form of a highly cross-linked, 4% agarose derivative (Pharmacia,1990). The degree of cross-linking of the agarose has been optimized to give high physical and chemical stability combined with excellent flow properties and high reproducibility on scaling-up. The rigidity of the matrix structure minimizes volume variations during changes in pH or ionic strength. On the other hand its chemical stability allows the gel to tolerate harsh working conditions and cleaning-in-place (CIP) routines. This matrix also displays a notable resistance to microbial attack, due to the presence of the unusual sugar 3,6-anhydro-L-galactose in the agarose structure (Pharmacia, 1992).
The particle size distribution of this matrix was measured by using an image analyzer Magiscan 2A system (Joyce-Loebl Ltd). A random sample of the gel beads was placed in a haemocytometer

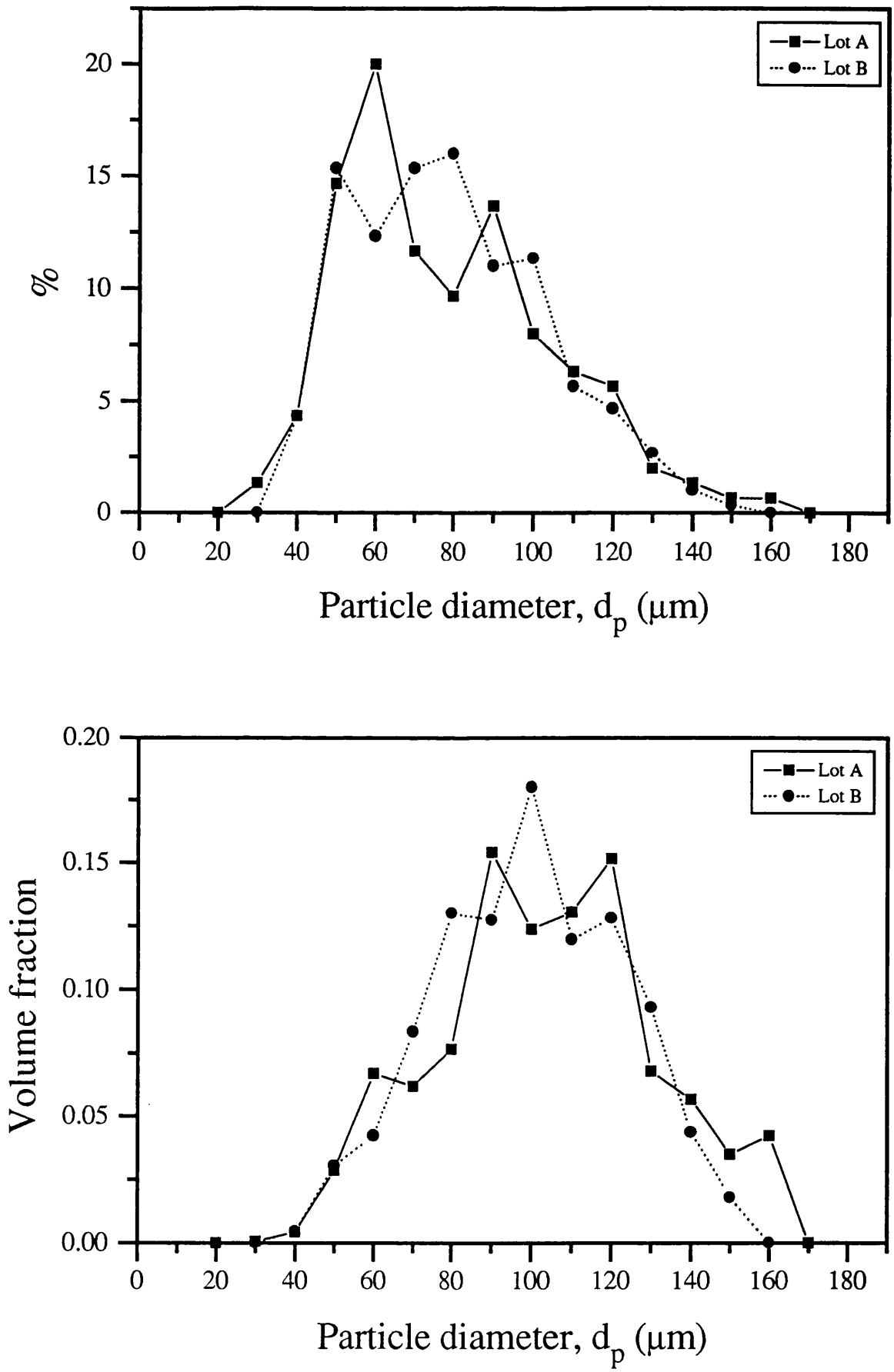

Fig. 5.1 Particle size distribution of the two lots of Sepharose 4 FF used in the fouling studies. Percentage frequency distribution (top) and volume fraction distribution (bottom).

(depth 0.2 mm) and the diameter of 300 beads was measured using the point to point function of the image analyzer. The particle size distribution obtained for the two different lots of Sepharose 4 FF used in this study are presented in fig. 5.1. The bead size range obtained compared very well with the manufacturer's reported range i.e. 45-165 μm. The matrix average particle radius R_p, was calculated directly from the measured particle size distribution according to eq. 2.17 (see section 2.3.2.4) where R_p represents the surface average radius, which according to Rasmuson (1985a) is the appropriate average radius to be used in chromatographic calculations. The values of R_p corresponding to the two lots of Sepharose 4 FF used in this study were 47.8 and 46.4 μm which compare very well with reported values of similar gels (Davies, 1989a; Boyer and Hsu, 1992).

5.2.1.2 Model proteins and void volume marker.

Two major sets of fouling experiments were carried out. In the first set three model proteins were used: cytochrome c, carbonic anhydrase and bovine serum albumin. These proteins were selected according to their molecular weight, availability, purity and cost. The second set utilised only two model proteins: cytochrome c and haemoglobin. The selection of these proteins was based not only on the difference of their molecular weights but primarily on their absorbance at 420 nm.
All proteins were bought from Sigma Chemical Co. Cytochrome c type IV from horse heart (cat. no. C-7752), had a purity of 99% based on H_2O content 4.6% and on molecular weight 12 384. Carbonic anhydrase was from bovine erythrocytes (cat. no. C-7025), with molecular weight of approx. 29 000. Bovine serum albumin was essentially fatty acid free (cat. no. A-0281) and had a purity of approx. 99% (agarose electrophoresis). Molecular weight 67 000. Bovine haemoglobin (cat. no. H-2500) probably containing up to 75% met-haemoglobin, balance primarily oxyhemoglobin. Molecular weight 64 000.
To measure bed void volume, blue dextran 2000 (Pharmacia LKB Biotechnology) was used.

5.2.1.3 Buffers.

The experiments were carried out utilising 20 mM phosphate buffer of three different ionic strengths which were obtained by using three different concentrations of sodium chloride (NaCl), i.e. 0.0 M, 0.5 M and 1.0 M. The pH was adjusted to 6.5 by adding 4 M sodium hydroxide solution. The phosphate buffers were prepared with di-sodium hydrogen orthophosphate (Na_2HPO_4) anhydrous AR (M.J. Patterson Scientific Ltd), sodium chloride (NaCl) SIGMA grade (Sigma

Chemical Co.) and sodium hydroxide (NaOH) Analar (BDH Ltd). All buffers were vacuum filtered (0.2 μm filter) and degassed prior to their use. The viscosity of the 0.5 M NaCl, 20 mM phosphate buffer was 1.12 mPa-s as measured by a rheometer Rheomat 115 (Contraves Industrial Products Ltd) at 20°C, using a cup and bob system. Its density was 1.029 g/ml as measured with a specific gravity bottle at 20 °C.

5.2.1.4 Experimental apparatus.

The experimental apparatus consisted of a FPLC system (Pharmacia LKB Biotechnology) which basic components and configuration have already been described in section 2.3.1.5. In the first set of experiments the FPLC system was used according to the configuration shown in fig. 4.3 which includes two high precision pumps P-500 and a single path UV monitor UV-1 (280 nm). The prefilter was not used in any of the fouling experiments so that the particulates concentration of the fouling stream was not affected. For the second set of experiments a pair of high precision pumps P-6000 (Pharmacia LKB Biotechnology) were added to the system and the UV monitor UV-1 was replaced by a variable wavelength Dynamax absorbance detector, model UV-1 (Rainin Instrument Co. Inc., USA).

In both of these types of pumps, pumping action is provided by a single gear box and a ball screw driving two alternating pistons. The pistons traverse reciprocally through two high precision glass cylinders so that liquid is drawn simultaneously into one cylinder and expelled from the other. Change of direction is activated by opto-electronic switches. The P-6000 pumps have a larger flow rate range, i.e. 0.1-99.9 ml/min, than the P-500 pumps. This means that the high precision glass cylinders of the P-6000 pumps are also larger than those of the P-500 pumps. This difference allows for a longer time between the switching of the pistons in the P-6000 pumps, for a particular flow rate. It is due to this advantage that the P-6000 pumps were added to the configuration in the second set of experiments. The P-500 pumps were used for column packing and for injecting the fouling stream onto the column while the P-6000 pumps were used during all the protein pulse response experiments.

The variable wavelength UV monitor was used so that absorbance could be measured at 280 nm as well as 420 nm. A jacketed glass column XK 16/20 (Pharmacia LKB Biotechnology) was used in all the experiments. A thermostatic bath LT/LB 8/72 (Grant Instruments Ltd) was used to keep the temperature of the buffer and the column constant at 20°C ± 0.2°C in all the experiments.

The data acquisition software and hardware were the same as those already described in section 2.3.1.5. In fig. 5.2 the complete experimental system used in the second set is shown.

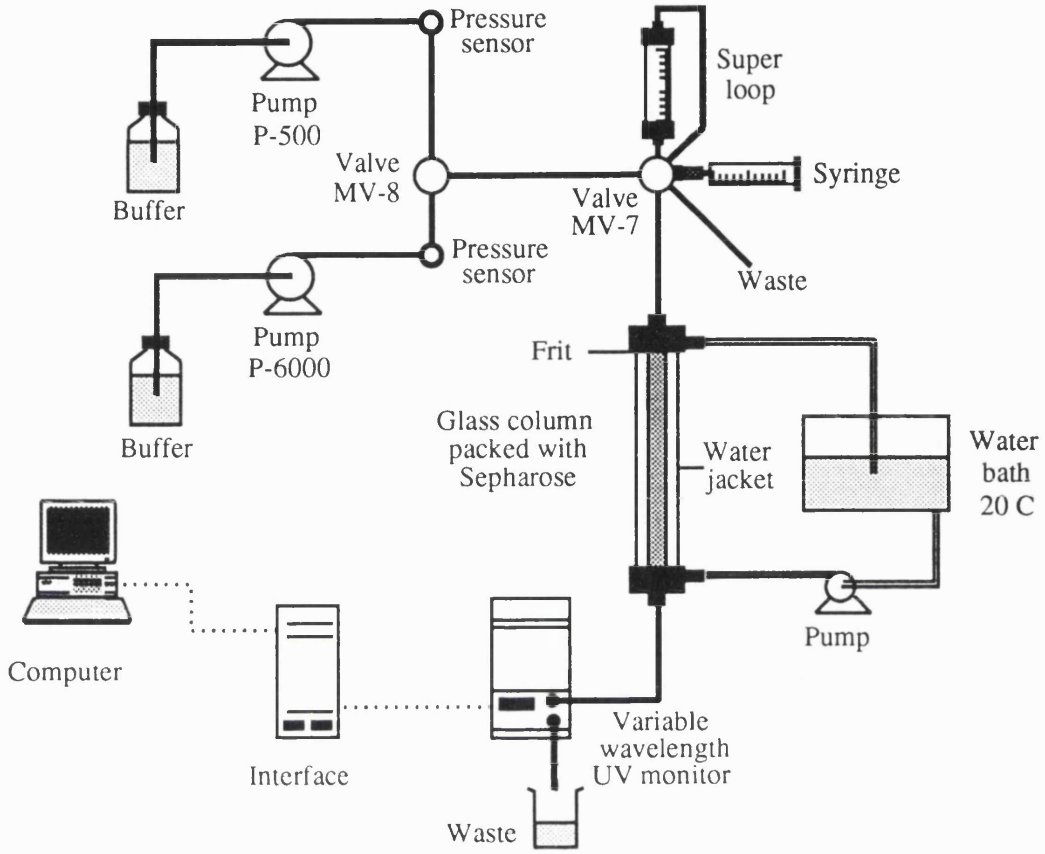

Fig. 5.2 Experimental apparatus used in the second set of the fouling experiments.

5.2.2 Experimental procedure.

Freshly packed columns were challenged with fouling streams of constant volume but containing different concentrations of foulants. This means that different amounts of foulants were actually injected to the column in each particular experiment. To assess the effects caused by matrix fouling on column performance, the transport and equilibrium parameters were measured before and after the columns were fouled and any change evaluated.

Columns were not reused since it was expected that for the higher foulant concentration experiments the bed structure could be dramatically modified rendering the column useless. Hence for each different foulant concentration tested a fresh new column was packed. In some cases the columns were cleaned-in-place and the transport and equilibrium parameters measured once the CIP procedure had finished. This enabled the effectiveness of the CIP to be determined.

Changes in all the transport and the equilibrium parameters were experimentally determined, with

the exception of those that may have occurred in the fluid-phase mass-transfer coefficient which were considered to be negligible. This coefficient was estimated by means of an engineering correlation (Ohashi et al, 1981) and was assumed not to be significantly affected by fouling. In reality it is expected that foulants will mainly deposit in the intra and interparticle space and only a very small fraction will deposit on the matrix outer surface blocking the matrix pores and therefore affecting the interphase mass transfer. Deposition of foulants inside the stationary phase will affect the inclusion porosity and the intraparticle diffusion, while deposition in the interparticle space will affect the bed structure and therefore the convective dispersion coefficient. Only if a very high deposition of foulants occurred in the interparticle space would the porosity of the stationary phase be considerably reduced and the fluid-phase mass-transfer coefficient affected. However, experience has shown that a high deposition of foulants in the interparticle space, enough to significantly reduce the matrix porosity, is never reached with these semi-rigid gels. This is because at lower levels of foulant deposition the bed permeability is sufficiently reduced to produce compression and the clogging of the bed. According to the above discussion it seems reasonable to assume that fouling does not have a significant effect on the fluid-phase mass-transfer coefficient and this coefficient was kept constant for all conditions, fouled and non-fouled. In order to experimentally determine the changes in the transport and equilibrium parameters effected by fouling, pulse analysis, and in particular the method of moments was used. It was not possible to use the HETP method (see section 4.2.1) since the chromatographic peaks obtained were far from being Gaussian. This involved the injection of pulses of protein at different flow rates before and after the column was fouled. The resulting chromatograms were then analyzed by the method of moments. The extracolumn contribution to peak dispersion was also experimentally determined so that the total peak dispersion could be corrected and only the peak dispersion due to the chromatographic bed considered in the evaluation of the transport parameters. A real process stream containing all types of biological fouling components, i.e. nucleic acids, proteins, lipids and particulates (cell debris), was produced in order to carry out our experiments in a very realistic manner. This fouling stream was produced strictly following the procedure outlined in the next section in order to obtain a stream with a fairly constant composition and characteristics. The stream was produced fresh every time a column was due to be fouled and it only was diluted to the required concentration for each particular experiment.

Therefore the effects of fouling on column performance, were those produced by a whole range of different types of foulants treated as a bulk. In order to determine the amount of fouling material retained by a column as well as to characterize the fouling components a series of assays were carried out. Samples were taken from the fouling stream and the column effluent during the fouling and washing procedures and were assayed for protein, nucleic acids, lipid, total organic

carbon and total dry weight.

Two major sets of experiments were conducted. In the first set the P-500 pump were used, but it was observed that after fouling the bed a spike was detected by the UV monitor (280 nm) every time the pump pistons switched direction (see section 5.2.1.4). These spikes were the result of the continuous foulant leakage from the beds and the momentary variations in flow rate occurring when the pistons switched. When the flow was constant the spikes did not appear, foulant leakage was detected as a constant background by the UV monitor. The presence of these spikes which could be large was a source of error in the moment analysis of the chromatograms resulting from the pulse response experiments with the model proteins. For the first set of experiments this problem was dealt with by extensively washing each column after the fouling procedure was finished. The washing procedure considerably reduced the foulant leakage but did not eliminate it completely.

After UV scanning the effluent stream from a fouled column, it was observed that the foulants present in this stream had maximum absorption around 280 nm, while their absorption away from this region was considerably lower. The UV spectrum of the effluent stream suggested that the foulants leaking from the column were mainly nucleic acids and possibly some proteins that had not been strongly retained by the matrix.

To reduce the error introduced by the spikes in the data analysis, a second set of experiments was conducted using cytochrome c and haemoglobin as the model proteins. Cytochrome c and haemoglobin due the presence of the haem group have a maximum UV absorption at around 420 nm. Therefore the column effluent stream was monitored at 420 nm. This eliminated or at least considerably reduce the size of the spikes caused by the foulant leakage. Also to make a further improvement in the quality and detection of the chromatograms, the P-6000 pumps were used to carry out the pulse experiments. Their use provided a longer period of time between the switching of the pistons (see section 5.2.1.4) for a particular flow rate as compared to the P-500 pumps. The extra time gained provided chromatograms with no spikes at all since each of the runs was finished before the switching of the pistons.

In each of the two sets of experiments different procedures were followed and different model proteins were utilised. The details of these experimental procedures as well as the above mentioned assays together with the method of moments are described in the following sections.

5.2.2.1 Preparation of fouling stream.

In order to foul the chromatographic columns in a realistic manner, a real biological process

stream containing a high concentration of diverse foulants was produced in the pilot plant. Baker's yeast (J. W. Pike Ltd) was used as the starting biological material.

The flow diagram for the preparation of this fouling stream is presented in fig. 5.3.

The homogenizer feed stream was prepared by dispersing 12 kg of Baker's yeast and 9.2 l of 20 mM phosphate buffer (pH 6.5) to make up a total volume of 20 l (the water content of Baker's yeast is ≈900 ml/kg, therefore 12 kg contain 10.8 l of water). In order to produce a homogeneous dispersion an electric stirrer model AXR (Silverston Machines Ltd) was used. The concentration of this stream, i.e. 600 g yeast/l was arbitrarily chosen in order to produce a final stream with a considerably high concentration of fouling materials. This cell concentration is close to the limit that can be processed by the homogenizer and the disk stack centrifuge in the subsequent steps. The dispersed yeast stream was then passed 5 times through a Manton-Gaulin high pressure homogenizer K3 (APV Co. Ltd). The pressure was set at 500 bar and the temperature was kept at 4-8 °C.

The resulting homogenate was then fed to a disk stack centrifuge SA00H 205 (Westfalia Separator AG) at a flow rate of 40 l/h. The centrifuge used 37 active disks and has a Q/Σ value of 1.87 x 10^{-8} m/s calculated according to Trowbridge (1962). The final pH of the supernatant was ≈6.5. The whole of this process took approx. 2.5 hours.

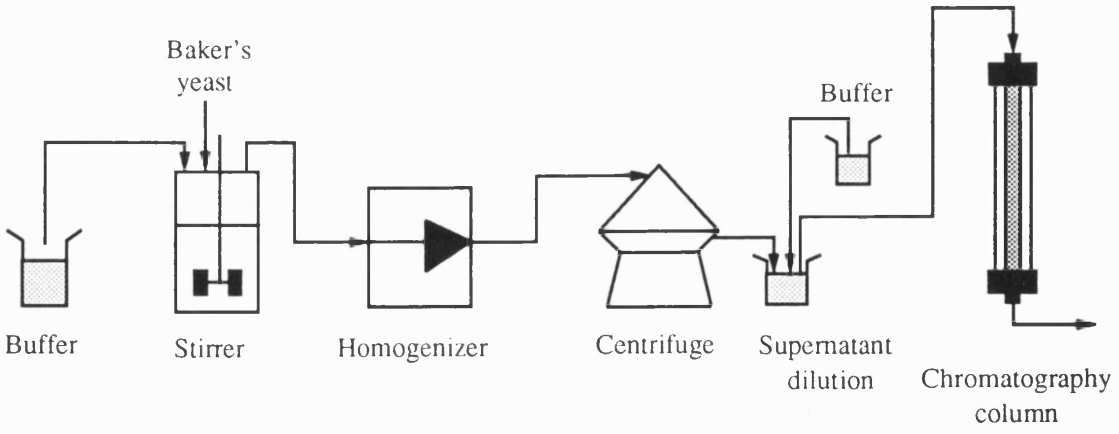

Fig. 5.3 Flow diagram describing the process followed in the production of the fouling stream.

The fouling stream was finally obtained by diluting the disk stack centrifuge supernatant with 20 mM phosphate buffer to the required concentration before its injection onto a chromatographic column. The pH of this stream was 6.5.
In the remaining part of this chapter, when reference is made to a % foulants concentration, the percentage is based on the degree of dilution to which the disk stack centrifuge supernatant was diluted previous to its injection onto a column.

5.2.2.2 Column packing procedure.

In order to be able to observe significant changes in the transport an equilibrium parameters, considerable fouling of the chromatographic columns was needed. This in turn required large volumes of fouling stream to be injected onto the columns. For this reason relatively short columns were used in this study. Short columns are more capable of withstanding the large pressure drops produced by the injection of fouling stream than the longer beds usually encountered in size-exclusion chromatography.
Columns 5.0 ± 0.1 cm long and 1.6 cm diameter (column volume of approx. 10 cm^3) were packed following two different packing procedures. The first procedure was conducted according to that employed by Pharmacia (Andersson, 1992) and the second is a modified version of the first. Only columns XK 16/20 (Pharmacia LKB Biotechnology) were utilized. Their protocols are as follows:

A) A required volume of Sepharose 4 FF slurry was degassed under vacuum at room temperature. The slurry contained approx. 50% gel and 50% filtered and deionized water. After eliminating air from the column dead spaces the gel suspension was poured down the side of the chromatographic glass tube to avoid bubble formation. Immediately after this the remainder of the column was filled with filtered and deionized water, the top adaptor was fitted to the column and connected to the P-500 pumps. The flow rate was then set to 14 ml/min (420 cm/h). The maximum packing flow rate recommended by the manufacturer (Pharmacia,1990) for this particular gel is 700 cm/h. The flow rate was maintained until a constant bed height had been reached. Next the top column adaptor was lowered just on top of the bed. Finally the top adaptor was manually lowered approx. 0.5 cm, compressing the bed to the final desired bed length[1]. This final step in the protocol was conducted following a suggestion by the manufacturer (Pharmacia, 1993). However, the bed void

[1] A more detailed description of the packing procedure is given by the manufacturer in their booklet "Ion Exchange Chromatography. Principles and Methods". Pharmacia, 1991.

fractions obtained with this procedure were lower than those usually found in gel filtration columns, i.e. 0.34-0.40. This is why this protocol was modified resulting in the following protocol.

B) The second packing procedure is virtually the same as the one above mentioned with the exception of the final step which was not conducted. Once the bed height was constant at a flow rate of 14 ml/min, the top adaptor was lowered on top of the bed without any further compression.

The columns packed following the first and second protocol were used respectively for the first and second set of experiments.

5.2.2.3 Pulse injection and column fouling procedure.

Once a column was packed it was equilibrated with 20 mM phosphate (0.5 M NaCl, pH 6.5) buffer. After equilibration pulses of different proteins were injected onto the column and eluted at constant flow rate. A range of flow rates were used with each particular protein, i.e. 1.0, 2.0, 3.0, 4.0 and 5.0 ml/min (u_o= 0.0083-0.0416 cm/s). All pulses had a constant volume of 200 µl and a concentration of 2 mg protein/ml, with the exception of those of haemoglobin which concentration was 3 mg/ml.

Cytochrome c, carbonic anhydrase and bovine serum albumin were used in the first set of experiments. The eluted peaks were detected by monitoring the absorbance at 280 nm of the column effluent. In the second set of experiments only two proteins were used, i.e. cytochrome c and haemoglobin. In this case a variable wavelength UV monitor was used and the eluting peaks were detected at 420 nm.

Column bed voidage was measured by the injection of a 200 µl pulse of blue dextran 2000 (Pharmacia LKB Biotechnology) with a concentration of 2.5 mg/ml. Bed voidage was evaluated according to maximum of the peak so obtained.

When the pulse experiments with a fresh column were finished the column was re-equilibrated with 20 mM phosphate buffer. Re-equilibration with buffer with the lowest ionic strength was carried out previously to the injection of the fouling stream, so that the conditions inside the bed were adequate for the retention of the fouling components.

A constant volume of 50 ml of fouling stream (approx. 5 column volumes) was then injected to the column by means of a 50 ml superloop (Pharmacia LKB Biotechnology) at a rather low flow rate, i.e. 1.6 ml/min. Previous experience had shown that loading the fouling stream at this flow rate or lower would not result in bed compression and clogging.

A stream containing a different concentration of fouling components was injected to each freshly packed column. The different foulant concentrations used were obtained by diluting down to 5, 10, 15 and 20% by volume the disk stack supernatant with 20 mM phosphate buffer. Higher foulant concentrations experimentally proved to greatly reduce bed porosity causing clogging, bed compression and channelling. The pH of the final stream was approx. 6.5. Prior to its injection the fouling stream was degassed under vacuum. This column fouling procedure was carried out in the same manner for both sets of experiments.

5.2.2.4 Column washing procedure and post-fouling pulse injection.

Immediately after the fouling of each column, one of two different washing procedures was conducted. The objective of the washing procedure was to reduce the amount of leakage of fouling material occurring during the following steps of each experiment and therefore to reduce the amount of interference in the chromatograms as detected by the UV monitor. Although the absorbance at 280 nm of the foulants leaking while the column was being washed, was high their mass was negligible. For this reason it was assumed that the fouling condition of the column did not significantly change with the washing procedure even if it was conducted in a very intensive manner.

The sequence of steps in the washing procedure carried out with the experiments that constituted the first set, and the objective of each of these steps are described in the following lines.

A) Initially 50 ml of 20 mM (pH 6.5) phosphate buffer were passed through each column at a flow rate of 1.6 ml/min in order to remove all the fouling components that were loosely bound or trapped by the gel matrix.

B) In order to remove most of the protein that had ionically or hydrophobically bound to the matrix, 90 ml of 20 mM phosphate, 1 M NaCl (pH 6.5) buffer were passed through each column at 1 ml/min. This was followed by another 90 ml of the same buffer but at a lower flow rate, i.e. 0.1 ml/min.

C) Then each column was washed with 20 mM phosphate, 0.5 M NaCl (pH 6.5) buffer until the baseline as detected by the UV monitor became stable and fairly flat, and the spikes produced by foulant leakage and the switching of the pump pistons did not appear or were small enough as to be considered negligible. This involved washing with 500 ml of buffer at 2.0 ml/min, followed by 720 ml at 1.0 ml/min. Then the flow rate was changed to 0.1 ml/min and 350 ml more were passed through the column. Finally a volume of buffer (250 to 1300 ml depending on the degree of fouling of the column) was passed at 3.0 ml/min. In total approx. 200 to 300 column volumes

(2000 to 3000 ml) of buffer were used to wash a column, the exact volume was proportional to the degree of fouling to which it had been subjected.

With the second set of experiments the number of column volumes used in the washing procedure was significantly reduced. This second washing procedure was therefore far more realistic than the previous one. It was carried out as follows:

A) Two gradients were run with the purpose of removing most of the protein that had ionically or hydrophobically bound to the column. Initially a gradient of 1.5 column volumes (15 ml) was conducted with 20 mM phosphate buffer from the lowest (0.0 M NaCl) to the highest ionic strength (1 M NaCl). The second gradient was carried out over two column volumes of 20 mM phosphate buffer, this time from the highest to the lowest ionic strength. Both gradients were run at 1.6 ml/min.

B) Washing with approx. 5 column volumes (50 ml) of 20 mM phosphate 0.5 M NaCl was carried out in order to remove the loosely bound or retained foulants, to bring the UV monitor baseline down to a stable and constant value and to reequilibrate the bed prior to the pulse injections.

In this latter procedure a total of approx. 8.5 column volumes (85 ml) of buffer were used.

Once a column was washed and reequilibrated pulse response runs were carried out with the model proteins so that the transport and equilibrium parameters could be determined for the fouled-column condition. The procedure followed was exactly the same as that described in the previous section, with the exception that with the most highly fouled columns, the flow rates used ranged from 0.5 up to 3.0 or 4.0 ml/min (0.00416-0.025 cm/s or 0.00416-0.0333 cm/s). A shorter range was used to avoid the development of high pressure drops that would have otherwise triggered the compression of the bed.

All these experimental procedures, i.e. pulse injections, column fouling and column washing were carried out at a constant temperature of 20 °C.

5.2.2.5 Extracolumn contribution to peak dispersion.

The measurement of the extracolumn sources of peak spreading were conducted following a procedure suggested by Arnold et al (1985). Pulses of the model proteins were injected into the XK 16/20 column (Pharmacia LKB Biotechnology), this time containing no matrix and in which the two distributors were pushed together. Protein samples of the same concentration (2 mg protein/ml of 0.5 M NaCL, 20 mM phosphate buffer for all model proteins except for haemoglobin

which concentration was 3 mg/ml) and size (200 µl) as those used for the pulse response experiments with the chromatographic bed were applied (see section 5.2.2.3). Therefore the measured dispersion due to the extracolumn effects would include not only the dispersion resulting from the presence of tubing connections, valves and column distributors but also the dispersion due to the initial bandwidth of the 200 µl pulses. Pulse experiments with cytochrome c, carbonic anhydrase and BSA were carried out using the basic FPLC configuration while cytochrome c and haemoglobin were used with the modified FPLC configuration (see section 5.2.1.4).

5.2.2.6 Cleaning-in-place procedure (CIP).

The cleaning-in-place procedure was carried out only with two columns from the first set of experiments. It consisted of the following steps:
A) Wash with 4 column volumes (approx. 40 ml) of 1 M NaOH at 1 ml/min (30 cm/h).
B) Wash with 1 M NaOH at 0.1 ml/min. This step was carried out in order to prolong the contact time with 1 M NaOH. The flow of alkali was sustained up to a total contact time of 3 hours (a total of 5.4 column volumes) with one of the two columns and up to 7 hours (a total of 7.8 column volumes) with the second one.
C) Wash with 5 column volumes of 20 mM phosphate, 1 M NaCl (pH 6.5) buffer. This step was conducted to bring the column pH down to 6.5.

This procedure followed the lines given by Pharmacia (Jägerston, 1993).
The CIP procedure was carried out with the objective of determining the extent to which the performance of a fouled column could be recovered by means of this treatment and to test the capability of the method of moments to measure changes in column performance. It was at the same time a test of the effectiveness of the CIP procedure.

5.2.3 Mass Balances.

In order to determine the total amount of fouling material retained by a column as well as the possible existence of a major fouling component in the column feed stream, a series of assays were carried out so that mass balances could be conducted. Nucleic acids, protein and lipids were assayed in order to determine the amount of these components in the column inlet and outlet

streams. Samples of these streams were taken during the fouling and washing procedures.
The amount of particulates (cell debris) in these streams was determined by means of dry weight measurements. The buffer used in the experiments contained a large amount of sodium chloride (see section 5.2.1.3). Since this salt was present in the dry weight samples, it was necessary to make a correction, so that the actual weight of the particulates could be determined. For this reason a sodium chloride assay was also conducted. Total organic carbon in the fouling stream and the column effluent was also assayed to determine the total amount of organic foulants retained by a column.
In the following sections the procedures and methods used to conduct the assays are described.

5.2.3.1 Protein assay.

The protein assay was a commercially available assay from Bio-Rad based on the Bradford assay. The assay was based on the principle of the shift of the absorbance maximum of an acidic solution of Coomassie Brilliant Blue G-250 from 465 to 595 nm when binding to protein occurs, first demonstrated by Bradford (1976). Over a ten-fold concentration range the extinction coefficient of a dye-albumin complex was constant, and therefore the Beer-Lambert law may be applied for accurate quantification of the protein in the sample.
In the assay, 50 µl of sample were mixed with 1.5 ml of the assay reagent in a cuvette and allowed to react for 5 minutes before the absorbance was measured at 595 nm. The standard curve was constructed using dilutions of BSA (Sigma Chemical Co) from 0.1 to 1 mg/ml, 50 µl of each dilution being reacted with 1.5 ml of reagent for 5 minutes before reading the absorbance at 595 nm.

5.2.3.2 DNA assay.

The assay for DNA was based on the reaction of 2-deoxyribose with a chromogenic reagent to give a coloured product which can be read in a spectrophotometer to give a quantitative value of DNA concentration. It is based on a method first described by Leyva and Kelly (1974).
The assay protocol was as follows. For the standards highly polymerised calf thymus DNA (BDH) was dissolved in 10 mM tris buffer containing 0.5 mg/ml of BSA (as a carrier) at pH 7.4. Standards were made from 0-250 µg of DNA in 200 µl and treated in the same way as samples. Samples had a volume from 50-100 µl depending on concentration. As protein was already

present, it was unnecessary to use a carrier protein in the samples. Samples and standards were precipitated with the addition of an equal volume of 0.4 M perchloric acid, and incubated at 4 °C for 30 minutes. The samples were then centrifuged at 16 000 rpm for 10 min in a bench top centrifuge and the supernatant discarded. The pellets were treated with 250 µl of 1 M perchloric acid and incubated in a water bath at 70 °C for 30 minutes. Subsequently they were cooled and 0.5 ml of the chromogenic reagent was added. The samples were then incubated at 37 °C overnight and read the following day in a spectrophotometer at 600 nm.
The chromogenic reagent was prepared as follows. 1.5 g of diphenylamine was dissolved in 100 ml of glacial acetic acid. A further 1.5 ml of concentrated sulphuric acid was added to this, and the reagent stored at 4 °C until use. Also 0.5 ml of acetaldehyde were mixed with 24.5 ml of distilled water and stored at 4 °C. The reagent was prepared immediately before use by adding 0.1 ml of the acetaldehyde solution to 20 ml of the diphenylamine solution. All chemicals used were Analar grade or equivalent, and were obtained from Sigma Chemical Co or BDH.

5.2.3.3 Lipid assay.

The amount of lipid in samples of fouling stream and column effluent was determined by firstly extracting the lipid and then quantifying the extracted lipid spectrophotometrically. The extraction method was that of Bligh and Dyer as modified by Kates (1986). 1 ml of the sample was extracted with 2:1 v/v mixture of chloroform:methanol, for 2 hours with occasional agitation. After this period the sample was centrifuged in stoppered glass vessels for 10 min, at 4 °C and 4000 rpm. The supernatant was reserved and 4.75 ml of methanol:chloroform:water in the ratio 2:1:0.8 v/v was added to the pellet. This was vigorously mixed and left to extract for another 2 hours. This mixture was then centrifuged under the same conditions, and the resulting supernatant added to the previously reserved supernatant. 2.5 ml each of chloroform and water were added to the combined supernatant, and the mixture shaken vigorously . The sample was then centrifuged to break the emulsion for about 5 minutes at 4000 rpm and 4 °C. The lower chloroform phase was drawn off and used for quantification in the next stages of the assay.

The spectrophotometric determination of lipids followed the phospho-vanillin reaction for determination of hydrophobic compounds described by Zollner and Kirsch (1962). The assay was prepared by dissolving 0.6 % w/v of vanillin (Sigma Chemical Co) in a 4:1 v/v phosphoric acid-water mixture. 50 µl of sample (chloroform layer) were mixed with 0.2 ml of concentrated sulphuric acid and placed in a boiling water bath for 10 minutes. The sample was cooled to room

temperature, and 4 ml of the vanillin reagent were added. The mixture was left for 30-50 minutes before reading in a spectrophotometer at 530 nm. Standards were obtained prediluted from Sigma Chemical Co. (Lipid Lin-Trol set).

5.2.3.4 Total dry weight.

The total dry weight was measured gravimetrically by drying 5 ml samples of fouling stream and column effluent in pre-weighed foil boats in an oven at 80 °C to constant weight (± 0.0005 g).

5.2.3.5 Sodium chloride assay.

The amount of NaCl present in the fouling stream and the column effluent was measured by means of a chloride analyzer model 926 (Corning Ltd). Samples of these streams were diluted hundred-fold with deionized water, so that their NaCl concentration would fall within the measuring range of the analyzer (10 to 999 mg/l). Accurately measured volumes of 0.5 ml of the diluted streams were analyzed.

5.2.3.6 Total organic carbon assay.

This assay was conducted utilizing a total organic carbon analyzer model TOC-5050 (Shimadzu Corporation). Volumes of 1 ml of the fouling stream and column effluent were diluted with 9 ml of deionized water in order to reduce their levels of salt. Samples of 50 µl of the resulting dilutions were injected into the combustion tube of the total organic carbon analyzer. The amount of organic carbon in the samples was given by the analyzer in ppm.

5.2.4 The method of moments and data analysis.

As mentioned in section 4.2.1 Schneider and Smith (1968) derived equations relating the first absolute and the second central moments of the chromatographic peak to the parameters that characterize performance. These equations constitute the general form of the pulse response analysis and are based on the statistical moments theory of Kubin (1965) and Kucera (1965). For

the particular case of size exclusion chromatography the equation of the first absolute moment is given by (see section 4.2.1):

$$\mu_1 = \frac{L}{u}\left(1+\frac{(1-\epsilon)\,\epsilon_p}{\epsilon}\right) + \frac{t_o}{2} \qquad (5.1)$$

and that of the second central moment by:

$$\mu_2' = \frac{2L}{u}\left[\frac{(1-\epsilon)}{\epsilon}\frac{R_p^2\epsilon_p^2}{15}\left(\frac{1}{D_e}+\frac{5}{k_f R_p}\right)+\frac{D_L}{u^2}\left(1+\frac{(1-\epsilon)}{\epsilon}\epsilon_p\right)^2\right]+\frac{t_o^2}{12} \qquad (5.2)$$

The generality of the method of moments resides in its applicability to all chromatographic peak shapes. However, it must be borne in mind its susceptibility to errors arising from the presence of small amounts of impurities, tailing and channelling or shifts in the detector baseline as well as the presence of noise, extracolumn effects and peak skewness, all of which can lead to large variations in the second central moment (Chesler and Cram, 1971). Indeed the use of the method of moments has been criticized as a result of the lack of control on these sources of error (Lenhoff, 1987).

However and despite of the possible errors involved the method of moments has been considerably used in the past. Rate parameters have been estimated from the peaks obtained from size exclusion chromatography of small molecules (Mehta et al, 1973; Suzuki, 1974; Nakanishi et al, 1977) and very recently the method of moments has also been used to determine transport parameters of large molecules, i.e. proteins (Ching et al, 1989; Boyer and Hsu, 1992; Ming and Howell, 1993). As in the case of the HETP method, the method of moments has been employed due to its easiness of application and because it does not require sophisticated equipment.

As already described the estimation of the transport and equilibrium parameters by means of the method of moments involves the conduction of pulse response experiments on a chromatography column at different liquid velocities. The first absolute and the second central moments are then evaluated by numerical integration of the resulting digitized chromatograms.

The first absolute moments are used to determine the value of the inclusion porosity, ϵ_p, also called intraparticle void fraction or intraparticle porosity. This is an equilibrium parameter which represents the volume fraction of intraparticle space available to the diffusing component. From eq. 5.1 it can be seen that a graph of μ_1-$t_o/2$ vs L/u results in a straight line. Then ϵ_p can be calculated from the slope of this line and by means of the value of ϵ, the bed void fraction.

The measurement of the transport parameters is conducted by the second moment analysis which

involves the rearrangement of eq. 5.2 to the following form:

$$\frac{\mu_2' - \frac{t_o^2}{12}}{\frac{2L}{u}} = \frac{(1-\epsilon)}{\epsilon}\frac{R_p^2 \epsilon_p^2}{15}\left(\frac{1}{D_e} + \frac{5}{k_f R_p}\right) + \frac{1}{u}\left[\frac{D_L}{u}\left(1 + \frac{(1-\epsilon)}{\epsilon}\epsilon_p\right)^2\right] \qquad (5.3)$$

In the experimental conditions usually encountered in size exclusion chromatography, both the fluid-phase mass-transfer coefficient k_f and the quantity D_L/u, are affected only very slightly by the interstitial velocity in the column as previously discussed in section 4.2.1. Therefore the left-hand side of eq. 5.3 gives a linear relation when plotted against the inverse interstitial velocity 1/u (Suzuki, 1974). The slope of this plot is related to the axial dispersion coefficient D_L while the y-intercept will depend on the intraparticle diffusivity D_e and the film mass transfer coefficient k_f. In the present study the method of moments was used to determine the inclusion porosity ϵ_p, the axial dispersion coefficient D_L and the intraparticle diffusion coefficient D_e, while the fluid-phase mass-transfer coefficient k_f was estimated by means of the correlation proposed by Ohashi (1981). This correlation has been used by other researchers (Liapis et al, 1989; Boyer and Hsu, 1992) and it appears to be the most suitable correlation to estimate k_f within the range of chromatographic operation (section 3.3.2).

Before the first moment analysis was carried out a correction was made to allow for the volume of the dead spaces, V_d in the system, according to the following equation (Suzuki, 1974):

$$\mu_1 = (\mu_1)_{measured} - \frac{V_d}{Q} \qquad (5.4)$$

where Q is the volumetric flow rate. The volume of the dead spaces V_d was calculated from the length and diameter of the connecting tubing, and was also determined from the retention time of blue dextran in a run in which the two column adaptors were pushed together inside the column in the absence of chromatography support.

In the second moment analysis only the peak dispersion produced by the non-equilibrium mechanisms occurring in the chromatographic bed itself should be taken into account for the evaluation of the transport parameters. According to chromatographic theory the total variance of a peak exiting a column is the sum of the variance from extracolumn effects and from the non-equilibrium interactions in the matrix:

$$\sigma_{Tot}^2 = \sigma_{extr}^2 + \sigma_{col}^2 \qquad (5.5)$$

The extracolumn contribution to peak dispersion was determined by means of the pulse response experiments referred in section 5.2.2.5. and the measurement of the second central moments of the

resulting peaks. Since the second central moment represents the variance of a chromatographic peak, the variance due to the non-equilibrium effects occurring inside the column was determined by subtracting the second central moment from the extracolumn effects from the second central moment representing the total variance of the peak according to the previous equation. The second central moments obtained in this manner were used in the evaluation of the axial dispersion coefficient and the intraparticle diffusivity.

The numerical integrations required to determine the first and second moments were carried out by means of the trapezoidal rule according to the following equations (Grushka et al, 1969):

$$\mu_1 = \frac{\sum_{all\ i} t_i y_i}{\sum_{all\ i} y_i} \tag{5.6}$$

$$\mu_2' = \frac{\sum_{all\ i} (t_i - \mu_1)^2 y_i}{\sum_{all\ i} y_i} \tag{5.7}$$

where y_i is the peak height "count" in the ith interval. The limits of integration were determined according to the criteria presented by Dyson (1990). A computer program was written in Pro-Matlab version 3.5i (The Mathworks, Inc) to carry out the determination of the limits of integration, to correct for the baseline drift and to conduct the numerical integrations and the evaluation of the normalised first absolute and second central moments of the chromatographic peaks. The program was run in a SUN SPARC station 1 (Sun Microsystems Europe, Inc).

5.3 Results and discussion.

To begin with it is important to stress that although some interactions might have occurred between the protein molecules injected as pulses and the foulant components deposited on the bed matrix, these interactions were negligible. The retention times of the outlet peaks resulting from the protein pulse injections were very similar before and after fouling the columns. Since the foulants retained by the bed occupied some of the void space, their presence occasioned slight variations in the protein retention times. If the interactions between the test protein and the foulants had been significant, then much larger variations in the retention times of the protein pulses would have been observed. In fact the retention times would have increased instead of slightly decreasing which was the general trend observed.

In section 5.2.2 the two sets of fouling experiments conducted in this study are described. In the first set carried out with the P-500 pumps (see section 5.2.1.4) a significant interference on the UV detector signal was produced by the foulants continuously leaking from the fouled column. This interference caused some distortion of the outlet peak profiles. In order to reduce the interference the columns in this set of experiments were subjected to very heavy washing, which probably removed an important amount of foulants from the bed. Due to the error resulting from the UV interference and to the possible error caused by the heavy washing the results from this set of experiments were unreliable and will not be presented. However, in some instances reference will be made to them in order to complement and enrich the discussion. The remaining part of this chapter will mainly deal with the results obtained with the second set of experiments described in section 5.2.2. This set of experiments was far more reliable and should therefore describe more accurately the effects of fouling on chromatographic performance.

Initially figs. 5.4 and 5.4a show the HETP vs u curves of cytochrome c and haemoglobin for the different fouling conditions to which the Sepharose 4 FF columns were subjected. Here it is important to stress that independently of the initial packing characteristics of a column the aim of the experiments resided in the evaluation of the changes effected by fouling on the column efficiency, this is in the HETP. Consequently the HETP vs u curve describing the initial efficiency of a column must be related to the corresponding curve describing its post-fouling condition, the interest is then focused on the difference between these two lines. From fig. 5.4 it can be observed that the difference between the initial and the final states of a particular column increased as the % of foulants injected to the column increased. This implies a direct relationship between the concentration or amount of foulants injected onto a column and the deterioration of its performance. It is also observed that the column which was more densely packed showed a slightly different behaviour (column fouled with a 10% foulant conc. stream, ε=0.3238, see table 5.1), its post-fouling curve shows a change in slope different to the general trend. This behaviour reflects the importance of bed permeability in the mechanisms of fouling as will be discussed later.

Unfortunately the assay results were not very meaningful and therefore it was not possible to carry out mass balances for the experiments. The results are presented in appendix B for completeness. The assays lack of accuracy and selectivity due to interferences caused by the many chemical species present in the fouling streams and column effluents. This is why in some cases the output exceeds the input (see appendix B). Although removal of most of the interfering chemical entities was considered in the protocols of each of the assays it seems that it may not have been sufficient. Consequently it was not possible to discriminate which of the main chemical groups, i.e. proteins, lipids, carbohydrates or cell debris, were more actively taking part in the fouling process. It is evident that more accurate and selective assays are required, as well as more strict assay protocols.

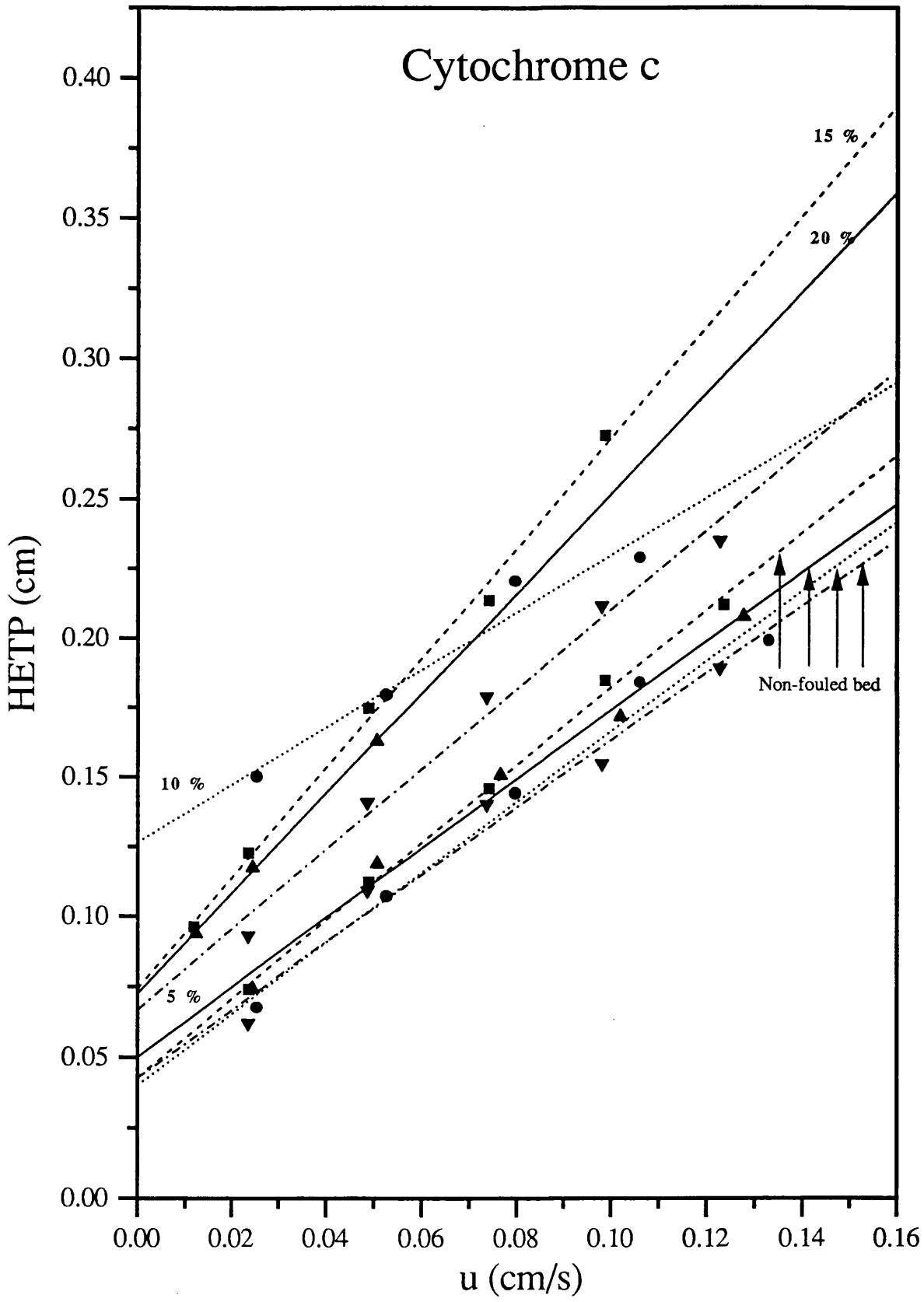

Fig. 5.4 Changes in plate height when Sepharose 4 FF columns were challenged with process streams containing different concentrations of foulants indicated as a percentage. The corresponding non-fouled and fouled HETP vs u curves for a particular column have been designated with the same symbol and line type to facilitate their association.

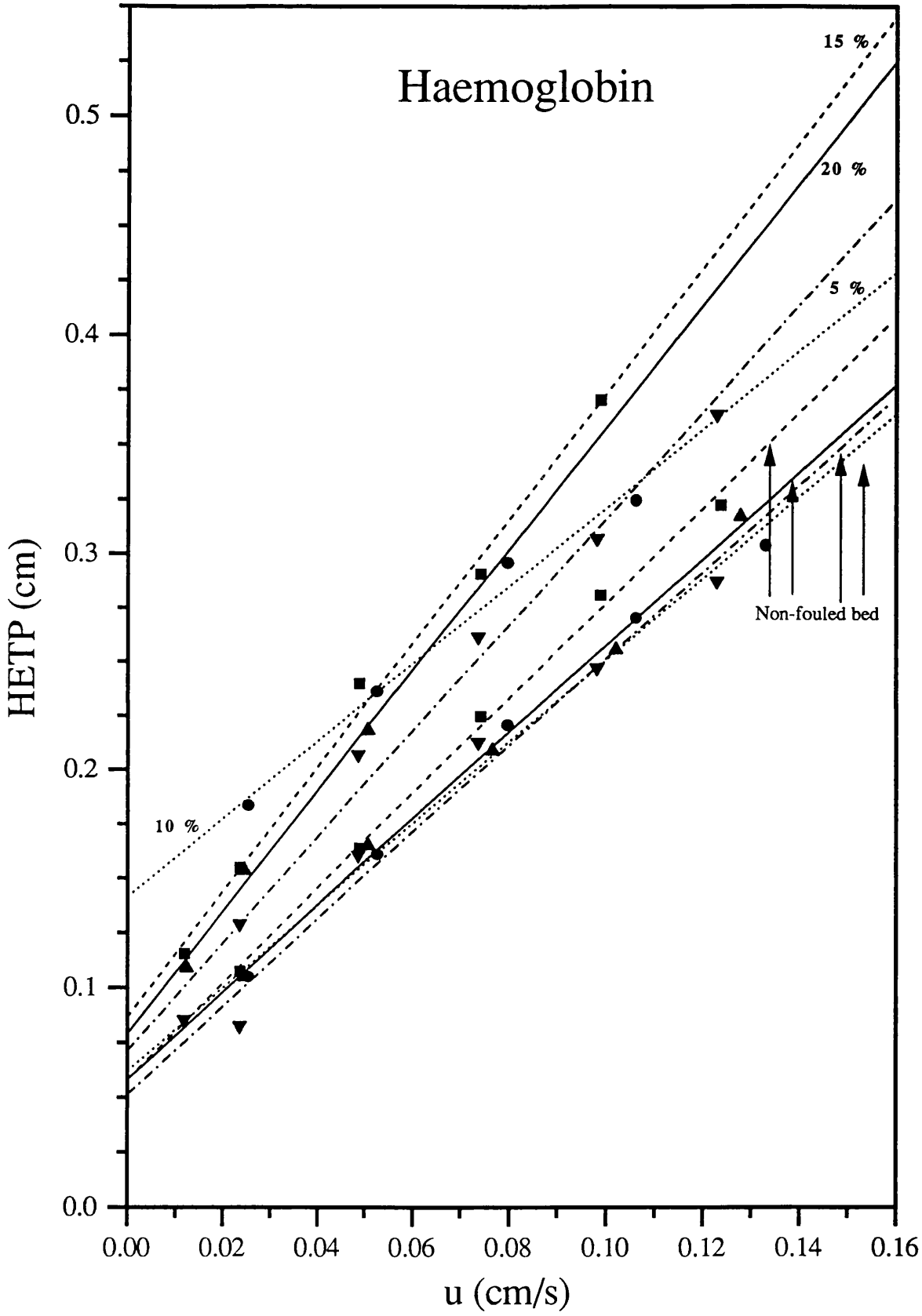

Fig. 5.4a Changes in plate height when Sepharose 4 FF columns were challenged with process streams containing different concentrations of foulants indicated as a percentage. The corresponding non-fouled and fouled HETP vs u curves for a particular column have been designated with the same symbol and line type to facilitate their association.

In particular a far more selective lipids assay is needed since this group of components is thought to participate greatly in matrix fouling.

Although it would have been convenient to distinguish which of the main chemical groups of foulants played a major role in the fouling process, in real separation processes a whole range of chemical species act together to foul and deteriorate a matrix, therefore in the present study all the fouling components have been considered as a bulk and no further attention has been paid to the chemical composition of the fouling stream and column effluent.

Table 5.1 summarizes the results obtained with the second set of fouling experiments. This table provides a global picture of the changes undergone by the equilibrium and transport parameters which in turn reflect the changes experienced by the matrix and bed structures. A single value of the bed void fraction ε is shown on this table. It seems that not much fouling material was trapped in the interstices between the matrix particles and therefore ε was not much affected. However, practical experience demonstrated that bed permeability was significantly reduced when a column was fouled since bed compression and channelling occurred in some of the failed experiments even at 10% foulant concentration. Also in some of the experiments of the first set (see section 5.2.2) a slight reduction in the bed void fraction was observed. These results suggest that although a relatively small amount of foulants was trapped in the interparticle space most must have been retained at a particular region of the bed, most likely the top, so as to be able to cause clogging and channelling. The foulants retained in the bed interparticle space are most likely to be cell debris which even in small quantities would significantly affect bed permeability.

The bed void fraction of a fresh gel bed is easily measured through the peak maximum of a pulse of blue dextran 2000. However, when a column was fouled the outlet blue dextran peak broadened and it became difficult to determine accurately the peak maximum. The spreading of the blue dextran peak was certainly caused by interactions between this molecule and the foulants deposited on the gel bed. In an attempt to measure the bed void fraction in a more precise manner, latex beads were employed to measure the interparticle void space of fresh Sepharose 4 FF beds, but the resulting bed void fraction was rather large ($\varepsilon \approx 0.41$) when compared with the values measured with blue dextran pulses ($\varepsilon \approx 0.33$). For this reason the bed void fraction was subsequently measured by means of the blue dextran pulses only. An improvement in the accuracy of this measurement, however, could be achieved if blue dextran 2000 is fractionated so that pulses of narrower molecular weight are injected. This would facilitate the determination of peak maxima under fouling conditions.

The efficacy of the cleaning-in-place (CIP) procedure is analyzed in fig. 5.5 and table 5.2. This figure shows the results obtained with the second CIP procedure described in section 5.2.2.6 in which the alkali contact time was of 7 hours. It can be observed that the column efficiency

Table 5.1 Transport and equilibrium parameters estimated by means of the method of moments with fresh and fouled Sepharose 4 FF columns.

Protein (MW)	Inclusion porosity [a] ε_p		D_t/u (cm)		Intraparticle diffusivity $D_e(cm^2/s)$		Foulant concentration. [b]	Column properties	
	Fresh bed	Fouled bed	Fresh bed	Fouled bed	Fresh bed	Fouled bed	%	Void fraction ε	Bed length L (cm)
	0.9368	0.9236	0.0174	0.0318	3.70×10^{-7}	3.16×10^{-7}	5	0.3508	4.95
Cytochrome c	0.9176	0.9162	0.0161	0.0645	3.38×10^{-7}	3.44×10^{-7}	10	0.3238	4.85
(12 400)	0.9368	0.9408	0.0221	0.0431	3.55×10^{-7}	2.78×10^{-7}	15	0.3482	5.05
	0.9315	0.9031	0.0243	0.0412	3.77×10^{-7}	2.67×10^{-7}	20	0.3372	4.90
	0.8658	0.8620	0.0160	0.0316	2.03×10^{-7}	1.69×10^{-7}	5	0.3508	4.95
Haemoglobin	0.8653	0.8453	0.0287	0.0703	2.21×10^{-7}	1.97×10^{-7}	10	0.3238	4.85
(64 000)	0.8669	0.8757	0.0287	0.0481	2.07×10^{-7}	1.74×10^{-7}	15	0.3482	5.05
	0.8671	0.8443	0.0312	0.0421	2.31×10^{-7}	1.54×10^{-7}	20	0.3372	4.90

[a] This parameter represents the fraction of intraparticle volume available to a molecule. It is equivalent to the equilibrium distribution coefficient K_{AV}.

[b] The % foulant concentration of the process stream injected to the columns is based on the concentration of the standard fouling stream which was produced with a constant intial concentration of Baker's yeast, i.e 600 g/l (see section 5.2.2.2).

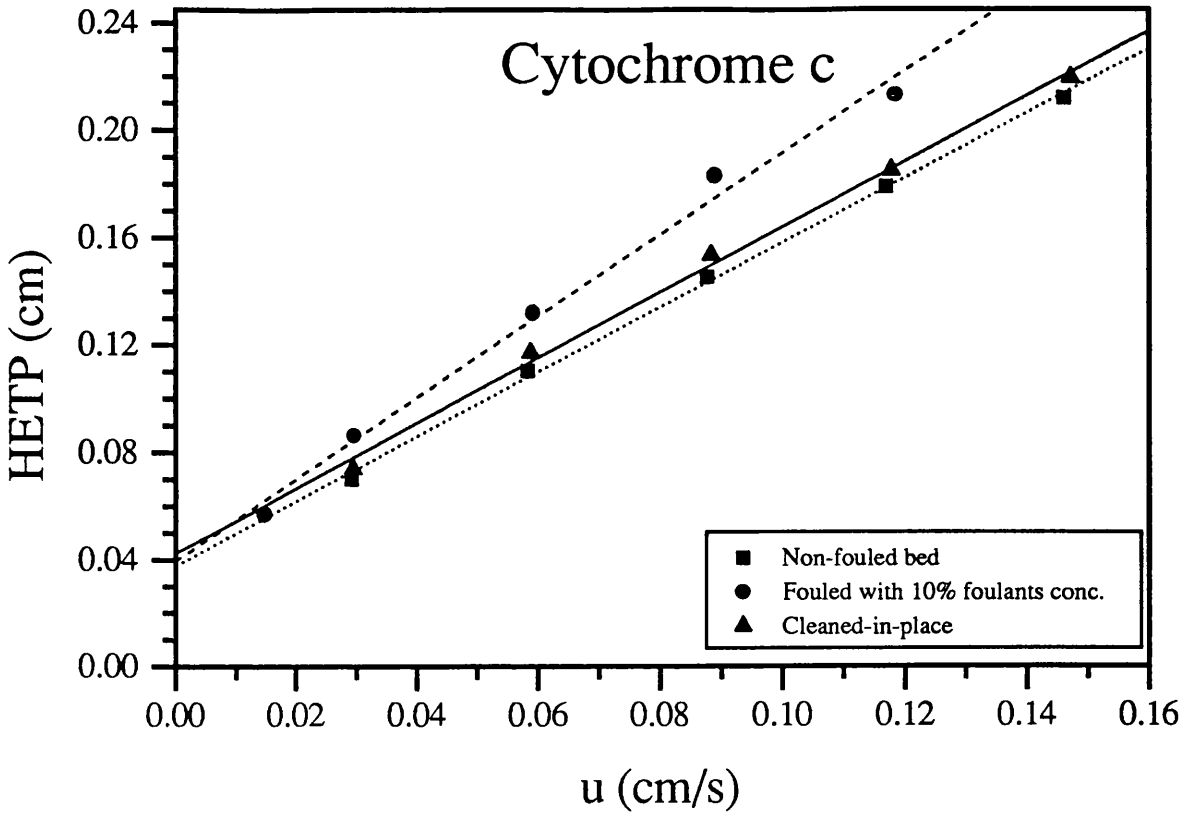

Fig. 5.5 Effectiveness of the cleaning-in-place (CIP) procedure on the efficiency of a Sepharose 4 FF bed fouled with a process stream containing 10% foulants.

Table 5.2 Comparison of the transport and equilibrium parameters determined by means of the method of moments for a Sepharose 4 FF column under non-fouled and fouled conditions and after the cleaning-in-place (CIP) procedure.

Cytochrome c			
Parameter	Fresh bed	Fouled bed	Cleaned-in-place bed
Inclusion porosity ε_p	0.8945	0.8871	0.8951
D_L/u (cm)	0.0191	0.0190	0.0205
Intraparticle diffusivity D_e (cm^2/s)	3.69×10^{-7}	3.31×10^{-7}	3.55×10^{-7}
Bed void fraction ε	0.2850	0.2810	0.2830

practically returned to its initial value, corresponding to the non-fouled bed condition, after the CIP procedure was carried out. This is clearly depicted by the closeness of the corresponding initial and post-CIP HETP vs u curves. In the first CIP experiment the NaOH contact time was only of 3 hours and proved not to be sufficient, this is why the contact time was increased to 7 hours in the second CIP experiment (see section 5.2.2.6). It appears that the cleaning procedure requires a longer than 7 hours contact time in order to be completely effective. It may be that the two CIP protocols used were not completely effective due to the smaller volumes and lower flow rates of 1 M NaOH utilised as compared with those proposed by the manufacturer (Pharmacia, 1992). However, the longer contact times used in these experiments should have compensated for the lower flow rates and volumes of 1 M NaOH employed.

From table 5.2 it can be observed that the bed almost recovered its initial performance after the CIP procedure was followed, only the intraparticle diffusivity was still lower with respect to its initial value. This is probably due to the presence of lipids and hydrophobic proteins which are not easily removed from the particle's interior by the CIP protocol followed in these experiments.

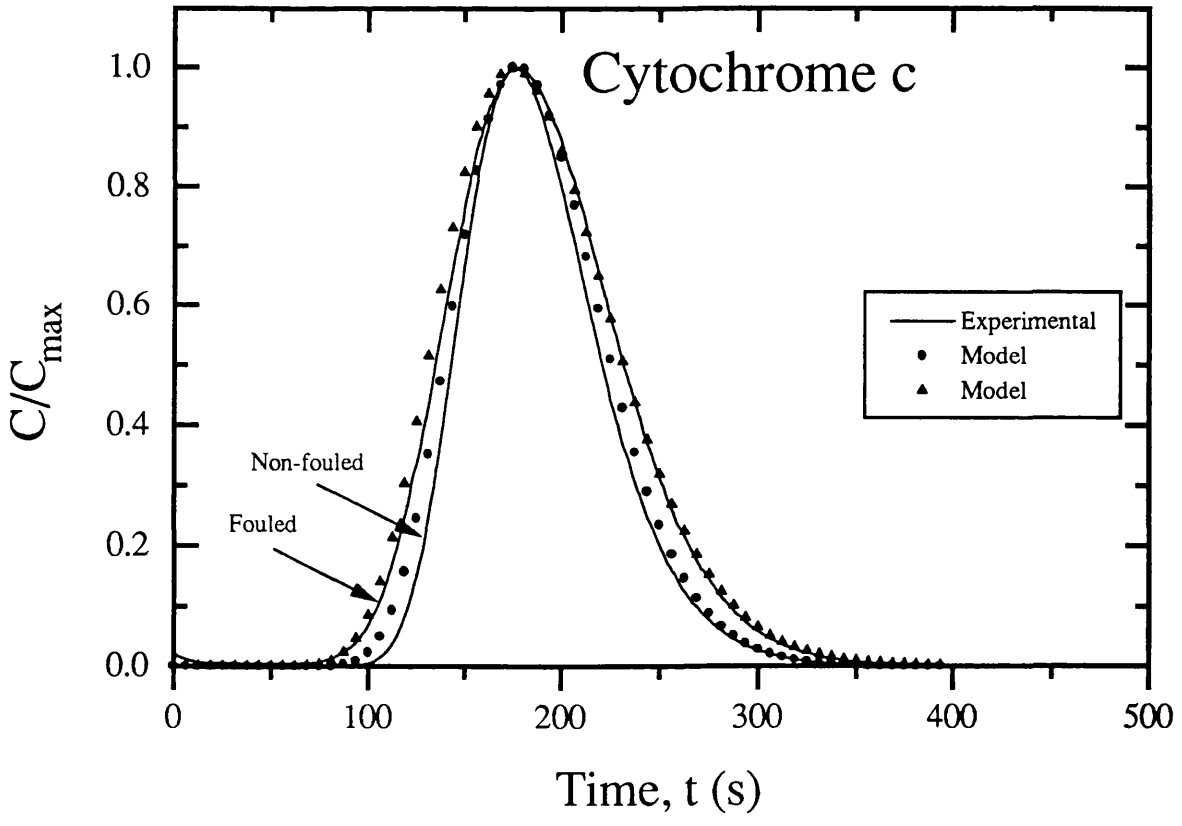

Fig. 5.6 Experimental and simulated peaks of cytochrome c, before and after fouling a Sepharose 4 FF column with a stream containing 15 % foulants concentration.

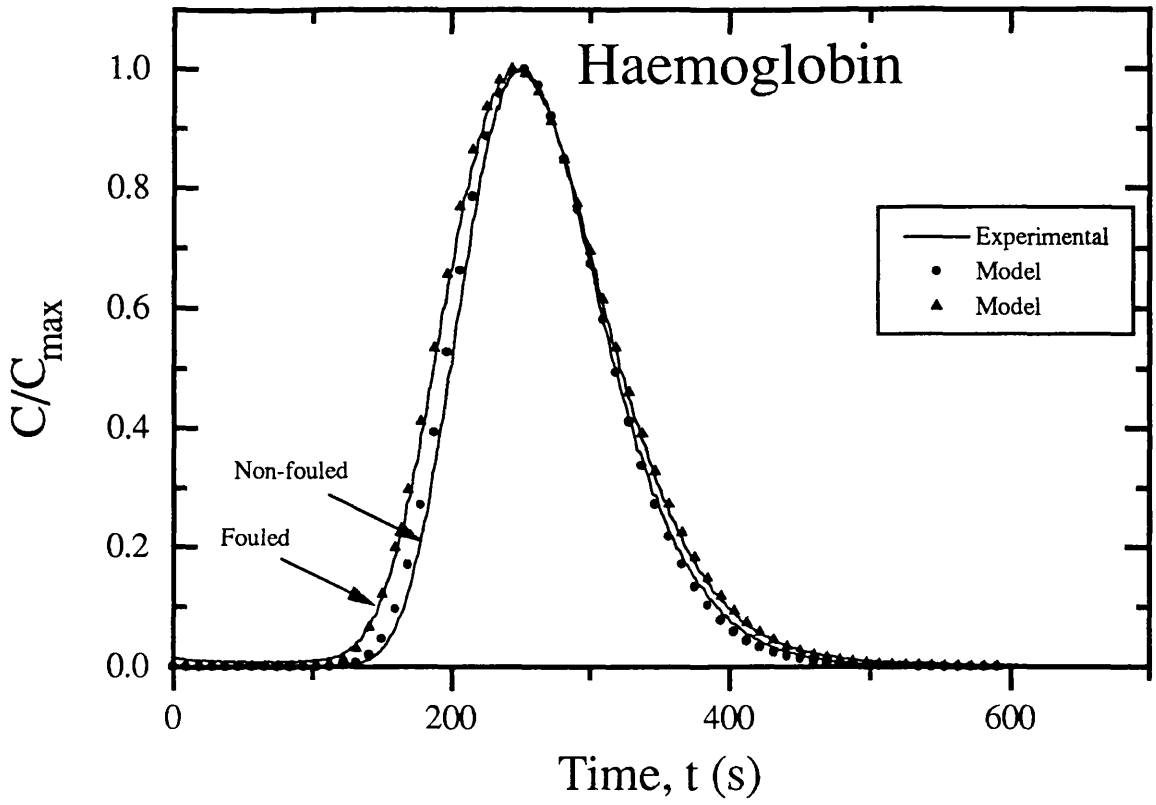

Fig. 5.7 Experimental and simulated peaks of haemoglobin, before and after fouling a Sepharose 4 FF column with a stream containing 5 % foulants concentration.

The validity of the parameters determined with the moments analysis was verified by comparing the experimental peaks under the non-fouled and the fouled condition with the peaks generated with the general rate model of size exclusion chromatography (see section 3.2.1). (In fig. 5.1 it can be seen that the Sepharose 4 FF matrix has a narrow particle size distribution and therefore the general rate model could be used to simulate column performance).

Figs. 5.6 and 5.7 show that the model simulations matched the experimental peaks very well. These simulations give confidence in the accuracy and reliability of the parameter values determined by means of the method of moments.

In the following sections the changes experienced by each of the parameters characterizing column performance will be analyzed in order to discriminate in a more precise manner how fouling alters the bed and matrix structure and therefore to define which are the major effects to consider.

5.3.1 Analysis of the equilibrium distribution coefficient.

An example of the first moment analysis of the protein outlet peaks is presented in fig. 5.8. The slope of the line corresponding to the cytochrome c is steeper than that for the haemoglobin. This

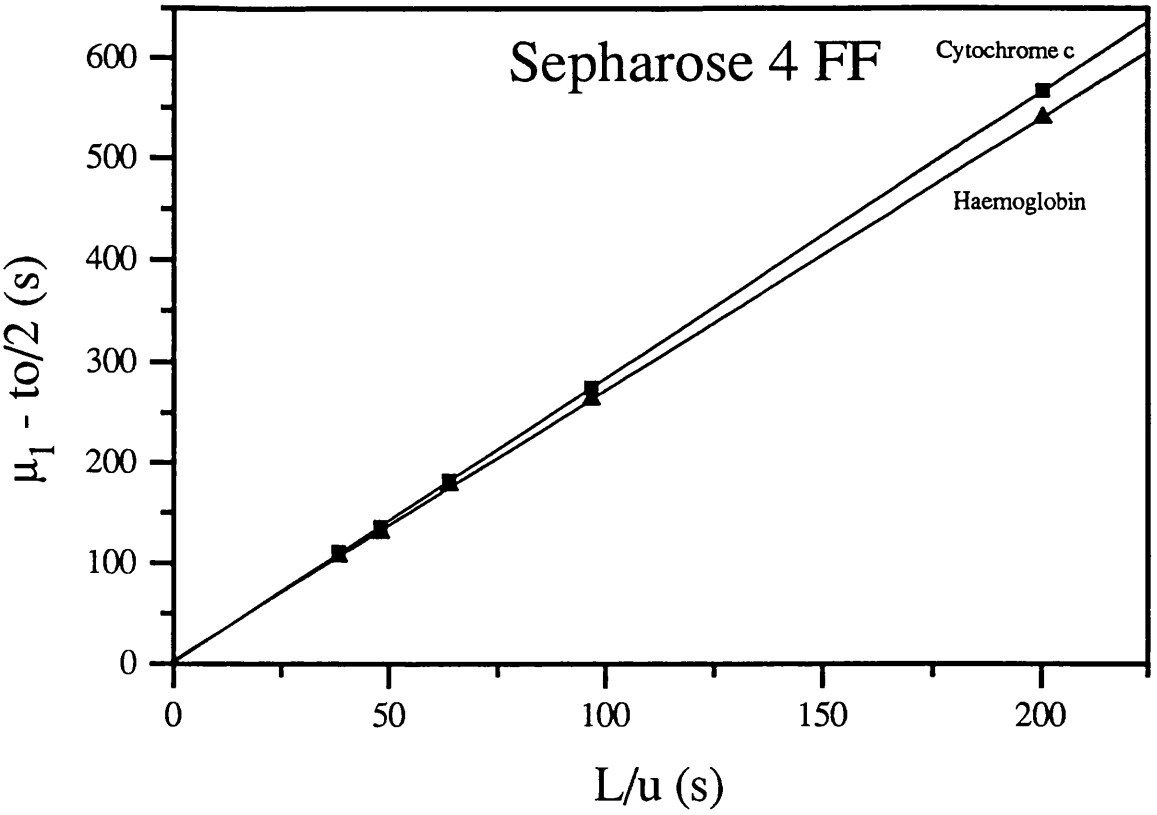

Fig. 5.8 First moment analysis of outlet peaks from protein pulses on a non-fouled Sepharose 4 FF column.

indicates the larger intraparticle space available to the smaller cytochrome c molecules reflected in table 5.3 by the inclusion porosity of cytochrome c being larger than that of haemoglobin.

The protein inclusion porosities obtained with the Sepharose 4 FF were larger (see table 5.3) than those obtained with proteins of similar molecular size (ribonuclease A and ovalbumin) with the Sepharose 6B and Cl-6B columns (see table 4.4) in the compression studies. This is in agreement with the difference in agarose concentration between the Sepharose 4 FF (4%) and the Sepharose 6B and Cl-6B (6%) gels. Although highly cross-linked the 4 FF gel possesses wider pores and greater porosity due to its lower agarose content. This is why the volume available to molecules of similar size is larger in this gel.

The changes effected by fouling on the equilibrium distribution coefficient ε_p of the cytochrome c and haemoglobin are shown graphically in fig. 5.9. As the concentration and hence the amount of foulants injected onto the Sepharose 4 FF columns increased, the value of ε_p linearly diminished. According to this figure the variations in the equilibrium distribution coefficient ε_p when a Sepharose 4 FF column is fouled can be predicted by means of the following relationship:

$$\epsilon_p' = \epsilon_p + b*(\%\ foulants) \qquad (5.8)$$

where ε_p' is the equilibrium distribution coefficient under fouling conditions, and the slope

Table 5.3 Equilibrium distribution coefficient or inclusion porosity of tested proteins as determined in Sepharose 4 FF columns under non-fouled and fouled conditions.

Protein (MW)	Inclusion porosity ε_p		Foulant conc. [a] %	Bed properties	
	Fresh bed	Fouled bed		Void fraction ε	Length L (cm)
Cytochrome c (12 400)	0.9368	0.9236	5	0.3508	4.95
	0.9176	0.9162	10	0.3238	4.85
	0.9368	0.9408	15	0.3482	5.05
	0.9315	0.9031	20	0.3372	4.90
Haemoglobin (64 000)	0.8658	0.8620	5	0.3508	4.95
	0.8653	0.8453	10	0.3238	4.85
	0.8669	0.8757	15	0.3482	5.05
	0.8671	0.8443	20	0.3372	4.90

a The % foulant concentration of the process stream injected to the columns is based on the concentration of the disk stack centrifuge supernatant which was produced with a constant concentration of Baker's yeast, i.e. 600 g/l (see section 5.2.2.1).

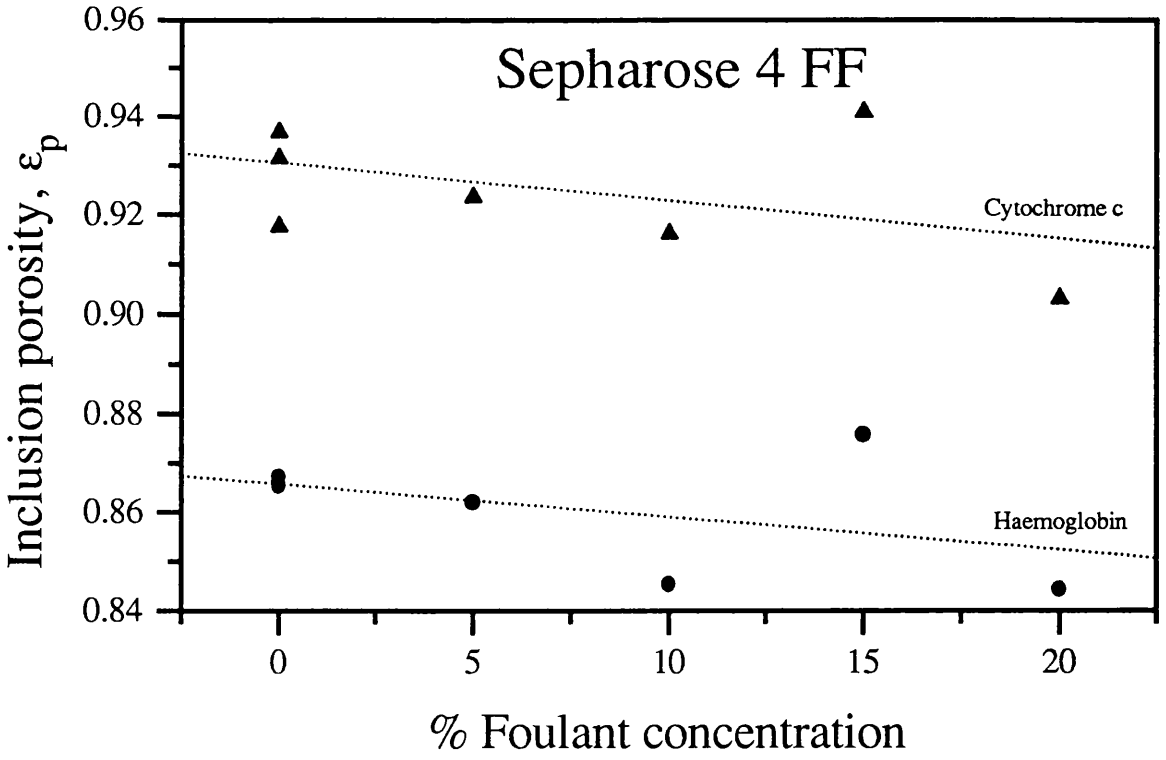

Fig. 5.9 Effect of foulant concentration in the stream injected onto the chromatographic column, on the inclusion porosity of cytochrome c and haemoglobin. The lines represent the least-squares linear fitting of the experimental points.

b= -0.00077 for cytochrome c and b= -0.00067 for haemoglobin.

The decrease in ε_p indicates the reduction in the intraparticle space available to the diffusing molecules which results from the deposition of foulants in the interior of the matrix particles. Since the changes in ε_p were slight it can be deduced that foulant deposition inside the matrix particles was very moderate.

The slope of the two lines in fig. 5.9 is very similar. This means that foulant deposition affected in very much the same degree the equilibrium distribution of the two molecules tested. This is a reasonable result since the size of the cytochrome c (MW=12 400) was not much smaller than the size of the haemoglobin molecule (MW= 64 000). A set of molecules of a wide range of molecular weights could be tested in order to assess the effects of foulant deposition on the inclusion porosity in relation to molecular size.

5.3.2 Analysis of the axial dispersion coefficient.

An example of the second moment analysis of the protein outlet peaks is shown in fig. 5.10. The slope of the lines is proportional to the axial dispersion of the column while the y-intercept depends inversely on the intraparticle diffusivity and the fluid film mass transfer. As the outlet peaks became broader due to the presence of foulants in the bed the lines became steeper and the y-intercept increased as can be seen in fig. 5.10. The lines corresponding to the haemoglobin for both the fresh and the fouled condition presented slightly steeper slopes than those corresponding to the cytochrome c. Accordingly the experimentally estimated values of D_L/u for the haemoglobin were in general slightly larger than those estimated from the cytochrome c peaks, as shown in table 5.4.

As previously mentioned under the range of operation of modern liquid chromatography the dispersion Péclet number ($Pe_L = ud_p/D_L$) is only very slightly affected by the interstitial velocity u in the column (see fig. 3.1), therefore the ratio D_L/u can be considered to be constant.

In table 5.4 the experimentally estimated values of D_L/u are compared with values of D_L/u evaluated by means of the correlations of Athalye et al (1992) and Hejtmánek et al (1993). These correlations appeared to be the most suitable to be used within the range of operation of importance to chromatographic practice (see section 3.3.1). It can be observed that the experimental values of D_L/u for the fresh bed condition lay in some cases very close to the values predicted with the correlation of Athalye et al (1992), while in other cases they were very close to the predictions of Hejtmánek et al (1993).

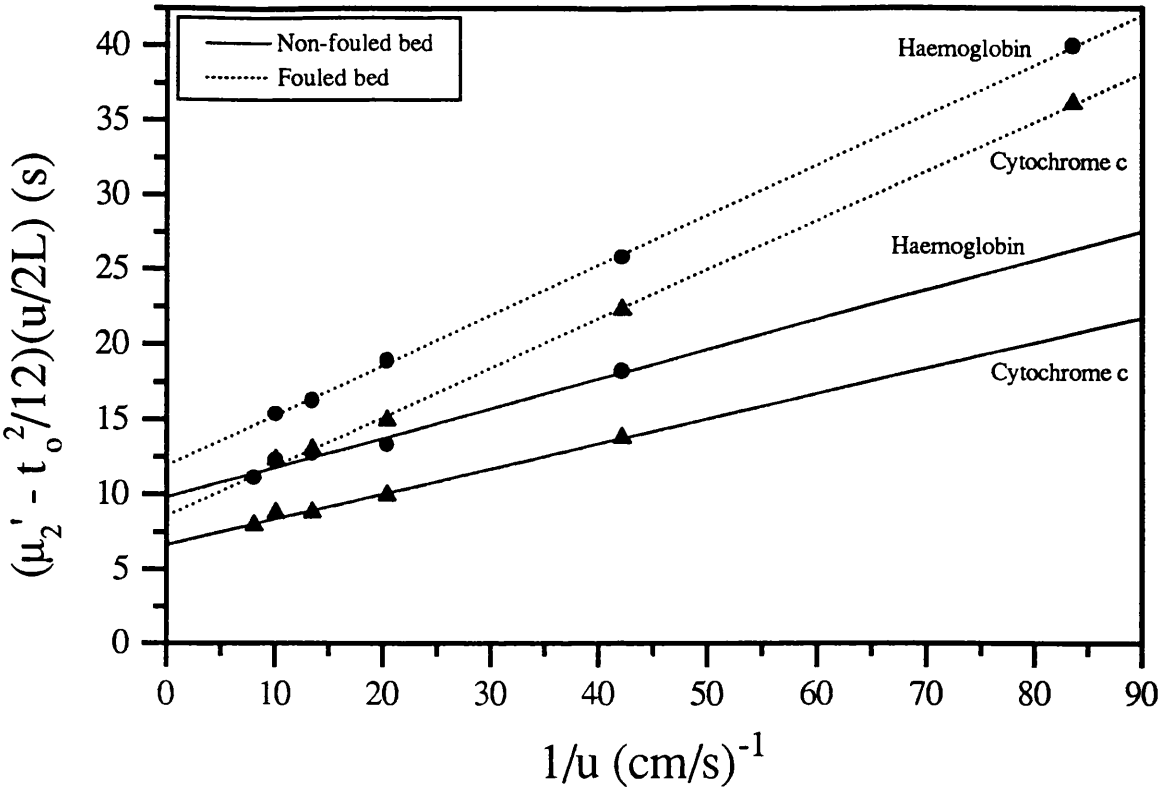

Fig. 5.10 Second moment analysis of protein pulses on a Sepharose 4 FF column before and after being fouled with a process stream containing 15 % foulants concentration.

Table 5.4 Comparison of experimentally estimated values of the axial dispersion coefficient in non-fouled and fouled Sepharose 4 FF with correlated values.

Protein (MW)	Foulant conc. [a] %	Experimental D_L/u (cm)		Correlated D_L/u (cm)		Bed properties	
		Fresh bed	Fouled bed	Athalye et al (1992)	Hejtmánek et al (1993)	void fraction ε	length L (cm)
Cytochrome c (12 400)	5	0.0174	0.0318	0.0238	0.0175	0.3508	4.95
	10	0.0161	0.0645	0.0237	0.0176	0.3238	4.85
	15	0.0221	0.0431	0.0238	0.0175	0.3482	5.05
	20	0.0243	0.0412	0.0237	0.0176	0.3372	4.90
Haemoglobin (64 000)	5	0.0160	0.0316	0.0259	0.0182	0.3508	4.95
	10	0.0287	0.0703	0.0257	0.0183	0.3238	4.85
	15	0.0287	0.0481	0.0259	0.0182	0.3482	5.05
	20	0.0312	0.0421	0.0258	0.0183	0.3372	4.90

[a] The % foulant concentration of the process stream injected to the columns is based on the concentration of the disk stack centrifuge supernatant stream which was produced with a constant concentration of Baker's yeast, i.e. 600 g/l (see section 5.2.2.1).

The pulse experiments were carried out in the creeping flow region within the Reynolds number range, 0.0070<Re<0.0367, while the reduced velocity (ReSc= $d_p u\varepsilon/D_m$) range was 67<ReSc<351 for cytochrome c and 111<ReSc<579 for haemoglobin. Since the correlation developed by Athalye et al (1992) is only valid within the range 7<ReSc<320, the correlation derived by Hejtmánek et al (1993) which is valid in the wider range 0.385<ReSc<580 (see section 3.3.1) appears to apply better to the present set of fouling experiments. In general the experimental values of D_L/u were slightly larger than the values predicted by the correlation of Hejtmánek et al (1993). Extracolumn band spreading was taken into account in the estimation of the parameters so it is not the cause of this slight discrepancy, and it is more likely to be the result of slight inhomogeneities in the initial structure of the fresh Sepharose 4 FF columns. Since the interest of this study is focused on the changes on performance produced by matrix fouling, the initial state of the fresh beds should not affect the results and the analysis.

Table 5.4 also shows the values of D_L/u obtained after the Sepharose 4 FF columns were fouled. It can be seen that in all cases a marked increase in the D_L/u values was experienced. Since the axial dispersion coefficient is very dependent on the bed structure it is clear that fouling of the columns caused modifications in the arrangement of the matrix beads and/or in the bed porosity which in turn altered the flow pattern producing greater dispersion.

Fig 5.11 depicts the changes undergone by the ratio D_L/u as the foulant concentration of the process stream injected onto the Sepharose columns was increased. It is observed that the axial dispersion increased as the amount of foulants injected increased. As the foulant concentration increases it is probable that a larger amount of fouling components (in particular cell debris) must have been retained or trapped in the bed interparticle space modifying in a more significant way its structure as above mentioned.

The values of D_L/u corresponding to 10% foulant concentration in fig. 5.11 are particularly higher. This was most certainly caused by the higher initial packing density of the column (ε=0.3238, see table 5.4). This column was the only one in this set packed following the first bed packing protocol outlined in section 5.2.2.2. The smaller permeability of this bed made it more susceptible to the perturbing action of the foulant components injected.

It seems that the dependence between D_L/u and the concentration of foulants could be expressed by the following relationship:

$$\frac{D_L'}{u} = \frac{D_L}{u} + b*(\%\ foulants) \qquad (5.9)$$

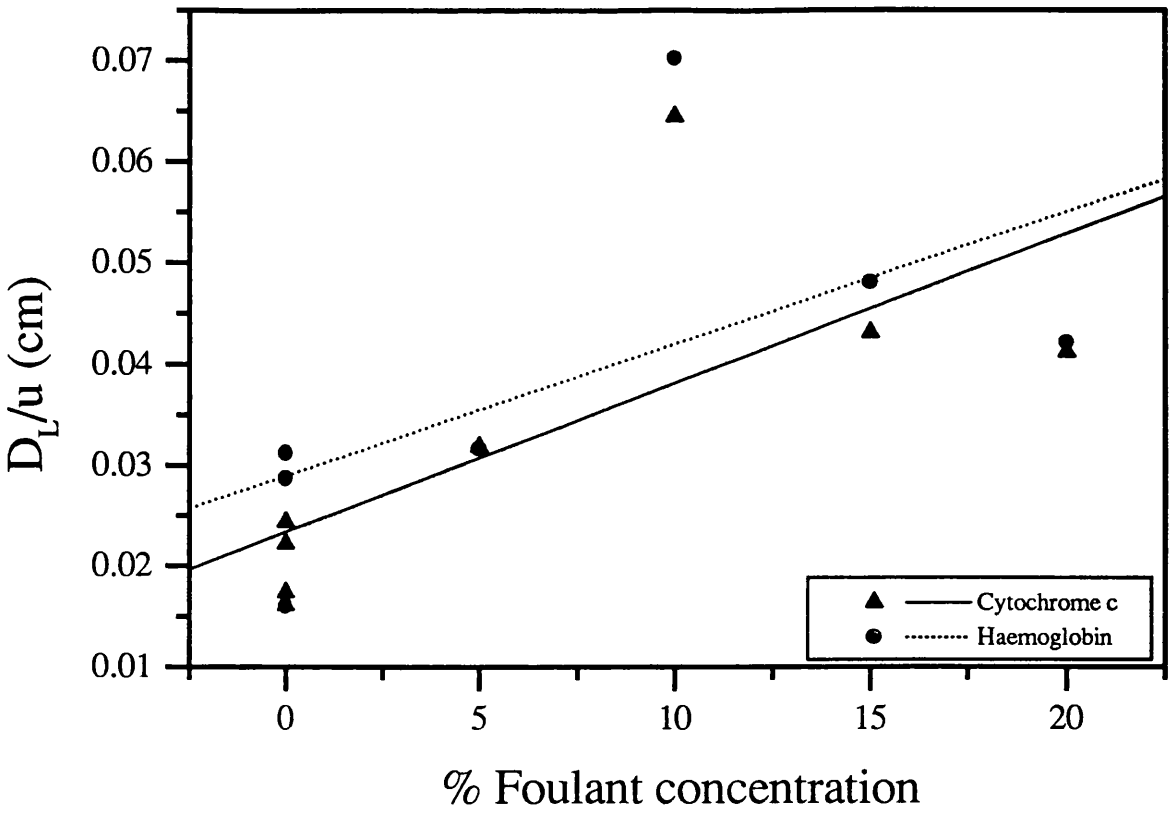

Fig. 5.11 Effect of foulant concentration on the axial dispersion coefficient D_L, when a process stream of varying foulant concentration is loaded onto a Sepharose 4 FF bed. The lines represent the least-squares linear fitting of the experimental points.

where D_L' is the axial dispersion coefficient under fouling conditions and the slope b= 0.0015 cm for cytochrome c and b= 0.0013 cm for haemoglobin.

However, it is apparent from fig. 5.11 that more experimental work is needed in order to verify the linearity of this dependence and to clearly establish the influence of initial bed porosity on the fouling process.

5.3.3 Analysis of the intraparticle diffusion coefficient.

The experimentally estimated values of protein intraparticle diffusivity D_e at the different levels of fouling carried out in this study are summarized in table 5.5.

The corresponding correlated values of D_e for the proteins studied are also shown. It is observed that the intraparticle diffusivity of cytochrome c was overestimated by the model proposed by Boyer and Hsu (1992) while the intraparticle diffusivity of the haemoglobin molecule was underestimated by the same model (the correlated values of D_e should be compared only with the experimental values obtained under non-fouled conditions). Although the model of Boyer and Hsu

(1992) was developed for agarose matrices, it does not take into account the influence of cross-linking the agarose fibres. Sepharose 4 FF is a highly cross-linked support (see section 5.2.1.1), and the presence of the linking chemical compound may have affected sterically the diffusion of the protein molecules.

Table 5.5 Intraparticle diffusivities of the tested proteins in the Sepharose 4 FF matrix under non-fouled and fouled conditions. Comparison with correlated values.

Protein (MW)	Foulant conc. [a] %	Experimental D_e (cm^2/s) (D_e/D_m) [b]		Predicted D_e [c] (cm^2/s) (D_e/D_m)	Bed properties	
		Fresh bed	Fouled bed		Void fraction ε	Length L (cm)
Cytochrome c (12 400)	5	3.70×10^{-7} (0.3248)	3.16×10^{-7} (0.2773)	4.5×10^{-7} (0.3943)	0.3508	4.95
	10	3.38×10^{-7} (0.2965)	3.44×10^{-7} (0.3018)		0.3238	4.85
	15	3.55×10^{-7} (0.3116)	2.78×10^{-7} (0.2440)		0.3482	5.05
	20	3.77×10^{-7} (0.3305)	2.67×10^{-7} (0.2339)		0.3372	4.90
Haemoglobin (64 000)	5	2.03×10^{-7} (0.2945)	1.69×10^{-7} (0.2456)	1.75×10^{-7} (0.2538)	0.3508	4.95
	10	2.21×10^{-7} (0.3211)	1.97×10^{-7} (0.2849)		0.3238	4.85
	15	2.07×10^{-7} (0.2995)	1.74×10^{-7} (0.2518)		0.3482	5.05
	20	2.31×10^{-7} (0.3346)	1.54×10^{-7} (0.2228)		0.3372	4.90

[a] The % foulant concentration of the process stream injected to the columns is based on the concentration of the disk stack centrifuge supernatant which was produced with a constant concentration of Baker's yeast, i.e. 600 g/l (see section 5.2.2.1).

[b] The free diffusivities D_m used in the calculations were experimental values reported in the literature: for cytochrome c $D_m = 11.4 \times 10^{-7}$ cm^2/s (Young et al, 1980), for haemoglobin $D_m = 6.9 \times 10^{-7}$ cm^2/s (Jones and Johnson, 1978).

[c] Predictions were carried out by means of the correlation proposed by Boyer and Hsu (1992), see section 3.3.3.

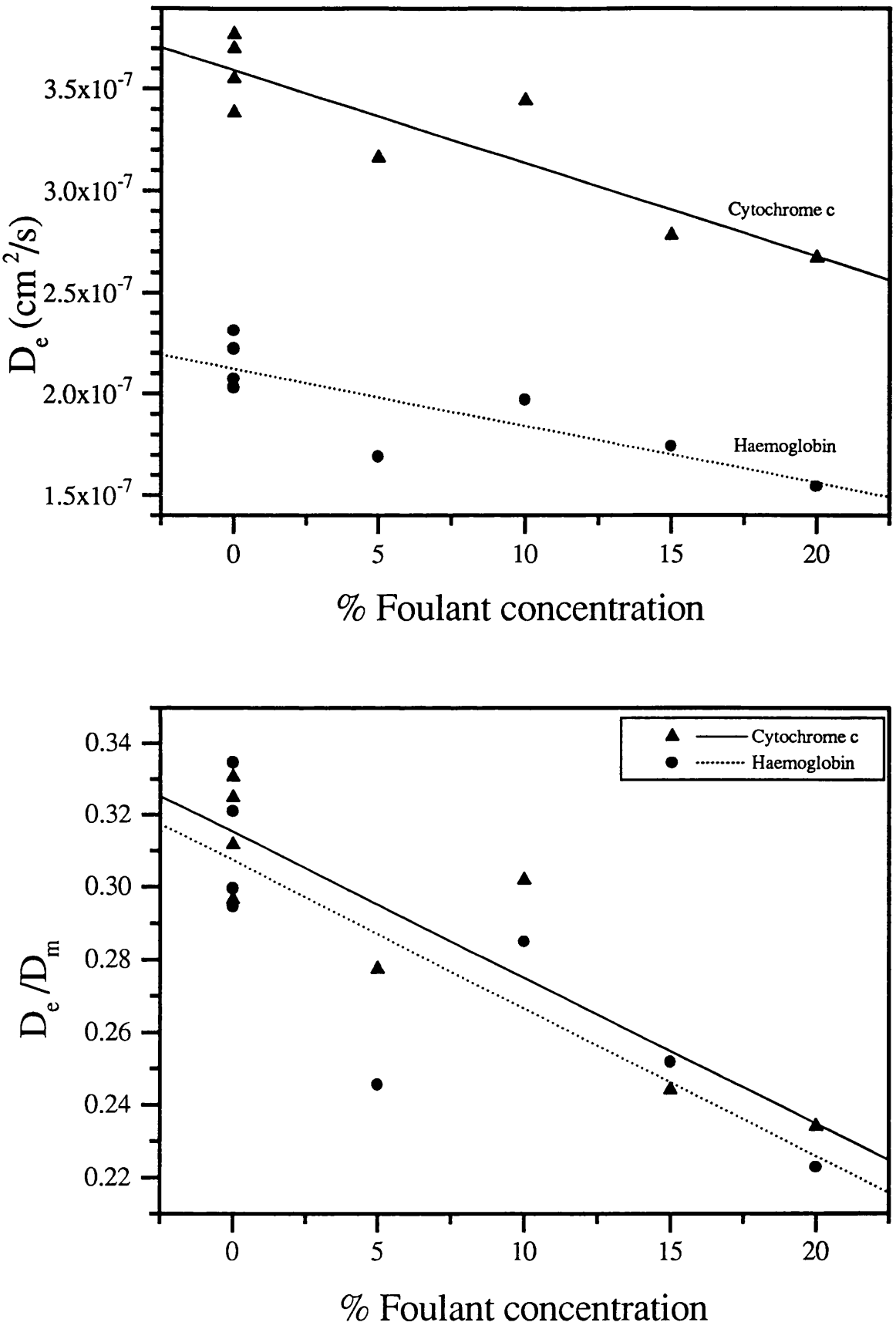

Fig. 5.12 Effect of foulant concentration on protein intraparticle diffusivity D_e, when a process stream of varying foulant concentration is loaded onto a Sepharose 4 FF bed. The lines represent the least-squares linear fitting of the experimental points.

The changes experienced by the intraparticle diffusion coefficient when the concentration of foulants in the injected stream increased are presented in fig. 5.12. As can be seen the intraparticle diffusivity of the proteins studied decreased linearly as the amount of foulants injected to the columns increased. This is in agreement with the slight reduction in the inclusion porosity of these proteins observed as the level of fouling increased (see section 5.3.1). A similar trend was observed with the results obtained from the first set of experiments (see section 5.2.2). Accordingly the dependence of D_e on the concentration of the fouling stream can be expressed as:

$$D_e' = D_e + b*(\%\ foulants) \qquad (5.10)$$

where D_e' is the intraparticle diffusivity under fouling conditions and the slope b= -4.57×10^{-9} cm^2/s for cytochrome c and b= -2.80×10^{-9} cm^2/s for haemoglobin.

The presence of the fouling components in the matrix inner space affected to a slightly greater extent the diffusion of the cytochrome c molecules as shown on the top graph of fig. 5.12, but the restricted diffusion D_e/D_m of both molecules decreased at the same rate as can be observed on the bottom graph of fig. 5.12.

In the light of the present experiments it appears that the intraparticle diffusion of proteins decreases linearly with the amount of fouling components injected onto a columns, however more experiments are needed to fully prove this relationship.

5.4 Further discussion and conclusions.

Due to its easiness of use and to the fact that no sophisticated pieces of equipment are required for its implementation, the method of moments has been employed in the present study. In spite of the errors involved in the estimation of equilibrium and transport parameters by means of this method, it is still widely used in the field of chromatography (Ching et al, 1989; Boyer and Hsu, 1992; Ming and Howell, 1993).

The present study illustrates the usefulness of the method of moments in the analysis of the effects of fouling on chromatographic matrices. Although not very accurate this method has proved to be very useful in determining the major fouling effects on the equilibrium and transport parameters and in showing the trends followed by these parameters as the degree of matrix fouling increased.

As an alternative to the method of moments for the estimation of the transport and equilibrium parameters, the SEC model could be used to fit the experimental outlet peaks. This procedure would produce more reliable estimations since it would not only make use of all the experimental points but would not involve the truncation errors inherent to the method of moments.

Foulant deposition in the interior of the matrix particles slightly affects the volume available for the diffusion of the protein molecules, that is their equilibrium distribution coefficient ε_p. As the amount of fouling components injected onto a column of Sepharose 4 FF increased ε_p decreased linearly. Further experiments employing a set of protein molecules with a wide range of molecular weights should be carried out in order to assess the effect of intraparticle foulant deposition on the inclusion porosity ε_p in relation to the molecular size.

As the foulant concentration in the stream injected onto a column increases the bed structure is increasingly modified as a result of the larger amount of fouling components being trapped in the interparticle space and/or as a result of rearrangements produced by the passage and the presence of the foulants themselves. Consequently a directly proportional increase in the axial dispersion is observed. The bed void fraction appears to influence the fouling process. It seems that the denser the column packing the more susceptible it is to structural modifications.

The intraparticle diffusivity of the two proteins studied decreased linearly as the concentration of the fouling stream increased. It seems that a greater steric hindrance was imposed on the diffusing protein molecules by the increasing amount of foulants deposited in the particles interior space. Since the intraparticle diffusivity is in general the rate limiting step in SEC separations, even small reductions in the value of this parameter have a significant effect on peak spreading and therefore on column performance. However, in the light of the present study it appears that depending on the bed density (bed void fraction), fouling could have a large effect on the bed structure and therefore on axial dispersion and peak spreading, which could even surpass the effects on intraparticle diffusion.

Possible changes occurring in the fluid film mass transfer have not been considered in this study. This parameter was estimated by means of the correlation developed by Ohashi et al (1981) and it was assumed to be constant under both non-fouled and fouled conditions. It is very unlikely that this parameter is the rate limiting step under chromatographic conditions (Gangwal et al, 1978), however fouling must have an effect on it by blocking some of the pores of the matrix particles. This effect must be small. Bed compression and channelling would occur before a significant number of pores would be blocked.

The results showed that there is a direct relationship between the concentration and total mass of foulants in the column input stream and the column performance (transport parameters). Although the observed trends in the change of the parameters as the degree of fouling increased appeared to be linear, this behaviour is not fully confirmed and the results of this study should be considered as preliminary. Further experimental work is needed in order to corroborate the observed trends and fully verify the linear relationship between the transport and equilibrium parameters and the degree of matrix fouling. These relationships constitute the basis on which the

performance of chromatographic columns operating under fouling conditions could be predicted. The parameters estimated in this study have been used to simulate chromatographic peaks from fresh and fouled beds. The experimental peaks were matched very well by the model simulations (see figs. 5.6 and 5.7), corroborating the validity of the parameters and the value of the above mentioned relationships in the prediction of chromatographic performance under very realistic conditions.

In real practice fouling is a time dependent process. Chromatographic matrices get fouled as samples containing certain amount of foulants are continuously injected onto a column. Although the time variable has not been considered in the present study the approach followed could still be useful for predicting column performance. If the total amount of foulants contained in a process stream is measured and then multiplied by the number of samples injected onto a column during a certain period of time, then the total amount of foulants actually entering a column is obtained. Assuming the effects produced by a certain amount of foulants is equal whether they are injected onto a column in a single sample or as a series of samples would allow the use of similar relationships to those derived in this study in the prediction of column performance. Clearly this assumption requires experimental verification.

As previously mentioned further work is required in order to fully characterize the effects of fouling on column performance. Future research should study the influence of bed void fraction (bed permeability), bed length and the injection flow rate of the fouling stream on the performance of columns operated under fouling conditions. Studies involving the time variable are necessary in order to evaluate the rate at which the foulants build up inside the bed and the matrix particles. Also more work is needed in order to characterize with greater accuracy the chemical composition of biological streams. The identification of the major fouling species will set the basis for more adequate and rational sample pretreatment protocols which will avoid excessive and costly pretreatment.

Finally it should be mentioned that the approach followed in this study could be used to evaluate the possibility of pushing a chromatographic step up in the downstream sequence. Determining how large an amount of foulants a particular chromatographic column could withstand, before losing its resolving power, is required to define the number of steps needed in a separation sequence and the position of the chromatographic step within it.

CHAPTER 6

CONCLUSIONS AND FUTURE WORK

6.1 Introduction.

In recent years there has been a rapidly increasing demand for highly purified proteins for use in both diagnostic and therapeutic applications. In the production of such highly purified proteins, chromatography plays a very important role. In particular in the case of therapeutic proteins, this unit operation has proved to be the only separation process capable of achieving the required high degree of purification demanded in their production. Licensing authorities require at least one chromatographic step to be included in the purification schemes of these biomolecules.
Despite the great relevance of chromatography in the bioprocess industry, its design, operation and scale-up is far from being optimum and a series of problems remain to be studied and solved. The present thesis has dealt with some of the problems related to the compressibility of the chromatographic matrices generally used in the purification of biomolecules as well as with problems arising due to the susceptibility of these matrices to fouling.
This chapter summarizes the contributions made by this work towards the study and the analysis of matrix compression and fouling and towards the improvement of the design, operation and scale-up of chromatographic separation steps. It also points out future developments that will further advance the understanding of these topics.

6.2 Column hydrodynamics and matrix compression.

Knowledge of the flow rate/pressure drop characteristics of compressible matrices is necessary for the design, operation, scale-up and optimisation of chromatographic separations employing this type of support. Therefore accurate prediction of the hydrodynamic behaviour of compressible packed beds is desirable. Among the models reported in the literature for the prediction of flow rate-pressure drop curves of compressible packed beds, those developed by Verhoff and Furjanic (1983) and by Davies (1989) appear to be the most relevant and complete. In the present work the predictive capabilities of these models were tested and verified against experimental data obtained with two soft chromatographic matrices, Sepharose 6B and CL-6B. It was shown that both models

are capable of predicting the maximum flow rate that can be achieved with packed columns of different dimensions, the model of Davies (1989) agreeing much more closely with the experimental flow rate-pressure drop curves. Accordingly both models are useful in the determination of the operating conditions and in the scaling-up of chromatographic columns packed with compressible matrices. However, further testing of these models employing different compressible matrices and larger column dimensions than those used in this study are necessary in order to fully prove their generality and applicability. Although the model of Verhoff and Furjanic (1983) is not as accurate as that of Davies (1989), the inclusion of a compressibility relationship as part of this model allows for the prediction of bed void fraction, a parameter which significantly affects the flow geometry and solute transport.

In order to carry out the model verifications, model parameters related to the matrix characteristics were estimated by means of methods generally used in soil mechanics. A novel procedure involving the oedometer-type cell has been developed in this work (see section 2.3.2.5). This method has been used to estimate friction coefficients between gel matrices and column walls, and provides a more accurate estimation than that obtained with conventional compression cells (section 2.3.2.5.). The small frictional forces involved in these systems made the former method more suitable for this evaluation. Refinements in the design and construction of the oedometer-type cell will lead to improvements in the accuracy of this parameter estimation technique.

The models tested in the present work are approximate, and the development of more accurate models would require a more precise description of the changes in permeability and/or interparticle and intraparticle space down a compressed bed. This would also result in the derivation of a more accurate compressibility relationship that would enable a better prediction of bed void fraction. Although the permeability of rigid porous materials has been long studied, the dependence of permeability on the degree of compression of soft porous materials has only very recently been approached (Kataja et al, 1992; Jönsson and Jönsson, 1992). These studies have adapted the permeability relationships used with rigid porous materials. Since these relationships are functions of porosity, they have expressed porosity in terms of the degree of compression (Kataja et al, 1992) or as function of the applied pressure (Jönsson and Jönsson, 1992). There is, however, a lack of experimental information concerning the variations in porosity that occur when pressure is applied on a compressible porous material. In this respect NMR imaging studies could play an important role (Ilg et al and Höpfel, 1992 and Bayer et al, 1989). This technique could be used to determine the changes in void volume and therefore the changes in porosity that occur when a compressible porous bed is under stress. The strains suffered by the compressed material could also be studied, and in the case of beds of beaded particles a relationship between the level of stress and the degree of particle compression (change in particle shape) could be derived. This

relationship would complete the hydrodynamic model of Verhoff and Furjanic (1983) (section 2.2). A more fundamental hydrodynamic model could be derived by integrating the steady state equation developed by Jönsson and Jönsson (1992) in order to describe fluid flow in compressible porous media. Its use would improve the description of column hydrodynamics and therefore the prediction of the flow rate-pressure drop curves.

Finally non-time-dependent and time-dependant bed length changes resulting from matrix compression should be accounted for by the models in order to complete the description of this phenomenon.

Although the models developed by Verhoff and Furjanic (1983) and by Davies (1989) have been tested against experimental data with success, it is necessary to carry out more experimental work to fully verify their predictive capabilities and generality. Also more theoretical work is needed in order to increase the understanding of the hydrodynamics of compressible packed beds which will lead to the development of improved models.

6.3 Matrix compression and column performance.

Although several researchers have reported improved performance of chromatographic beds that have been highly compressed (Edwards and Delft, 1970; Fishman and Barford, 1970; Hjertén and Liao, 1988; Horváth, 1990) a satisfactory explanation concerning this improvement has not been provided.

In the present work a contribution has been made towards the elucidation and understanding of the effects of bed compression on column performance. The approach aimed at distinguishing which of the transport and equilibrium parameters characterizing the performance of size exclusion chromatography (SEC) were more affected when a bed was progressively compressed, and the extent of these effects. The HETP method was used in order to estimate these parameters.

This approach has enabled the changes caused by compression on the matrix and bed structures to be studied, leading to the assessment and identification of the major effects.

Within the levels of bed compression achieved in this study it appeared that the reduction of bed volume was mainly caused by a reduction in the interparticle void volume, with only a very small fraction of intraparticle void volume being lost. Accordingly it was observed that bed compression did not significantly affect the protein distribution coefficients (inclusion porosities) ε_p nor the protein intraparticle diffusivities D_e. The major effect occasioned by bed compression was on the value of the coefficient of axial dispersion D_L which increased as the bed compressed. Therefore

it can be concluded that although the matrix particles may have been deformed under compression, the deformation was not sufficient to cause a variation in the intraparticle space available to the diffusing molecules. On the other hand bed structural modifications caused by compression were more significant as signalled by the marked increase in D_L.

In spite of the increase undergone by D_L, in the case of the Sepharose 6B column a slight improvement in performance was observed as the bed compressed (see section 4.3.4). This improvement could be attributed to the reduction in the interparticle distances travelled by the diffusing molecules (Hjertén, 1988) or to a reduction in the resistances to interparticle transport (Horváth, 1990) resulting in a faster attainment of equilibrium. It appears therefore that bed compression could have a beneficial effect on column performance by accelerating the partition of the solute molecules but this must be balanced against deleterious effects caused by bed structural modifications which result in flow non-uniformities and hence in greater dispersion.

The validity of the transport and equilibrium parameters determined in this study by means of the HETP method was confirmed by matching the experimental outlet peaks with the simulated peaks generated by means of the general rate model of SEC (section 3.2.1). The very good match also proved the capability of this model to describe accurately the chromatographic peaks.

Further experimental work is needed in order to understand better the effects of bed compression on column performance. In particular experiments should be carried out at higher degrees of bed compression in order to assess fully the effects on the intraparticle diffusion coefficient and the equilibrium distribution coefficient. Since bed compression may produce a reduction in the interparticular diffusion resistances (Horváth, 1990), further experimental work in this area should also envisage the estimation of the effects of compression on the fluid film mass transfer coefficient.

It is evident that the methodology used in this study enables a deeper analysis of the effects of compression by separating all the contributions affecting column performance.

6.4 Fouling and column performance.

Matrix fouling is an important problem in chromatographic separation and purification because its occurrence has a detrimental effect on column performance and hence on the costs of separation. In the present thesis a methodology involving the method of moments has been developed in order to analyze the effects that different levels of foulants contained in a process stream and injected onto a chromatographic column have on its performance. This methodology aimed at analysing the different effects in a separate manner by estimating the transport and equilibrium parameters

that characterize column performance. The variations caused by fouling on the value of these parameters can serve to infer the different changes undergone by the bed and matrix structure and the manner in which foulant deposition occurs.

It was found that as the amount of foulants injected onto the column increased the equilibrium distribution coefficient and the intraparticle diffusivities of the proteins tested decreased linearly, while the axial dispersion coefficient increased also in a linear fashion. This behaviour allowed for the derivation of mathematical relationships that could be used in the prediction of the chromatographic performance of columns operated under fouling conditions.

Again the validity of the parameters estimated by means of the method of moments was corroborated by comparing the experimental peaks with those simulated by using the SEC model. The matching of the peaks gave confidence in the validity of the parameters and proved the possibility of employing this methodology for the analysis of chromatographic separations carried out under fouling conditions and for the derivation of mathematical relationships that would enable the simulation and prediction of these separations.

Further experimental work is required in order to verify fully the linearity of the relationships between the values of the transport and equilibrium parameters and the amount of foulants injected onto a column. It is evident that the amount of foulants accepted by the column before its performance is considerably deteriorated or before it gets clogged is dependent on a series of variables related to the column and matrix characteristics. The methodology developed in this work could be used to study the effects of fouling on the performance of columns of different dimensions or packed with matrices of different characteristics. The packing density has certainly an effect on the ability of a column to handle particulates and lipids. Accordingly columns with different bed void fractions could be examined. With respect to the operating conditions, the flow rate and the temperature at which the stream containing the fouling material is loaded to the column should affect the response of the column to fouling. The effects of these variations could also be analyzed by means of the method employed in this thesis.

Another important variable to be considered in the fouling of chromatographic columns is the time variable. A series of samples of constant composition could be injected onto a single column and its performance monitored after a constant number of samples have been injected in order to evaluate the time dependency of fouling or the degree of fouling in relation to the number of samples and/or the total amount of contaminants injected. This would provide information about the lifetime of a column operating under certain specified conditions and the required frequency of cleaning cycles. In this respect and as shown by the preliminary tests reported in this work the techniques employed could also easily be used in the evaluation of the effectiveness of cleaning protocols.

The use of more selective assays will reduce the errors arising from the interference produced by the large number of different chemical species present in real biological process streams. This in turn would allow the identification of the chemical entities mostly responsible for matrix fouling. However, if interferences could not be eliminated or reduced, pure contaminants could be injected onto a column and its performance analyzed. Although this approach is not very realistic, the identification of major fouling components would certainly provide a strong basis on which the effects of more complex streams on column performance could be inferred and on which sample pretreatment protocols could be designed.

Although this thesis has focused on the study of the performance of size exclusion chromatography, due to its simplicity when compared with other types of chromatography, the methods developed here could also be used to analyze the effects of fouling on the capacity of adsorptive matrices as well as on the rate parameters involved in the adsorption step and are therefore of generic utility.

APPENDIX A

Program listing

```
% Solution of the Gel Filtration model by Laplace transformation and by
% numerical inversion of the solution in the Laplace domain utilising
% Fast Fourier Transform algorithm.

% Chromatography parameters

% C - solute concentration in mobile phase
% Cp- solute concentration in particle pores
% Co- pulse concentration (mg/cm3)
 Co= input('Sample concentration-mg/ml= 1.5(default)');
 if isempty(Co)
   Co= 1.5;
 end
% Flow rate (cm3/min)
 Frate= input('Flow rate-cm3/min= 0.1(default)');
 if isempty(Frate)
   Frate= 0.1;
 end
% E - column void fraction
 E= input('Bed void fraction= 0.3538(default)');
 if isempty(E)
  E= 0.3538;
 end
% u - mean interstitial mobile phase velocity (cm/s)
 u= Frate/(2*E*60);
% DL- axial dispersion coefficient (cm2/s)
 DLu= input('Enter value of DL/u-cm= 0.0076(default)');
 if isempty(DLu)
  DLu= 0.0076;
 end
```

```
 DL= DLu*u;
% kf- film mass transfer coefficient (cm/s)
 kf= input('Film mass transfer coefficient-cm/s= 4.13d-4(default)');
 if isempty(kf)
  kf= 4.13d-4;
 end
% Ep- intraparticle void fraction
 Ep= input('Intraparticle void fraction= 0.6816(default)');
 if isempty(Ep)
  Ep= 0.6816;
 end
% R - average radius of particles (cm)
 R= input('Average particle radius-cm= 4.4d-3(default)');
 if isempty(R)
  R= 4.4d-3;
 end
% De- effective intraparticle diffusivity (cm2/s)
 De= input('Effective intraparticle diffusivity-cm2/s= 1.11d-7(default)');
 if isempty(De)
  De= 1.11d-7;
 end
% to- sample injection time (s)
% this time is negligible and therefore not considered
% z - axial distance from column outlet (cm)
% Solution of model is carried out only at the column outlet, therefore
% z is equal to the column length
 z= input('Column length-cm= 51.2(default)');
 if isempty(z)
  z= 51.2;
 end
% r - intraparticle radial position
% m - volume ratio
m= E/(1-E);
```

```
% FFT algorithm parameters

% Period is equal to 2T (s)
T= input('Period T required by the FFT algorithm= 30000.0(default)');
if isempty(T)
 T= 30000.0;
end
% Constant along which the line integration is carried out. For this
% particular case a should be 0.0, but this results in an error in the
% calculation (NaN) due to the appearance of an infinite number (division
% by zero) therefore a should be made as small as possible
a= 0.000001;
% Number of time steps and frequency steps. N must be a power of two.
N= input('Number of time steps= 128(default)');
if isempty(N)
 N= 128;
end
% Time step
DT= 2*T/N;
% Frequency step
Dw= pi/T;
% Maximum frequency
wmax= N*pi/(2*T);


% Parameters required by the program
U= u/(2*DL);
% Evaluation of the real and imaginary parts of the transformed function

for k= 0:1:N/2
  l= k + 1;
  w(l)= k*pi/T;
  s= a + j*w(l);
  RT= sqrt(Ep*s/De);
  RTR= RT*R;
  alp= (RT*cosh(RTR)-(1/R)*sinh(RTR))/(RT*cosh(RTR)+(kf/De-1/R)*sinh(RTR));
```

```
  C(l)= Co*exp((U-sqrt(U^2+s/DL+(3*kf*alp)/(m*DL*R)))*z);
  x(l)=real(C(l));
  y(l)=imag(C(l));
  x(N-l+2)= x(l);
  y(N-l+2)= -y(l);
end

y(N/2+1)= 0.0;
[x' y'];

for k= 0:1:N-1
  l= k + 1;
  w(l)= k*pi/T;
  CC(l)= x(l) + y(l)*j;
  t(l)= k*DT;
end

CF= conj(CC);
[w.' CC.' CF.'];

% Fast Fourier Transform Algorithm
cf= fft(CF);
[cf];
f= conj(cf);
[f];

for i= 0:1:N-1
   n= i + 1;
   c(n)= (exp(a*i*DT)/(2*T))*f(n);
end

% Normalizing peak
 cc= c/max(c);
plot(t,cc,'--')
```

```
% Evaluating retention time (min)
[mval,ind]= max(cc);
tR= t(ind)/60
```

APPENDIX B Results of all the assays conducted in the fouling studies [a]

Foulant conc.[g] %	Total solids [b] (g)		Total protein (g)		Total salt in buffer [c] (g)		DNA (g)		Lipids (g)		Cell debris [d] (g)		NaCl (g)		Total organic carbon (g)	
	Inlet [e] stream	Outlet[f] stream	Inlet stream	Outlet stream	Inlet stream	Outlet stream	Inlet stream	Outlet stream	Inlet stream	Outlet stream	Inlet stream	Outlet stream	Inlet stream	Outlet stream	Inlet stream	Outlet stream
5	0.5087	1.8543	0.0950	0.1083	0.144	0.3024	0.0029	0.0047			0.2668	0.3784	0.0	1.0605	0.2510	0.2308
10	0.8763	2.1840	0.215	0.1928	0.144	0.3024	0.0049	0.0067			0.5114	0.6216	0.0	1.0605	0.3435	0.3355
15	1.2530	2.6460	0.3879	0.2929	0.144	0.3024	0.0065	0.0084			0.7146	0.9818	0.0	1.0605	0.7538	0.7190
20	1.6133	2.9134	0.5974	0.5205	0.144	0.3024	0.0078	0.0110			0.8641	1.0190	0.0	1.0605	0.6595	0.6533

[a] The experimental procedure followed in the conduction of each of the assays is described in section 5.2.3. All the assays were carried out three times, the results shown in this table correspond to the average values.

[b] The values in these columns are the results of the total dry weight measurements carried out according to the procedure presented in section 5.2.3.4.

[c] The values in these columns were calculated from the composition of the buffers used in these experiments (see sections 5.2.1.3 and 5.2.2)

[d] The amount of cell debris present in the different streams was calculated as : Cell debris= Total solids-Protein-Salt in buffer-DNA.

[e] The volume of this stream was constant and equal to 50 ml. The quantities of the different components shown in this table were contained in this volume.

[f] The volume of this stream was constant and equal to 105 ml. The quantities of the different components shwon in this table were contained in this volume.

[g] The % foulant concentration of the process stream injected onto the Sepharose 4 FF columns is based on the concentration of the disk stack centrifuge supernatant, which was produced with a constant concentration of Baker's yeast, i.e. 600 g/l (see section 5.2.2.1).

APPENDIX C

List of company names and addresses.

Anachem. Charles Street, Luton, Beds. LU2 OEB, UK.

The A.P.V. Company Ltd. Manor Royal, Crawley, Sussex, UK.

BDH Laboratory Supplies. Merck Ltd. Hunter Boulevard, Lutterworth, Leicestershire LE17 4XN, UK.

Bio-Rad Laboratories Ltd. Bio-Rad House, Maylands Avenue, Hemel Hempstead, Hertfordshire HP2 7TD.

Brookhaven Instruments, Ltd. Chapel House, Stock Wood, Worcestershire B96 6ST, UK.

Contraves Industrial Products Ltd. Times House, Station Approach, GB-Ruislip, Middlesex HA4 8LH, UK.

Corning Medical and Scientific. Corning Ltd. Halstead, Essex CO9 2DX, England.

Entran Ltd. 19-19a Garston Park Parade, Garston, Watford, Herts WD2 6LQ, England.

Grant Instruments (Cambridge) Ltd. Barrington, Cambridge CB2 5QZ, UK.

Joyce-Loebl Ltd. Dukesway, Team Valley, Gateshead, Tyne & Wear NE11 OPZ, UK.

J. W. Pike Ltd. Yeast Merchants & Baker's Sundriesmen. Unit 4, Eley Estate, Eley Road, Edmonton, London N18 3BH, UK.

The Mathworks, Inc. 21 Eliot Street, South Natick, MA 01760, USA.

M.J. Patterson (Scientific) Ltd. Unit 21, Apex Business Centre, Boscombe Road, Dunstable, Beds. LU5 4UB, UK.

Perkin-Elmer Ltd. Post Office Lane, Beaconsfield, Buckinghamshire, England HP9 1QA.

Pharmacia LKB Biotechnology. Davy Avenue, Knowlhill, Milton Keynes MK5 8PH, UK.

Pharmacia LKB Biotechnology AB. Björkgatan 30, S-751 82 Uppsala, Sweden.

Shimadzu Corporation. 3, Kanda-Nishikicho 1-chome, Chiyoda-ku, Tokyo 101, Japan.

Sigma Chemical Co. P.O. Box 14508, St. Louis MO, 63178 USA.

Silverston Machines Ltd. Waterside, Chesham, Bucks, UK.

Sun Microsystems Europe, Inc. Sun House, 31-41 Pembroke Broadway, Camberley, Surrey GU15 3XD, England.

Westfalia Separator AG. D-4740 Oelde, Germany.

NOMENCLATURE

A	column cross-sectional area	cm^2
A	constant in Knox equation (eq. 1.19)	dimensionless
A'	constant in eq. 1.9	$(s/cm)^{1/3}$
A_o	constant in Van Deemter equation (eq. 1.18)	cm
B	constant that relates wall shear stress and vertical stress	dimensionless
B	constant in Knox equation (eq. 1.19)	dimensionless
B_o	constant in Van Deemter equation (eq. 1.18)	cm^2/s
Bo	Bodenstein number, defined as ud_p/D_L	dimensionless
C	solute concentration in mobile phase	mg/cm^3
C	constant in Knox equation (eq. 1.19)	dimensionless
C_o	constant in Van Deemter equation (eq. 1.18)	s
C	Laplace domain solute concentration in mobile phase	mg/cm^3
$\hat{C}$	solute conc. in stationary phase, averaged over entire particle	mg/cm^3
C^*	equilibrium solute concentration in mobile phase	mg/cm^3
C_{DO}	drag coefficient for single particle fixed in liquid flowing at rate u_o	dimensionless
c_f	polymer (fibre) concentration in particles	g/cm^3
C_{max}	maximum concentration observed in a chromatographic peak	mg/cm^3
C_o	pulse or sample concentration	mg/cm^3
C_p	solute concentration in particle, based on accessible particle volume	mg/cm^3
C_s	solute concentration in stationary phase	mg/cm^3
D_a	apparent dispersion coefficient	cm^2/s
d_c	column diameter	cm
d_e	absolute size constant	cm
D_e	effective intraparticle diffusivity of solute	cm^2/s
D_L	convective axial dispersion coefficient	cm^2/s
D_m	solute diffusivity in unbounded solution	cm^2/s
d_p	stationary phase mean particle diameter	cm
D_s	solute diffusivity in stationary phase	cm^2/s
E	energy dissipation rate per unit mass of fluid	cm^2/s
F	total force on bed	N
F_F	force acting on bed due to fluid flow	N
F_g	force exerted on bed due to gravity	N

F_w	force on bed resulting from support of column walls	N
g	acceleration of gravity (equal to 9.81)	m/s^2
h	reduced plate height, H/d_p	dimensionless
H	height equivalent to a theoretical plate (HETP), or plate height	cm
K	permeability	m^2
k′	capacity factor	dimensionless
K′	ratio of lateral to vertical pressure	dimensionless
k_B	Boltzman constant= 1.3805 X 10^{-16}	$g \cdot cm^2/s^2 \cdot °K$
K_d	equilibrium distribution coefficient	dimensionless
k_f	fluid-phase mass transfer coefficient	cm/s
k_m	apparent mass transfer coefficient	s^{-1}
k_m'	apparent mass transfer coefficient	s^{-1}
k_o	retention factor	dimensionless
K_o	permeability of unstressed bed	m^2
k_s	screening coefficient	cm^{-1}
L	bed length	cm
L_{avg}	average bed length	cm
m	$\varepsilon/(1-\varepsilon)$	dimensionless
M	molecular weight	daltons
N	plate number or number of theoretical plates	dimensionless
Nu	Nusselt number, defined as $k_f d_p/D_m$	dimensionless
p	empirical parameter in Gunn's correlation	dimensionless
P	fluid pressure	kPa
Pe_L	dispersion Péclet number, defined as $d_p u/D_L$	dimensionless
P_F	solids pressure due to fluid flow	kPa
P_g	solids pressure due to the weight of the particles	kPa
P_s	total solids pressure exerted on bed	kPa
P_W	solids pressure associated with the wall support	kPa
q	equilibrium solute concentration in the stationary phase	mg/cm^3
Q	volumetric flow rate	cm^3/s
r	radial distance from centre of particle	cm
R	retardation factor (chapter 1)	dimensionless
R	column radius	cm
Re	Reynolds number, defined as $d_p u \varepsilon \rho/\mu$	dimensionless
Re^f	modified Reynolds number, defined as $E^{1/3} d_p^{4/3} \rho/\mu$	dimensionless
r_f	radius of matrix fibre	cm

r_o	interaction radius between polymer fibre and protein inside particle	cm
R_p	stationary phase particle radius	cm
r_s	radius of solute molecule	nm
r_s	solute Stokes radius	cm
R_s	chromatographic resolution	dimensionless
s	Laplace transform variable	s^{-1}
S	lateral surface area of column	m^2
Sc	Schmidt number, defined as $\mu/\rho D_m$	dimensionless
Sh	Sherwood number, defined as $k_f d_p/D_m$	dimensionless
t	time	s
T	temperature	°K
t_o	input pulse time	s
t_R	retention time	s
u	interstitial fluid velocity, based on the area εA	cm/s
u_o	superficial fluid velocity	cm/s
V_c	total column volume	cm^3
V_d	volume of dead spaces in chromatograph	cm^3
v_f	volume of matrix fibres per total volume	dimensionless
V_F	sample volume	cm^3
V_i	intraparticle void volume (volume of liquid imbibed by gel particles)	cm^3
V_m	volume of mobile phase in interparticle space	cm^3
V_o	interparticle void volume	cm^3
V_R	elution or retention volume	cm^3
V_s	total volume of stationary phase (matrix and intraparticle space)	cm^3
V_T	total void volume (interparticle and intraparticle void space)	cm_3
w	peak width	s
z	axial coordinate in a packed bed	cm

GREEK SYMBOLS

α	matrix compressibility	kPa^{-1}
α	parameter in the correlation for Nusselt number (chapter 3)	dimensionless
α	selectivity (chapter 1)	dimensionless
α_1	smallest zero of the Bessel function $J_o(\cdot)$; *ca.* 2.405	dimensionless
β	low ReSc asymptote of the Nusselt number	dimensionless

γ	obstruction factor to diffusion in interparticle space	dimensionless
γ_s	obstruction factor to diffusion in stationary phase	dimensionless
δ	angle of friction against glass wall	degrees
$\Delta\rho$	$(\rho_s-\rho_L)g$	kPa/cm
ΔP	fluid pressure drop	kPa
ε	interparticle void fraction in a packed bed	dimensionless
ε_o	initial void fraction of unstressed bed	dimensionless
ε_p	intraparticle inclusion porosity of a solute	dimensionless
θ	angle of internal friction	degrees
λ	flow-geometry dependent constant	dimensionless
μ	fluid viscosity	g/cm·s
μ'	coefficient of wall friction	dimensionless
μ_1	first absolute moment	s
μ_2'	second central moment	s^2
ν	reduced velocity, ud_p/D_m	dimensionless
ρ	fluid density	g/cm^3
ρ_L	density of liquid phase	g/cm^3
ρ_s	density of stationary phase	g/cm^3
σ	effective interparticulate stress acting directly along the column axis	kPa
σ^2_{col}	peak variance due to non-equilibrium effects in the column	s^2
σ^2_{extr}	peak variance due to extracolumn effects	s^2
σ^2_{Tot}	total variance of a chromatographic peak	s^2
σ_L	peak standard deviation measured in column length units	cm
σ_o	constant used to scale σ in eq..., representing matrix rigidity	kPa
σ_t	peak standard deviation measured in time units	s
σ_V	peak standard deviation measured in volume units	cm^3
τ	tortuosity factor for a packed bed	dimensionless
Φ	shape factor	dimensionless
ω	wall support coefficient	cm^{-1}

BIBLIOGRAPHY

Ackers, G. K. and Steere, R. L. Purification and Separation of Tobacco Mosaic Virus and Southern Bean Mosaic Virus by Agar-Gel Filtration. *Nature.* **194**:114-116 (1962).

Afeyan, N. B., Scott, P. F., Gordon, N. F., Mazsaroff, I., Várady, L. and Regnier, F. E. Perfusion Chromatography and Approach to Purifying Biomolecules. *Bio/Technology.* **8**:203-206 (1990).

Aguilera Soriano, G. and Titchener-Hooker, N. A Hydrodynamic Study of Compression in Beds of Chromatographic Matrix. IChemE Research Event. Manchester. 101-103 (1992).

Andersson, T. Pharmacia LKB Biotechnology. Uppsala, Sweden. Personal communication. 1992.

Andersson, T., Carlsson, M., Hagel, L. and Pernemalm, P-Å. Agarose-Based Media for high-Resolution Gel Filtration of Biopolymers. *J. Chromatogr.* **326**:33-44 (1985).

Andrei, D. C., Briscoe, B. J., Luckham, P. F. and Williams D. R. Study of the Micro-Deformability of Individual Particles. IChemE Research Event. University College London. 1994.

Arnold, F. H., Blanch, H. W. and Wilke, C. R. Analysis of Affinity Separations. II: The Charaterization of Affinity Columns by Pulse Techniques. *The Chem. Eng. J.* **30**:B25-B36 (1985).

Arve, B. H. and Liapis, A. I. Modeling and Analysis of Biospecific Adsorption in a Finite Bath. *AIChE J.* **33**:179-193 (1987).

Arve, B. H. and Liapis, A. I. Biospecific Adsorption in Fixed and Periodic Countercurrent Beds *Biotechnol. Bioeng.* **32**:616-627 (1988).

Athalye, A., Gibbs, S. J. and Lightfoot, E. N. Predictability of Chromatographic Protein Separations. Study of Size-Exclusion Media with Narrow Particle Size Distributions. *J. Chromatogr.* **589**:71-85 (1992).

Basset, R. H., Reader in Geotechnics. Dept. of Civil Engineering. UCL, UK. Personal communication. 1992.

Bayer, E., Müller, W., Ilg, M. and Albert, K. Visualization of Chromatographic Separations by NMR Imaging. *Angew. Chem. Int. Ed. Engl.* **28(8)**:1029-1032 (1989).

Bear, J. *Dynamics of Fluids in Porous Media.* American Elsevier, New York. 1972.

Beeckman, J. W. and Froment, G. F. Catalyst Deactivation by Active Site Coverage and Pore Blockage. *Ind. Eng. Chem. Fundam.* **18**(3):245-256 (1979).

Biot, M. A., Theory of Elasticity and Consolidation for a Porous Anisotropic Solid. *J. Appl. Phys.* **26**:182-185 (1955).

Bird, R. B., Stewart, W. E. and Lightfoot, E. N. *Transport Phenomena.* Wiley, New York. 1960.

Bjerrum, L. Engineering Geology of Norwegian Normally-Consolidated Marine Clays as Related to Settlements of Buildings. *Géotechnique.* **17**:81-188 (1967).

Blake, F. C. Resistance of Packing to Fluid Flow. *Trans. Amer. Inst. Chem. Engrs.* **14**:415-421 (1922).

Bogue, D. C. A Note on the Theory of Solid Phase Diffusion in Chromatography. *Anal. Chem.* **32**(13):1777-1778 (1960).

Bonnerjea, J., Oh, S., Hoare, M. and Dunnill, P. Protein Purification: the Right Step at the Right Time. *Bio/Technology.* 4:954-957 (1986).

Boyer, P. M. and Hsu, J. T. Experimental Studies of Restricted Protein Diffusion in an Agarose Matrix. *AIChE J.* **38**(2):259-272 (1992).

Bradford, M. M. A Rapid and Sensitive Method for the Quantitation of Microgram Quantities of Protein Utilizing the Principle of Protein-Dye Binding. *Anal. Biochem.* **72**:248-254 (1976).

Bristow, P. A. and Knox, J. H. Standardization of Test Conditions for High Performance Liquid Chromatography Columns. *Chromatographia.* **10**(6):279-289 (1977).

Buchholz, K. and Godelmann, B. Pressure Drop Across Compressible Beds. *Enzyme Engng.* **4**:89-92 (1978).

Builder, S. E. and Hancock, W. S. Analytical and Process Chromatography in Pharmaceutical Protein Production. *Chem. Eng. Prog.* 42-46 (1988).

Carman, P. C. A Study of the Mechanism of Filtration. Part I. *J.S.C.I.* **52**:280-282 (1933).

Carman, P. C. Fluid Flow Through Granular Beds. *Trans. Inst. Chem. Eng. London.* **15**:150-166 (1937).

Carta, G. Exact Analytic Solution of a Mathematical Model for Chromatographic Operations. *Chem. Eng. Sci.* **43**:2877-2883 (1988).

Carta, G. and Bauer, J. S. Analytic Solution for Chromatography with Nonuniform Sorbent Particles. *AIChE J.* **36**(1):147-150 (1990).

Chen, T-L. and Hsu, J. T. Prediction of Breakthrough Curves by the Application of Fast Fourier Transform. *AIChE J.* **33**(8):1387-1390 (1987).

Chesler, S. N. and Cram, S. P. Effect of Peak Sensing and Random Noise on the Precision and Accuracy of Statistical Moment Analysis from Digital Chromatographic Data. *Anal. Chem.* **43**(14):1922-1933 (1971).

Chilcote, D. D. and Scott, C. D. A Theoretical Derivation of the Axial Diffusion Coefficient in Chromatography. *J. Chromatogr.* **87**:315-323 (1973).

Ching, C. B., Uddin, M. S. and Hidajat, K. Diffusional Kinetics of Monoclonal Antibody, Transferrin and Bovine Serum Albumin on Sephacryl S-200 HR Gel. *Chem. Eng. J.* **42**:B47-B52 (1989).

Chisti, Y. and Moo-Young, M. Large Scale Protein Separations: Engineering Aspects of Chromatography. *Biotech. Adv.* **8**:699-708 (1990).

Clonis, Y. D. Large-Scale Affinity Chromatography. *Bio/Technology.* **5**:1290-1293 (1987).

Colin, H. Contribution of Packing Cost to Overall Cost. *Genetic Eng. News.* July/August, 22 (1988).

Colin, H., Hilaireau, P. and Tournemire, J. Dynamic Axial Compression Columns for Preparative High Performance Liquid Chromatography. *LC-GC Intl.* 3(4):40-48 (1990).

Cooney, J. M. Chromatographic Gel Media for Large Scale Protein Purification. *Bio\Technology.* **2**(1):41-55 (1984).

Cox, G. B. The Design of Large-Diameter Columns for Preparative Liquid Chromatography. *LC-GC Intl.* **3**(10):10-16 (1990).

Craig, L. C. Identification of Small Amounts of Organic Compounds by Distribution Studies. *J. Biol. Chem.* **155**:519-534 (1944).

Crone, H. D. Ion-Exclusion Effects on the Chromatography of Acetyl-Cholinesterase and other Proteins on Agarose Columns at Low Ionic Strength. *J. Chromatogr.* 92:127-135 (1974).

Crump, K. S. Numerical Inversion of Laplace Transforms Using a Fourier Series Approximation. *J. Assoc. Comp. Machinery.* **23**(1):89-96 (1976).

Cukier, R. I. Diffusion of Brownian Spheres in Semidilute Polymer Solutions. *Macromol.* **17**:252-255 (1984).

Darcy, H. *Les Fontaines Publiques de la Ville de Dijon.* Victor Dalmont, Paris. 1856.

Davies, P. A. *Physical and Engineering Aspects of Protein Separation Processes.* PhD Thesis. University of Oxford, 1989.

Davies, P. A. Determination of Diffusion Coefficients of Proteins in Beaded Agarose by Gel Filtration. *J. Chromatogr.* **483**:221-237 (1989a).

Davies, P. A. and Bellhouse, B. J. Permeability of Beds of Agarose-Based Particles. *Chem. Eng. Sci.* **44**(2):452-455 (1989).

Dawkins, J. V. Packings in Size Exclusion Chromatography. In: *Packings and Stationary Phases in Chromatographic Techniques. Chromatographic Science Series*, Vol. 38. Unger, K. K., ed. Marcel Dekker, New York. 1990.

Dawkins, J. V., Stone, T. and Yeadon, G. High Performance G.P.C. with Crosslinked Polystyrene Gels: Influence of Particle Size Distribution. *Polymer* **18**:1179-1184 (1977).

Dawson, R. M. C., Elliott, D. C., Elliott, W. H. and Jones, K. M. *Data for Biochemical Research.* 3rd Ed. pp. 545. Oxford University Press, New York. 1987

De Ligny, C. L. The Contribution of Eddy Diffusion and of the Macroscopic Mobile Phase Velocity to the Plate Height in Chromatography. *J. Chromatogr.* **49**;393-401 (1970).

Delaney, R. A. M. *Industrial Gel Filtration of Proteins.* Ch. 10 in: *Applied Protein Chemistry.* Grant, R. A., ed. pp 233-280. Applied Science Publishers Ltd., London. 1989.

Dewaele, C. and Verzele, M. Influence of the Particle Size Distribution of the Packing Material in Reversed-Phase High-Performance Liquid Chromatography. *J. Chromatogr.* **260**:13-21 (1983).

Dubner, H. and Abate, J. Numerical Inversion of Laplace Transforms by Relating Them to the Finite Fourier Cosine Transform. *J. Assoc. Comp. Machinery.* **15**(1):115-123 (1968).

Dullien, F. A. *Porous Media. Fluid Transport and Pore Structure.* pp 157-163. Academic Press, New York. 1979.

Dwyer, J. L. High Performance Liquid Chromatography as a Process Tool. *AICHE Symposium Series.* **82(250)**:120-127 (1986).

Dyson, N. *Chromatographic Integration Methods.* Smith, R. M. editor. pp 87-156. Royal Society of Chemistry, Cambridge, UK. 1990.

Ebach, E. A. and White, R. R. Mixing of Fluids Flowing Through Beds of Packed Solids. *AIChE J.* **4**:161-169 (1958).

Eble, J. E., Grob, R. L., Antle, P. E. and Snyder, L. R. Simplified Description of High-Performance Liquid Chromatographic Separation Under Overload Conditions, Based on the Craig Distribution Model. I. Computer Simulations for a Single Elution Band Assuming Langmuir Isotherm. *J. Chromatogr.* **384**:25-44 (1987).

Edgington, S. M. Surviving the 90's: Can Biotech Master Clinical Trials?. *Bio/Technology.* **12**:977-

979 (1994).

Edwards, M. F. and Richardson, J. F. Gas Dispersion in Packed Beds. *Chem. Eng. Sci.* **23**:109-123 (1968).

Edwards, V. H. and Helft, J. M. Gel Chromatography: Improved Resolution Through Compressed Beds. *J. Chromatogr.* **47**:490-493 (1970).

Ernst, U. P. and Hsu J. T. Estimation of Rate Parameters in Chemical Flow Systems by the Fast Fourier Transform Technique. *Proc. Computer Simulation Conf.*, D. Pace, ed., 579-582 (1991).

Fane, A. G. and Fell, C. J. D. Modeling Fouling Mechanisms in Protein Ultrafiltration. *J. Membrane Sci.* **27**:181-193 (1986).

Fane, A. G. and Fell, C. J. D. A Review of Fouling and Fouling Control in Ultrafiltration. *Desalination.* **62**:117-136 (1987).

Fedkiw, P. S. and Newman, J. Low Péclet Number Behaviour of the Transfer Rate in Packed Beds. *Chem. Eng. Sci.* **33**:1043-1048 (1978).

Fedkiw, P. S. and Newman, J. Mass-Transfer Coefficients in Packed Beds at Very Low Reynolds Numbers. *Int. J. Heat Mass Transfer.* **25**(7):935-943 (1982).

Fishman, M. L. and Barford, R. Increased Resolution of Polymers Through Longitudinal Compression of Agarose Gel Columns. *J. Chromatogr.* **52**:494-496 (1970).

Flannery, W. H. and Teukolsky, S. A. *Numerical Recipes. The Art of Scientific Computing (FORTRAN version).* pp. 547-554. Cambridge University Press, New York. 1989.

Furui, M. and Yamashita, K. Horizontal Baffle Effects on Compaction of Immobilized Cell Catalyst Beds. *J. Ferment. Technol.* **63**(10):73-78 (1985).

Gangwal, S. K., Hudgins, R. R. and Silveston, P. L. Conditions Needed for Satisfactory Measurement of Mass Transfer Coefficients, Internal Diffusivity and Adsorption rate Constants. *Can. J. Chem. Eng.* **56**:554-557 (1978).

Ghrist, B. F. D., Stadalius, M. A. and Snyder, L. R. Predicting Bandwidth in the High-Performance Liquid Chromatographic Separation of Large Biomolecules. I. Size-Exclusion Studies and the Role of Solute Stokes Diameter *versus* Particle Pore Diameter. *J. Chromatogr.* **387**:1-19 (1987).

Gibbs, J. S. *Protein Diffusion and Chromatography.* Ph.D. Thesis, University of Wisconsin, Madison. 1989.

Gibbs, S. J. and Lightfoot, E. N. Scaling Up Gradient Elution Chromatography. *Ind. Eng. Chem. Fundam.* **25**:490-498 (1986).

Gibbs, S. J., Karrila, S. J. and Lightfoot, E. N. Mass Transfer to a Sphere with a Non-uniform Boundary Layer: Implications in Chromatographic Analysis. *Chem. Eng. J.* **36**:B29-B27 (1987).

Gibbs, S. J., Chu, A. S., Lightfoot, E. N. and Root, T. W. Ovalbumin Diffusion at Low Ionic Strength. *J. Phys. Chem.* **95**:467-471 (1991).

Gibbs, S. J., Lightfoot, E. N. and Root, T. W. Protein Diffusion in Porous Gel Filtration Chromatography Media Studied by Pulse Field Gradient NMR Spectroscopy. *J. Phys. Chem.* **96**:7458-7462 (1992).

Giddings, J. C. *Dynamics of Chromatography. Part I: Principles and Theory. Chromatographic Science Series*, Vol. 1, Marcel Dekker, New York. 1965.

Giddings, J. C. and Eyring, H. A Molecular Dynamic Theory of Chromatography. *J. Phys. Chem.* **59**:416-421 (1955).

Giddings, J. C., Kucera, E., Russell, C. P. and Myers, M. N. Statistical Theory for the Equilibrium Distribution of Rigid Molecules in Inert Porous Networks. Exclusion Chromatography. *J. Phys. Chem.* **72**:4397-4408 (1968).

Glueckauf, E. Theory of Chromatography. Part 10.-Formulae for Diffusion into Spheres and theri Application to Chromatography. *Trans. Faraday Soc.* **51**:1540-1551 (1955).

Golden, L. S. and Irving, J. Osmotic and Mechanical Strength in Ion-Exchange Resins. *Chemistry and Industry.* 837-844 (1972).

Golshan-Shirazi, S. and Guiochon, G. The Equilibrium Dispersive Model of Chromatography. Proceedings of the NATO Advanced Study Institute on: *Theoretical Advancement in Chromatography and Related Separation Techniques*. Dondi, F. and Guichon, G. Eds. NATO ASI Series. Series C: Mathematical and Physical Sciences. Vol. 383. pp. 61-92. Kluwer Academic Publishers. 1992a.

Golshan-Shirazi, S. and Guiochon, G. Review of the Various Models of Linear Chromatography, and their Solutions. Proceedings of the NATO Advanced Study Institute on: *Theoretical Advancement in Chromatography and Related Separation Techniques*. Dondi, F. and Guichon, G. Eds. NATO ASI Series. Series C: Mathematical and Physical Sciences. Vol. 383. pp. 61-92. Kluwer Academic Publishers. 1992b.

Goward, C. R., Stevens, G. B., Collins, I. J., Wilkinson, I. R. and Scawen, M. D. Use of Macrosorb Kieselguhr Composite and CM-Sepharose Fast Flow for the Large-Scale Purification of L-Asparaginase from *Erwinia chrysanthemi*. *Enzyme Microb. Technol.* **11**:811-814 (1989).

Grace, H. P. Resistance and Compressibility of Filter Cakes. *Chem. Eng. Prog.* **49**:303-318 (1953).

Graham, E. E. and Fook, C. F. Rate of Protein Absorption and Desorption on Cellulosic Ion Exchangers. *AIChE J.* **28**(2):245-250 (1982).

Grushka, E., Myers, M. N., Schettler, P. D. and Giddings, J. C. Computer Characterization of Chromatographic Peaks by Plate Height and Heigher Central Moments. *Anal. Chem.* **41**(7):889-892 (1969).

Grushka, E. Chromatographic Peak Shapes. Their Origin and Dependence on the Experimental Parameters. *J. Phys. Chem.* **76**(18):2586-2593 (1972).

Guiochon, G. and Katti, A. Preparative Liquid Chromatography. *Chromatographia.* **24**:165-189 (1987).

Gunn, D. J. Theory of Axial and Radial Dispersion in Packed Beds. *Trans. Instn. Chem. Engrs.* **47**:T351-T359 (1969).

Gunn, D. J. Transfer of Heat or Mass to Particles in Fixed and Fluidised Beds. *Int. J. Heat Mass Transfer*. **21**:467 (1978).

Gunn, D. J. Axial and Radial Dispersion in Fixed Beds. *Chem. Eng. Sci.* **42**(2):363-373 (1987).

Gunn, D. J. and Pryce, C. Dispersion in Packed Beds. *Trans. Instn. Chem. Engrs.* **47**:T341-T350 (1969).

Gunn, D. J. and DeSouza J. F. C. Heat Transfer and Axial Dispersion in Packed Beds. *Chem. Eng. Sci.* **29**:1363-1371 (1974).

Guowei, Z., Genfu, X., Guirong, Z. and Xiuzhen, L. A Study on Mechanism of Silica Fouling of Anion Exchange Resins. *Reactive Polymers.* **7**:289-292 (1988).

Haën, C. de, Molecular Weight Standards for Calibration of Gel Filtration and Sodium Dodecyl Sulfate-Polyacrylamide Gel Electrophoresis: Ferritin and Apoferritin. *Anal. Biochem.* **166**:235-245 (1987).

Hagel, L. in *Protein Purification, Methods for High Resolution Protein Separation and Analysis.* Janson, J-C. and Rydén, L. editors. Ch. 3. VCH, Deerfield Beach, FL. 1989.

Hagel, L., Lundström, H., Andersson, T. and Lindblom H. Properties, in Theory and Practice, of Novel Gel Filtration Media for Standard Liquid Chromatography. *J. Chromatogr.* **476**:329-344 (1989).

Han, N-W., Bhakta, J. and Carbonell, R. G. Longitudinal and Lateral Dispersion in Packed beds: Effect of Column Length and Particle Size Distribution. *AIChE J.* **31**(2):277-288 (1985).

Hearle, D.C., Aguilera Soriano, G., Wiksell, E. and Titchener-Hooker, N. J. Quantifying the Fouling Effects of a Biological Process Stream on Chromatographic Supports. IChemE Research Event. University College London. 174-176 (1994).

Hejtmánek, V. and Schneider, P. Axial Dispersion Under Liquid-Chromatography Conditions. *Chem. Eng. Sci.* **48**(6):1163-1168 (1993)

Hiby, J. W. Longitudinal and Transverse Mixing During Single-Phase Flow Through Granular Beds, in *Proceedings of Symposium on Interaction Between Fluids and Particles.* A. Rottenburg (Editor). pp. 312-325. Institution of Chemical Engineers, London. 1962.

Hjertén, S. and Eriksson, K-O. High-Performance Molecular Sieve Chromatography of Proteins on Agarose Columns: The Relation between Concentration and Porosity of the Gel. *Anal. Biochem.* **137**:313-317 (1984).

Hjertén, S. and Liao, J-L. High-Performance Liquid Chromatography of Proteins on Compressed, Non-Porous Agarose Beads. I. Hydrophobic-Interaction Chromatography. *J. Chromatogr.* **457**:165-174 (1988).

Hjertén, S., Mohammad, J., Eriksson, K.-O. and Liao, J.-L. General Methods to Render Macroporous Stationary Phases Nonporous and Deformable, Exemplified with Agarose and Silica Beads and their Use in High-Performance Ion-exchange and Hydrophobic-Interaction Chromatography of Proteins. *Chromatographia.* **31**(1-2):85-94 (1991).

Hodgson, J. Affinity Innovations for Bioprocessing. *Bio/Technol.* **8**:864 (1990).

Horstmann, B. J. and Chase, H. A. Modelling the Affinity Adsorption of Immunoglobulin G to Protein A Immobilized to Agarose Matrices. *Chem. Eng. Res. Dev.* **67**:243-254 (1989).

Horváth, C. NATO Advanced Study Institute on *Chromatographic and Membrane Processes in Biotechnology*. São Miguel, Açores, Portugal. July 15-27, 1990.

Hsu, T-A. *Computer Automation of Cascade Chromatography and the Application of Fast Fourier Transform to Distributed Parameter Model Problems*. Ph. D. Thesis. Northwestern University, Evanston. 1979.

Hsu, J. T. and Chen, T-L. Theoretical Analysis of the Asymmetry in Chromatographic Peaks. *J. Chromatogr.* **404**:1-9 (1987).

Hsu, J. T. and Dranoff, J. S. Numerical Inversion of Certain Laplace Transforms by the Direct Application of Fast Fourier Transform (FFT) Algorithm. *Comput. Chem. Engng.* **11**(2):101-110 (1987).

Hussain, S., Metha, M. S., Kaplan, J. I. and Dubin, P. L. Experimental Evaluation of Conflicting Models for Size Exclusion Chromatography. *Anal. Chem.* **63**:1132-1138 (1991).

Ilg, M., Maier-Rosenkranz, J., Müller, W., Albert, K., Bayer, E. and Höpfel, D. Imaging of the

Chromatographic Process. *J. Magnetic Resonance.* **96**:335-344 (1992).

Jägerston, C. Pharmacia LKB Biotechnology. Uppsala, Sweden. Personal communication. 1993.

Jagschies, G. *Process-Scale Chromatography.* In: Ullman's Encyclopedia of Industrial Chemistry. 5th Ed. Vol. B3 pp (10-1)-(10-44). VCH Publishers. Weinheim, 1988.

Jaky, J. The Coefficient of Earth Pressure at Rest. *Journal of Society of Hungarian Architects and Engineers.* 355-358 (1944).

Janson, J-C. and Hedman, P. Large-Scale Chromatography of Proteins. In *Chromatography*; Fiechter, A. Ed.; Adv. Biochem. Eng. **25**:43-99 (1982).

Janson, J-C. and Jönsson, J-A. Introduction to Chromatography. In: *Protein Purification Principles, High Resolution Methods and Applications.* Janson, J-C. and Rydén, L., eds. VCH Publishers, N. Y. 1989.

Johanson, J. R. Two-Phase-Flow Effects in Solids Processing and Handling. *Chem. Eng.* 77-86 (1979).

Johnson, G. W. and Kapner, R. S. The Dependence of Axial Dispersion on Non-Uniform Flows in Beds of Uniform Packing. *Chem. Eng. Sci.* **45**:3329-3339 (1990).

Johnston, A. and Hearn, M. T. W. High-Performance Liquid Chromatography of Amino Acids, Peptides and Proteins. CXIV. Protein Interactions with Porous Coulombic Sorbents: Comparison of Experimental Findings with Predictions of Several Adsorption Models. *J. Chromatogr.* **557**:335-358 (1991).

Jones, C. R. and Johnson, C. S. Photon Correlation Spectroscopy of Hemoglobin: Diffusion of Oxy-HbA and Oxy-HbS. *Biopolymers.* **17**:1581-1593 (1978).

Jönsson, J. Å. Elution Curves and Statistical Moments in Non-Ideal, Linear Chromatography. *Chromatographia.* **18**(8):427-433 (1984).

Jönsson, J. Å. Dispersion and Peak Shapes in Chromatography, in *Chromatographic Theory and Principles.* Chromatographic Science Series. Vol. 38, pp. 27-102. Marcel Dekker, Inc. 1987.

Jönsson, K. A-S. and Jönsson, B. T. L. Fluid Flow in Compressible Porous Media: I: Steady-State Conditions. *AIChE J.* **38(9)**:1340-1348 (1992).

Joustra, M. K., Emnéus, A. and Tibbling, P. Large Scale Gel Filtration. *Protides Biol. Fluids.* **15**:575-579 (1967).

Karabelas, A. J., Wegner, T. H. and Hanratty, T. J. Use of Asymptotic Relations to Correlate Mass Transfer Data in Packed Beds. *Chem. Eng. Sci.* **26**:1581-1589 (1971).

Kataoka, T., Yoshida, H. and Ueyama, K. Mass transfer in Laminar Region Between Liquid and Packing Material Surface in the Packed Bed. *J. Chem. Eng. Japan.* **5**(2):132-136 (1972).

Kates, M. *Laboratory Techniques in Biochemistry and Molecular Biology. Techniques of Lipidology. Isolation, Analysis and Identification of Lipids.* Burdon, R. H. and Knippenberg, P. H. editors. Volume 3, part 2, pp. 106-107. Elsevier, New York. 1986.

Katz, E., Ogan, K. L. and Scott, R. P. W. Peak Dispersion and Mobile Phase Velocity in Liquid chromatography: The Pertinent Relationship for Porous Silica. *J. Chromatogr.* **270**:51 (1983).

Kawai, T., Egashira, R. and Kawasaki, J. Axial Dispersion of Liquid Phase in Fixed Bed of Fine Particles. *Kagaku Kogaku Ronbunshu.* **18**(6):965-969 (1992).

Kehinde, A. J., Hudgins, R. R. and Silveston, P. L. Measurement of Axial Dispersion in Packed Beds at Low Reynolds Numbers by Imperfect Pulse Chromatography. *J. Chem. Eng. Japan.* **16**(6):476-482 (1983a).

Kehinde, A. J., Hudgins, R. R. and Silveston, P. L. Measurement of Mass Transfer in Packed Beds at Low Reynolds Numbers by Imperfect Pulse Chromatography. *J. Chem. Eng. Japan.* **16**(6):483-489 (1983b).

Key, P. Y. and Sellen, D. B. A Laser Light-Scattering Study of the Structure of Agarose Gels. *J. Polym. Sci.: Polym. Phys. Ed.* **20**:659-679 (1982).

Kissinger, S. L. and Khang, S-J. The Pore-Filling Model for a Macroporous Catalyst Pellet with Three Different Types of Fouling Mechanisms. *Chem. Eng. Sci.* **44**(2):417-426 (1989).

Klein, J., Washausen, P., Kluge, M. and Eng, H. Characterization of Microbial Biocatalysts. pp. 277-299. Verlag Chemie. 1979.

Knox, J. H. Practical Aspects of LC Theory. *J. Chromatogr. Sci.* **15**:352-364 (1977)

Knox, J. H. Kinetic Factors Influencing Column Design and Operation. In: *Techniques in Liquid Chromatography*. C. F. Simpson, Ed. Ch. 2 pp. 31-38. Wiley Heyden Publishers. Chichester, 1982.

Knox, J. H. and Parcher, J. F. Effect of Column to Particle Diameter Ratio on the Dispersion of Unsorbed Solutes in Chromatography. *Anal. Chem.* **41**(12):1599-1606 (1969).

Knox, J. H. and Scott, H. P. Theoretical Models for Size-Exclusion Chromatogaphy and Calculation of Pore Size Distribution from Size-Exclusion Chromatography Data. *J. Chromatogr.* **316**:311-332 (1984).

Knox, J. H. and Pyper, H. M. Framework for Maximazing Throughput in Preparative Liquid Chromatography. *J. Chromatogr.* **363**:1-30 (1986).

Koch, D. and Brady, J. F. Dispersion in Fixed Beds. *J. Fluid. Mech.* **154**:399-427 (1985).

Kril, M. B., Janauer, G. E. and Fitzpatrick, T. Effect of Fouling on Dynamic Column Capacities of Activated Charcoal and Ion Exchanges Resins. *Reactive Polymers.* **5**(1):109 (1987).

Kroeff, E. P., Owens, R. A., Campbell, E. L., Johnson, R. D. and Marks, H. I. Production Scale Purification of Biosynthetic Human Insulin by Reversed-Phase High-Performance Liquid Chromatography. *J. Chromatogr.* **461**:45-61 (1989).

Kubin, M. Beitrag zur Theorie der Chromatographie. *Collection Czechoslov. Chem. Commun.* **30**:1104-1118 (1965).

Kucera, E. Contribution to the Theory of Chromatography. Linear Non-equilibrium Elution Chromatography. *J. Chromatogr.* **19**:237-248 (1965).

Lapidus, L. and Amundson. N. R. Mathematics of Adsorption in Beds. VI. The Effect of Longitudinal Diffusion in Ion Exchange and Chromatographic Columns. *J. Phys. Chem.* **56**:984-988 (1952).

Laurent, T. C. and Killander, J. A Theory of Gel Filtration and its Experimental Verification. *J. Chromatogr.* **14**:317-330 (1964).

Laurent, T. C. Determination of the Structure of Agarose Gels by Gel Filtration. *Biochim. Biophys. Acta.* **136**:199-205 (1967).

Lee, A. L., Velayudhan, A. and Horváth, C. *Preparative HPLC. Int. Biotechnol. Symp., 8th.* Durand, G., Bobichon, L. and Florent, J., editors. Soc. Fran. Microbiol. Vol. 1, pp. 593-610. Paris. 1988.

Lenhoff, A. M. *Convective Dispersion and Interphase Mass Transfer.* PhD Thesis. University of Wisconsin, Madison. 1985.

Lenhoff, A. M. Significance and Estimation of Chromatographic Parameters. *J. Chromatogr.* **384**:285-299 (1987).

Lenhoff, A. M. and Lightfoot, E. N. Convective Dispersion and Interphase Mass Transfer. *Chem. Eng. Sci.* **41**(11):2795-2810 (1986).

Levison, P. R., Badger, S. E., Toome, D. W., Butts, E. T., Koscielny, M. L. and Lane, L. Influence of Column Design on Chromatographic Performance of Ion-Exchange Media. Upstream and Downstream Processing in Biotechnology III. Mechanical Separation and Particle Technology. Technologisch Institut-Kviv. **16**:3.21-3.28 (1991).

Leyva, A. and Kelly, W. N. Measurement of DNA in Cultured Human Cells. *Anal. Biochem.* **62**:173-179 (1974).

Liao, J.-L. and Hjertén, S. High-Performance Liquid Chromatography of Proteins on Compressed, Non-Porous Agarose Beads. II. Anion-Exchange Chromatography. *J. Chromatogr.* **457**:175-182 (1988).

Liapis, A. I., Anspach, B., Findley, M. E., Davies, J., Hearn, M. T. W. and Unger, K. K. Biospecific Adsorption of Lysozyme onto Monoclonal Antibody Ligand Immobilized on Nonporous Silica Particles. *Biotech. Bioeng.* **34**:467-477 (1989).

Lightfoot, E. N., Gibbs, S. J., Athalye, A. M. and Scholten, T. H. Designing Large-Scale

Adsorptive Separations. *Israel J. Chem.* **30**:229-237 (1990).

Lin, B., Ma, Z. and Guiochon, G. Influence of the Choice of the Boundary Conditions on the Results of the Dynamic Chromatography Model. *J. Chromatogr.* **542**:1-18 (1991).

Magnico, P. and Martin. M. Dispersion in the Interstitial Space of Packed Columns. *J. Chromatogr.* **517**:31-49 (1990).

Majors, R. E. Measuring Particle-Size Distribution of HPLC Packings. *LC-GC Int.* 7:8-13 (1994).

Martin, H. Low Péclet Number Particle-to-Fluid Heat and Mass Transfer in Packed Beds. *Chem. Eng. Sci.* **33**:913-919 (1978).

Martin, A. P. and Synge, R. L. M. A New From of Chromatogram Employing Two Liquid Phases. 1. A Theory of Chromatography. 2. Application to the MIcro-Determination of the Higher Monoamino-Acids in Proteins. *Biochem. J.* **35**:1358-1368 (1941).

Martin, M., Eon, C. and Guiochon, G. Study of the Pertinency of Pressure in Liquid Chromatography. Problems in Equipment Design. *J. Chromatogr.* **108**:229-241 (1975).

McCabe, W. L. and Smith, J. M. *Unit Operations of Chemical Engineering.* pp 196-201 and pp 809-817, McGraw-Hill, New York. 1976.

McCormick, D. Currents in Chromatography. *Bio/Technology.* **5**:246-250 (1987).

McCoy, M. A. and Liapis, A. Evaluation of Kinetic Models for Biospecific Adsorption and its Implications for Finite Bath and Column Performance. *J. Chromatogr.* **548**:25-60 (1991).

McGreavy, C. Andrade Jr., J. S. and Rajagopal, K. Size Exclusion Chromatography in Pore Networks. *Chromatographia.* **30**(11/12):639-644 (1990).

Mehta, R. V., Merson, R. L. and McCoy, B. J. Moment Analysis of Experiments in Gel Permeation Chromatography. *AIChE J.* **19**(5): 1068-1070 (1973).

Miller, S. F. and King, C. J. Axial Dispersion in Liquid Flow Through Packed Beds. *AIChE J.* **12**(4):767-773 (1966).

Ming, F. and Howell, J. A. Parameter Estimation for a Column Adsorption Model Incorporating Axial Dispersion - Application to a Novel Monolithic Ion-Exchange Column. *Trans. I. Chem. E.* **71**:267-272 (1993).

Miyauchi, T., Kikuchi, T. and Hsu, K-H. Limiting Sherwood Number of Sphere Packed Beds by Electrical Method. *Chem. Eng. Sci.* **31**:493-498 (1976).

Mohammad, A. W., Stevenson, D. G.and Wankat, P. C. Pressure Drop Correlations and Scale-up of Size Exclusion Chromatography with Compressible Packings. *Ind. Eng. Chem. Res.* **31**:549-561 (1992).

Moussaoui, M., Benlyas, M. and Wahl, P. Diffusion of Proteins in the Chromatographic Gel AcA-34. *J. Chromatogr.* **558**:71-80 (1991).

Moussaoui, M., Benlyas, M. and Wahl, P. Diffusion of Proteins in Sepharose Cl-B Gels. *J. Chromatogr.* **591**:115-120 (1992).

Nakanishi, K., Yamamoto, S., Matsuno, R. and Kamikubo, T. Analysis of Dispersion Mechanism in Gel Chromatography. *Agric. Biol. Chem.* **41**(8):1465-1473 (1977).

Nakanishi, K., Yamamoto, S., Matsuno, R. and Kamikubo, T. Effect of Particle Size Distribution on Column Efficiency in Gel Chromatography. *Agric. Biol. Chem.* **42**(10):1943-1945 (1978).

Nishio, I., Reina, J. C. and Bansil, R. Quasielastic Light-Scattering Study of the Movement of Particles in Gels. *Phys. Rev. Lett.* **59**(6):684-687 (1987).

Norsker, O., Gibson, K. and Zittan, L. Experience with Empirical Methods for Evaluating Pressure Drop Properties of Immobilized Glucose Isomerase. *Starch/Stärke.* **31**(1):13-16 (1979).

Öbrink, B. Characterization of Fiber Parameters in Agarose Gels by Light Scattering. *J. Chromatogr.* **37**:329-330 (1968).

Ogston, A. G., Preston, B. N. and Wells, J. D. On the Transport of Compact Particles Through Solutions of Chain-Polymers. *Proc. R. Soc. London.* **333A**:297-316 (1973).

Ohashi, H., Sugawara, T., Kikuchi, K-I. and Konno, H. Correlation of Liquid-Side Mass Transfer

Coefficient for Single Particles and Fixed Beds. *J. Chem. Eng. Japan.* **14**(6):433-438 (1981).

Olbrich, R. *The Characterisation and Recovery of Protein Inclusion Bodies from Recombinant Escherichia coli*. Ph. D. Thesis. University College London. pp. 108. 1989.

Östergren, K. and Trägårdh, C. A Study of Permeability and Hydrodynamic Dispersion Under Conditions of Chromatographic Flow, in *Separations for Biotechnology*. D. L. Pyle Ed. Vol. 2, pp 632-41. SCI Elsevier Applied Science. 1990.

Östergren, K. and Trägårdh, C. Modelling of Flow and Hydrodynamic Dispersion in a Chromatographic Column. Poster presented at: The NATO Advanced Study Institute on *Theoretical Advancement in Chromatography and Related Separation Techniques*. Ferrara, Italy. 18-30 August 1991.

Parker, K. H., Metha, R. V. and Caro, C. G. Steady Flow in Porous, Elastically Deformable Materials. *J. Appl. Mech.* **54**:794-800 (1987).

Pettersson, T. *Optimization in Chromatography. Column Maintenance.* Biochemical Engineering Hands-on Course. University College London. U.K. Summer 1989.

Pharmacia LKB Biotechnology. *Protein A Sepharose 4 Fast Flow. Data File. Affinity media.* Uppsala, Sweden. 1990.

Pharmacia LKB Biotechnology. *Gel Filtration. Principles and Methods.* 5th ed. Rahms i Lund, Sweden. 1991a.

Pharmacia LKB Biotechnology. *Ion Exchange Chromatography. Principles and Methods.* 3rd Ed. Uppsala, Sweden. 1991b.

Pharmacia LKB Biotechnology. *Sepharose Fast Flow Ion Exchangers. Data File. Ion Exchange Media.* Uppsala, Sweden. 1992.

Pharmacia LKB Biotechnology. Personal communication. 1993.

Pirotta, M. *Ion Exchange Resins and Adsorbents in the Chromatographic Extraction of Antibiotics.* M. S. Verral Ed. Ch. 7, pp. 98-114. Ellis Horwood, Ltd. Chichester, U.K. 1985.

Rasmuson, A. The Effect of Particles of Various Size, Shape and Properties on the Dynamics of Fixed Beds. *Chem. Eng. Sci.* **40**:621-629 (1985a).

Rasmuson, A. Exact Solution of a Model for Diffusion in Particles and Dispersion in Packed Beds: Numerical Evaluation. *AIChE J.* **31**:518-519 (1985b).

Ravindranath, B. *Principles and Practice of Chromatography*. First ed. pp 64-85. Ellis Horwood Series. U.K. 1989.

Reyes, S. C. and Iglesia, E. Monte Carlo Simulations of Structural Properties of Packed Beds. *Chem. Eng. Sci.* **46**(4):1089-1099 (1991).

Richards, D. Process LC Techniques Assume Greater Role as Biotech Drugs Readied for Market; Purity vs. Speed Trade-Offs. *The Med. Business J.* 202-204. November 30, 1989.

Ritcey, G. M. Silica Fouling in Ion Exchange, Carbon-in-Pulp and Solvent Extraction Circuits. *Canadian Metal. Quarterly.* **25**(1):31-43 (1986)

Rumpf, H. and Gupte, A. R. Einflüsse der Porosität und Korngrössenverteilung im Widerstandgesetz der Porenstömung. *Chem. Ing. Tech.* **43**:367-375 (1971).

Ruth, B. F., Montillon, G. H. and Montonna, R. E. Studies in Filtration: I. Critical Analysis of Filtration Theory; II. Fundamentals of Constant Pressure Filtration. *Ind. Engng. Chem.* **25**:76-82, 153-161 (1933).

Sachs, D. H. and Painter, E. Improved Flow Rates with Porous Sephadex Gels. *Science.* **175**:781-782 (1972).

Saffman, P. G. Dispersion Due to Molecular Diffusion and Macroscopic Mixing in Flow Through a Network of Capillaries. *J. Fluid. Mech.* 7:194-208 (1960).

Satterfield, C. N., Colton, C. K. and Pitcher, Jr. W. H. Restricted Diffusion in Liquids Within Fine Pores. *AIChE J.* **19**:628-635 (1973).

Scawen, M. D., Hammond, P. M., Sherwood, R. F. and Atkinson, T. Large-Scale Protein Extraction and Isolation. *Biochem. Soc. Trans.* 18:231-233 (1990).

Schmidt, Jr., D. E., Glese, R. W., Conron, D. and Karger, B. L. High Performance Liquid Chromatography of Proteins on a Diol-Bonded Silica Gel Stationary Phase. *Anal. Chem.* 52:177-182 (1980).

Schneider, P. and Smith, J. M. Adsorption Rate Constants from Chromatography. *AIChE J.* **14**(5):762-771 (1968).

Scott, C. R. *An Introduction to Soil Mechanics and Foundations.* 1st ed. Maclaren and Sons Ltd, London. 1969.

Skidmore, G. L., Horstmann, B. J. and Chase, H. A. Modelling Single-Component Protein Adsorption to the Cation Exchanger S-Sepharose FF. *J. Chromatogr.* **498**:113-128 (1990).

Smith, M. H., in *Handbook of Biochemistry. Selected Data for Molecular Biology.* 2nd ed., Sober, H. A., editor. pp. C3-C39. Chemical Rubber Company, Cleveland, USA. 1970.

Sofer, G. Increasing Media Lifetime for Cost-Effective Chromatography. *Bio/Technology.* **5**:341-342 (1987).

Sofer, G. K. and Nyström, L. E. *Process Chromatography. A Practical Guide.* 1st ed. Academic Press Ltd. London, UK. 1989.

Sørensen, J. P. and Stewart, W. E. Computation of Forced Convection in Slow Flow Through Ducts and Packed Beds. Parts I-IV. *Chem. Eng. Sci.* **29**:811-837 (1974).

Stewart, W. E. Forced Convection: IV. Asymptotic Forms for Laminar and Turbulent Transfer Rates. *AIChE J.* **33**(12):2008-2016 (1987).

Stewart, D. J., Purvis, D. R. and Lowe, C. R. Affinity Chromatography on Novel Perfluorocarbon Supports. *J. Chromatogr.* **510**:177-187 (1990).

Suzuki, M. Zone Spreading in Gel Chromatography. *J. Chem. Eng. Japan.* **7**(4):262-266 (1974).

Suzuki, M. and Smith, J. M. Kinetic Studies by Chromatography. *Chem. Eng. Sci.* **26**:221-235 (1971).

Tiller, F. M. Compressible Cake Filtration. In *The Scientific Basis of Filtration.* K. J. Ives, ed. Noordhoof, Lyden. 1975.

Trowbridge, M. E. O'K. Problems in the Scaling-up of Centrifugal Separation Equipment. *The Chem. Engineer.* A73-A87 (1962).

Tsou, H-S. and Graham, E. E. Prediction of Adsorption and Desorption of Protein on Dextran Based Ion-Exchange Resin. *AIChE J.* **31**(12):1959-1966 (1985).

Tyn M. T. and Gusek, T. W. Prediction of Diffusion Coefficients of Proteins. *Biotech. & Bioeng.* **35**:327-338 (1990).

Unger, K. K. and Janzen, R. Packings and stationary Phases in Preparative Column Liquid Chromatography. *J. Chromatogr.* 373:227-264 (1986).

Van Vliet, B. M. and Weber Jr., W. J. Particle Surface Roughness Effects on the Interfacial Mass Transfer Dynamics of Microporous Adsorbents. *Chem. Eng. Comm.* **68**:165-176 (1988).

Van Deemter, J. J., Zuiderweg, F. J. and Klinkenberg, A. Longitudinal Diffusion and Resistance to Mass Transfer as Causes of Nonideality in Chromatography. *Chem. Eng. Sci.* **5**:271-289 (1956).

Verhoff, F. H. and Furjanic, Jr. J. J. Compressible Packed Bed Fluid Dynamics with Application to a Glucose Isomerase Reactor. *Ind. Eng. Chem. Process Des. Dev.* **22**:192-198 (1983).

Verzele, M., Dewaele, C. and De Weerdt, M. Inner Wall Coating of Micro-LC Columns. Wall Effects in LC. *J. High Resolution Chromatogr.* **12**:164-168 (1989).

Verzele, M. Preparative Liquid Chromatography. *Anal. Chem.* **62**(4):265A-269A (1990).

Villermaux, J. Deformation of Chromatographic Peaks Under the Influence of Mass Transfer Phenomena. *J. Chromatogr. Sci.* **12**:822-831 (1974).

Wakao, N. and Funazkri, T. Effect of Fluid Dispersion Coefficients on Particle-to-Fluid Mass Transfer Coefficients in Packed Beds. *Chem. Eng. Sci.* **33**:1375-1384 (1978).

Wakao, N. and Kaguei, S. *Heat and Mass Transfer in Packed Beds.* Gordon and Breach Science

Publishers, Inc. New York. 1982.

Wakeman, R. J. A Numerical Solution of the Differential Equations Describing the Formation of and Flow in Compressible Filter Cakes. *Trans. Instn. Chem. Engs.* **56**:258-265 (1978).

Walters, R. R. High-Performance Affinity Chromatography: Pore-Size Effects. *J. Chromatogr.* **249**:19-28 (1982).

Werner, R. G. Potential and Efficiency in the Biotechnical Process. *Pharm. Tech. Europe.* 20-28 May (1994).

Wilson, E. J. and Geankoplis, C. J. Liquid Mass Transfer at Very Low Reynolds Numbers in Packed Beds. *Ind. Eng. Chem. Fundam.* **5**:9-14 (1966).

Wu, J-Y., Chen, T-L. and Weng, H-S. Simulation of Nonlinear Fixed-Bed Adsorbers by Orthogonal Collocation with the Aid of Fast Fourier Transform. *J. Chem. Eng. Japan.* **24**(3):391-394 (1991).

Yamamoto, S., Nakanishi, K., Matsuno, R. and Kamikubo, T. Operational Conditions for Gel Chromatography -Prediction of Elution Curves-. *Agric. Biol. Chem.* **43**(12):2499-2506 (1979).

Yamamoto, S., Nomura, M. and Sano, Y. Scaling up of Medium-Performance Gel Filtration Chromatography of Proteins. *J. Chem. Eng. Jpn.* **19**(3):227-231 (1986).

Yamamoto, S., Nakanishi, K. and Matsuno, R. *Ion-Exchange Chromatography of Proteins.* Chromatographic Science Series, Vol. 43. Marcel Dekker, New York. 1988.

Yamamoto, S. and Sano, Y. Predicting the Performance of Production-Scale Chromatography. In: *Biochemical Engineering for 2001. Proceedings of Asia-Pacific Biochemical Engineering Conference 1992.* Furusaki, S., Endo, I. and Matsuno, R. Eds. pp 548-550. Springer-Verlag. Tokyo. 1992.

Young, M. E., Carroad, P. A. and Bell, R. L. Estimation of Diffusion Coefficients of Proteins. *Biotech. & Bioeng.* **22**:947-955 (1980).

Zollner, N. and Kirsch, K. *Z. Ges. Exp. Med.* **135**:545-561 (1962).